



Dysfonction mitochondriale et réponse immune de l'hôte au cours de la pneumopathie à *Streptococcus pneumoniae*: impact de la ventilation mécanique ?

Mathieu Blot

► To cite this version:

Mathieu Blot. Dysfonction mitochondriale et réponse immune de l'hôte au cours de la pneumopathie à *Streptococcus pneumoniae*: impact de la ventilation mécanique ?. Médecine humaine et pathologie. Université Bourgogne Franche-Comté, 2020. Français. NNT : 2020UBFCI002 . tel-03353672

HAL Id: tel-03353672

<https://theses.hal.science/tel-03353672>

Submitted on 24 Sep 2021

HAL is a multi-disciplinary open access archive for the deposit and dissemination of scientific research documents, whether they are published or not. The documents may come from teaching and research institutions in France or abroad, or from public or private research centers.

L'archive ouverte pluridisciplinaire **HAL**, est destinée au dépôt et à la diffusion de documents scientifiques de niveau recherche, publiés ou non, émanant des établissements d'enseignement et de recherche français ou étrangers, des laboratoires publics ou privés.

THESE DE DOCTORAT DE L'ETABLISSEMENT UNIVERSITE BOURGOGNE FRANCHE-COMTE
PREPAREE A L'UFR DES SCIENCES SANTE DE DIJON

Ecole doctorale n°554

Environnement Santé

Doctorat de Science de la vie

Par

Mr Blot Mathieu

Dysfonction mitochondriale et réponse immune de l'hôte au cours de la pneumopathie à *Streptococcus pneumoniae* : impact de la ventilation mécanique ?

Thèse présentée et soutenue à Dijon, le 28 mai 2020

Composition du jury :

Pr. Florence ADER,	Université Lyon 1,	Rapporteuse
Pr. Pierre-Emmanuel CHARLES,	Université Bourgogne-Franche Comté,	Directeur de Thèse
Pr. Pascal CHAVANET,	Université Bourgogne-Franche Comté,	Président du Jury
Pr. Sébastien GIBOT,	Université de Lorraine,	Rapporteur
Pr. Benoit GUERY,	Université de Lausanne,	Examinateur
Pr. David MASSON,	Université Bourgogne-Franche Comté,	Examinateur

Je dédie ce travail à ma femme Pauline, et mes 3 petits gars Marius, Louis et Camille

Remerciements

A Monsieur le Professeur Pierre-Emmanuel CHARLES

Merci de m'avoir accueilli dans votre équipe depuis 2014, à l'occasion de mon Master 2. Tous ces travaux accomplis, ces réunions d'équipes, ces nombreuses discussions scientifiques et tous vos conseils avisés m'ont beaucoup appris et surtout donné une grande motivation à poursuivre en ce sens, sur cette thématique des infections respiratoires. Merci pour votre patience, et surtout votre entière confiance tout au long de ces années.

A Monsieur le Professeur Pascal CHAVANET

C'est un honneur que vous me faites de présider ce jury. Vous m'avez accueilli en 2011 en tant qu'interne dans votre service et désormais dans l'équipe de Maladies Infectieuses. Ces travaux au laboratoire n'auraient pas été possible sans vous, et j'en suis profondément reconnaissant. Vous avez construit un « univers » autour de la recherche en infectiologie et ainsi déposé une première pierre, et j'espère pouvoir continuer dans ce sens. Merci de me faire partager votre expérience et d'évaluer désormais ce travail de thèse de Science.

A Madame le Professeur Florence ADER

Merci Florence d'accepter de rapporter ce travail. Nous connaissons ton intérêt pour la réponse immunitaire au cours de la pneumopathie et ton dynamisme pour développer la recherche sur les infections respiratoires, comme en témoigne ton investissement actuel dans l'étude DISCOVERY. C'est un honneur que tu me fais pouvoir juger ce travail.

A Monsieur le Professeur Sébastien GIBOT

Je vous remercie sincèrement d'accepter de juger ce travail. Vous connaissez de longue date l'équipe du Pr Pierre Emmanuel Charles et nous avons pu à plusieurs reprises échanger sur ces travaux. Je vous remercie pour vos conseils avisés et cette rigueur scientifique.

A Monsieur le Professeur David MASSON

Merci David de me faire l'honneur de juger ce travail. Merci pour ta confiance dans nos travaux au sein de l'équipe Lipness. Merci aussi pour tes nombreux soutiens.

A Monsieur le Professeur Benoit GUERY

Je vous remercie de me faire l'honneur de juger de ce travail. Je suis admiratif de votre dynamisme dans la recherche en infectiologie et connais votre intérêt pour la réponse immunitaire au cours de la pneumopathie.

Je remercie aussi le Professeur Lionel PIROTH pour sa confiance et son soutien sans faille durant ces années passées dans le service. Merci aussi pour sa rigueur scientifique.

Je remercie les Professeurs Didier Payen et Tarek Sharshar qui m'ont guidé et conseillé tout au long de cette thèse en tant que membre du comité de suivi de thèse.

A ma femme Pauline et nos 3 petits gars Marius, Louis et Camille. Ce travail n'aurait pas été possible sans vous, tous ces sacrifices que vous avez fait pour me soutenir.

A mes parents que je ne remercierai jamais assez !

A mes frères et sœur (Elvina, David, Pierre, Thomas et Antoine), et mes belles sœurs et beaux-frères.

A ma grand-mère Monique.

A toute ma famille

A mes beaux-parents Pascale et Clause et toute ma belle-famille.

A tous mes amis.

A toute l'équipe de Maladies Infectieuses,

A toute l'équipe Lipness, en particulier le Dr Laurent Lagrost qui nous a permis d'intégrer l'équipe il y a quelques années. A tous mes collègues du B3, à Laure Anne qui m'a accueilli dans l'équipe et appris à pipeter ! à tous les étudiants qui ont participé à ces travaux dont Chloé, Stéphanie, Jennifer, Camille, Charline et Marine.

A toutes les personnes qui m'ont aidé, soutenu et appris au labo, l'équipe de la plateforme de cytométrie, de l'animalerie, de Cellimap...

A Mr le Professeur Jérôme Pugin, Irène Dunn-Siegriest et Serge Grazioli pour cette collaboration sur l'étude des alarmines.

A Mme la Professeure Bensoussan Danièle, Loic Reppel et Caroline Laroye pour cette belle collaboration ayant permis d'investiguer les CSMs dans notre modèle.

Table des matières

Liste des travaux réalisés et présentés dans ce manuscrit :	8
Autres travaux réalisés et discutés dans le manuscrit :	8
Communications orales.....	9
Communication affichée	9
Liste des Tableaux	10
Liste des Figures	10
Abréviations	12
1 Introduction	14
1.1 Pneumopathie aigue communautaire	14
1.1.1 Généralités	14
1.1.2 Réponse immunitaire (exemple de la pneumopathie à pneumocoque)	17
1.1.3 Stratégies thérapeutiques au cours de la PAC: passé, présent, (futur ?).....	19
1.2 Altérations immunitaires et d'organes au cours du sepsis : rôle des mitochondries ?	20
1.2.1 Altérations immunitaires au cours du sepsis et perspectives thérapeutiques immunostimulatrices.....	20
1.2.2 Rôle des mitochondries dans la réponse immunitaire innée.....	23
1.2.3 Dysfonction mitochondriale et dysfonctions d'organe au cours du sepsis.....	36
1.3 Ventilation mécanique et Ventilator-Induced Lung Injury	37
1.3.1 Ventilator-Induced Lung Injury.....	38
1.3.2 Stratégies de « VM protectrice ».....	40
1.3.3 Impact de la ventilation mécanique sur l'homéostasie mitochondriale.....	41
1.4 Les cellules souches/stromales mésenchymateuses	42
1.4.1 Définition, propriétés et perspectives au cours du sepsis	42
1.4.2 Propriétés immunomodulatrices.....	43
1.4.3 Propriétés microbicides.....	43
1.4.4 Résolution de la dysfonction d'organe.....	44
2 Objectifs des travaux	48
2.1 Article 1 (Genève/Dijon, Plos One)	48
2.2 Article 2 (Dijon, Scientific Reports 2018)	69
2.3 Article 3 : Dysfonction mitochondriale et réponse immune de l'hôte au cours de la pneumopathie à <i>Streptococcus pneumoniae</i> : impact de la ventilation mécanique ? (Travail en cours de publication).....	93
3 Travaux cliniques en cours.....	149
3.1 Etude PNEUMOCHONDRIE.....	149
3.2 Etude Ancillaire PNEUMOCHONDRIE COVID-19	154

3.3 Etude LYMPHONIE.....	157
3.4 Etude ancillaire LYMPHONIE Covid-19.....	157
4 Perspectives	159
5 Conclusion générale.....	161
6 Bibliographie	165

Liste des travaux réalisés et présentés dans ce manuscrit :

Article 1

- ⊕ Mitochondrial alarmins are tissue mediators of ventilator-induced lung injury and ARDS.
Grazioli S, Dunn-Siegriest I, Pauchard LA, **Blot M**, Charles PE, Pugin J. **Plos One 2019.**

Article 2

- ⊕ **Blot M**, Pauchard LA, Dunn I, Donze J, Malnuit S, Rebaud C, Croisier D, Piroth L, Pugin J, Charles PE. Mechanical ventilation and *Streptococcus pneumoniae* pneumonia alter mitochondrial homeostasis. **Scientific reports 2018.**

Article 3

- ⊕ **Blot M**, Jacquier M, Pauchard LA, Thomas C, Croisier D, Bensoussan D, Reppel L, Charles PE. Mesenchymal stem cells as an adjunctive therapy during severe ventilated pneumococcal pneumonia. (Article en préparation, abstract accepté aux Journées Nationales d'Infectiologie 2020).

Autres travaux réalisés et discutés dans le manuscrit :

- ⊕ Pauchard LA, **Blot M**, Bruyere R, Barbar SD, Croisier D, Piroth L, Charles PE. Linezolid and atorvastatin impact on pneumonia caused by *Staphylococcus aureus* in rabbits with or without mechanical ventilation. **Plos One 2017.**
- ⊕ **Blot M**, Croisier D, Péchinot A, Vagner A, Putot A, Fillion A, Baudouin N, Quenot JP, Charles PE, Bonniaud P, Chavanet P, Piroth L. A leukocyte score to improve clinical outcome predictions in bacteremic pneumococcal pneumonia in adults. **Open forum Infectious Diseases 2014.**
- ⊕ **Blot M**, Pivot D, Bourredjem A, Salmon-Rousseau A, de Curraize C, Croisier D, Chavanet P, Binquet C, Piroth L. Effectiveness of and obstacles to antibiotic streamlining to amoxicillin monotherapy in bacteremic pneumococcal pneumonia. **International Journal of Antimicrobial Agents 2017.**
- ⊕ **Blot M**, Chavanet P, Piroth L. Procalcitonin to distinguish viral from bacterial origin of pneumonia: no premature conclusion! **Clinical Infectious Diseases 2019**
- ⊕ **Blot M**, Chavanet P, Piroth L. Influenza infection: An update for clinicians. **Revue Medecine Interne 2019.**
- ⊕ **Blot M**, Salmon-Rousseau A, Chavanet P, Piroth L. Corticosteroids in treating community-acquired pneumonia: Has the time really come? **Clinical Microbiology and Infection 2017.**
- ⊕ **Blot M**, Salmon-Rousseau A, Chavanet P, Piroth L. Do we know enough to recommend corticosteroids in acute respiratory distress syndrome? **Critical Care 2017.**

Communications orales

- ✚ Quel rôle des alarmines mitochondrielles au cours de la pneumopathie à *Streptococcus pneumoniae* et la ventilation mécanique. (**Journées de Recherche Respiratoires 2015, Dijon**)
- ✚ Les alarmines mitochondrielles : quel impact au cours de la pneumopathie à *Streptococcus pneumoniae* chez le lapin soumis à la ventilation mécanique ? (**Journées Nationales d'Infectiologie, 2015**)
- ✚ Les cellules souches/stromales mésenchymateuses améliorent le pronostic et corrigent les altérations immunes et mitochondrielles au cours de la pneumopathie à pneumocoque ventilée. (**Journées Nationales d'Infectiologie, 2020, soumis**)

Communication affichée

- ✚ Which role for mitochondrial alarmins in rabbit with *Streptococcus pneumoniae* pneumonia and mechanical ventilation? (**ESCMID 2015, Copenhague**)

Liste des Tableaux

Tableau 1. Définitions de la pneumopathie aigue communautaire

Tableau 2. Facteurs de virulence de *Streptococcus pneumoniae* capables de compromettre la réponse immune au cours de la colonisation ou de l'invasion bactérienne

Liste des Figures

Figure 1. Principaux déterminants du devenir clinique au cours de la pneumopathie aigue communautaire

Figure 2. Reconnaissance des PAMPs de *Streptococcus pneumoniae* par les PRRs

Figure 3. Altérations de la réponse immunitaire innée au cours du sepsis.

Figure 4. Mitochondrie visualisée par microscopie électronique à transmission.

Figure 5. Alarmines mitochondrielles.

Figure 6. Reconnaissance de l'ADNmt circulant et activation de la réponse immunitaire innée.

Figure 7. Chaîne respiratoire mitochondriale.

Figure 8. Reprogrammation métabolique au cours du sepsis.

Figure 9. Apoptose via la voie intrinsèque.

Figure 10. Régulation de l'homéostasie mitochondriale.

Figure 11. Dommages pulmonaires et inflammation produites par une ventilation mécanique agressive.

Figure 12. Effet des CSMs sur la dysfonction d'organe aux cours du sepsis.

Figure 13. Mécanismes d'action des CSMs au cours du SDRA

Figure 14. Hypothèses des déterminants et conséquences de la libération des alarmines mitochondrielles : modèle de pneumopathie à pneumocoque sous ventilation mécanique.

Figure 15. Analyse morphologique des mitochondries d'un lapin sain par microscopie électronique d'un pneumocyte de type II et (B) d'un hépatocyte.

Figure 16. Réponse immunitaire et déterminants mitochondriaux dans les compartiments alvéolaires et systémiques

Figure 17. Réponse immunitaire et déterminants mitochondriaux dans les compartiments alvéolaires et systémiques

Figure 18. Effet des CSMs au cours de la pneumopathie à pneumocoque grave ventilée.

Abréviations

- °NO : monoxyde d'azote
- ADNmt : Acide désoxyribonucléique mitochondrial
- ADP : adénosine diphosphate
- ATP : adénosine triphosphate
- Bcl-2 : protéine B cell lymphoma 2
- CHU : centre hospitalier universitaire
- CIO⁻ : ion hypochlorite
- CMH : complexe majeur d'histocompatibilité
- CSMs : cellules souches mésenchymateuses stromales
- FiO₂ : fraction inspirée en oxygène
- fMLP : N-formyl-methionyl-leucyl-phenylalanine
- FPR : formyl peptide receptor
- H₂O₂ : peroxyde d'hydrogène
- HMGB1 : high mobility group box 1
- IL : interleukin
- LPS : lipopolysaccharide
- MAPK : Mitogen-activated protein kinase
- NADPH : Nicotinamide adénine dinucléotide phosphate
- NETs : neutrophil extracellular traps
- NF-κB : nuclear factor- κB
- NLRP3 : NOD-like receptor family, pyrin domain containing 3
- NO : monoxyde d'azote
- NRF2 : nuclear respiratory factors 1 et 2
- O₂[•] : anion superoxyde
- ONOO[•] : peroxynitrite
- OXPHOS : oxydative Phosphorylation
- PAC : pneumopathie aigue communautaire
- PAMPs : pathogen associated molecular patterns
- PaO₂ : pression artérielle en oxygène
- PEEP : pression expiratoire positive

PGC1 α : peroxysome-proliferator-activated receptor γ coactivator 1 α

Pink1 : PTEN-induced putative kinase 1

PMNs : polymorphonuclear leukocytes

Pplat: pression de plateau

PRRs : pattern recognition receptors

ROS : Reactive Oxygen Species

S.p. : *Streptococcus pneumoniae*

SD : standard deviation

SDRA : syndrome de détresse respiratoire aigue

TFAM : transcription factor A for the mitochondrion

TLR: toll like receptor

USI : unité de soins intensifs

VILI : ventilator induced lung injury

VM : ventilation mécanique

VO₂ : volume of oxygen

V_T : volume courant

$\Delta\Psi_m$: potentiel de membrane mitochondrial

1 Introduction

1.1 Pneumopathie aigue communautaire

1.1.1 Généralités

La littérature ne permet pas de dégager de définition consensuelle de la pneumopathie aigue communautaire (1,2). Les sociétés savantes Britanniques, Américaines et Européennes proposent des définitions, la première purement clinique, et la deuxième radio-clinique (Tableau 1).

Pneumopathie aigue communautaire

→ Définition purement clinique selon la British Thoracic Society (3)

- Symptômes d'infection aigue des voies aériennes inférieures (toux + au moins un autre symptôme)
- Signes physiques de foyer infectieux pulmonaire focal
- ≥ 1 signe d'atteinte systémique (température > 38°C et/ou frissons, sueurs, douleurs)
- Pas d'autre explication expliquant les symptômes et décision clinique de traiter la pathologie comme une pneumopathie par des antibiotiques.

→ Définition clinico-radiologique pour l'Infectious Diseases Society of America (IDSA)/American Thoracic Society (ATS) (4) et l'European Respiratory Society (ERS) / European Society for Clinical Microbiology and Infectious Diseases (ESCMID) (5)

- Symptômes et signes aigus d'infection des voies aériennes inférieures
 - Pour les recommandations européennes :
 - Présents depuis moins de 3 semaines
 - Toux + ≥ 1 autre signe respiratoire (crachat productif, dyspnée, respiration sifflante et douleur thoracique) + fièvre depuis plus de 4 jours
 - Nouvel infiltrat radiologique du parenchyme pulmonaire
 - Sans autre cause pouvant les expliquer
- ##### → Caractère communautaire
- Pneumopathie présente ou diagnostiquée dans les 48 heures suivant l'admission à l'hôpital

Tableau 1. Définitions de la pneumopathie aigue communautaire (selon les recommandations britanniques, américaines et européennes)

L'incidence des PAC en Europe est estimée à 1,7-11,6 cas pour 1000 personnes par an, soit environ 3 370 000 cas par an, dont environ 1 000 000 requièrent une hospitalisation avec une sous-estimation probable liée aux données disponibles essentiellement issues d'études en milieu hospitalier et à la difficulté d'estimer l'incidence des PAC en ambulatoire (6,7).

Le poids de la maladie est avant tout humain. La PAC demeure la principale cause de décès d'origine infectieuse dans le monde, d'après les données de l'organisation mondiale de la santé (OMS)

(8). Les infections respiratoires basses seraient responsables dans le monde de 35,4 (33,8 – 36,8) décès par 100 000 personnes par an, tout âge confondu, soit environ 2 558 600 décès par an (9). Au cours d'une PAC pris en charge à l'hôpital, la mortalité à 30 jours touche 6 à 17% des patients, et 30% pour ceux admis en réanimation (10–13). Néanmoins, une tendance à la diminution de cette mortalité semble être observée ces deux dernières décennies (12,14).

Parmi ces décès, un tiers surviennent précocement dans les 2 premiers jours, témoignant de la sévérité initiale de la pathologie (10).

- Les principales **causes de décès précoces** au cours de la PAC sont la survenue d'une **détresse respiratoire, d'un choc septique/défaillance multi-organe, ou d'une complication cardiaque** (insuffisance cardiaque ou arythmie) (10). **Le syndrome de détresse respiratoire (SDRA)** survient chez 2% des patients hospitalisés pour une PAC, et 13% des patients admis en unité de soins intensifs (USI) (15). En cas de pneumopathie bactériémique à *S.p.* nous avions retrouvé dans notre cohorte au centre hospitalier universitaire (CHU) de DIJON, 15% de patients présentant un SDRA (16). Cette complication définie par la présence d'une insuffisance respiratoire aigüe non expliquée par une dysfonction cardiaque, des opacités parenchymateuses bilatérales et un rapport $\text{PaO}_2/\text{FiO}_2 < 300$ avec une pression expiratoire positive (PEEP) $\geq 5 \text{ cmH}_2\text{O}$, est associée à une mortalité de plus de 50% (17).
- Les **causes de décès plus tardifs** sont plus attribuables aux comorbidités, en particulier neurologiques et cardiaques (18). A plus long terme, il existe aussi une augmentation du risque de décès toutes causes (aHR 1,65 IC95% 1,57-1,73) (19), et d'évènements cardiovasculaires (risque d'insuffisance cardiaque à 10 ans (HR 1,61 IC95% 1,44-1,81) (20)), par-rapport à la population générale (21).

Le poids est aussi économique. Le cout moyen ajusté estimé à un an, de la prise en charge d'un patient hospitalisé pour une PAC est de 55 391 dollars dans une étude américaine récente (22). L'impact économique est plus important lorsque la PAC est due à *Streptococcus pneumoniae* (*S.p.*), que d'une autre origine (7). L'étude prospective française PNEUMOCOST, évaluait le cout moyen associé à la prise en charge d'une pneumopathie à pneumocoque hospitalisée à 7293 euros (SD 7363 euros) et le cout du suivi à 1242 euros (SD 3000 euros), avec un poids important des comorbidités associées et du niveau de sévérité initiale (23).

L'origine des PAC est principalement bactérienne et *S.p.* la principale bactérie responsable (24), retrouvé dans environ un tiers des cas (12 à 85%) dans les séries européennes (7,25), et 27% (IC95% 24-31) dans le monde (26). *Haemophilus influenzae* et *Staphylococcus aureus* sont aussi fréquemment responsables, plus rarement des bactéries intracellulaires (*Mycoplasma pneumoniae*,

Chlamydia pneumoniae, *Legionella pneumophila*...) (25). Les virus respiratoires (influenzae, virus respiratoire syncytial, rhinovirus, adénovirus, coronavirus, parainfluenzae ...) sont fréquemment retrouvés (27). Il s'agit le plus souvent de co-infections (28), le virus facilitant la surinfection bactérienne secondaire (29). Bien que des données épidémiologiques récentes avancent que les virus sont la principale cause de PAC, car plus fréquemment retrouvés que les bactéries (27), ce résultat est probablement plus le reflet des progrès effectués dans le diagnostic moléculaire des virus respiratoires sur le site nasopharyngé (facile d'accès), alors que parallèlement, aucun progrès substantiel n'a été effectué pour le diagnostic bactériologique pulmonaire (30).

La physiopathologie de la PAC résulte de la relation complexe entre la virulence bactérienne et la réponse immunitaire de l'hôte (Figure 1). L'intensité de cette dernière est conditionnée par de nombreux facteurs (génétique, âge du patient déterminant le niveau de maturation ou de senescence de l'immunité, survenue d'une infection virale préalable, immunosuppression...). Les principaux facteurs de risque de PAC sont ainsi principalement liés à des altérations des défenses immunitaires locales (arbre respiratoire) et/ou systémique (immunodépression). Une condition facilitant l'inhalation de sécrétions contaminées est un autre facteur de risque significatif (31). Une clairance bactérienne rapide et précoce facilitée par l'administration d'une antibiothérapie efficace détermine le pronostic des PAC, mais une telle prise en charge pourrait entraîner une réponse immune inappropriée en lien avec la lyse bactérienne.

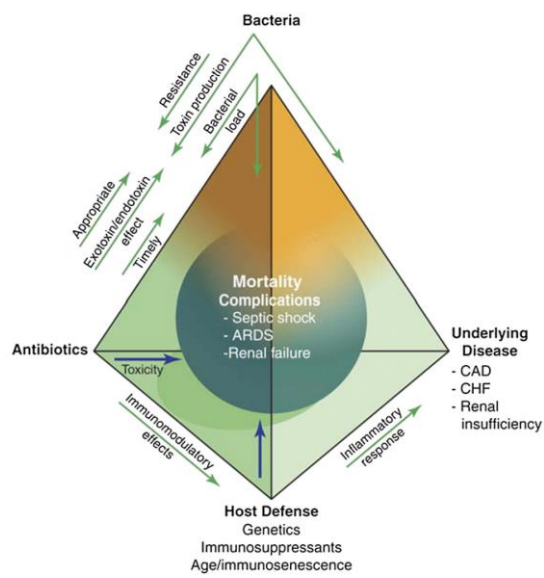


Figure 1. Principaux déterminants du devenir clinique au cours de la pneumopathie aigue communautaire (D'après Waterer et al (32))

1.1.2 Réponse immunitaire (exemple de la pneumopathie à pneumocoque)

Au cours de l'agression infectieuse, la réponse immunitaire innée permet l'élimination des pathogènes responsables de l'invasion. Chez un certain nombre de patients, cette réponse peut s'avérer inadaptée, soit insuffisante pour éradiquer l'agent infectieux, soit au contraire excessive et pouvant être responsable de dommages pulmonaires, voire plus à distance. Un juste équilibre entre la balance pro et anti-inflammatoire détermine ainsi le devenir des patients (33).

La réponse immunitaire innée antibactérienne est principalement orchestrée par les cellules épithéliales, les macrophages alvéolaires, les polynucléaires neutrophiles (PMNs, polymorphonuclear leukocytes) et les cellules lymphocytaires T. Elle met en jeu des récepteurs spécifiques, les PRRs (pattern recognition receptors) qui reconnaissent des « signaux de danger », soit portés par les micro-organismes (les PAMPs pour Pathogen Associated Molecular Patterns), soit endogènes, libérés par les cellules endommagées, (les DAMPs pour Damage Associated Molecular Patterns) (34). Au cours de la pneumopathie à pneumocoque, les nombreux facteurs de virulence de *S.p.* sont reconnus à différents niveaux par le système immunitaire (Figure 2).

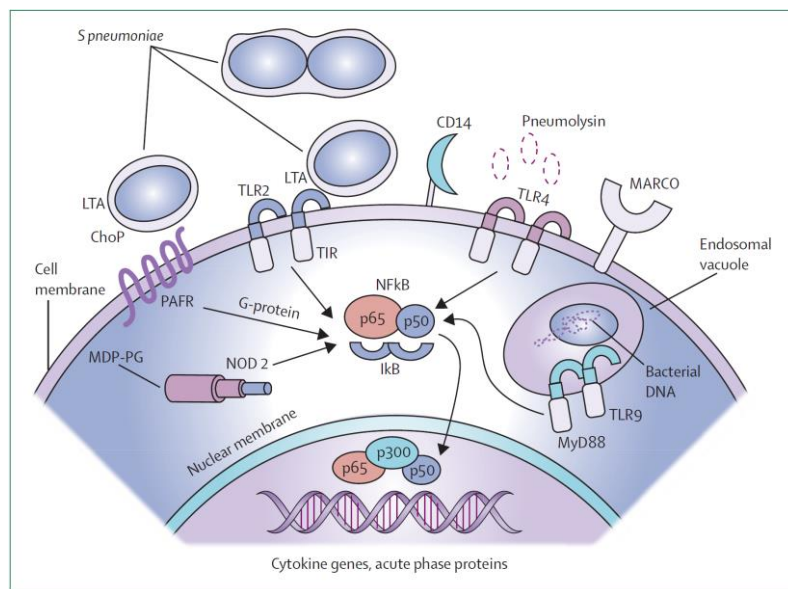


Figure 2. Reconnaissance des PAMPs de *Streptococcus pneumoniae* par les PRRs (D'après Van der Poll et Opal (24)).

Les macrophages alvéolaires représentent la 1^{ère} ligne de défense immune, capable de phagocytter et de tuer une grande partie des pneumocoques (24). La reconnaissance des PAMPs et des DAMPs par les PRR active les cellules épithéliales et les macrophages alvéolaires qui produisent et libèrent des cytokines chimiotactiques de la famille des CXC (dont l'interleukine 8 (IL-8)), entraînant le

recrutement de PMNs sur le site pulmonaire qui deviennent alors la principale cellule phagocytaire (35).

Les PMNs jouent un rôle clé et précoce dans la défense anti-infectieuse par le biais de 3 grands mécanismes : 1) la **phagocytose**, 2) la **dégranulation**, 3) la **libération de NETs (neutrophil extracellular traps)**, mais leur activation massive peut être à l'origine de lésions tissulaires importantes, comme celles observées au cours du SDRA. La phagocytose permet l'élimination des pathogènes par des mécanismes oxydatifs et non oxydatifs (36). Elle active d'une part le système *NADPH oxydase* générant une large quantité de ROS, agissant en puissants microbicides. D'autre part, elle implique la libération de granules protéolytiques, contenant des peptides antibactériens (défensines, cathélicidines, etc...), et des protéases (myélopéroxydase, sérine protéase, élastases, etc...) permettant la dégradation du micro-organisme dans le phagolysosome. Parallèlement, des formations riches en contenu nucléaire (ADN et histone) et granulaire (protéases), les NETs sont libérés en extracellulaire pour former un réseau fibrillaire neutralisant les bactéries, puis dégradant les facteurs de virulence bactériens par l'action protéolytiques des protéases qu'ils contiennent, et entraînant *in fine* la mort bactérienne (37). Longtemps considéré comme un mécanisme de mort cellulaire suicide du PMN, il existe aussi une forme de Nétose, n'impliquant pas la mort du PMN (38). La fonction du PMN est parfois dichotomique, avec un choix nécessaire entre phagocytose et Nétose. Ainsi, les situations d'échec de la phagocytose pourraient précipiter le PMN vers la Nétose (39). Parallèlement, les macrophages alvéolaires modulent la réponse inflammatoire en participant à la clairance des PMNs apoptotiques (40).

L'afflux massif de PMNs sur le site pulmonaire est une marque de fabrique de la pneumopathie et du SDRA secondaire, et son intensité est corrélée au pronostic (41). La persistance de PMNs sur le site agressé pourrait être rendu possible par une **apoptose retardée** de ceux-ci, allongeant ainsi leur durée de vie. L'importance de ce phénomène est corrélée au pronostic au cours du SDRA (42).

La compréhension de la physiopathologie du sepsis pulmonaire implique aussi de prendre en compte le concept de **compartimentalisation de la réponse inflammatoire**. Il traduit les variations qualitatives et quantitatives de la réponse inflammatoire selon que l'on considère le compartiment pulmonaire ou systémique. Souvent, cette réponse est plus intense sur le site pulmonaire infecté, qu'au niveau systémique, ou encore au niveau du poumon infecté, en comparaison au poumon controlatéral en cas de pneumopathie unilatérale (43,44). Cette compartmentalisation pourrait être le reflet d'un gradient de cytokines inflammatoires (en particulier d'IL-8), avec des concentrations plus fortes sur les lieux de l'agression bactérienne, permettant d'y recruter les PMNs. Peu de données existent sur la régulation de ce gradient, en particulier à un stade plus tardif de l'infection, ou en cas de résolution de la réponse inflammatoire. Les modalités de cette compartmentalisation semblent

associées au devenir des patients infectés. En effet, des auteurs ont retrouvé chez des patients présentant une PAC sévère, en comparaison à ceux présentant une PAC non sévère, une réponse inflammatoire plus intense au niveau systémique (plasma) et moins intense au niveau respiratoire (concentrations cytokiniques dans les crachats) (45).

1.1.3 Stratégies thérapeutiques au cours de la PAC: passé, présent, (futur ?)

L'antibiothérapie est le traitement de référence de la PAC, qui a permis durant ces dernières décennies de faire chuter drastiquement la mortalité associée aux PAC. Malgré cette avancée majeure, mais aussi les progrès effectués dans le domaine de la vaccination des populations à risque, et celui des soins de support en réanimation, il demeure une mortalité incompressible qui impose de trouver de nouvelles thérapies adjuvantes à l'antibiothérapie.

La réponse immunitaire, et en particulier les déterminants de la réponse inflammatoire, se sont rapidement montrés être des cibles prometteuses, sur la base de données pré-cliniques. Néanmoins, force est de constater que pas moins de 150 études évaluant pour la majorité des stratégies anti-inflammatoires dans le sepsis/choc septique, n'ont pas permis de démontrer de bénéfice sur la survie (46), en sachant que la majorité des patients considérés dans ces études présentaient une pneumopathie.

Pour autant, plusieurs stratégies anti-inflammatoires sont toujours investiguées au cours du sepsis et en particulier de la PAC :

- Pour exemple, suite aux résultats de plusieurs méta-analyses mettant en évidence un possible effet bénéfique de la corticothérapie sur la survie et la stabilité clinique au cours des PAC sévères (47), 2 essais cliniques de phase III, randomisés contre placebo, investiguent actuellement l'effet de la corticothérapie comme thérapie adjuvante à l'antibiothérapie au cours de la PAC sévère : essai CAP-CODE (NCT02517489) et essai ESCAPe (NCT01283009).
- Par leur propriétés anti-inflammatoires et antimicrobiennes, les statines font toujours l'objet de travaux au cours de la PAC. Des études rétrospectives ont montré que l'utilisation préalable de statines était associée à une réduction du risque de survenue d'une PAC et d'une amélioration du pronostic en cas de survenue d'une PAC. Néanmoins, les essais thérapeutiques randomisés contrôlés contre placebo n'ont pas permis de mettre en évidence un effet sur la survie (48).
- En dehors de leur effet antibiotique, les macrolides ont des propriétés immunomodulatrices et des données rétrospectives montrent que leur utilisation en association à une β-lactamine pourrait être associée à une meilleur devenir, même si l'ensemble des essais randomisés sur

le sujet n'a pas permis de mettre en évidence un bénéfice sur la survie, en association à une β -lactamine (49).

1.2 Altérations immunitaires et d'organes au cours du sepsis : rôle des mitochondries ?

1.2.1 Altérations immunitaires au cours du sepsis et perspectives thérapeutiques immunostimulatrices.

Si la phase initiale d'un sepsis est caractérisée par une réponse immune inflammatoire parfois intense, elle laisse rapidement place à une réponse anti-inflammatoire compensatrice, créant un véritable état d'immunodépression tout aussi intense, et qui serait responsable d'une morbi-mortalité en lien avec des infections secondaires ou d'autres complications (50). L'agression infectieuse induit des altérations quantitatives et fonctionnelles de l'ensemble des cellules de l'immunité innée et adaptative, incluant (33,50,51) (Figure 3):

- Désactivation des monocytes (diminution de l'expression d'HLA-DR),
- Apoptose de l'ensemble des cellules immunes (en particulier les lymphocytes T),
- Expansion des lymphocytes T régulateurs,
- Diminution du chimiotactisme des PMNs (52,53) et de la production de ROS,
- Immaturité des cellules myéloïdes.

L'apoptose des cellules immunitaire est un phénomène capital. Pour exemple, un neutrophile apoptotique perd ses fonctions de sécrétion de cytokine, ses capacités chimiotactiques, de phagocytose, de burst oxydatif et de dégranulation (54).

Parmi les conséquences de ces altérations immunitaires induites par le sepsis, une altération de la clairance microbienne lors de l'épisode septique initial, des réactivations virales ou la survenue d'infections secondaires (50). Il serait néanmoins réducteur de penser que ces 2 phases, hyper et hypoinflammatoire, se suivent, certaines altérations immunitaires survenant parfois très précocement et chevauchant la phase hyper-inflammatoire.

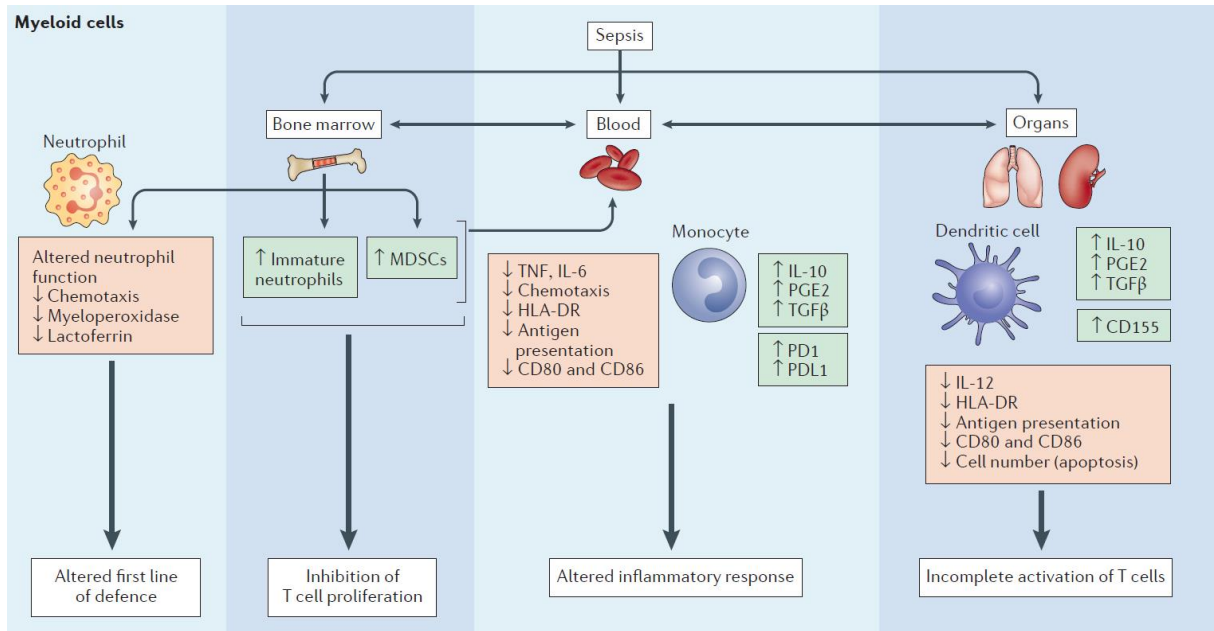


Figure 3. Altérations de la réponse immunitaire innée au cours du sepsis. Exemple des cellules myéloïdes. D'après Venet et al. (51)

Parmi les déterminants de ces altérations immunitaires, l'on peut citer le rôle de l'infection virale préalable, et l'impact des facteurs de virulence bactériens. Une des situations les mieux décrites est la survenue d'une grippe compliquée d'une PAC à *S.p.* (55). L'infection virale préalable compromet l'intégrité de la barrière immunitaire muqueuse en entraînant l'apoptose des cellules épithéliales et des macrophages alvéolaires au cours de la réplication virale. Parallèlement, l'activité ciliaire et la production de surfactant par les pneumocytes de type II sont altérées. Les facteurs de virulence viraux (comme la neuraminidase virale) exposent les récepteurs du pneumocoque en clivant les acides sialiques. Enfin, la production d'interféron de type I à visée antivirale altère les fonctions phagocytaires des macrophages alvéolaires et des neutrophiles, limitant ainsi la clairance bactérienne et facilitant l'invasion (29,55). Par ailleurs, *Streptococcus pneumoniae* possède un arsenal de facteurs de virulence, capables de compromettre l'efficacité de la réponse immunitaire de l'hôte (Tableau 2).

Facteurs de virulence	Mécanismes d'échappement du système immunitaire
Capsule polysaccharidique	Facilite la pénétration dans le mucus Résistance à la phagocytose par les macrophages alvéolaires
Pneumolysine	Résiste à la clairance muqueuse Paralysie ciliaire Altération du burst oxydatif Lyse des cellules de l'hôte, en particulier immunitaires et épithéliales
Pili	Inhibition de la phagocytose
Protéases IgA	Inhibition de la réponse immune muqueuse IgA médiée
DNases	Clive l'ADN bactérien Clive les NETs (Neutrophil Extracellular Traps)
Pneumococcal protein A et C surface	Altère la maturation des cellules dendritiques Diminution de la réponse cellulaire T

Tableau 2. Facteurs de virulence de *Streptococcus pneumoniae* capables de compromettre la réponse immune au cours de la colonisation ou de l'invasion bactérienne (d'après Grousd et al., Van der Poll et al. (24,56)).

Au cours du sepsis, ces découvertes ont ouvert de nouvelles pistes thérapeutiques immuno-stimulatrices, adjuvantes de l'antibiothérapie. Elles ciblent essentiellement les lymphocytes (anti-PD1/PDL1, interleukine 7), ou les cellules myéloïdes (Interféron γ) (50,57). Néanmoins, si ces altérations, aussi complexes qu'elles soient, sont de mieux en mieux décrites, l'impact de leurs corrections sur le pronostic des patients reste incertain.

D'autre part, certains auteurs avancent l'idée selon laquelle une approche thérapeutique personnalisée (concept de théranostique) est nécessaire pour sélectionner les patients véritablement susceptibles de bénéficier de telles thérapies ciblant la réponse immune. En effet, une hétérogénéité importante a été identifiée. Ainsi, les réponses transcriptionnelles évaluées chez les leucocytes circulants des patients septiques sont très variables selon les individus, certains ayant plutôt des profils « hyper-inflammatoires », quand d'autres sont jugés plutôt « hypo-inflammatoires » (58,59). Pour preuve, dans une analyse ancillaire de l'essai VANISH évaluant notamment l'intérêt de la corticothérapie au cours du sepsis, la classification à posteriori des patients selon leur profil hypo ou hyperinflammatoire, prédisait la réponse aux corticoïdes. Ainsi, les patients ayant un phénotype qualifié d'« immunocompétent» avait une moins bonne survie que les autres (60). C'est pourquoi une

meilleure caractérisation de la réponse immunitaire des patients (« immune-profiling »), pourrait permettre de personnaliser la prise en charge des patients afin de proposer des thérapies adjuvantes immunomodulatrices ciblées (33,51,61).

Cependant, les mécanismes cellulaires et moléculaires qui concourent à ces altérations immunes sont peu connus. Il est important de les explorer car ils pourraient ouvrir un champ nouveau d'investigation et la découverte de nouveaux biomarqueurs susceptibles d'aiguiller les thérapies ciblées. Des travaux récents suggèrent notamment le rôle de l'altération des fonctions métaboliques des cellules immunitaires dans le déterminisme de leur réponse antimicrobienne (62,51).

1.2.2 Rôle des mitochondries dans la réponse immunitaire innée

1.2.2.1 Mitochondries : origine, structure, fonctions

Les mitochondries sont des organites intracellulaires qui dériveraient de l'endosymbiose d'une α -protéobactérie *Rickettsia prowazekii*, par une cellule eucaryote, il y a 1,5 billion d'années (63). Pour preuve, l'ADN mitochondrial (ADNmt), a des caractéristiques très proches de l'ADN bactérien (64) (65). Le rôle des mitochondries dans la réponse immunitaire fait l'objet de nombreux travaux de recherche, étant donné leur rôle majeur dans le métabolisme cellulaire, et leur capacité à alerter le système immunitaire au cours d'agressions diverses et notamment infectieuses (66).

Le nombre de mitochondries par cellule varie fortement d'un type cellulaire à un autre, et d'une situation à une autre (besoin énergétiques différents), avec environ 200 à 2000 mitochondries par cellule. Les mitochondries sont en mouvement dans la cellules et subissent des phénomènes de fusion et de fission, eux même sous une régulation étroite (67).

La mitochondrie comprend plusieurs compartiments (Figure 4):

- **La matrice** qui correspond au compartiment interne de la mitochondrie, siège de nombreuses voies métaboliques dont le cycle de Krebs ou l'oxydation des acides gras. Elle renferme aussi l'ADN mitochondrial.
- **La membrane externe** constituée d'une bicouche lipidique, perméable grâce à une protéine transmembranaire, VDAC (Voltage-Dependant Anion Channel).
- **La membrane interne**, riche en protéines, qui comprend de nombreux replis formant les crêtes mitochondrielles. Sa composition lipidique particulière, riche en cardiolipine, détermine un potentiel électrochimique via le transport des électrons pour la synthèse d'ATP.
- **L'espace intermembranaire** qui contient une forte quantité de protons accumulé par la chaîne respiratoire

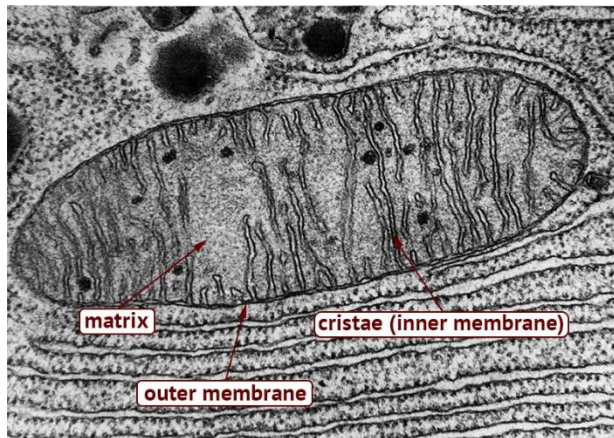


Figure 4. Mitochondrie visualisée par microscopie électronique à transmission. Image issue de <https://www.philpoteducation.com/mod/book/view.php?id=805&chapterid=1076#/>.

1.2.2.2 Mitochondrie et réponse immunitaire innée

Les mitochondries permettent d'initier, d'amplifier et de réguler la réponse immunitaire innée. Cela passe par la libération de médiateurs jouant le rôle de signal de Danger (les alarmines mitochondrielles), par le relargage de ROS aux actions microbicides, et par une complexe régulation de la fonction des cellules immunitaires dont les mécanismes permettant la résolution de la réponse inflammatoire.

1.2.2.2.1 Les alarmines mitochondrielles

Le modèle « du danger » a été développé par Polly Matzinger pour rendre compte aussi bien des éléments qui déclenchent une réponse immunitaire, que de ceux qui permettent un état de tolérance (68,69). Une version récente du modèle implique fortement la réponse immunitaire innée et suggère qu'au cours de l'évolution, les tissus ont acquis la capacité d'envoyer des signaux de détresse lorsqu'ils étaient altérés ou agressés. Au cours de traumatismes sévères, un tableau clinique semblable à celui d'une infection avec de la fièvre, associés à une réponse immunitaire (production cytokinique, chimiotactisme et activation des neutrophiles...) est décrit (65,70). Cette réponse immunitaire « stérile » est attribuée à la libération de DAMPs, comprenant des protéines intracytoplasmiques (HMGB1, protéines du choc thermique HSP, protéines S100), mais aussi des molécules d'origines mitochondrielles (ADNmt, ATP (adénosine triphosphate), fMLP (N-formyl-L-methionyl-L-leucyl-phenylalanine)) et d'autres molécules (65,70).

Ces molécules mitochondrielles rappellent l'origine commune avec les bactéries, puisque 1) l'ADNmt est circulaire, non méthylé, et arborant des motifs CpG, tout comme l'ADN bactérien, et ainsi reconnu par le même récepteur endosomal TLR-9, 2) l'ATP mitochondrial, tout comme l'ATP bactérien,

active l'inflammasome NLRP3 (NOD-like receptor family, pyrin domain containing et 3) le fMLP mitochondrial, qui a aussi une origine bactérienne, active le chimiotactisme des neutrophiles via son récepteur membranaire FPR (formyl peptide receptor) (Figure 5) (66,71,72).

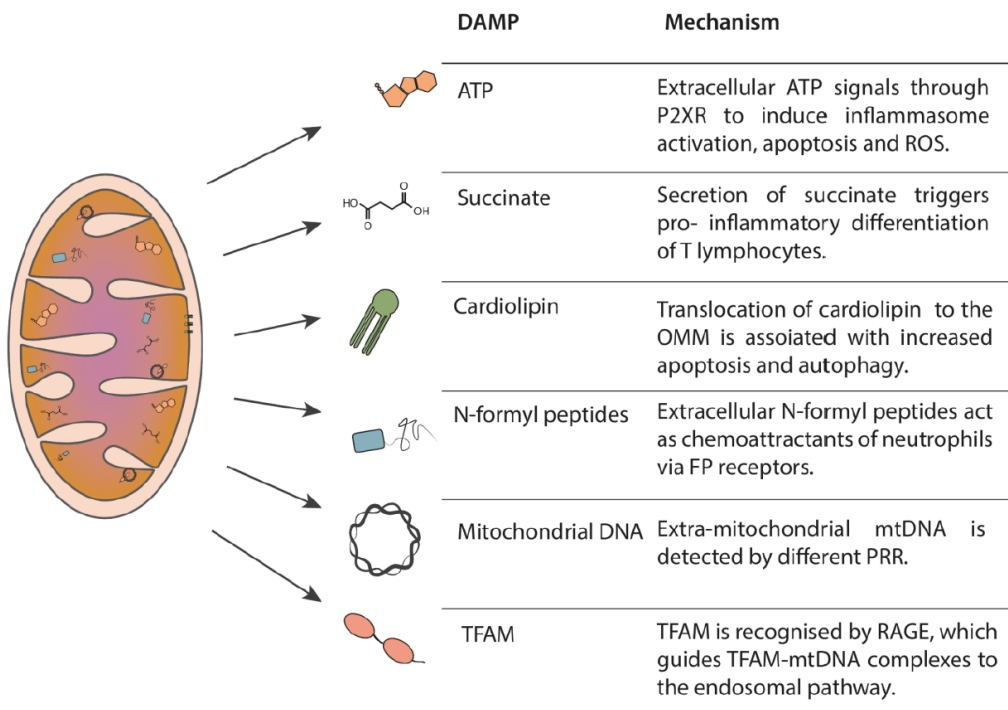


Figure 5. Alarmes mitochondrielles. D'après Rodriguez-Nuevo (73).

➤ ADN mitochondrial

Une mitochondrie contient plusieurs copies d'ADN mitochondrial, circulaire, qui représente moins de 1% de l'ADN total de la cellule. Si l'ADNmt code pour des certaines protéines mitochondrielles impliquées dans la chaîne respiratoire (NADH-déshydrogénase, ubiquinone cytochrome b réductase, cytochrome c oxydase et ATP synthase), la plupart des protéines mitochondrielles sont codées par le génome nucléaire. Lorsqu'il se situe en situation cytoplasmique, l'ADNmt est capable de déclencher une réponse inflammatoire, qui semble impliquée dans la physiopathologique de nombreuses situations d'inflammation stérile comme l'ischémie-reperfusion, les traumatismes sévères (Crush syndrome ...), le cancer, mais aussi dans celle des infections (65,72,74).

Les mécanismes conduisant à la libération d'ADNmt au niveau cytoplasmique ou extracellulaire sont probablement partiellement connus. Les mieux décrits sont :

- Au cours de la nécrose cellulaire, par la rupture incontrôlée des membranes libérant le contenu intracellulaire dans la circulation, dont l'ADN mitochondrial (65).
- A cours de l'apoptose ou d'autres stress mitochondriaux, par l'activation des pores de perméabilité membranaires (PPM) (75,76).

- Au cours de la Nétose, les PMNs libérant de l'ADN nucléaire, mais aussi de l'ADN mitochondrial pour former les Neutrophil Extracellular Traps (NETs) qui vont permettre la clairance bactérienne (77).
- Lors de l'accumulation de mitochondries défectueuses. Un défaut d'activation ou un dépassement de la mitophagie, est associée à la libération d'ADNmt cytosolique (78).

L'ADNmt en position extracellulaire ou cytoplasmique, est capable d'activer 3 voies distinctes dont (Figure 6):

➔ **La voie TLR-9**

Il s'agit du principal récepteur de l'ADNmt. Puisqu'il est localisé au niveau endosomal, son activation requiert que l'ADNmt présent au niveau cytoplasmique (75). L'ADNmt en position extracellulaire doit ensuite être internalisé pour atteindre sa cible endosomale, sous le contrôle de protéines chaperonnes comme HMGB1 (pour High mobility group box 1), une alarmine d'origine nucléaire, elle aussi libérée au cours des dommages cellulaires (79). La liaison à TLR-9 permet l'activation de voies de transcription des cytokines inflammatoires.

➔ **L'inflammasome NLRP3**

Les dysfonctions de la chaîne respiratoire mitochondriale sont responsables d'un relargage d'ADNmt, mais aussi d'une production de ROS. L'ADNmt ne comprenant pas d'histones, il ne peut être compacté, et est de ce fait plus vulnérable vis-à-vis du stress oxydatif. Par ailleurs, plusieurs mécanismes capables de réparer l'ADN nucléaire, ne sont pas actifs sur l'ADN mitochondrial (80). Ainsi, ce stress oxydatif est capable de produire des dommages de l'ADNmt : modifications de bases, cassures simple ou double brin, voire délétions parfois étendues (81). Ainsi, l'ADNmt oxydé peut ainsi être relargué dans le cytosol, et alors susceptible d'activer l'inflammasome NLRP3 (82).

De plus, l'accumulation de dommages de l'ADNmt (délétions), va également entraîner la perte de certains gènes d'où une possible dysfonction mitochondriale, pouvant conduire à la mort cellulaire (80).

Ces phénomènes ont bien été décrits au cours de certaines maladies chroniques. Ainsi, certaines délétions sont associées à des maladies neuro-musculaires rares, tandis que d'autres, plus fréquentes (une délétion de 4988 paires de bases par exemple), sont associées à la survenue de certains cancers ou de maladies cardio-vasculaires (80,81).

Afin de se protéger contre ces phénomènes, l'autophagie est capable de prévenir le transfert d'ADNmt dans le cytoplasme, en entraînant le recyclage des mitochondries défectueuses, et ainsi de limiter l'activation de l'inflammasome NLRP3 (78).

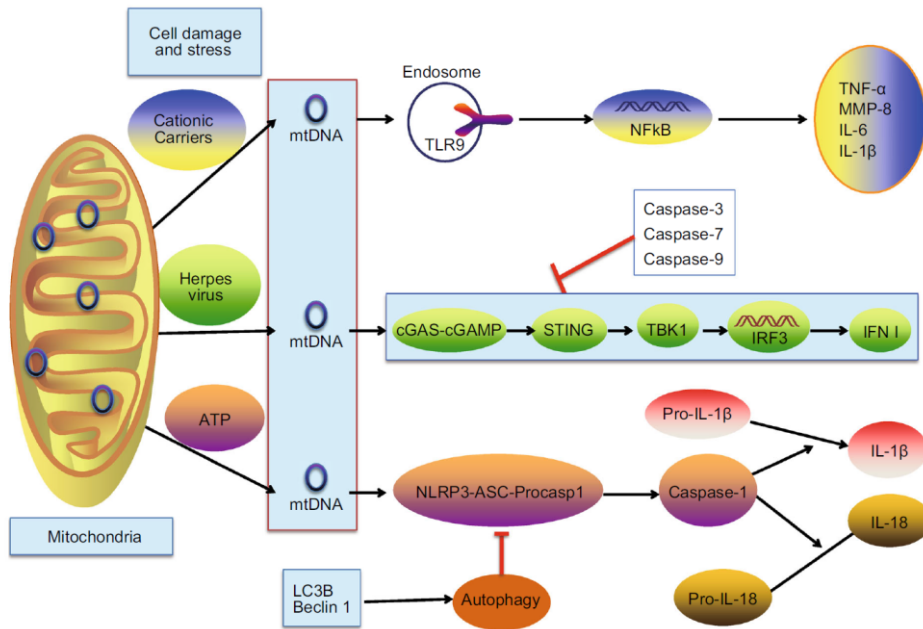


Figure 6. Reconnaissance de l'ADNmt circulant et activation de la réponse immunitaire innée. D'après Fang et al. (71).

→ Données obtenues au cours du sepsis

Plusieurs modèles précliniques montrent qu'il existe une **augmentation des concentrations d'ADNmt dans le plasma** au cours du sepsis (83). Cependant les données cliniques sont plus contradictoires. En effet, Krychtiuk *et al* observaient une élévation des concentrations d'ADNmt dans le plasma de patients admis en soins intensifs, ces concentrations étant prédictives du pronostic (84). Timmermans et al, ont aussi retrouvé une élévation des concentrations d'ADNmt chez des patients en choc septique, en comparaison à des contrôles sains, mais sans corrélation au pronostic (85). A l'inverse, Puskarich et al ne retrouvaient aucune différence en termes de concentrations d'ADNmt plasmatiques entre des patients septiques et des contrôles sains, mais il existait une corrélation avec la sévérité dans la mesure où ceux en choc septique avaient des concentrations d'ADNmt circulantes inférieures aux autres (86). Ces données cliniques contradictoires soulèvent certaines questions. Il serait nécessaire : (i) de mieux comprendre les mécanismes qui régulent la libération extracellulaire d'ADNmt au cours du sepsis ; (ii) d'étudier les variations d'ADNmt circulant dans des populations plus homogènes de patients (ou dans des modèles expérimentaux), les patients admis en soins intensifs ayant souvent subi des agressions répétées, infectieuses ou traumatiques, (iii) enfin de mieux définir le moment optimal du dosage de l'ADNmt, sa libération suivant une cinétique qui reste à déterminer.

➤ **ATP mitochondrial et voies de signalisation purinergique**

Autre alarmine, l'ATP mitochondriale est aussi libérée au cours des phénomènes de nécrose ou d'apoptose, et reconnue soit directement soit après son hydrolyse sous forme d'ADP (adénosine diphosphate) par :

- Les récepteurs P2Y ET P2X permettant :
 - **Le chimiotactisme et le contrôle du gradient des PMNs vers le site de l'infection** (87,88).
 - L'agrégation plaquettaire (89).
- **L'inflamasome NLRP3**, s'activant, et permettant la maturation de la pro IL-1 β en IL-1 β (88,90).

Une augmentation des concentrations plasmatiques en ATP, particulier d'origine mitochondriale est décrite dans des modèles précliniques de sepsis. Elle serait nécessaire à l'activation des PMNs (91,92).

➤ **fMLP mitochondrial**

Le fMLP mitochondrial, comme le fMLP d'origine bactérienne, est reconnu par FPR1 à la surface des neutrophiles, activant leur **chimiotactisme**. Le blocage de FPR1 par un anticorps spécifique ou la ciclosporine H inhibe le chimiotactisme des neutrophiles suite à la nécrose cellulaire (88).

1.2.2.2 Fonction mitochondriale et immuno-métabolisme

➔ **Phosphorylation oxydative**

Les mitochondries contribuent à la **production de l'énergie utilisable par la cellule sous forme d'ATP**, par le biais de la **phosphorylation oxydative** (OXPHOS pour Oxydative Phosphorylation), à partir des produits du catabolisme des glucides, protéines et lipides (93,94) (Figure 7). Trois grands facteurs régulent ce qui est également appelé respiration mitochondriale : la pression d'oxygène tissulaire , la concentration en monoxyde d'azote (NO), et l'apport en ADP (95). Plusieurs étapes sont nécessaires à son fonctionnement :

- (1) Le catabolisme des glucides (glycolyse), des protéines et des lipides permettant la production de pyruvate puis d'Acétyl-CoA,
- (2) La consommation de l'Acétyl-CoA par le cycle de Krebs permettant la production de 2 principaux substrats, riche en énergie (NADH et FADH₂) et qui vont servir de source d'électrons,
- (3) la mise en jeu de la **chaine respiratoire** proprement dite, associant des complexes protéiques accepteurs d'électrons au sein de la membrane interne de la mitochondrie, va

utiliser l'énergie de NADH et FADH₂, sous forme de transferts d'électrons, créant ainsi un gradient transmembranaire de protons. Une chaîne de réactions d'oxydoréduction reposant sur 4 complexes est mise en jeu (complexe I : NADH-ubiquinone réductase, II : succinate-UQ réductase, III : UQH₂-cytochrome c réductase, IV : cytochrome oxydase), permettant la création du **potentiel de membrane mitochondrial**, en transférant des protons (H⁺) de la matrice vers l'espace intermembranaire. L'énergie résultant de la génération de ce gradient de protons est ensuite utilisée par un 5^{ème} complexe (V : ATP synthase), pour assurer la phosphorylation de l'ADP en ATP. Les électrons de basses énergies libérés à la fin de la chaîne respiratoire réagiront ainsi avec les molécules d'oxygène et les protons présents dans la matrice mitochondriale afin de former des molécules d'eau.

En situation d'anaérobiose, une autre voie, appelée fermentation, transforme directement le pyruvate en lactate (**fermentation lactique**).

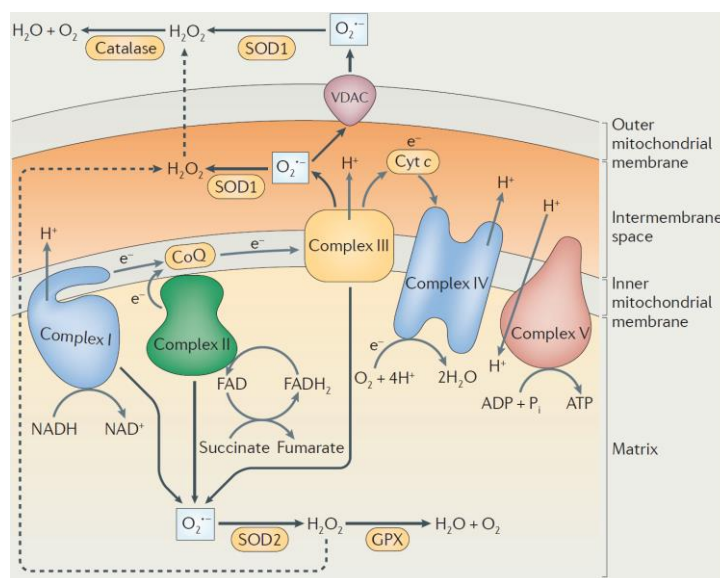


Figure 7. Chaîne respiratoire mitochondriale : complexes impliqués dans la génération d'un gradient de protons (I-IV), la production d'ATP (V) et de ROS. D'après West et al (96).

Les modèles précliniques et des études cliniques montrent qu'il existe une **altération de la respiration mitochondriale au cours du sepsis sévère et choc septique dans l'ensemble des cellules immunitaires** circulantes dont les lymphocytes (97,98), les monocytes (99), ou les leucocytes résidants sur le site infecté (100). Ces altérations se traduisent par une chute du ΔΨm (100), qui s'associe à une altération de leur fonction. Pour exemple, la chute du ΔΨm des PMNs, suite à une stimulation bactérienne ou par le LPS, diminue le chimiotactisme et le burst oxydatif de ceux-ci (101–103).

Ces défauts de l'homéostasie mitochondriale pourraient donc contribuer aux altérations immunitaires observées au cours du sepsis.

→ Immunométabolisme

L'immunométabolisme s'intéresse aux interactions étroites qui existent entre métabolisme et fonctions immunitaires. Ainsi, l'adaptation des cellules immunitaires aux variations de leur environnement en termes de substrats énergétiques et d'oxygène pourrait contribuer à la nature de leur réponse immune à l'agression (i.e., polarisation inflammatoire ou anti-inflammatoire), et vice versa. Ainsi par exemple, l'activation des cellules immunitaires augmente leur demande en nutriments. Par exemple, la prolifération lymphocytaire, ou la présentation d'antigène par les cellules myéloïdes implique notamment l'augmentation de la production d'acides gras et/ou d'acides nucléiques, en raison notamment de l'activation de la transcription de nombreux gènes (104).

Des données expérimentales et cliniques suggèrent qu'il existe ainsi **une reprogrammation métabolique de la production d'énergie** par les leucocytes dans certaines situations, et notamment en cas de stimulation par des produits microbiens. Ce phénomène nommé « **effet Warburg** », initialement décrit au cours du cancer, est aussi retrouvé au cours des situations de stress infectieux. Il s'agit, en contexte d'**aérobiose**, d'un **switch de la phosphorylation oxydative vers la glycolyse anaérobie, suivie d'une fermentation lactique dans le cytosol**, afin de produire directement et donc très rapidement de l'ATP indispensable au déclenchement de l'activation immune initiale de l'hôte (62,104) (Figure 8). A l'inverse, l'immunotolérance des leucocytes induite par un sepsis (i.e., situations d'immuno-paralysie), est associée à des dysfonctionnements métaboliques, touchant à la fois la glycolyse et la phosphorylation oxydative (Figure 8). Ces altérations sont réversibles, spontanément après la résolution du sepsis, ou bien partiellement sous l'effet d'un traitement par l'interféron- γ (62).

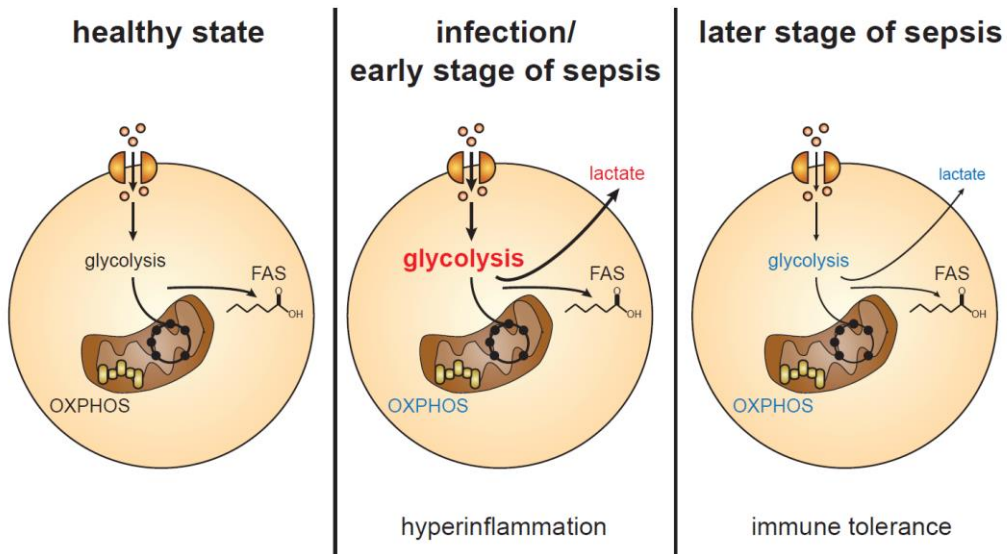


Figure 8. Reprogrammation métabolique au cours du sepsis. En phase initiale, l'effet Warburg est observé au niveau des cellules immunitaire en situation d'anaérobiose, avec un switch du métabolisme de la phosphorylation oxydative à faible glycolyse, vers une glycolyse accrue et une fermentation lactique pour produire l'ATP. A une phase plus tardive, la glycolyse est down-régulée, avec pour conséquence une diminution de la production d'ATP et une diminution des fonctions cellulaires (phase d'immuno-tolérance). D'après Sienstra et al. (104).

Outre son implication dans le déclenchement de l'immunité innée et la régulation de son intensité, le métabolisme énergétique intervient aussi, par des mécanismes de régulation épigénétique, dans la capacité de la réponse immunitaire à garder en mémoire les caractéristiques d'une stimulation antigénique antérieure, afin de lui permettre de s'adapter plus rapidement et efficacement en cas de nouvelle agression, par une réponse non spécifique. L'on parle de « **trained immunity** » ou d'immunité mémoire innée (105).

1.2.2.2.3 Espèces réactives de l'oxygène

Une des conséquences du transport d'électrons à travers les complexes de la phosphorylation oxydative mitochondriale, est la production des « Reactive Oxygen Species » (ROS) (Figure 7). Les mitochondries représentent ainsi la principale source de ROS, molécules produites par réaction entre l'oxygène et une petite proportion d'électrons échappant aux complexes I et III de la chaîne respiratoire mitochondriale (66). L'autre source de ROS est le système NADPH oxydase. Ces espèces oxygénées activées ont différentes fonctions :

- En situation physiologique, les ROS contribuent à la régulation de différentes fonctions cellulaires :

- **Contrôle de l'apoptose**, par un contrôle de la surcharge calcique et de la perméabilité membranaire mitochondriale.
 - **Signalisation cellulaire**, les ROS activant certaines voies de la transcription et activant la prolifération cellulaire.
- En situation de stress infectieux, les ROS interviennent dans la défense antimicrobienne (96):
- **Soit directement, en participant à la lyse bactérienne** au sein des phagocytes (macrophages et PMNs) qui les produisent, créant un environnement oxydatif (burst oxydatif) permettant la destruction des bactéries. L'anion superoxyde (O_2^-) est la principale espèce radicale, pouvant conduire à la production de ROS plus agressives : peroxyde d'hydrogène (H_2O_2), monoxyde d'azote ($^{\circ}NO$), peroxynitrite ($ONOO^-$) ou encore l'ion hypochlorite (ClO^-), contenu dans la solution de Dakin.
 - **Soit indirectement, en activant les voies de signalisation pro-inflammatoires que sont NF-κB** (nuclear factor- κB) et MAPK (Mitogen-activated protein kinase), ou encore **l'inflamasome NLRP3**.

Un puissant système de détoxification composé d'enzymes (superoxyde dismutase, catalase, glutathion peroxydase...), et de protéines chaperonnes ou autres (vitamines C et E), permet d'éviter tout stress oxydant en situation basale.

Lorsqu'ils sont produits en excès, par exemple en situation de diminution de la pression tissulaire en oxygène, les ROS peuvent dépasser les capacités de ce système de détoxification (balance redox déséquilibrée), et réagir avec les protéines, lipides et l'ADN de la cellule (nucléaire mais surtout mitochondrial), entraînant des dysfonctions et/ou la mort cellulaire. Une des conséquences de ces phénomènes est la chute du $\Delta\psi_m$, l'inhibition de la chaîne respiratoire mitochondriale et le relargage de signaux pro-apoptotiques activant les caspases à l'origine de l'apoptose (106).

1.2.2.2.4 Apoptose mitochondriale

Les mitochondries contrôlent la voie intrinsèque de l'apoptose cellulaire, elle-même contrôlée par différents facteurs (concentrations en ROS et dommages oxydatifs de l'ADN, calcium, céramide...). La formation de pores de transition de perméabilité dans la membrane mitochondriale externe, s'accompagne d'une diminution du $\Delta\psi_m$, suivi du gonflement de la matrice mitochondriale, d'une interruption du métabolisme énergétique aérobie et d'un stress oxydatif. Il s'ensuit une libération dans le cytosol, du cytochrome c, qui conduit à l'activation des caspases (Figure 9). L'intégrité de la membrane mitochondriale externe est sous le contrôle de protéines appartenant à la superfamille de la protéine B cell lymphoma 2 (Bcl-2).

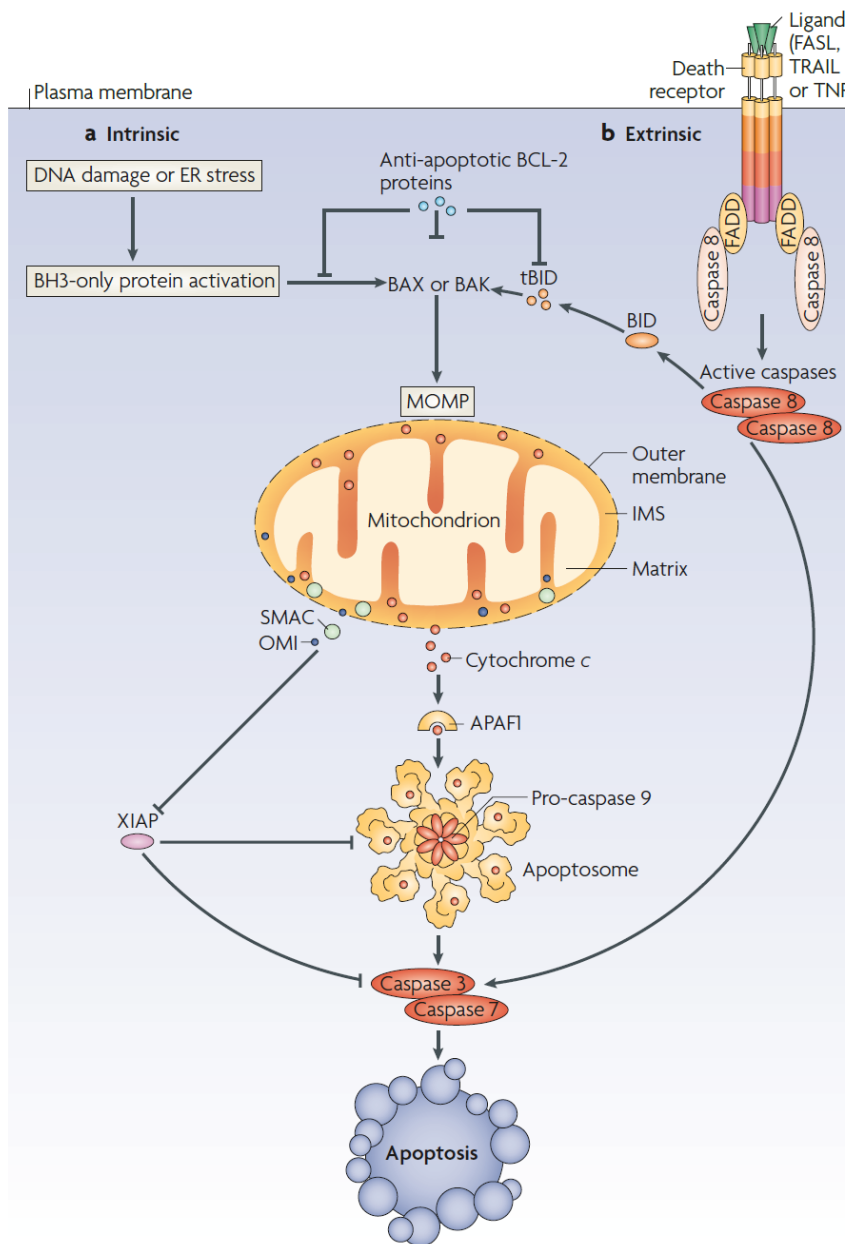


Figure 9. Apoptose via la voie intrinsèque, déclenchée par différent stimuli comme les dommages de l'ADN, ou le stress du réticulum endoplasmique (RE). D'après Tait et al. (107)

Parmi les altérations de la réponse immune au cours du sepsis, l'apoptose représente un événement capital, décrit comme capable de réguler et de limiter une réponse inflammatoire trop intense, mais pouvant concourir à la survenue d'une immunodépression secondaire délétère si elle est excessive et dérégulée (50). Il semble qu'à la fois la voie intrinsèque mitochondriale, mais aussi la voie extrinsèque, soient impliquées, expliquant en partie la lymphopénie post septique (50,108). Ainsi, les cellules lymphocytaire en cours d'apoptose présentent un phénotype marqué par une diminution de l'expression du complexe majeur d'histocompatibilité (CMH) de classe II et une augmentation de la production en IL-10 (phénotype « T-cell exhaustion ») (109).

Cependant, le rôle de l'apoptose mitochondriale dans la survenue de ces altérations immunes est encore imparfaitement compris. Et à l'inverse, le défaut d'apoptose observé au cours du sepsis chez certaines cellules immunes comme les PMNs, pourrait être délétère pour l'hôte, comme cela a été décrit au cours du SDRA. Le rôle de l'apoptose mitochondriale dans ces phénomènes reste méconnu.

1.2.2.2.5 Contrôle qualité mitochondriale et régulation de la réponse immune

Les mitochondries étant au cœur de la régulation de certains aspects de la réponse immune comme cela vient d'être décrit, en plus de ses fonctions clé dans le métabolisme énergétique, un contrôle de la qualité et de l'homéostasie mitochondriale est indispensable au bon fonctionnement de la cellule.

La régulation de l'homéostasie mitochondriale, est le fruit d'une balance entre plusieurs mécanismes régulateurs : le turnover des mitochondries par la mitophagie, la biogénèse mitochondriale, et la fission et fusion mitochondrielles (110) (Figure 10).

- ➔ La mitophagie est l'autophagie sélective des mitochondries. Son rôle est de surveiller les populations mitochondrielles et d'éliminer les mitochondries « superflues » ou endommagées, permettant de réguler la survie et la fonction cellulaire en réponse à un stress, traumatique ou infectieux par exemple (111). Elle implique une machinerie moléculaire permettant la fusion de la mitochondrie défectueuse avec un phagophore, formant l'autophagosome, qui lui-même va fusionner avec le lysosome contenant un milieu acide et riche en enzymes protéolytiques qui vont permettre la dégradation. La mitophagie est régulée par plusieurs voies dont le couple de protéines PINK1 (PTEN-induced putative kinase 1)/parkin qui est recruté dans la membrane mitochondriale externe en réponse à une chute du $\Delta\Psi_m$ (111). En plus de l'élimination sélective des mitochondries endommagées, elle permet aussi d'ajuster le nombre de mitochondries (pool mitochondrial) aux besoins métaboliques (112).
- ➔ La biogénèse mitochondriale permet de contrôler la masse (nombre et taille des mitochondries) ainsi que la fonction mitochondriale, en particulier en augmentant et augmentant la production de protéines mitochondrielles, d'enzymes de la glycolyse et facilitant ainsi la phosphorylation oxydative. Ce processus est médié par PGC1 α (peroxysome-proliferator-activated receptor γ coactivator 1 α) qui active les facteurs de transcription NRF1 et NRF2 (nuclear respiratory factors 1 et 2). Les protéines NRF1 et 2 augmentent l'expression de TFAM (transcription factor A for the mitochondrion) qui active à son tour la transcription

de l'ADNmt et ainsi la production de protéines mitochondrielles nécessaires à l'activité de la chaîne respiratoire (110).

→ La fusion et fission permet l'organisation du réseau mitochondrial au sein de la cellule. Les mitochondries fusionnent et fissionnent continuellement et l'équilibre entre les 2 mécanismes conditionne la dynamique et la fonction mitochondriale (113). Par exemple, un déficit en protéines qui contrôlent la fusion (Mitofusin-2), ou de la fission (DRP-1), est associé à une altération du $\Delta \Psi m$ et à une diminution de la consommation en oxygène (114). Il existe une étroite coopération entre ces mécanismes. La fission isole les mitochondries dépolarisées et inhibe le processus de fusion, afin de prévenir la réintégration dans le réseau de mitochondries dysfonctionnantes, facilitant ensuite leur mitophagie (113).

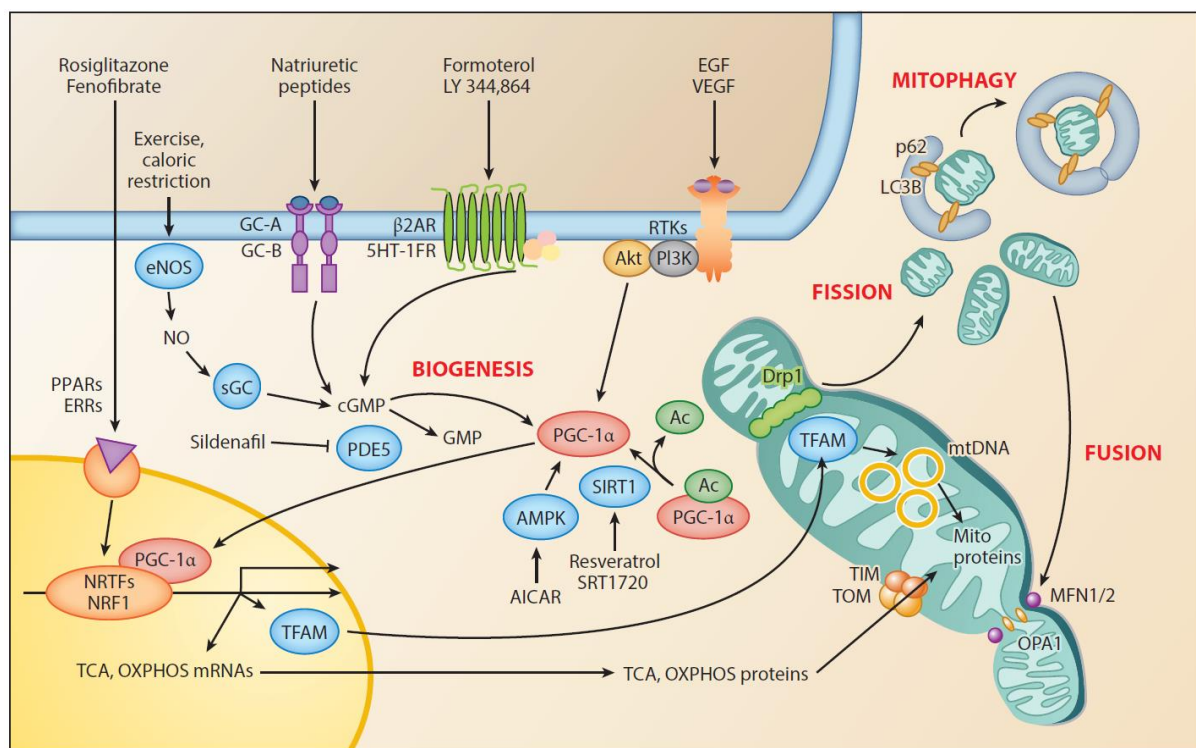


Figure 10. Régulation de l'homéostasie mitochondriale. D'après Whitaker et al. (110).

Une altération de la biogénèse mitochondriale est observée précocement (J1) dans les cellules mononucléées circulantes de patients septiques. Elle s'associe à une chute du nombre de copies d'ADN mitochondrial intracellulaire, et à une augmentation des concentrations d'ADN mitochondrial plasmatiques. Dans cette même étude, une restauration de l'activation transcriptionnelle de la biogénèse et du pool mitochondrial était décrite dès J5, et de façon plus précoce chez les patients septiques ayant le meilleur pronostic (115).

Les données cliniques relatives à la mitophagie dans les cellules immunes au cours du sepsis sont en revanche quasi inexistantes.

1.2.3 Dysfonction mitochondriale et dysfonctions d'organe au cours du sepsis

La physiopathologie de la dysfonction d'organe au cours du sepsis est complexe et probablement mal comprise (116). **Le défaut d'oxygénation des tissus** apparaît comme un évènement clé. Les anomalies macrocirculatoires (e.g., débit cardiaque insuffisant, diminution de la pression artérielle altérant sa distribution) susceptibles de réduire le transport de l'O₂, ou du moins de le rendre inadéquate vis-à-vis de la demande tissulaire, contribuent largement à ce phénomène. Il est néanmoins intéressant de remarquer que des dysfonctions d'organe peuvent aussi survenir en l'absence d'altération significative de la macrocirculation (114). C'est pourquoi on parle alors de choc microcirculatoire. Il en résulte une hyperlactatémie qui contraste avec des marqueurs de transport en oxygène normaux, voire supranormaux (e.g., ScVO₂ supérieure à 70%), témoignant en fait d'une extraction cellulaire en O₂ effondrée. Il s'agit d'un **défaut d'utilisation de l'O₂** par les cellules, aussi appelé « cellular metabolic shutdown » (117). Une agression infectieuse prolongée conduit progressivement à cette réduction de la consommation en O₂, alors qu'un rebond du métabolisme est observé au cours de la phase de récupération (117–119).

Parce que les mitochondries utilisent plus de 90% de la consommation d'oxygène totale du corps humain pour produire l'ATP, il est admis que les perturbations de la VO₂ (volume of oxygen, témoin de la consommation en oxygène) décrites au cours du sepsis sont associées à des dysfonctions mitochondrielles (120). En effet, la réponse inflammatoire systémique excessive, pourrait avoir les conséquences suivantes au niveau des différents tissus :

- (1) **Un défaut de phosphorylation oxydative mitochondriale**, par défaut d'apport en O₂ faisant suite aux troubles circulatoires.
- (2) **Une production accrue de ROS mitochondriaux**, qui inhibent la respiration mitochondriale et entraînent des dommages de l'ADN, des protéines et des lipides mitochondriaux avec pour conséquence un dysfonctionnement mitochondrial.
- (3) **Une down régulation précoce de l'expression des gènes codant pour certaines protéines mitochondrielles**. Ce phénomène fut initialement décrit chez des volontaires sains recevant une injection de LPS (121), puis confirmé chez des patients en réanimation (122).
- (4) **Des altérations hormonales** comme le syndrome de T3 basse, survenant au cours du sepsis impactent directement la fonction mitochondriale.
- (5) **Une diminution du pool mitochondrial** (119)

(6) Des anomalies ultrastructurales des mitochondries (gonflement mitochondrial...) (119,122)

Les conséquences sont un **défaut de production d'ATP mitochondrial par les tissus, entraînant une diminution du métabolisme cellulaire et de leurs fonctions**. L'intensité de ce phénomène serait corrélée au pronostic. Brealey *et al* montraient ainsi que les concentrations musculaires d'ATP étaient plus basses dans les muscles de patients septiques qui décédaient, comparativement à ceux qui survivaient, et s'associant à un défaut d'activité du complexe I (123). Il s'ensuit un remplacement de la production d'ATP, par l'activation de la glycolyse, mais ce phénomène est transitoire et insuffisant (114).

Constatation intéressante, les tissus de patients septiques conservent une histologie relativement bien préservée, en dehors de l'infiltrat cellulaire inflammatoire et de l'œdème, avec un degré de mort cellulaire relativement bas comparativement à l'intensité du stress oxydatif (124,125). Certains auteurs expliquent cela par un « shutdown » bioénergétique et métabolique (ou hibernation cellulaire). Cette phase de « shutdown », transitoire, protégerait la cellule, du stress oxydatif intense, avant le retour progressif à un niveau fonctionnel antérieur (117).

Cette phase de récupération pourrait être induite par la biogénèse mitochondriale comme l'atteste les données de Haden *et al* dans un modèle murin de sepsis à *Staphylococcus aureus* où le métabolisme cellulaire, le pool mitochondrial et l'expression des gènes mitochondriaux hépatiques sont secondairement restaurés, parallèlement à l'activation de l'expression des gènes de la biogénèse mitochondriale (PGC1 α , NRF1 et 2). Ces données ont ensuite été corroborées par Carré *et al* retrouvant que l'expression des gènes de la biogénèse mitochondriale étaient seulement augmentée chez les patients survivants, comparativement à ceux qui décèdent en situation de réanimation (122).

1.3 Ventilation mécanique et Ventilator-Induced Lung Injury

La survenue d'un SDRA au cours d'une PAC, impose le plus souvent le recours à la VM invasive. L'objectif est d'assurer les échanges gazeux, mais cela se fait au prix d'un étirement cyclique des cellules pulmonaires, ce d'autant si le volume courant (V_T) est excessif et/ou que les volumes pulmonaires sont diminués (i.e., concept de « baby lung ») ou encore que la compliance du système respiratoire est effondrée. Ce volotraumatisme génère une inflammation stérile (i.e., biotrauma) et des dommages tissulaires (i.e. Ventilator-Induced Lung Injury [VILI]), capables d'induire des dysfonctions cellulaires et de modifier la réponse immune à l'agression infectieuse (126).

1.3.1 Ventilator-Induced Lung Injury

La physiopathologie du VILI est complexe et encore mal comprise. La surdistension des alvéoles est un facteur important, déterminé par l'importance du V_T (volume courant) (126). Des phénomènes d'ouverture et de fermeture cycliques des alvéoles ont aussi été incriminés. En effet, la pression d'ouverture de certaines alvéoles est augmentée au sein d'un poumon lésé, avec pour conséquence leur fermeture lors de la ventilation spontanée. Lors de la ventilation mécanique, la pression positive appliquée à l'inspiration peut les rouvrir, mais il existe un risque de fermeture à chaque baisse de pression dans les voies aériennes durant l'expiration. L'apport d'une PEEP permet de prévenir ce phénomène. C'est pourquoi on considère qu'une ventilation associant un V_T réduit et l'application d'une PEEP comme étant « protectrice » au cours du SDRA. Dans le cas contraire (V_T élevé et absence de PEEP), on parle de ventilation « agressive » ou « délétère ».

La surdistension des alvéoles au cours de la VM induit un biotrauma, caractérisé par la libération de différents médiateurs intracellulaires, résultant de l'activation de différentes voies de signalisation cellulaire conduisant à une activation transcriptionnelle dans les cellules épithéliales, endothéliales, et immunitaires. Ainsi on observe la libération de **cytokines inflammatoires** (IL-1 β , IL-6, IL-8, TNF- α , CXCL1 et 10...) dans l'espace alvéolaire, une up-regulation de certains PRR comme TLR-2 (127), à l'origine notamment d'un recrutement et d'une activation des PMNs sur le site pulmonaire (126) (Figure 11).

L'étirement cyclique des voies aériennes pourrait aussi être à l'origine de la libération de **DAMPs** par les cellules alvéolaires agressées. Des données expérimentales et cliniques démontrent la présence de DAMPs dans le surnageant de liquide broncho-alvéolaire chez des patients présentant des lésions de VILI, parmi lesquelles des constituants de la matrice extracellulaire (le hyaluronan, l'heparan sulfate, le versican), les Heat shock protéines (HSP), HMGB1, S100A12, l'acide urique et l'ATP (128) (Figure 2). Une conséquence est l'activation de la réponse immunitaire innée, un certain nombre de ces DAMPs étant reconnus par des PRRs (TLR, NLRP3, RAGE...), participant ainsi à la genèse de l'inflammation stérile déterminant le VILI (128) (Figure 11).

Le rôle des PMNs dans la genèse du VILI ne fait plus de doute. Ainsi une déplétion préalable en PMNs chez des lapins soumis à une VM « agressive » (i.e., haut V_T) limite fortement la survenue de lésions de VILI (129). En effet les médiateurs libérés (cytokines inflammatoires et DAMPs) sont à l'origine d'un **recrutement et de l'activation des PMNs** dans les alvéoles, ces cellules pouvant ensuite agraver les phénomènes inflammatoires et les dommages tissulaires par la libération d'enzymes protéolytiques (métalloprotéases 8 et 9...) et de ROS (130). Des phénomènes de Nétose ont aussi été mis en évidence, mais leur rôle pathogénique dans le VILI reste controversé (131).

La double agression VM/pneumopathie, représente une situation clinique d'intérêt. Dans notre modèle de pneumopathie chez le lapin, de précédents travaux montraient qu'un schéma de VM jugé « agressif » et prolongé aggravait le pronostic de pneumopathies aussi bien à bactéries Gram + (*Streptococcus pneumoniae* (132), *Staphylococcus aureus* (133,134)), que Gram – (*Enterobacter aerogenes* (135,136)). Cette aggravation du pronostic se caractérise par une plus forte mortalité, des pneumopathies multifocales, des dommages pulmonaires histologiques plus marqués et une altération de la clairance bactérienne pulmonaire et systémique (132,135,137). En comparaison aux animaux en respiration spontanée, les animaux ventilés présentaient une inflammation pulmonaire (expressions géniques et concentrations d'IL-8 et TNF- α , expression génique de TLR-2), et systémique (TNF- α) plus marquées (133).

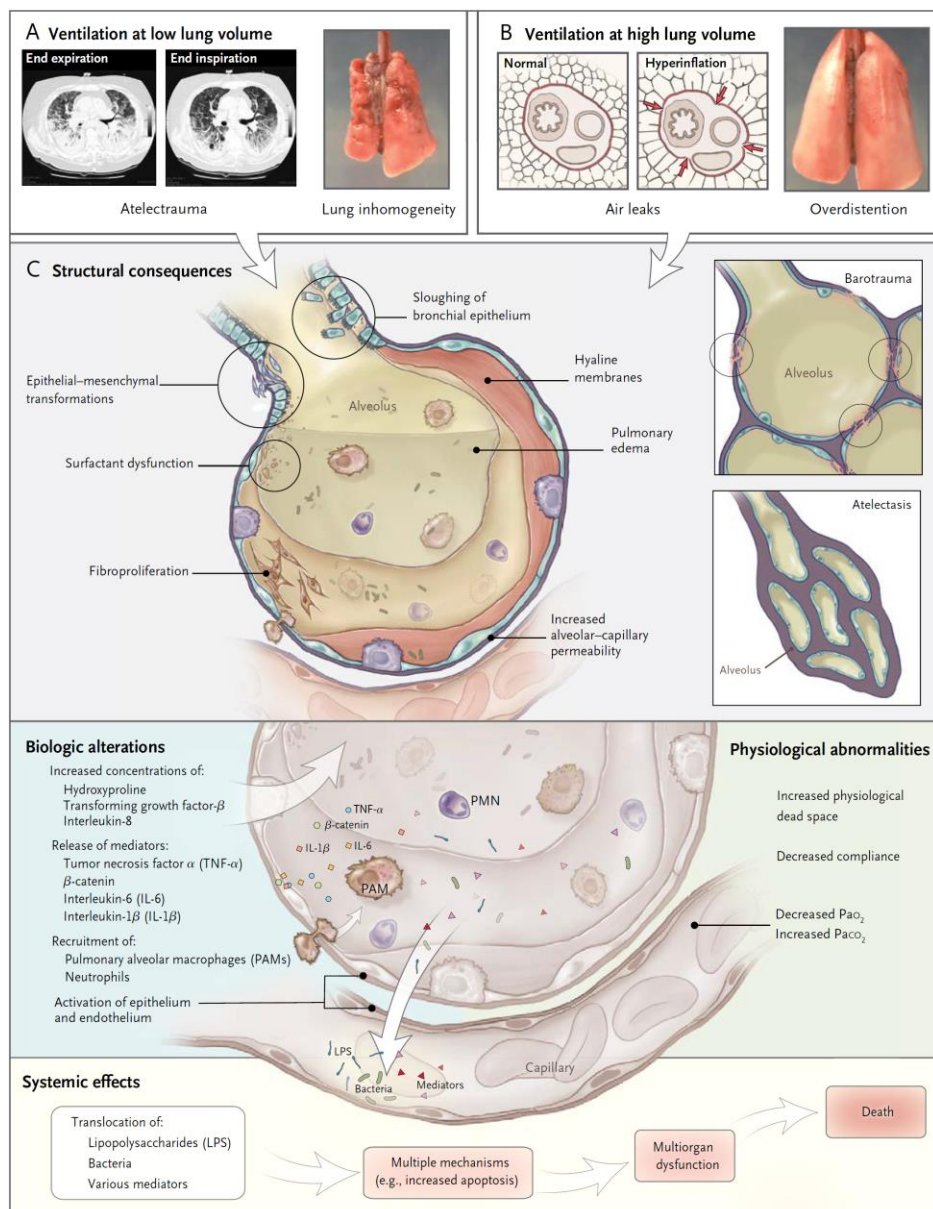


Figure 11. Dommages pulmonaires et inflammation produites par une ventilation mécanique agressive. D'après Slutsky and Ranieri (126)

1.3.2 Stratégies de « VM protectrice »

Les recommandations internationales sont désormais d'appliquer une VM associant un V_T de 4-8 ml/kg de poids prédit par la taille pour une pression de plateau (P_{plat}) ≤ 30 cmH₂O. Une pression positive en fin d'expiration ≥ 5 cmH₂O est par ailleurs recommandée. Cette stratégie « protectrice », est associée à une diminution de la mortalité de l'ordre de 9% (138). Dans une méta-analyse de 3 essais randomisés, la mortalité augmentait lorsque la PEEP était basse, en comparaison à une PEEP élevée (139). Enfin, de nombreuses données précliniques et quelques travaux cliniques démontrent qu'en comparaison à un schéma de VM agressive, un schéma jugé plus protecteur est capable de limiter le biotrauma (136,135,140).

En cas de SDRA, lorsque le rapport PaO_2/FiO_2 est inférieur à 150 mmHg, la mise en décubitus ventral (ou prone position) est aussi associé à une réduction significative de la mortalité (141), raison pour laquelle cette mesure est actuellement recommandée. Chez les lapins, les travaux de l'équipe montraient qu'au cours de la pneumopathie ventilée à *Enterobacter aerogenes*, le décubitus ventral était associé à une amélioration de la clairance bactérienne et à une diminution du VILI en termes de dommages pulmonaires et d'inflammation pulmonaire (136).

Cependant, malgré ces stratégies ventilatoires jugées « protectrices », la mortalité au cours du SDRA reste élevée, de l'ordre de 40-50%. De plus, il faut insister sur le fait qu'environ un tiers des patients en SDRA présentent des signes de distension alvéolaire, en dépit d'une VM « protectrice ». Ces patients ont de plus des niveaux d'inflammation alvéolaire plus élevés et une durée de VM plus longue que les autres (142). Dans une large cohorte de 3562 patients en SDRA, la pression motrice (PM), considérée comme un marqueur de distension alvéolaire (« alveolar strain ») et qui correspond à la P_{plat} moins la PEEP, était le paramètre ventilatoire le plus fortement associé au risque de décès (143). Ainsi, une valeur de PM supérieure ou égale à 15 cmH₂O serait fortement associée à la mortalité au cours du SDRA, malgré l'application d'une stratégie « protectrice » (144).

Pour cela, de nouvelles pistes physiopathologiques doivent être explorées afin d'ouvrir le champs à de nouvelles stratégies thérapeutiques capable de limiter le VILI et d'améliorer le pronostic des patients en SDRA.

1.3.3 Impact de la ventilation mécanique sur l'homéostasie mitochondriale

La VM pourrait en elle-même causer des dysfonctions mitochondrielles.

Des données *in vitro* issues de 2 travaux montrent que le stretch de cellules épithéliales pulmonaires chez l'homme ou le rat active NFkB et entraîne une production de ROSmt, dont l'anion superoxyde (145,146).

In vivo, la VM agressive de rats, induit la production de ROSmt, augmentant la perméabilité membranaire de l'épithélium alvéolaire, phénomène limité par l'injection de Tiron, un ROS « scavenger » (146). D'autres données chez des souris néonatales montrent qu'une VM agressive (V_T à 15 µl/g) pendant 8 heures, diminuent la production d'ATP et l'activité de la chaîne respiratoire mitochondriale, compromettant le développement alvéolaire des souriceaux (147). Récemment, un travail chez le rat trachéotomisé montrait que l'exposition à une VM agressive pendant 4 heures induisait du VILI, associés à l'accumulation de ROS, à une augmentation des concentrations d'ADNmt ainsi qu'à une chute du potentiel de membrane mitochondrial des cellules épithéliales alvéolaires. Ces altérations étaient limitées par l'injection de chloroquine, un bloqueur de TLR-9, suggérant le rôle de la voie ADNmt/TLR9 dans la genèse du VILI (148). Néanmoins, des données contradictoires ont été publiées par une autre équipe qui a montré que la délétion de TLR9 chez la souris ne permettait pas de limiter le VILI chez des souris soumises à une VM protectrice (V_T à 8ml/kg) ou plus aggressive (32 ml/kg) pendant 4 heures. En effet, les concentrations alvéolaires d'ADN nucléaire étaient augmentées significativement au cours de la VM mais celles d'ADNmt ne l'étaient pas (149).

Le rôle de la biogénèse mitochondriale dans le VILI ont été étudiés dans un modèle murin. Des souris NRF2-/ ventilées pendant 2 heures présentaient, en comparaison aux souris NRF2+/, une plus grande perméabilité alvéolaire et vasculaire, et une réponse inflammatoire plus marquée, suggérant un rôle protecteur de la protéine NRF2 (150).

Enfin, plusieurs travaux montrent aussi l'impact de la VM sur la dysfonction diaphragmatique, et le rôle possible de la dysfonction mitochondriale des cellules musculaires dans sa survenue (151).

En conclusion, les données évaluant l'impact de la VM sur l'homéostasie mitochondriale, reposent essentiellement sur des modèles *in vitro* de stretch de cellules pulmonaires, et des schémas de VM très courts (maximum 8 heures) chez des petits rongeurs. Les données concernant l'impact d'une VM prolongée sur l'homéostasie mitochondriale sont en revanche limitées et parfois contradictoires. Néanmoins, au cours d'une pneumonie bactérienne, ces phénomènes pourraient contribuer au VILI et au plus mauvais pronostic observé dans les modèles animaux. C'est pourquoi il serait intéressant d'explorer expérimentalement ces hypothèses.

1.4 Les cellules souches/stromales mésenchymateuses

Parmi les thérapies adjuvantes de l'antibiothérapie envisagées dans le sepsis, et notamment dans des situations telles que la pneumopathie bactérienne compliquée de SDRA, l'administration de cellules souches/stromales mésenchymateuses (CSMs) seraient une piste prometteuse. Leur effet bénéfique pourrait reposer notamment sur la restauration de l'homéostasie mitochondriale.

1.4.1 Définition, propriétés et perspectives au cours du sepsis

Les CSMs ont initialement été identifiées dans la moelle osseuse. Elles ont un pouvoir de différenciation en cellules mésodermiques (ostéocytes, adipocytes, chondrocytes), ou non mésodermiques, selon leur environnement cellulaire (152). Elles sont caractérisées par l'expression de certains marqueurs de surface (CD73, CD90, CD105) et l'absence d'expression d'autres marqueurs (CD45, CD14, CD79A et HLA-DR). On les retrouve dans d'autres tissus que la moelle osseuse : le poumon, le cœur, le muscle, le cordon ombilical... (153).

Les CSMs ont des propriétés immunomodulatrices et anti-infectieuses, mais aussi leur capacités régénératrices des tissus agressés en font une candidate attractive en tant que thérapie adjuvante de l'antibiothérapie dans le sepsis. D'autre part, leur disponibilité dans des compartiments tels que la moelle osseuse, la graisse, le placenta ou le cordon fœtal permet d'imaginer que les CSMs pourront être utilisées à plus large échelle que celle des essais cliniques. Ensuite, il est possible de les cultiver largement *ex vivo* en un temps limité. De plus, ces cellules sont peu immunogènes, car elles expriment peu le CMH de type I et pas celui de type II, limitant ainsi le risque de rejet que l'on observe classiquement avec les cellules souches hématopoïétiques. Enfin, à la différence des CSMs d'origine embryonnaires, elles ont un faible pouvoir tumorigène, et une courte durée de vie (153–156).

Le traitement par CSMs a été associé à une amélioration du devenir dans différents modèles précliniques de sepsis bactérien ou d'endotoxémie, en particulier de la survie, avec des résultats contrastés cependant (153). Il faut de plus souligner la diversité des modèles utilisés, des modes d'administration et du nombre de cellules administrées ($3 \times 10^5/\text{kg}$ à $30 \times 10^6/\text{kg}$), du nombre d'injection, et du timing d'injection des CSMs (i.e., simultanément à l'agression, ou après un certain délai suivant son induction) (153). La relevance clinique de ces résultats est donc à nuancer en fonction de ces éléments.

Si les mécanismes sous-tendant les effets bénéfiques des CSMs au cours du sepsis ne sont pas parfaitement compris, plusieurs ont été mis en évidence (157):

- La différenciation des CSMs en cellules de l'organe agressé (ex : cellules épithéliales pulmonaires) favorisant la réparation du tissu lésé
- La réparation de cellules agressées, grâce à la fusion des CSMs avec celles-ci
- Une sécrétion paracrine de molécules de signalisation capable de réparer le tissu ou de prévenir certains dommages par des propriétés immunomodulatrices
- Un transport d'organelles et/ou de molécules des CSMs vers les cellules agressées à travers des nanotubes membranaires (tunnelling nanotube), en particulier le transfert de mitochondries
- Une signalisation par le relargage par les CSMs d'exosomes ou de microvésicules

1.4.2 Propriétés immunomodulatrices

Plusieurs travaux précliniques et cliniques de sepsis ou d'endotoxémie ont démontré les propriétés immunomodulatrices des CSMs. Les CSMs réduisent les concentrations plasmatiques de cytokines inflammatoires (en particulier IL-6, IL-1 β , IL-12, IL-2 et IL17), mais aussi au niveau de l'organe atteint. L'effet des CSMs sur l'IL-10 est plus controversé (153,158). Suite à une injection de LPS chez des volontaires sains, une injection unique de CSMs entraînait une réponse à la fois pro et anti-inflammatoire, dépendant en partie du temps d'évaluation après l'injection (158).

1.4.3 Propriétés microbicides

L'effet des CSMs sur la clairance bactérienne est variable selon les travaux (153). Bien que dépourvues de propriétés de phagocytose, les CSMs pourraient permettre d'améliorer la clairance bactérienne via une augmentation de la phagocytose des cellules myéloïdes :

- Chez les monocytes, via une reprogrammation en augmentant l'expression des gènes impliqués dans la phagocytose et la mort bactérienne (159). Cet effet n'a été observé que dans un environnement « septique » (159).
- Chez les macrophages alvéolaires dans un modèle de pneumopathie à E. coli (160)
- Chez les neutrophiles in vitro et dans un modèle de CLP chez la souris (161)

Cependant la déplétion en neutrophiles chez la souris n'annulait que partiellement les effets bénéfiques des CSMs, alors que la déplétion en macrophages les annulait complètement (160), suggérant le rôle clef de ces cellules.

Enfin, à cet effet immunostimulant, s'ajoute la sécrétion par les CSMs de peptides dotés de propriétés antimicrobiennes comme le LL-37 (162) et l'hepcidine (163).

1.4.4 Résolution de la dysfonction d'organe

Les CSMs s'avèrent efficaces au cours du sepsis expérimental pour améliorer la fonction de la plupart des organes atteints (poumon, rein, système circulatoire dont le cœur, foie, muscle) (153). Les critères de jugement sont le plus souvent la réduction de l'infiltrat neutrophile et de l'œdème, des dommages histologiques. Il pourrait s'agir d'un effet immunomodulateur précédemment décrit dans la mesure où s'y associe une réduction des concentrations locales en cytokines inflammatoires. La fonction des organes est aussi améliorée (e.g., force musculaire (164), clairance de la créatinine, transaminases (165), contractilité myocardique (166)...) (Figure 12).

Une amélioration de la dysfonction circulatoire a aussi été observée, notamment dans un modèle de choc septique par péritonite fécale chez le cochon (diminution de la lactatémie, diminution des besoins en norépinephrine), corrélée à une amélioration de la survie (167).

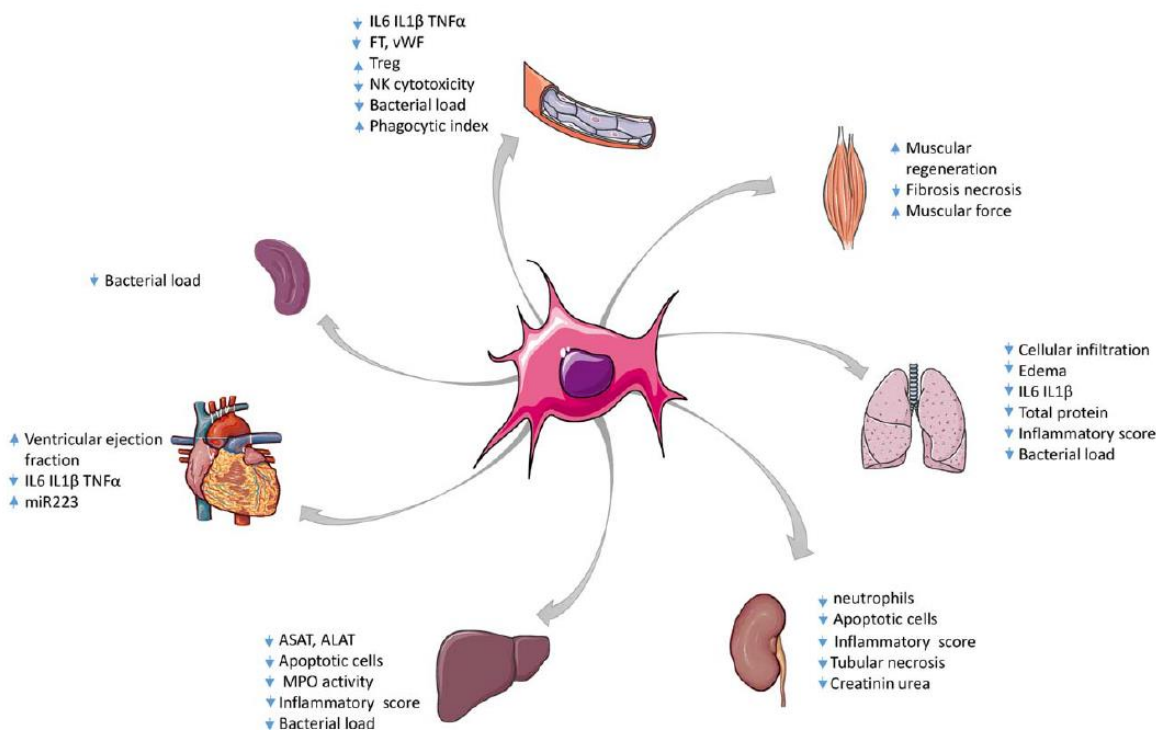


Figure 12. Effet des CSMs sur la dysfonction d'organe aux cours du sepsis. D'après Laroye et al (153)

Dans la majorité de ces travaux, les CSMs étaient le seul traitement testé. A notre connaissance, une seule étude a évalué l'effet des CSMs en comparaison à l'antibiothérapie, mais aussi en association

avec celle-ci. Il s'agissait d'un modèle murin de péritonite (i.e., « cecal ligation and puncture » (CLP)). Une amélioration de la survie, de la clairance bactérienne, ainsi qu'une réduction des dysfonctions d'organe associée à une diminution des concentrations en cytokines inflammatoires étaient mises en évidence (163).

1.4.4.1 Au cours de la pneumopathie et du SDRA

Les effets bénéfiques des CSMs ont également été mis en évidence dans différents modèles pré-cliniques de SDRA : réduction de l'œdème pulmonaire, des dommages endothéliaux, de la réponse inflammatoire intra-pulmonaire, et amélioration de la survie (Figure 13) (155). Dans ces modèles, les CSMs étaient injectées par voie intraveineuse ou intratrachéale (168).

Chez l'homme, deux essais de phase I investiguant l'effet des CSMs au cours du SDRA ont retrouvé une bonne tolérance de celles-ci, de même que l'essai de phase 2a (START) comparant une injection unique de CSMs (10×10^6 /kg de poids prédict) au placebo (169–172).

Au cours de la pneumopathie sévère, l'essai randomisé contrôlé contre placebo, SEPCELL (NCT03158727) de phase Ib/IIa, est actuellement en cours pour évaluer l'effet d'une injection de deux injections CSMs issues de la graisse (chacune de 160×10^6 CSMs) à J1 et J3.

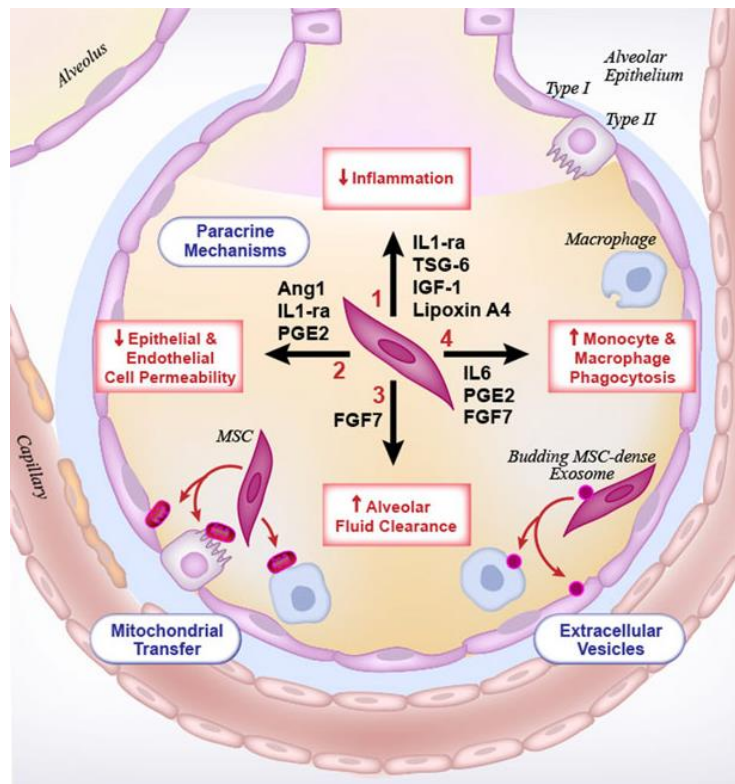


Figure 13. Mécanismes d'action des CSMs au cours du SDRA. D'après Huppert et al (155)

1.4.4.2 Effet des CSMs au cours du VILI (hors contexte infectieux)

Plusieurs travaux précliniques ont évalué l'effet des CSMs sur le VILI. Ces études reposaient sur l'exposition de rats à des stratégies de VM jugées agressives (volumes élevés, absence de PEEP). Ces travaux montrent que dans ce contexte, les CSMs améliorent la fonction pulmonaire et diminuent les dommages histologiques associés au VILI, avec une efficacité supérieure lorsque les CSMs sont administrées par voies intraveineuse ou intratrachéale, comparativement à la voie intrapéritonéale (173–175).

Néanmoins, la pertinence de ce modèle de VILI était discutable dans la mesure où la stratégie ventilatoire utilisée était associée à une mortalité de l'ordre de 40% (173). D'autre part, aucun modèle n'a évalué l'effet des CSMs au cours de la double agression pneumopathie bactérienne et VM.

1.4.4.3 CSMs et restauration de l'homéostasie mitochondriale

Dans plusieurs travaux précliniques, l'effet bénéfique des CSMs a été associé à une amélioration de l'homéostasie mitochondriale. En effet, plusieurs publications ont rapporté des résultats montrant que les CSMs étaient capables de transférer leur propres mitochondries dans les cellules épithéliales ou endothéliales pulmonaires agressées, restaurant ainsi leur métabolisme énergétique cellulaire et leurs fonctions (176–178). Ce transfert se ferait soit directement par des nanopores, soit à distance par des vésicules extracellulaires relarguées contenant des mitochondries (153,176).

Ainsi, dans un modèle murin de SDRA secondaire à une pneumopathie à *E. coli*, Jackson *et al* ont montré que les CSMs amélioraient les capacités phagocytaires des macrophages alvéolaires via le transfert de mitochondries (160).

D'autres auteurs ont observé que les CSMs étaient aussi capables d'améliorer la fonction d'organe, en restaurant l'homéostasie mitochondriale. Pour exemple, dans un modèle d'agression musculaire post-septique (CLP) ou toxique chez la souris, l'injection de CSMs améliorait la fonction musculaire dans le même temps qu'une résolution de l'inflammation et qu'une restauration du pool et de la fonction mitochondriale, rétablissant ainsi la production d'ATP (164).

En conclusion, à la lumière de données pré-cliniques, les CSMs apparaissent comme une stratégie thérapeutique adjuvante prometteuse au cours de la pneumopathie bactérienne grave, capable de corriger certaines dysfonctions d'organe tout en modulant la réponse immune. Leurs effets méritent d'être investigués au cours de la double agression pneumopathie et VM, et plus particulièrement de la pneumopathie à pneumocoque, situation clinique la plus fréquente. D'autre part, il est nécessaire de mieux comprendre les mécanismes sous-jacents, et en particulier l'éventuelle restauration de l'homéostasie mitochondriale des tissus agressés ou des cellules immunitaires associée à l'administration de CSMs.

Enfin, une des raisons avancées pour expliquer l'échec des nombreuses thérapies immuno-modulatrices au cours du sepsis est l'hétérogénéité des patients, de leur réponse immunitaire, du moment où ils sont pris en charge par rapport à l'histoire naturelle de l'infection. Les CSMs pourraient apparaître comme une thérapie « intelligente », capable de s'adapter à la situation immune de l'hôte, et ainsi représenter en quelque sorte une réponse thérapeutique personnalisée, ou théranostique.

2 Objectifs des travaux

2.1 Article 1 (Genève/Dijon, Plos One)

➔ Objectifs de l'étude

Le premier travail a été réalisé en collaboration avec l'équipe du Pr Jérôme Pugin à Genève. L'hypothèse formulée était que les alarmines mitochondrielles (ADNmt, fMLP, ATP) pourraient être libérées par les cellules épithéliales pulmonaires, en réponse à l'agression mécanique que représente l'étirement cyclique, et agir comme des médiateurs de l'inflammation stérile contribuant au développement du VILI.

Deux modèles expérimentaux ont été utilisés :

- Le modèle *in vitro* de cellules épithéliales pulmonaires humaines soumises à l'étirement cyclique (analyse des surnageants)
- Le modèle *in vivo* de lapins soumis à une VM agressive pendant 8 heures (analyse des liquides de LBA)

La pertinence clinique de ces données a ensuite été testée grâce à l'analyse du surnageant de LBA humains issus de patients ventilés présentant un SDRA, en comparaison à des témoins sains.

➔ Participation personnelle à l'étude

La partie expérimentale chez le lapin a été réalisée à Dijon, avant mon arrivée dans le laboratoire. Ma participation à ce travail a concerné l'interprétation des résultats, l'analyse statistique et la rédaction du manuscrit.

RESEARCH ARTICLE

Mitochondrial alarmins are tissue mediators of ventilator-induced lung injury and ARDS

Serge Grazioli^{1,2*}, Irène Dunn-Siegrist^{1*}, Laure-Anne Pauchard^{3,4*}, Mathieu Blot⁵, Pierre-Emmanuel Charles^{3,4}, Jérôme Pugin¹

1 Intensive Care Laboratory, Department of Microbiology and Molecular Medicine, University Hospitals of Geneva & Faculty of Medicine, Genève, Switzerland, **2** Department of Pediatrics, Division of Neonatal and Pediatric Intensive Care, University Hospital of Geneva, Genève, Switzerland, **3** Intensive Care Unit, University Hospital of Dijon, Dijon, France, **4** U.M.R. 1231, I.N.S.E.R.M, Burgundy University, Dijon, France, **5** Department of Infectious Diseases, University Hospital of Dijon, Dijon, France

* These authors contributed equally to this work.

* serge.grazioli@hcuge.ch



Abstract

OPEN ACCESS

Citation: Grazioli S, Dunn-Siegrist I, Pauchard L-A, Blot M, Charles P-E, Pugin J (2019) Mitochondrial alarmins are tissue mediators of ventilator-induced lung injury and ARDS. PLoS ONE 14(11): e0225468. <https://doi.org/10.1371/journal.pone.0225468>

Editor: Heinz Fehrenbach, Forschungszentrum Borstel Leibniz-Zentrum für Medizin und Biowissenschaften, GERMANY

Received: April 14, 2019

Accepted: November 5, 2019

Published: November 22, 2019

Copyright: © 2019 Grazioli et al. This is an open access article distributed under the terms of the [Creative Commons Attribution License](#), which permits unrestricted use, distribution, and reproduction in any medium, provided the original author and source are credited.

Data Availability Statement: All relevant data are within the article and its Supporting Information files.

Funding: This study was supported by a grant from the Swiss National Foundation for Scientific Research (#310030-141143) to JP. <http://www.snf.ch/en/Pages/default.aspx> The funders had no role in study design, data collection and analysis, decision to publish, or preparation of the manuscript.

Rationale

Endogenous tissue mediators inducing lung inflammation in the context of ventilator-induced lung injury (VILI) and acute respiratory distress syndrome (ARDS) are ill-defined.

Objectives

To test whether mitochondrial alarmins are released during VILI, and are associated with lung inflammation.

Methods

Release of mitochondrial DNA, adenosine triphosphate (ATP), and formyl-Met-Leu-Phe (fMLP) peptide-dependent neutrophil chemotaxis were measured in conditioned supernatants from human alveolar type II-like (A549) epithelial cells submitted to cyclic stretch *in vitro*. Similar measurements were performed in bronchoalveolar lavage fluids from rabbits submitted to an injurious ventilatory regimen, and from patients with ARDS.

Measurements and main results

Mitochondrial DNA was released by A549 cells during cell stretching, and was found elevated in BAL fluids from rabbits during VILI, and from ARDS patients. Cyclic stretch-induced interleukin-8 (IL-8) of A549 cells could be inhibited by Toll-like receptor 9 (TLR9) blockade. ATP concentrations were increased in conditioned supernatants from A549 cells, and in rabbit BAL fluids during VILI. Neutrophil chemotaxis induced by A549 cells conditioned supernatants was essentially dependent on fMLP rather than IL-8. A synergy between cyclic stretch-induced alarmins and lipopolysaccharide (LPS) was found in monocyte-derived macrophages in the production of IL-1 β .

Competing interests: The authors have declared that no competing interests exist.

Conclusions

Mitochondrial alarmins are released during cyclic stretch of human epithelial cells, as well as in BAL fluids from rabbits ventilated with an injurious ventilatory regimen, and found in BAL fluids from ARDS patients, particularly in those with high alveolar inflammation. These alarmins are likely to represent the proximal endogenous mediators of VILI and ARDS, released by injured pulmonary cells.

Introduction

Mechanical ventilation has been lifesaving in many patients with respiratory failure since its introduction several decades ago. It has also been associated with lung damage due to cyclic stretch imposed by positive pressure mechanical ventilation, particularly when the lung is injured or infected. This phenomenon is nowadays known as ventilator-induced lung injury (VILI) [1, 2]. It is also now widely accepted that ventilatory strategies aimed at decreasing airway overstretching are associated with better outcome in patients with and without acute respiratory distress syndrome (ARDS) [3, 4].

An important part of VILI is due to lower airway inflammation mediated by pro-inflammatory cytokines, chemokines, and blood neutrophils recruited to the airways [5–7]. *In vitro* experiments with isolated lung cells [8, 9] and animal studies with intact lungs [10–12] could demonstrate that cyclic stretch *per se* induced pro-inflammatory mediators such as monocyte chemoattractant protein-1 (MCP-1) and interleukin-8 (IL-8), prototypical chemokines for myeloid cells. Although it could be shown that cyclic stretch induces *de novo* transcription of IL-8 gene [13], it remains unclear whether this was a direct transcriptional effect of the mechanical strain or a secondary effect of endogenous mediator(s) released by lung cells injured by cyclic stretch.

Mechanical ventilation and cyclic stretch of lung cells have been shown to induce cell membrane breaks with spillover of intracellular cell content [14, 15]. Recent evidence suggests that injured cells release alarmins (also called damage-associated molecular patterns, DAMPs) originating from mitochondria [16–18], and that these alarmins may play a role in mediating VILI [19–22]. The release by injured cells of mitochondrial alarmins, such as mitochondrial DNA, N-formyl-methionyl-leucyl-phenylalanine (fMLP), and adenosine triphosphate (ATP) produces a local and sometimes systemic inflammatory response. This response is mainly dependent on the local production of interleukin-1 β (IL-1 β) via the assembly of the NOD-like-receptor protein 3 (NLRP3) inflammasome and the recruitment of neutrophils to injured tissues [16–18, 23]. Since IL-1 β is a prominent and bioactive pro-inflammatory cytokine in the lower airways from patients with ARDS [6, 7, 24], we hypothesized that mitochondrial alarmins may be released by airway cells submitted to cyclic stretch due to mechanical ventilation, and represent the missing link between cell stretch and downstream inflammatory cytokines.

Methods

In vitro cell stretching

The human alveolar type II-like A549 cells (ATCC, Manassas, VA) were cultured onto silastic membranes (Bioflex® plates, Dunn Labortechnik, Asbach, Germany), and submitted to cyclic stretch using the FX-3000 Flexcell® system (Flexcell International, Hillsborough, NC, USA), as previously described [13, 25]. In some experiments, we substituted A459 cells for primary

human monocyte-derived macrophages [8]. In other experiments, macrophages submitted to cyclic stretch were co-incubated with 100 ng/mL of *E.coli* K12 LPS (UltraPure® LPS, Invivogen). ATP (Roche) was used at 100 µM concentration, and the Toll-like receptor 9 (TLR9) antagonist ODN TTAGGG (Invivogen) was used at 1 µM concentration. Detailed methods are described in the online data supplement. Cell viability before and after cell stretching was assessed using phase contrast optic microscopy and fluorescence microscopy (Live/Dead kit®, Thermo Fisher Scientific, USA), and by flow cytometry (FACS, 7-AAD, BioRad). Briefly, cells were incubated for 15 min in the fluorescently-labeled calcein-AM (live cells, green) and propidium iodide (dead cells, red) solution, and analyzed by fluorescent microscopy. FACS analysis of static vs. stretched cells was done using the 7-AAD reagent (BioRad) staining live cells, excluding dead cells.

Measurement of alarmins in conditioned supernatants

Mitochondrial DNA. For mitochondrial DNA isolation, collected conditioned media from A549 cells and BAL were first centrifuged at 2000 x g for 10min to remove cell debris, followed by DNA extraction using Qiagen DNAEasy kit (Qiagen, Hilden, Germany). Quantitative PCR was used to measure levels of mitochondrial DNA(mtDNA) in cell-free supernatants and BAL using mitochondrial specific PCR primers for cytochrome B, cytochrome C oxidase subunit III (COXIII), and NADH dehydrogenase subunit I (ND1) as previously described [17]. In addition, we performed droplet digital PCR (ddPCR) that allowed us to determine the copy number of mtDNA and genomic DNA (gDNA) by amplifying mitochondrial COX III and genomic ribonuclease protein subunit p30 (RPP30) respectively.

In some experiments, 2 µM of the TLR9 antagonist ODN TTAGGG (Invivogen, San Diego, CA, USA) was added to the A549 cell cultures just before starting cell stretch. IL-8 secreted in conditioned supernatants was measured as a marker of cell activation.

Cell reporter assay. In order to study TLR9 activation, supernatants from stretched cells were added to HEK293 Blue® cells expressing TLR9 (Invivogen). HEK293 Blue® cells respond to TLR9 agonists such as bacterial and mitochondrial DNA by secreting embryonic alkaline phosphatase (SEAP) [26, 27]. Cell activation was measured using an alkaline phosphatase substrate present in the colorimetric HEK-Blue™ detection system (Caya-Invivogen Europe, Toulouse, France), quantified using an ELISA reader at 655 nm, and expressed as optical densities. Those experiments were repeated with human bronchoalveolar lavage (BAL) samples.

ATP. Extracellular ATP released by A549 cells was quantified in conditioned supernatants using the ATP bioluminescence assay kit CLS II with a detection range of 10^{-11} – 10^{-6} M (Roche Applied Science, Mannheim, Germany). For optimal measurements with this method, pH of the samples was set at pH 7.7 using Tris buffer. A standard curve was performed with purified ATP.

Chemotactic factors. Chemotaxis of human neutrophils induced by supernatants from stretched A549 cells was measured using a modified Boyden chamber as previously described [28]. For each experiment, serial dilutions of prototypical chemotactic factors, such as human IL-8 (a gift from C. Power, MerckSerono, Geneva, Switzerland) and the bacterial/mitochondrial formylated peptide fMLP (Sigma, St. Louis, MO) served to control a maximal rate of neutrophil chemotaxis. In some experiments, neutrophils were pre-incubated 30 min prior to start the chemotaxis assay with an anti-formyl peptide receptor 1 (FPR1) monoclonal mouse antibody (blocking the human surface receptor for fMLP, R&D, Minneapolis, MN, USA) or an anti-C-X-C motif chemokine receptor 1 (CXCR1) blocking antibody (Abcam). More detailed methods are described in the online data supplement.

IL-8 and IL-1 β . Conditioned supernatants collected after A549 cell stretching were centrifuged at 1,200 rpm for 5 min at 4°C to remove cell debris. IL-8 levels were measured in supernatants using a sandwich ELISA using a pair of monoclonal antibodies as previously described [25]. IL-1 β levels were measured in conditioned supernatants and in cell lysates from monocyte-derived macrophages (cell lysed using a Triton-X-based cell lysis buffer) using a sandwich ELISA (Perbio Science Switzerland SA). This antibody pair does not differentiate pro-IL-1 β from mature IL-1 β . Monocyte-derived macrophages were also cultured with the TLR9 agonist (ODN TTAGGG, Invivogen), ATP, or both. The secretion of IL-1 β in conditioned supernatants from monocyte-derived macrophages was also assessed using a Western blot technique as described by Wu et al. [22].

Mechanical ventilation in rabbits

Animals. Male New Zealand white rabbits (3.0 to 3.3 kg) were obtained from the “élevage scientifique des Dombes” (Romans, France) and bred in the University of Burgundy animal facility (Dijon, France). They were placed in individual cages, had free access to water, and were fed in accordance with current recommendations described in the *Guide for the Care and Use of Laboratory Animals*, National Institutes of Health No. 92–23, revised version of 1985. The protocol for animal studies was approved by the local veterinary committee (Ethics committee for animal research, C2EA grand campus of Dijon #105). Experiments were performed according to European laws and regulations on animal welfare. A central venous catheter was surgically inserted into every rabbit the day before MV.

Experimental protocol. Twenty-four hours after jugular catheterization, animals were orally intubated with a 2.5mm tracheal cuffed tube (Mallinckrodt™, Covidien®, U.S.A.) under general anesthesia obtained with ketamine 20 mg/Kg (Panpharma, France) and xylazine 1.5 mg/Kg (Rompun®, Bayer, Germany). Animals were put in the supine position on a heating blanket and connected to a volume-controlled ventilator (Servo ventilator 900C, Siemens®, Germany) (20 mL/kg of tidal volume with zero end-expiratory pressure [ZEEP], a respiratory rate of 30 bpm and a fraction of inspired oxygen at 0.5). Ventilated rabbits were perfused with isotonic saline and kept anesthetized and paralyzed throughout the experiment with 0.2mg/kg/h midazolam (Hypnovel®, Roche, Switzerland) and, 0.8mg/kg/h cisatracurium besilate (Nimbelex®, GlaxoSmithKline, U.K.). Animals were sacrificed after 4 hrs. or 8 hrs. of mechanical ventilation (MV). Intubated, but spontaneously breathing (SB) rabbits were used as controls (n = 8). At the end of the experiments, animals were exsanguinated by venous puncture, and autopsied aseptically to harvest the lungs. Bronchoalveolar lavage (BAL) followed by surgical removal of the lungs was performed at the end of the experiment as described [25]. Briefly, BAL was performed in the lower pulmonary lobe using an appropriate catheter with 5 mL of sterile 0.9% NaCl. The collected BAL fluid was divided into aliquots, and stored at -80°C until analyses were performed. The remaining tissue was homogenized in sterile water. Lung homogenates were then frozen, and stored at -80°C until tissue concentrations of cytokines were measured. Measurement of inflammatory mediators in BAL fluids and in lung tissues, as well as the assessment of a histological lung injury score was done as described elsewhere [25]. More detailed methods can be found in the online data supplement, including the quantitative measurement of mitochondrial DNA in BAL fluids. Methods for the quantification of chemotactic attraction of human neutrophils by rabbit BAL fluids are also described in the online data supplement.

Patients with ARDS

BAL fluid was obtained through fiberoptic bronchoscopy in intubated and mechanically ventilated patients at day 1 and day 7 after the onset of ARDS (Harborview Medical Center, Seattle,

WA, USA) [29] after having obtained an informed consent from the patient or the next-of-kin. BAL fluid was also obtained in 3 healthy volunteers, centrifuged and kept frozen at -80°C [29]. Total DNA was extracted from cell-free human BAL fluids and quantitative PCR was done measuring levels of the mitochondrial cytochromes B and C oxidase III DNA, as described above for supernatants from stretched cells. BAL samples were defined as “highly inflammatory” if they contained > 80% neutrophils and > 2 mg/mL proteins. Others were defined as “low inflammatory”.

Statistical analysis

Data are presented as median with interquartile range. Because the majority of the data were not normally distributed or had low sample size, non-parametric tests were used. The Mann-Whitney *U* test or the Kruskall-Wallis test were used to compare variables between two or multiple groups respectively. To account for multiple comparisons, the *P*-value was adjusted for a false discovery rate (FDR) using the Benjamini and Hochberg method. A FDR (or *q*-value) of 0.05 was considered significant. Data were analyzed with the GraphPad Prism® software [30].

Results

Human type II-like alveolar epithelial cells submitted *in vitro* to cyclic stretch release mitochondrial DAMPs

First, we investigated whether mitochondrial DAMPs are released during mechanical stretch using an *in vitro* model of mechanical ventilation. We found that mitochondrial DNA levels were significantly increased in culture supernatant from A549 cells exposed to mechanical stretch as compared to unstretched cells for all stretch periods (Fig 1A). This result was further validated by digital droplet PCR showing a significant increase in the mtDNA/gDNA ratio in the supernatant of cells exposed to 24h stretch as compared to unstretched cells (S1 Fig). In addition to mtDNA, we also measured an increase in extracellular ATP in supernatants from A549 cells exposed to 24 hrs. of stretch as compared to unstretched cells (Fig 1B). Although

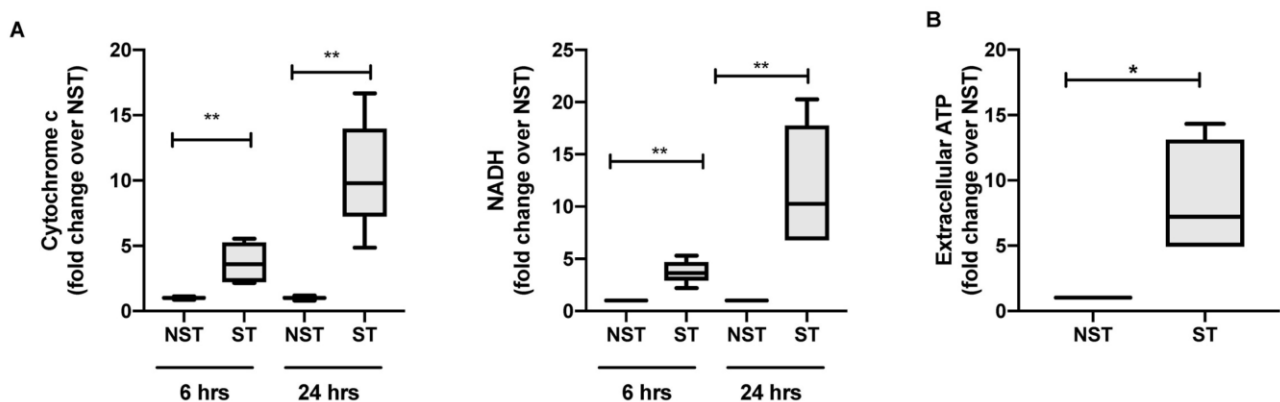


Fig 1. Mitochondrial DAMPs are released during cyclic mechanical stretch. (A) Mitochondrial DNA (cytochrome C oxidase III and NADH) release in conditioned supernatants from human alveolar type II-like epithelial A549 cells submitted to cell stretching for 6 and 24 hours or kept in static conditions, expressed as fold changes over non stretched cells. (B) Extracellular ATP quantified by luciferase assay in conditioned supernatants from human alveolar type II-like epithelial A549 cells submitted to cell stretching for 24 hours, and from cells kept in static conditions, expressed as fold changes over non stretched cells. Data represent median with interquartile range of at least three independent experiments. **P* < 0.05, ***P* < 0.01, Mann-Whitney test (A-B). NST: non stretch, ST: stretch, NADH: nicotinamide adenine dinucleotide.

<https://doi.org/10.1371/journal.pone.0225468.g001>

little differences were observed in stretched cells using phase contrast and fluorescent microscopy, we measured by FACS a small increase in the number of dead cells (or cells with permeable/ruptured membranes) after cell stretching compared with cells kept in static conditions ([S2 Fig](#)). These data demonstrate that mitochondrial DAMPs are released in the extracellular space during cyclic mechanical stretch.

Conditioned media from cell exposed to stretch activates TLR9 signaling

To determine whether the mitochondrial DAMPs released by mechanical stretch are biologically active, we exposed HEK BlueTM hTLR9 reporter cell line to the supernatant from stretched and unstretched cells. Supernatant from stretched cells induced a significant increase in TLR9 signaling as measured by SEAP production as compared to supernatant from unstretched cells ([Fig 2](#)). Co-incubation of conditioned media from stretch cells with TLR9 antagonist ODN TTAGGG caused a decrease in SEAP production. These data demonstrate the presence of biologically active TLR9 agonists in conditioned media from cells exposed to mechanical stretch.

Mechanical stretch causes the extracellular release of IL-8 via a TLR9 dependent mechanism

Next, we explored whether mtDAMPs may be involved in stretch-induced IL-8 secretion through TLR9 signaling. We measured the production of the IL-8 chemokine in media from cells exposed to stretch and co-incubated with the TLR9 antagonist ODN TTAGGG. We found that IL-8 concentrations increased in the supernatant from stretched cells as compared to unstretched cells for every time period in a time-dependent manner ([Fig 3A](#)). Interestingly, stretch-induced IL-8 secretion decreased with co-incubation with a TLR9 antagonist ([Fig 3B](#)).

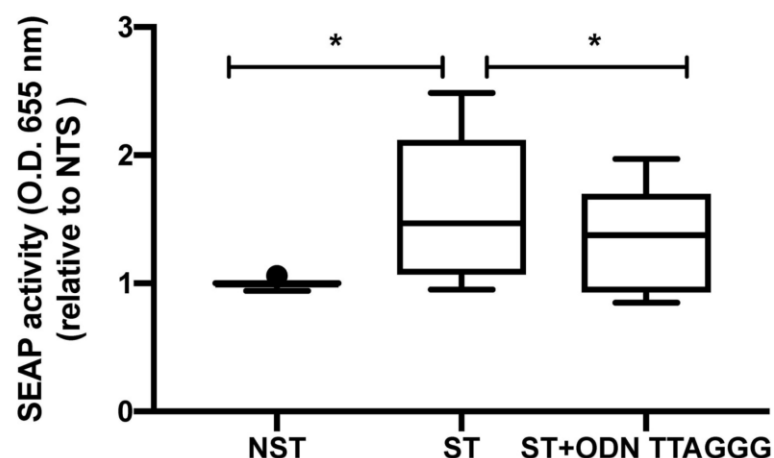


Fig 2. Supernatant from 24 hours stretched A549 cells induces TLR9 signaling that can be blocked with TLR9 antagonists. Supernatant collected from 24 hours stretched A549 cells and from unstretched cells were co-incubated with HEK-Blue hTLR9 reported cell line either alone or with TLR9 antagonists ODN TTAGGG. After 24 hours supernatants were analyzed for activity by spectroscopy of the target transgene NF- κ B induced secreted embryonic alkaline phosphatase absorbance at 655 nm. Data are expressed as fold change over NST and represent median with interquartile range of at least three independent experiments. * $P < 0.05$, Mann-Whitney test (NST vs ST) and Wilcoxon signed-rank test (ST vs ST+ ODN TTAGGG) with FDR correction. NST: non stretch, ST: stretch.

<https://doi.org/10.1371/journal.pone.0225468.g002>

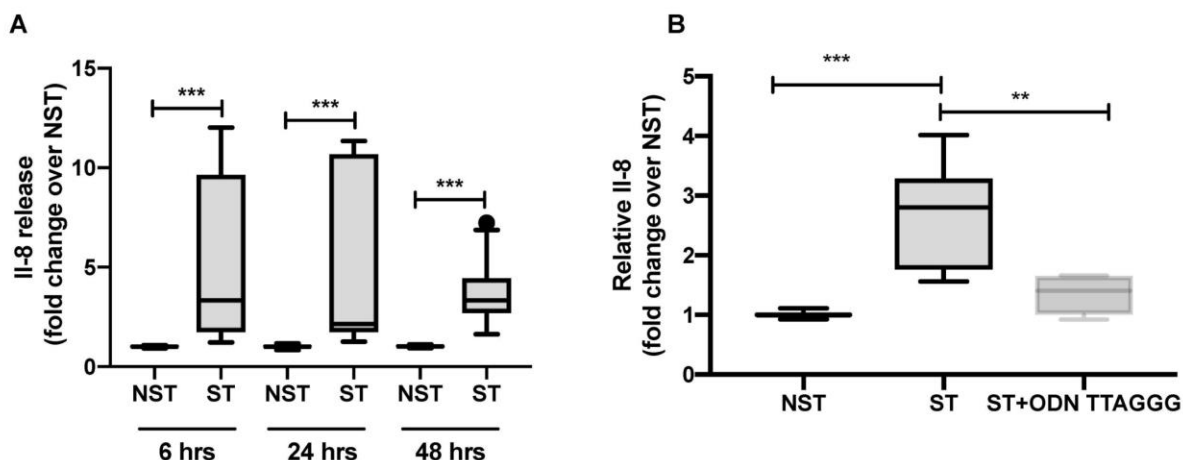


Fig 3. Mechanical stretch induces extracellular secretion of pro-inflammatory cytokine IL-8 that can be blocked with TLR9 antagonists. (A) IL-8 concentration measured in supernatant collected from A549 cells submitted to cyclic mechanical stretch for 6, 24 and 48 hours and their control unstretched cells. (B) IL-8 concentration measured in supernatant collected from A549 cells stretched for 24 hours and co-incubated with TLR9 antagonist ODN TTAGGG. Data are expressed as fold change over NST and represent median with interquartile range of at least three independent experiments. ** $P < 0.01$, *** $P < 0.001$, Mann-Whitney test (A), Kruskall-Wallis test with FDR correction (B). NST: non stretch, ST: stretch.

<https://doi.org/10.1371/journal.pone.0225468.g003>

Since mtDNA promotes TLR9-mediated inflammation, these data suggest that mtDNA may represent a potential TLR9 agonist in our *in vitro* stretch model. Once released in the extracellular milieu by stretch, mtDNA may elicit a paracrine pro-inflammatory effect through TLR9 signaling.

Mechanical stretch induces the production and secretion of IL-1 β by stretched monocyte-derived macrophages

Lung macrophages are tissue-resident immune cells that play a critical role in maintaining homeostasis and fighting infection in the lungs. We investigated whether mechanical stretch could synergistically activate macrophages with TLR agonists either directly and/or indirectly. IL-1 β concentrations were measured in conditioned media, and in cell lysates from activated macrophages. Using immunoblotting and ELISA, we found that IL-1 β concentration significantly increase in supernatant from monocyte-derived macrophages submitted to 24 hrs. of mechanical stretch as compared to unstretched cells (Fig 4A). However, there was no difference in IL-1 β production in cell lysates of stretched monocyte-derived macrophages as compared to unstretched monocyte-derived macrophages (Fig 4B). Interestingly, we found a synergistic effect between mechanical stretch and the TLR4 agonist LPS for IL-1 β production and secretion in supernatant and cell lysates from monocyte-derived macrophages. These experiments suggest that mechanical stretch induces the secretion of IL-1 β by monocyte-derived macrophage with a synergistic effect with LPS.

Conditioned media from stretched A549 cells induces chemotaxis of human neutrophils

Since IL-8 and fMLP are both neutrophil chemokines, we evaluated next the chemoattractant properties of supernatants collected from A549 cells exposed to cyclic mechanical stretch. Conditioned media from A459 cells exposed to mechanical stretch for 24 hrs. induced chemotaxis of human neutrophils as compared to unstretched cells (Fig 5A). Blocking formyl peptide

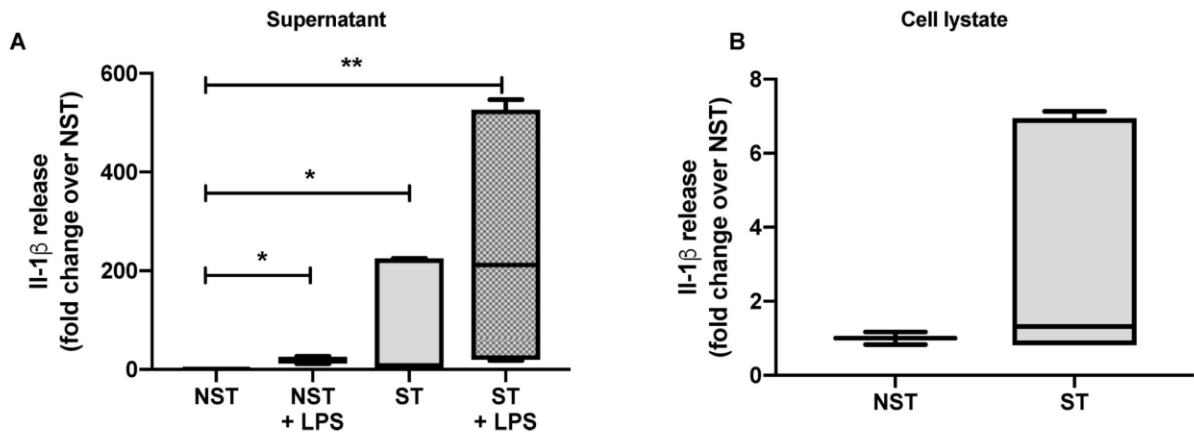


Fig 4. Mechanical stretch and TLR4 agonists LPS have a synergistic effect on pro-inflammatory cytokines IL-1 β secretion in monocytes derived macrophages submitted to mechanical stretch. (A) IL-1 β concentration measured by ELISA in supernatant isolated from monocytes derived macrophages submitted to 24 hours cyclic mechanical stretch and/or co-incubated with LPS. (B) IL-1 β concentration measured by ELISA in cell lysates from monocytes derived macrophages submitted to 24 hours mechanical stretch and unstretched cells. Data are expressed as fold change over NST and median with interquartile range of at least three independent experiments. * $P < 0.05$, ** $P < 0.01$, Kruskall-Wallis test with FDR correction (A), Mann-Whitney test (B). NST: non stretch, ST: stretch, LPS: lipopolysaccharide.

<https://doi.org/10.1371/journal.pone.0225468.g004>

receptors or CXR1 receptors alone were not sufficient to decrease stretch-induced chemotaxis (Fig 5B). Interestingly when both receptors were blocked, we measured a significant decrease in chemotaxis after both 6 and 24 hrs of mechanical stretch. Those results suggest that

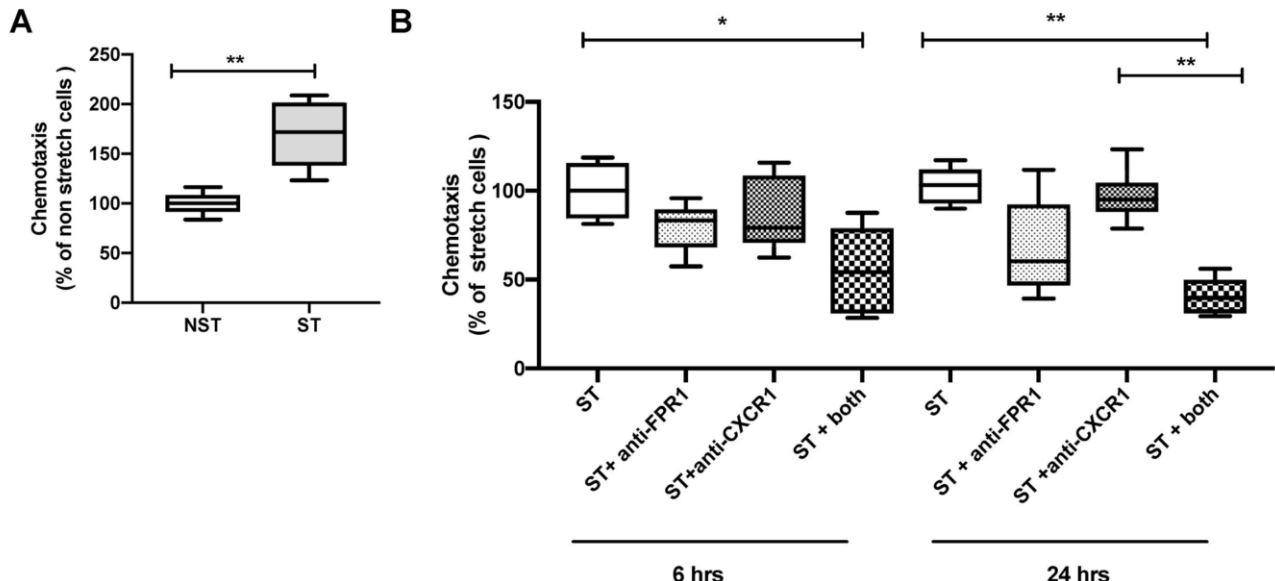


Fig 5. Supernatant from stretched A549 cells induces neutrophils chemotaxis mediated principally by chemoattractant fMLP. Boyden chamber chemotaxis assay of human primary neutrophils stimulated with (A) conditioned supernatants collected from A549 cells submitted mechanical stretch for 24 hours and unstretched A549 cells and (B) antibodies against the fMLP receptor (anti-FPR1) and the IL-8 receptor (anti-CXCR1). Data are expressed as percentage of NST (A) and ST (B) and represent median with interquartile range of at least three independent experiments. * $P < 0.05$, ** $P < 0.01$, Mann-Whitney test (A), Kruskall-Wallis test with FDR correction (B). NST: non stretch, ST: stretch, FPR1: anti-formyl peptide receptor 1, CXCR1: C-X-C motif chemokine receptor 1.

<https://doi.org/10.1371/journal.pone.0225468.g005>

mitochondrial fMLP may be released by A549 cells during stretch, and may act synergistically with IL-8 to induce neutrophil chemotaxis.

Lung inflammation and alarmins in rabbits submitted to adverse mechanical ventilation

We next tested whether our *in vitro* findings could be translated into a rabbit model of VILI. In the rabbit model, an injurious mechanical ventilation (MV) regimen induced significant lung injury and neutrophil recruitment, as compared with control spontaneously breathing (SB) animals (Fig 6A, 6B and 6C). Despite the development of lung injury, pro-inflammatory cytokines were only mildly elevated in the lung tissue of ventilated rabbit as compared to SB animals. MV increased TNF- α gene expression and BAL concentration, but not IL-8 (Fig 7). Mitochondrial DNA could be detected in BAL fluids from both SB and MV animals (Fig 8A, 8B and 8C). Although mitochondrial DNA concentration increased overtime in BAL from MV animals as compared to SB animals, the difference was not statistically different.

Significantly higher ATP was found in BAL fluids from rabbits subjected mechanically ventilated for 8 hrs. (Fig 9A). Similar to supernatants from stretched A549 cells, BAL fluids from MV animals induced *in vitro* chemotaxis of human neutrophils, particularly in BAL fluids originating from animals ventilated for 8 hrs. (Fig 9B). Taken together, these results suggest

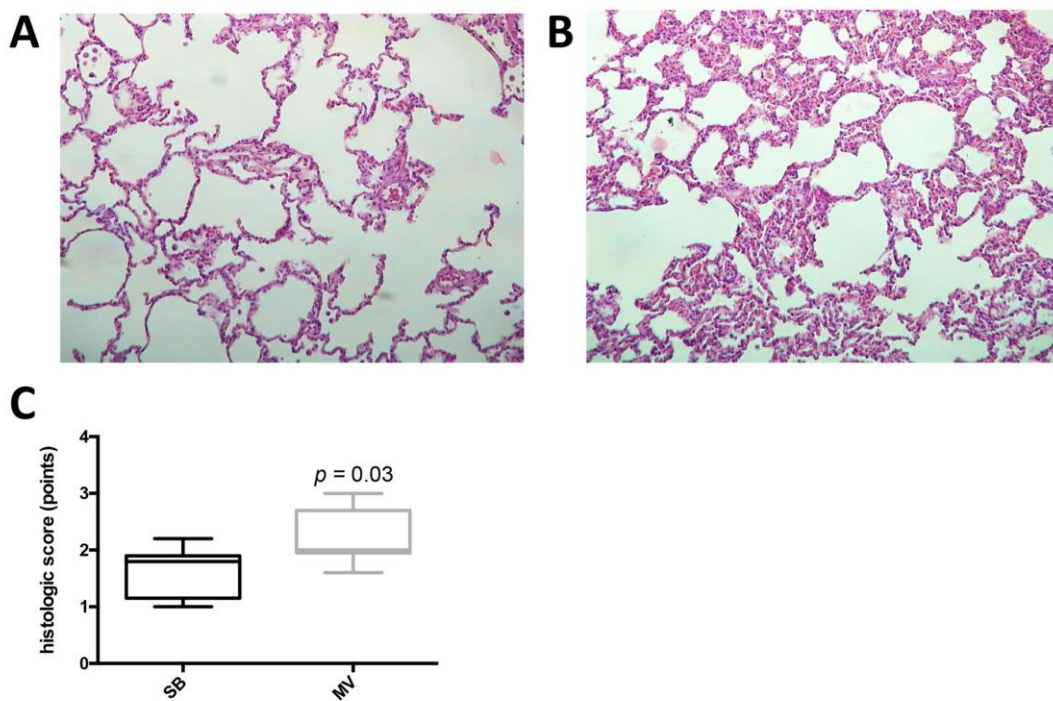


Fig 6. Rabbits exposed to injurious mechanical ventilation present signs of lung injury characterized by massive neutrophil infiltration. Representative lung histology (hematoxylin-eosin stain) in spontaneously breathing rabbits (A) and in rabbits submitted to mechanical ventilation for 4 hours (B). Histological lung injury score in rabbits submitted to mechanical ventilation compared to spontaneously breathing (SB) animals. Tissue injury was scored based on the degree of polymorphonuclear infiltration, hemorrhage, and edema in the interstitial and alveolar spaces on a scale from 0 to 3 points (C). Data represent median with interquartile range of at least three independent experiments. $P < 0.05$ as indicated, Mann-Whitney test. MV: mechanical ventilation, SB: spontaneously breathing.

<https://doi.org/10.1371/journal.pone.0225468.g006>

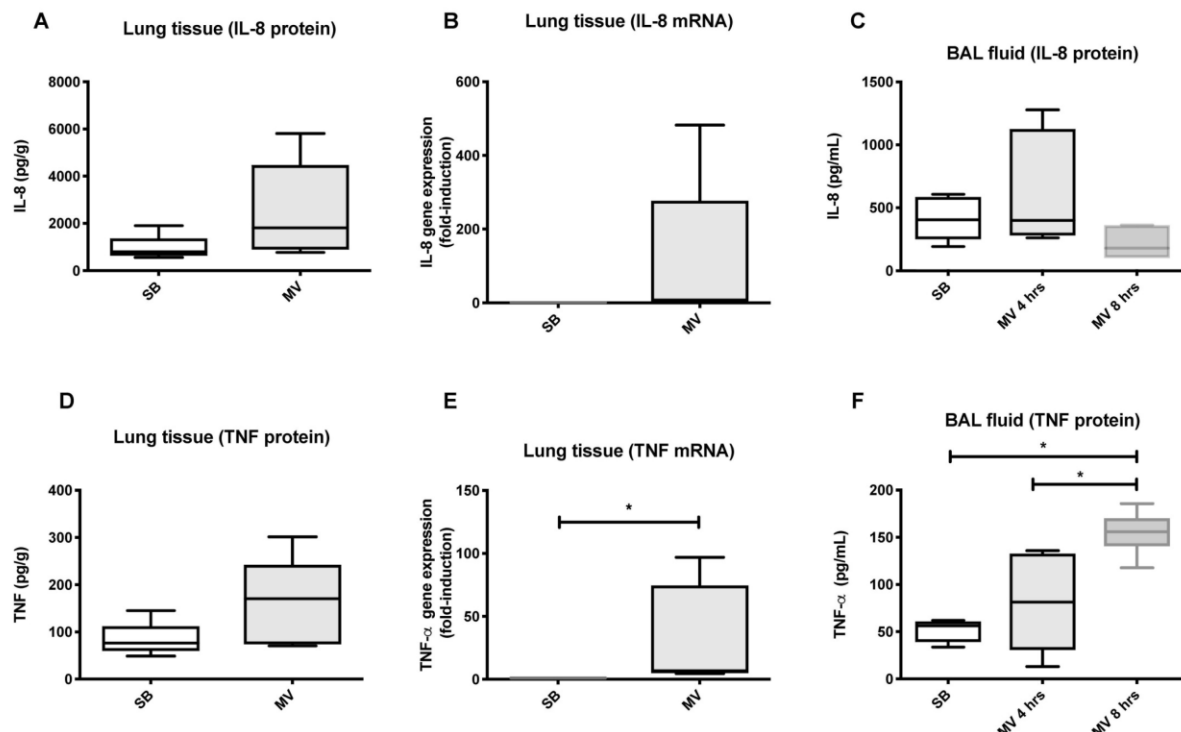


Fig 7. Injurious mechanical ventilation induces a pro-inflammatory response in the lungs of ventilated rabbits. Lung production (lung tissue mRNAs and proteins) and secretion into the alveolar space (bronchoalveolar lavage [BAL] fluid) of the IL-8 chemokine (A, B, and C) and the pro-inflammatory cytokines TNF- α (D, E, and F) by rabbits submitted to mechanical ventilation and by spontaneously breathing animals. Data represent median with interquartile range of at least three independent experiments. * $P < 0.05$, Mann-Whitney test (A,B,D, and E), Kruskall-Wallis test with FDR correction (C and F). MV: mechanical ventilation, SB: spontaneously breathing.

<https://doi.org/10.1371/journal.pone.0225468.g007>

that mitochondrial alarmins are released in the lower airways of rabbits submitted to an injurious MV and induces neutrophils chemotaxis. Further studies will be required to determine

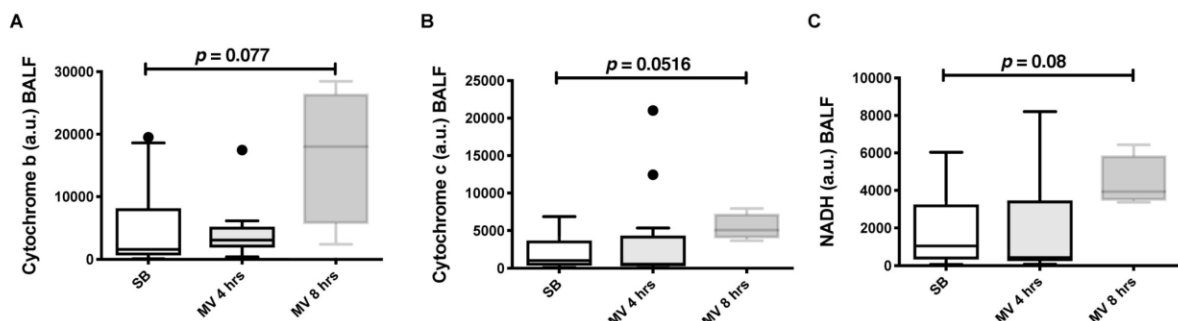


Fig 8. Injurious mechanical ventilation causes the extracellular release of mitochondrial DNA in ventilated rabbits. Mitochondrial DNA (cytochrome B, [A]; cytochrome C oxidase III, [B] and NADH, [C]) measured by quantitative PCR in bronchoalveolar lavage (BAL) fluid from rabbits submitted to mechanical ventilation for 4 and 8 hours and in spontaneously breathing animals. Data represent median with interquartile range of at least three independent experiments. Kruskall-Wallis test with FDR correction (A-C). MV: mechanical ventilation, SB: spontaneously breathing.

<https://doi.org/10.1371/journal.pone.0225468.g008>

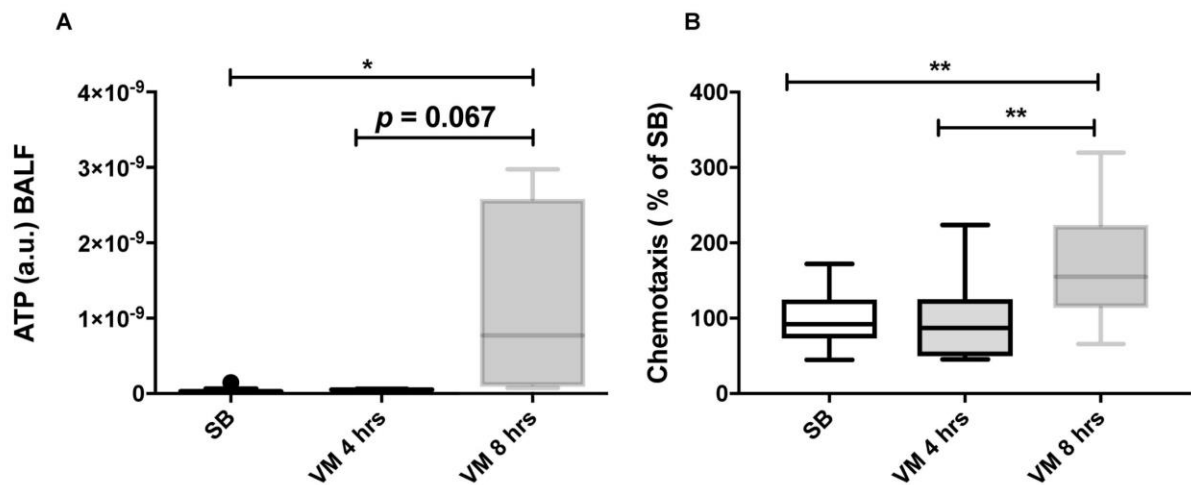


Fig 9. BAL fluid from ventilated rabbits presents elevated ATP level and has chemotactic activity. (A) Extracellular ATP measured in bronchoalveolar lavage (BAL) fluid from rabbits submitted to mechanical ventilation for 4 and 8 hours and in spontaneously breathing animals. (B) Chemotactic activity of BAL fluid from rabbits submitted to mechanical ventilation for 4 and 8 hours and in spontaneously breathing animals. Human primary neutrophil chemotaxis was measured in a 96-well Boyden chamber and expressed as percentage migration compared to SB. Data represent median with interquartile range of at least three independent experiments. * $P < 0.05$, ** $P < 0.01$, Kruskall-Wallis test with FDR correction (A-B). MV: mechanical ventilation, SB: spontaneously breathing.

<https://doi.org/10.1371/journal.pone.0225468.g009>

whether the release of mitochondrial DAMPs during mechanical ventilation is caused by an active process or the result of cell death.

Mitochondrial DNA in bronchoalveolar lavage fluids from ARDS patients

Finally, we investigated the human relevance of our experimental and animal data by analyzing BAL fluids from human patients with ARDS.

Mitochondrial DNA was detectable by qRT PCR in BALF from patients with low and high inflammatory ARDS, defined as a neutrophil count of $> 80\%$ and protein levels $> 2 \text{ mg/mL}$. Mitochondrial DNA concentration was the highest in the BALF from patients on day 1 of high inflammatory ARDS as compared to healthy volunteers and declined at day 7 of ARDS (Fig 10).

BAL fluids from ARDS patients at Day 1 with a high inflammatory profile induced TLR9 signaling in exposed HEK Blue™ hTLR9 reporter cells (S3A Fig), and this activity was inhibited by the TLR9 antagonist ODN TTAGGG (S3B Fig).

Discussion

Herein, we show that mitochondrial DNA, ATP and fMLP are released from human type II-like A459 lung alveolar cells submitted to cyclic stretch. Similarly, the same pro-inflammatory alarmins are found in the airways of rabbits submitted to a short injurious MV regimen, and mitochondrial DNA concentrations were found to be markedly elevated in BAL fluids from patients with ARDS. Conditioned media from stretched cells and BAL from ventilated rabbits were shown to induce neutrophil chemotaxis, attributable to the mitochondrial fMLP chemo-kine with a possible synergistic effect with IL-8. In addition, conditioned media from stretched cells could modulate stretch-induce IL-8 secretion through TLR9 signaling, suggesting that mtDNA may be a TLR9 agonist in this system.

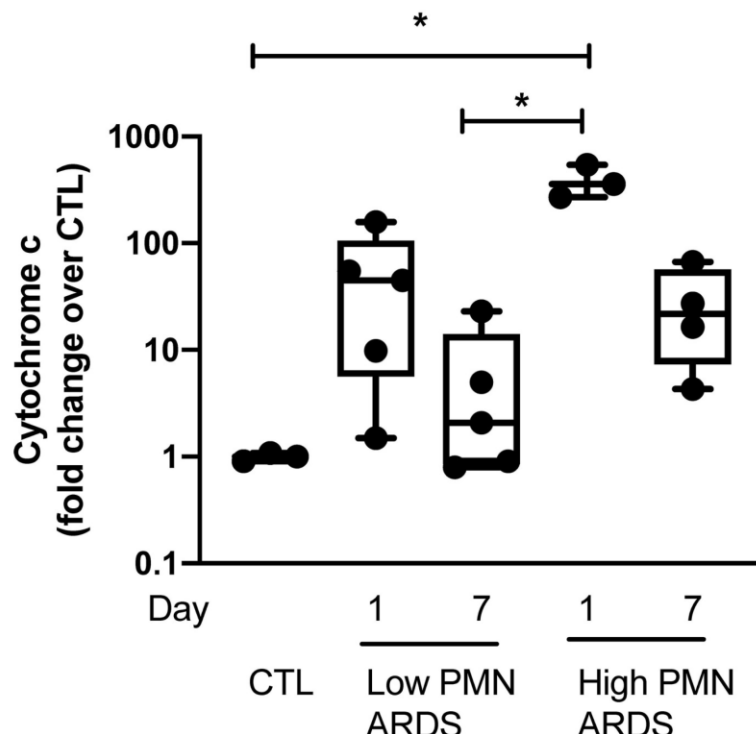


Fig 10. Mitochondrial DNA are released in BALF of patients with ARDS. Mitochondrial DNA (cytochrome C oxidase III) measured by quantitative PCR in bronchoalveolar lavage fluid of patients with ARDS at day 1 and day 7 of presentation and healthy volunteers. Patients with ARDS were categorized as “highly inflammatory” (high PMN) if they contained > 80% neutrophils and > 2 mg/mL proteins or “low inflammatory” (low PMN) if they did not meet those criteria. Data are expressed as fold change over healthy volunteers and represent median with interquartile range of at least three independent experiments. * $P < 0.05$, Kruskall-Wallis test with FDR correction (A-B). CTL: controls (healthy volunteers), PMN: polymorphonuclear, ARDS: acute respiratory distress syndrome.

<https://doi.org/10.1371/journal.pone.0225468.g010>

Lung inflammation is a hallmark of acute lung injury and ARDS [7, 31]. Lung inflammation originates from the primary lung insult (pneumonia, sepsis, gastric fluid aspiration, trauma, etc.). It has become evident that MV could *per se* induce airway inflammation, and more importantly synergized with the primary lung injury. Supporting this, ARDS patients receiving lung protective ventilator strategy have lower levels of alveolar and systemic inflammation, in particular less alveolar neutrophils, and lower levels of the pro-inflammatory cytokines IL-1 β and TNF- α [32].

Recent studies demonstrated that during cell death and organ injuries, certain molecules released from mitochondria such as mtDNA, fMLP and ATP may function as DAMPs and activate the innate immune system [17, 33]. The role of mitochondrial DAMPs in the pathogenesis of lung inflammation were highlighted in an animal study by Zhang et al [34], who demonstrated that intravenous mtDNA injection in rats induced acute lung injury through activation of the TLR9/NF- κ B signaling pathway.

In the present study, we demonstrated that mechanical stretch causes extracellular release of mitochondrial DNA and ATP in both our experimental and animal model of MV. Cellular necrosis and disruption of cytoplasmic membrane may constitute a potential mechanism for

the extracellular release of mitochondrial DAMPs in our stretch model. However, recent experimental and human studies with trauma patients [35, 36] have demonstrated that extracellular release of mitochondrial DNA in absence of markers of cellular necrosis, suggesting another mechanism for mitochondrial DAMPs release after trauma. Experimental studies of mitochondrial injury have shown that disruption of mitochondrial membrane integrity lead to leakage of free-mtDNA fragments into the cytosol followed by extracellular release [37]. In addition, mitochondrial components of injured mitochondria may also be actively released into the extracellular milieu through autophagy [38] and mitochondrial derived vesicles [39], without disruption of the cytoplasmic membrane integrity. Since mitochondria anchor to the cytoskeleton, they may also function as mechanotransducers and respond directly to cyclic mechanical stretch. This was suggested by Ali et al. [40] who showed that mechanical strain in endothelial cells induces reactive oxygen species (ROS) production by mitochondria that was abrogated after treatment with cytochalasin D, a known disruptor of cytoskeletal network. In our in vitro experiments, no significant necrosis or apoptosis was observed in stretched cells. This suggests that stretch-induced mtDAMPs release in our study may be the result of an active process triggered by cyclic strain rather than the result of disruption of cellular integrity.

Plasma release of cell-free mtDNA has been shown to occur in patients with trauma and sepsis [18]. In VILI animal models mtDNA release has been inconsistently found. Increased mtDNA has been measured in BAL fluids from mice in an acid-induced lung injury model [41], as well as in rats exposed to injurious ventilation [42]. In other MV-induced lung injury in mice [43] and rabbits [44], MV was not associated with an increase in mtDNA concentrations in BAL fluid. In our model, mtDNA was released within the airway from ventilated rabbits but there was high variability in mtDNA content among different animal groups for the three mitochondrial primers tested. A possible explanation for these apparent discrepant results is that levels of lung injury were different in these VILI models, with lower tidal volumes [44], and protective PEEP [43]. Difference in mtDNA concentration in BAL fluid among different VILI models may also be explained by heterogeneity in cellular capacity to restore mitochondrial density following injury resulting in progressive loss of intracellular mtDNA copy number. This was demonstrated by Haden et al. [45] in a murine model peritonitis induced by *Staphylococcus aureus*, showing that initial mitochondrial injury and loss of mitochondrial DNA copy number could be restored through the activation of mitochondrial biogenesis.

After demonstrating that mechanical stretch causes extracellular release of mtDNA and ATP, we explored next whether mitochondrial DAMPs released by stretch were biologically active. Mitochondrial DNA activates the immune response directly via the activation of TLR9 pathways resulting in a pro-inflammatory response [37]. Zhang et al. showed that mitochondrial DNA injected IV to rats induced lung inflammation, increased permeability of the alveolar capillary barrier [17], and upregulated TLR9 in lung tissue [34]. In line with those findings, we show that conditioned media from stretched A549 cells as well as BAL fluid from ventilated rabbits both triggered TLR9 signaling in a HEK-Blue hTLR9 reported cell line. Interestingly, mitochondrial DNA seems to be more potent as a TLR9 agonist when it is oxidized [46]. The production of reactive oxygen species by different alveolar cells is thought to be an important pathogenic and pro-inflammatory mechanism during ARDS, due to inflammation and hyperoxic environment [47]. Aside from protein and lipid oxidation, oxidation of mitochondrial DNA could then well represent an important pro-inflammatory mediator of acute lung injury. To further support the role of TLR9 signaling in pro-inflammatory response induced by stretch, blockade of the mitochondrial DNA receptor TLR9 by the TLR9 antagonist ODN TTAGGG abrogated the stretch-induced IL-8 secretion by these cells. This strongly suggests autocrine and paracrine cell activation by cytoplasmic alarmins released during cell cyclic stretch.

Polymorphonuclear neutrophil recruitment to the lung and neutrophil-dependent tissue damage have been proposed as key pathogenic factors in VILI and ARDS [5, 48]. It was long thought that the main neutrophil chemotactic and activation factor was the CXC chemokine IL-8. It was however recently shown in a murine model of aseptic thermal hepatic injury that mitochondrial fMLP released by injured cells was the essential chemotactic factor bringing neutrophils to the necrotic lesion, overriding the effect of CXC chemokines [16]. The formylated peptide fMLP found in both bacterial and mitochondrial walls attracts and activates neutrophils either directly by binding to fMLP receptor-1 (FPR1) or indirectly by inducing IL-8 secretion [49]. Chemoattractant properties on human neutrophils could be demonstrated in both conditioned media from stretched cells and in BAL fluid from ventilated rabbits, supporting previous results in rabbit VILI models [44]. Interestingly, the neutrophil chemotactic activity present in supernatants from stretched lung cells could be reduced with FPR1 blocking alone and completely inhibited by combined CXCR1 and FPR1 blockade. This suggests that the main chemotactic factor present in conditioned supernatants from stretched cells was the mitochondrial fMLP.

IL-1 β has been shown to play a major role as a local pro-inflammatory mediator in the context of ARDS and VILI, and is secreted by alveolar macrophages and by alveolar epithelial cells [6, 7, 31, 50]. IL-1 β can be secreted in response to various stimuli, including bacterial molecules such as Gram-negative lipopolysaccharide (LPS). The production of bioactive IL-1 β is tightly regulated and follows a multistep pathway. It requires both the upregulation of the pro-IL-1 β gene expression, and the posttranslational cleavage of pro-IL-1 β into mature IL-1 β . This latter step is dependent on the activation of caspase-1, part of the NALP3 inflammasome complex [51]. It was recently recognized that endogenous danger signals (alarmins) originating from injured/necrotic cells could trigger the production of IL-1 β , and be responsible for aseptic inflammation. Mitochondrial DNA, when released from injured cells, upregulates the IL-1 β gene through its interaction with its receptor, TLR9. Extracellular ATP, which is also released by injured/necrotic cells, induces the assembly of the NALP3 inflammasome and caspase-1 activation through its interaction with the P2X₇ receptor, resulting in the cleavage of pro-IL-1 β into bioactive IL-1 β [16, 17]. Our results confirm that cyclic stretch of human monocyte-derived macrophages induced the production and the release of IL-1 β , and that cyclic stretch synergized with co-treatment of macrophages with LPS. We therefore postulate that cyclic stretch induces the release by lung cells of mitochondrial DNA (TLR9 agonist), and ATP, and that this leads to the production of IL-1 β by macrophages, and plays an important local pro-inflammatory signal in the lung submitted to (injurious) mechanical ventilation.

Recent work supports the role of NLRP3 inflammasome in the pathogenesis of VILI. NLRP3 inflammasome gene expression was upregulated in ventilated patients, and also in mice ventilated with high tidal volumes, with increased caspase-1 activation, and increased uric acid levels, another NLRP3 agonist [52]. Finally, NLRP3-deficient mice showed less signs of VILI, and IL-1 receptor antagonist partially protected mice against VILI, supporting previously published data [24, 52]. ATP released into the airways during VILI [30] may also therefore be an agonist for NLRP3 in this context. Interestingly, Wu et al. recently reported that mechanical ventilation in mice and *in vitro* alveolar macrophage cyclic stretch induced the assembly of NLRP3 and activated caspase-1, leading to the production and secretion of bioactive IL-1 β [22]. Caspase-1 activation was dependent on the generation of reactive oxygen species by mitochondria, but the possible implication of extracellular ATP as a trigger for inflammasome activation was not directly tested.

Recent clinical studies in patients with sepsis or ARDS suggest that mtDNA levels may be used as a biomarker reflecting the severity of critical illness and predicting mortality. In a large clinical study, Nakahira et al [53], demonstrated that elevated cell-free mtDNA level was

associated with ICU mortality. In the present study, we showed that mtDNA could be measured in BAL fluid from patients with ARDS and increased with the degree of lung inflammation. Further studies are needed to address the relevance of alveolar release of mtDNA in ARDS, as a marker or a potential mediator of lung injury.

Our study has some limitations. First, we cannot exclude the participation of bacterial DNA in BAL fluids from patients for TLR9-dependent activation of target inflammatory cells. However, we excluded the presence of bacterial DNA using 16S PCR primers in cell supernatants and in BAL fluids from ventilated rabbits, suggesting that TLR9 was activated in those models by mtDNA. Second, we compared in our animal model an injurious ventilatory regimen (large tidal volume and zero end-expiratory pressure) to spontaneously breathing animals. This choice was made to compare extreme experimental conditions regarding lung cyclic stretch but may be viewed as not clinically relevant. However, in certain circumstances, such as in the operating room, some patients may be ventilated with similar regimens. Future animal studies including non-injurious mechanical ventilation groups will be required to further validate the clinical relevance of our findings. In addition, because of the pulmonary heterogeneity in ARDS, significant portions of the lungs may receive large volumes, despite “protective ventilation” protocols.

In conclusion, our data support a model of VILI based on an aseptic local inflammation due to pro-inflammatory endogenous alarmins released from lung cells injured by airway overstretching, mainly of mitochondrial origin. The presences of mitochondrial alarmins in conditioned media from stretched alveolar epithelial cells and BAL from ventilated rabbits may participate in the pro-inflammatory response induced by mechanical ventilation by attracting neutrophils (fMLP) and stimulating the secretion of pro-inflammatory cytokines by alveolar cells in an autocrine and paracrine manner (mtDNA). These lung alarmins may represent the missing molecular links between the mechanical stress imposed to lung cells, and the observed airway inflammation in critically ill patients submitted to mechanical ventilation. This model also fits with the “danger theory” in which inflammatory and immune cells will respond to mediators of cell injury, rather than to innocuous non-self molecules [54, 55]. It remains to be demonstrated if alarmins released locally by airway stretch act synergistically with other types of lung injury or infection to generate lung inflammation, as suggested by animal studies [11, 25, 56]. It also remains to be tested whether a pharmacologic modulation of alarmin pathways will prevent VILI, and decrease lung inflammation and impairment of pulmonary functions in patients with acute lung injury and ARDS.

Supporting information

S1 Fig. Mitochondrial DNA/genomic DNA ratio increases in supernatant from stretched A549 cells. Mitochondrial DNA (cytochrome C oxidase III) and genomic DNA (RPP30, single copy nuclear gene) measured in conditioned supernatants from human alveolar type II-like epithelial A549 cells submitted to cell stretching for 24 hours or kept in static conditions by digital droplet PCR. Results are expressed as mtDNA/gDNA ratio and represent median with interquartile range of at least three independent experiments. * $P < 0.05$, Mann-Whitney test. NST: non stretch, ST: stretch, mtDNA: mitochondrial DNA, gDNA: genomic DNA. (EPS)

S2 Fig. Cells exposed to mechanical stretch present not significant morphological difference on phase contrast microscopy examination but a small increase in cellular permeability. A549 cells viability after 24 hrs of cell stretching. Upper panels, phase contrast microscopy; middle panels, fluorescence microscopy (calcein(+)live cells in green, and propidium iodide (+)nuclei of dead cells in red); lower panels, flow cytometry analysis of stretched vs. static cells;

7-AAD(+)dead cells in red, 7-AAD(-)live cells in green, percentage of live cells indicated. (TIF)

S3 Fig. BALF from patients with high inflammatory ARDS induces TLR9 signaling that can be blocked with TLR9 antagonists. BALF collected from patients with ARDS at day 1 of presentation and healthy were co-incubated with HEK-Blue hTLR9 reported cell line either alone (**A**) or with TLR9 antagonists ODN TTAGGG (**B**). Patients with ARDS were categorized as “highly inflammatory” (high PMN) if they contained > 80% neutrophils and > 2 mg/mL proteins or “low inflammatory” (low PMN) if they did not meet those criteria. After 24 hours BALF were analyzed for activity by spectroscopy of the target transgene NF- κ B induced secreted embryonic alkaline phosphatase absorbance at 655 nm. Data are expressed as fold change over healthy volunteers (**A**) or in arbitrary units (**B**) and represent median with interquartile range of at least three independent experiments with the exception of the group of healthy volunteers ($n = 2$). * $P < 0.05$, Mann-Whitney test (**B**). CTL: controls (healthy volunteers), PMN: polymorphonuclear, ARDS: acute respiratory distress syndrome. A.U: arbitrary units. (EPS)

S1 File. Supplementary method.
(DOCX)

Acknowledgments

The authors thank Thomas R. Martin (University of Washington, Seattle, WA) for the gift of BAL samples from ARDS patients and healthy volunteers.

Author Contributions

Conceptualization: Pierre-Emmanuel Charles, Jérôme Pugin.

Data curation: Serge Grazioli.

Formal analysis: Serge Grazioli.

Funding acquisition: Pierre-Emmanuel Charles, Jérôme Pugin.

Investigation: Serge Grazioli, Irène Dunn-Siegrist, Laure-Anne Pauchard.

Methodology: Serge Grazioli, Irène Dunn-Siegrist, Laure-Anne Pauchard, Pierre-Emmanuel Charles, Jérôme Pugin.

Supervision: Pierre-Emmanuel Charles, Jérôme Pugin.

Writing – original draft: Serge Grazioli.

Writing – review & editing: Serge Grazioli, Mathieu Blot, Pierre-Emmanuel Charles, Jérôme Pugin.

References

1. Pugin J. Is the ventilator responsible for lung and systemic inflammation? *Intensive Care Med.* 2002; 28 (7):817–9. <https://doi.org/10.1007/s00134-002-1320-8> PMID: 12349817.
2. Tremblay L, Valenza F, Ribeiro SP, Li J, Slutsky AS. Injurious ventilatory strategies increase cytokines and c-fos m-RNA expression in an isolated rat lung model. *J Clin Invest.* 1997; 99(5):944–52. <https://doi.org/10.1172/JCI119259> PMID: 9062352; PubMed Central PMCID: PMC507902.

3. Ventilation with lower tidal volumes as compared with traditional tidal volumes for acute lung injury and the acute respiratory distress syndrome. The Acute Respiratory Distress Syndrome Network. N Engl J Med. 2000; 342(18):1301–8. <https://doi.org/10.1056/NEJM200005043421801> PMID: 10793162.
4. Serpa Neto A, Cardoso SO, Manetta JA, Pereira VG, Esposito DC, Pasqualucci Mde O, et al. Association between use of lung-protective ventilation with lower tidal volumes and clinical outcomes among patients without acute respiratory distress syndrome: a meta-analysis. JAMA. 2012; 308(16):1651–9. <https://doi.org/10.1001/jama.2012.13730> PMID: 23093163.
5. Kawano T, Mori S, Cybulsky M, Burger R, Ballin A, Cutz E, et al. Effect of granulocyte depletion in a ventilated surfactant-depleted lung. J Appl Physiol. 1987; 62(1):27–33. <https://doi.org/10.1152/jappl.1987.62.1.27> PMID: 3558186.
6. Pugin J, Ricou B, Steinberg KP, Suter PM, Martin TR. Proinflammatory activity in bronchoalveolar lavage fluids from patients with ARDS, a prominent role for interleukin-1. Am J Respir Crit Care Med. 1996; 153(6 Pt 1):1850–6. <https://doi.org/10.1164/ajrccm.153.6.8665045> PMID: 8665045.
7. Pugin J, Vergheze G, Widmer MC, Matthay MA. The alveolar space is the site of intense inflammatory and profibrotic reactions in the early phase of acute respiratory distress syndrome. Crit Care Med. 1999; 27(2):304–12. <https://doi.org/10.1097/00003246-199902000-00036> PMID: 10075054.
8. Dunn I, Pugin J. Mechanical ventilation of various human lung cells in vitro: identification of the macrophage as the main producer of inflammatory mediators. Chest. 1999; 116(1 Suppl):95S–7S. https://doi.org/10.1378/chest.116.suppl_1.95s PMID: 10424615.
9. Pugin J, Dunn I, Jolliet P, Tassaux D, Magnenat JL, Nicod LP, et al. Activation of human macrophages by mechanical ventilation in vitro. Am J Physiol. 1998; 275(6 Pt 1):L1040–50. <https://doi.org/10.1152/ajplung.1998.275.6.L1040> PMID: 9843840.
10. Bregeon F, Roch A, Delpierre S, Ghigo E, Autillo-Touati A, Kajikawa O, et al. Conventional mechanical ventilation of healthy lungs induced pro-inflammatory cytokine gene transcription. Respir Physiol Neurobiol. 2002; 132(2):191–203. [https://doi.org/10.1016/s1569-9048\(02\)00069-1](https://doi.org/10.1016/s1569-9048(02)00069-1) PMID: 12161332.
11. Charles PE, Martin L, Etienne M, Croisier D, Piroth L, Lequeu C, et al. Influence of positive end-expiratory pressure (PEEP) on histopathological and bacteriological aspects of pneumonia during low tidal volume mechanical ventilation. Intensive Care Med. 2004; 30(12):2263–70. <https://doi.org/10.1007/s00134-004-2442-y> PMID: 15536527.
12. Vaneker M, Halbertsma FJ, van Egmond J, Netea MG, Dijkman HB, Snijdelaar DG, et al. Mechanical ventilation in healthy mice induces reversible pulmonary and systemic cytokine elevation with preserved alveolar integrity: an in vivo model using clinical relevant ventilation settings. Anesthesiology. 2007; 107(3):419–26. <https://doi.org/10.1097/01.anes.0000278908.22686.01> PMID: 17721244.
13. Oudin S, Pugin J. Role of MAP kinase activation in interleukin-8 production by human BEAS-2B bronchial epithelial cells submitted to cyclic stretch. Am J Respir Cell Mol Biol. 2002; 27(1):107–14. <https://doi.org/10.1165/ajrcmb.27.1.4766> PMID: 12091253.
14. Streetz RW, Vlahakis NE, Walters BJ, Schroeder MA, Hubmayr RD. Validation of a new live cell strain system: characterization of plasma membrane stress failure. J Appl Physiol. 2001; 90(6):2361–70. <https://doi.org/10.1152/jappl.2001.90.6.2361> PMID: 11356803.
15. Vlahakis NE, Hubmayr RD. Invited review: plasma membrane stress failure in alveolar epithelial cells. J Appl Physiol. 2000; 89(6):2490–6; discussion 7. <https://doi.org/10.1152/jappl.2000.89.6.2490> PMID: 11090606.
16. McDonald B, Pittman K, Menezes GB, Hirota SA, Slaba I, Waterhouse CC, et al. Intravascular danger signals guide neutrophils to sites of sterile inflammation. Science. 2010; 330(6002):362–6. <https://doi.org/10.1126/science.1195491> PMID: 20947763.
17. Zhang Q, Raoof M, Chen Y, Sumi Y, Sursal T, Junger W, et al. Circulating mitochondrial DAMPs cause inflammatory responses to injury. Nature. 2010; 464(7285):104–7. <https://doi.org/10.1038/nature08780> PMID: 20203610; PubMed Central PMCID: PMC2843437.
18. Grazioli S, Pugin J. Mitochondrial Damage-Associated Molecular Patterns: From Inflammatory Signaling to Human Diseases. Front Immunol. 2018; 9:832. <https://doi.org/10.3389/fimmu.2018.00832> PMID: 29780380; PubMed Central PMCID: PMC5946030.
19. Kuipers MT, van der Poll T, Schultz MJ, Wieland CW. Bench-to-bedside review: Damage-associated molecular patterns in the onset of ventilator-induced lung injury. Crit Care. 2011; 15(6):235. <https://doi.org/10.1186/cc10437> PMID: 22216838; PubMed Central PMCID: PMC3388678.
20. Matsuyama H, Amaya F, Hashimoto S, Ueno H, Beppu S, Mizuta M, et al. Acute lung inflammation and ventilator-induced lung injury caused by ATP via the P2Y receptors: an experimental study. Respir Res. 2008; 9:79. <https://doi.org/10.1186/1465-9921-9-79> PMID: 19077288; PubMed Central PMCID: PMC2627837.
21. Pugin J. How tissue injury alarms the immune system and causes a systemic inflammatory response syndrome. Ann Intensive Care. 2012; 2(1):27. <https://doi.org/10.1186/2110-5820-2-27> PMID: 22788849; PubMed Central PMCID: PMC3488542.

22. Wu J, Yan Z, Schwartz DE, Yu J, Malik AB, Hu G. Activation of NLRP3 inflammasome in alveolar macrophages contributes to mechanical stretch-induced lung inflammation and injury. *J Immunol.* 2013; 190(7):3590–9. <https://doi.org/10.4049/jimmunol.1200860> PMID: 23436933; PubMed Central PMCID: PMC3608749.
23. Martinon F, Burns K, Tschopp J. The inflammasome: a molecular platform triggering activation of inflammatory caspases and processing of proIL- β . *Mol Cell.* 2002; 10(2):417–26. [https://doi.org/10.1016/s1097-2765\(02\)00599-3](https://doi.org/10.1016/s1097-2765(02)00599-3) PMID: 12191486.
24. Frank JA, Pittet JF, Wray C, Matthay MA. Protection from experimental ventilator-induced acute lung injury by IL-1 receptor blockade. *Thorax.* 2008; 63(2):147–53. <https://doi.org/10.1136/thx.2007.079608> PMID: 17901159.
25. Charles PE, Tissieres P, Barbar SD, Croisier D, Dufour J, Dunn-Siegrist I, et al. Mild-stretch mechanical ventilation upregulates toll-like receptor 2 and sensitizes the lung to bacterial lipopeptide. *Crit Care.* 2011; 15(4):R181. <https://doi.org/10.1186/cc10330> PMID: 21794115; PubMed Central PMCID: PMC3387624.
26. Mortaz E, Adcock IM, Ito K, Kraneveld AD, Nijkamp FP, Folkerts G. Cigarette smoke induces CXCL8 production by human neutrophils via activation of TLR9 receptor. *Eur Respir J.* 2010; 36(5):1143–54. <https://doi.org/10.1183/09031936.00062209> PMID: 19840968.
27. Panigrahi S, Ma Y, Hong L, Gao D, West XZ, Salomon RG, et al. Engagement of platelet toll-like receptor 9 by novel endogenous ligands promotes platelet hyperreactivity and thrombosis. *Circ Res.* 2013; 112(1):103–12. <https://doi.org/10.1161/CIRCRESAHA.112.274241> PMID: 23071157; PubMed Central PMCID: PMC3537845.
28. Drifte G, Dunn-Siegrist I, Tissieres P, Pugin J. Innate immune functions of immature neutrophils in patients with sepsis and severe systemic inflammatory response syndrome. *Crit Care Med.* 2013; 41(3):820–32. <https://doi.org/10.1097/CCM.0b013e318274647d> PMID: 23348516.
29. Park WY, Goodman RB, Steinberg KP, Ruzinski JT, Radella F 2nd, Park DR, et al. Cytokine balance in the lungs of patients with acute respiratory distress syndrome. *Am J Respir Crit Care Med.* 2001; 164(10 Pt 1):1896–903. <https://doi.org/10.1164/ajrccm.164.10.2104013> PMID: 11734443.
30. Rich PB, Douillet CD, Mahler SA, Husain SA, Boucher RC. Adenosine triphosphate is released during injurious mechanical ventilation and contributes to lung edema. *J Trauma.* 2003; 55(2):290–7. <https://doi.org/10.1097/01.TA.0000078882.11919.AF> PMID: 12913640.
31. Ware LB, Matthay MA. The acute respiratory distress syndrome. *N Engl J Med.* 2000; 342(18):1334–49. <https://doi.org/10.1056/NEJM200005043421806> PMID: 10793167.
32. Ranieri VM, Suter PM, Tortorella C, De Tullio R, Dayer JM, Brienza A, et al. Effect of mechanical ventilation on inflammatory mediators in patients with acute respiratory distress syndrome: a randomized controlled trial. *JAMA.* 1999; 282(1):54–61. <https://doi.org/10.1001/jama.282.1.54> PMID: 10404912.
33. Tschopp J. Mitochondria: Sovereign of inflammation? *Eur J Immunol.* 2011; 41(5):1196–202. <https://doi.org/10.1002/eji.201141436> PMID: 21469137.
34. Zhang JZ, Liu Z, Liu J, Ren JX, Sun TS. Mitochondrial DNA induces inflammation and increases TLR9/NF- κ B expression in lung tissue. *Int J Mol Med.* 2014; 33(4):817–24. <https://doi.org/10.3892/ijmm.2014.1650> PMID: 24535292.
35. McIlroy DJ, Jarnicki AG, Au GG, Lott N, Smith DW, Hansbro PM, et al. Mitochondrial DNA neutrophil extracellular traps are formed after trauma and subsequent surgery. *J Crit Care.* 2014; 29(6):1133 e1–5. <https://doi.org/10.1016/j.jcrc.2014.07.013> PMID: 25128442.
36. McIlroy DJ, Bigland M, White AE, Hardy BM, Lott N, Smith DW, et al. Cell necrosis-independent sustained mitochondrial and nuclear DNA release following trauma surgery. *J Trauma Acute Care Surg.* 2015; 78(2):282–8. <https://doi.org/10.1097/TA.0000000000000519> PMID: 25602756; PubMed Central PMCID: PMC4323572.
37. Yao X, Carlson D, Sun Y, Ma L, Wolf SE, Minei JP, et al. Mitochondrial ROS Induces Cardiac Inflammation via a Pathway through mtDNA Damage in a Pneumonia-Related Sepsis Model. *PLoS One.* 2015; 10(10):e0139416. <https://doi.org/10.1371/journal.pone.0139416> PMID: 26448624; PubMed Central PMCID: PMC4598156.
38. Unuma K, Aki T, Funakoshi T, Hashimoto K, Uemura K. Extrusion of mitochondrial contents from lipopolysaccharide-stimulated cells: Involvement of autophagy. *Autophagy.* 2015; 11(9):1520–36. <https://doi.org/10.1080/15548627.2015.1063765> PMID: 26102061; PubMed Central PMCID: PMC4590602.
39. McLellan GL, Soubannier V, Chen CX, McBride HM, Fon EA, Parkin and PINK1 function in a vesicular trafficking pathway regulating mitochondrial quality control. *EMBO J.* 2014; 33(4):282–95. <https://doi.org/10.1002/embj.201385902> PMID: 24446486; PubMed Central PMCID: PMC3989637.
40. Ali MH, Pearlstein DP, Mathieu CE, Schumacker PT. Mitochondrial requirement for endothelial responses to cyclic strain: implications for mechanotransduction. *Am J Physiol Lung Cell Mol Physiol.* 2004; 287(3):L486–96. <https://doi.org/10.1152/ajplung.00389.2003> PMID: 15090367.

41. Davidson BA, Vethanayagam RR, Grimm MJ, Mullan BA, Raghavendran K, Blackwell TS, et al. NADPH oxidase and Nrf2 regulate gastric aspiration-induced inflammation and acute lung injury. *J Immunol.* 2013; 190(4):1714–24. <https://doi.org/10.4049/jimmunol.1202410> PMID: 23296708; PubMed Central PMCID: PMC3563868.
42. Lin JY, Jing R, Lin F, Ge WY, Dai HJ, Pan L. High Tidal Volume Induces Mitochondria Damage and Releases Mitochondrial DNA to Aggravate the Ventilator-Induced Lung Injury. *Front Immunol.* 2018; 9:1477. <https://doi.org/10.3389/fimmu.2018.01477> PMID: 30018615; PubMed Central PMCID: PMC6037891.
43. Timmermans K, Kox M, Vaneker M, Pickkers P, Scheffer GJ. Mitochondrial DNA and TLR9 Signaling Is Not Involved in Mechanical Ventilation-Induced Inflammation. *Anesth Analg.* 2017; 124(2):531–4. <https://doi.org/10.1213/ANE.0000000000001554> PMID: 28099322
44. Blot M, Pauchard LA, Dunn I, Donze J, Malnuit S, Rebaud C, et al. Mechanical ventilation and *Streptococcus pneumoniae* pneumonia alter mitochondrial homeostasis. *Sci Rep.* 2018; 8(1):11718. <https://doi.org/10.1038/s41598-018-30226-x> PMID: 30082877; PubMed Central PMCID: PMC6078986.
45. Haden DW, Suliman HB, Carraway MS, Welty-Wolf KE, Ali AS, Shitara H, et al. Mitochondrial biogenesis restores oxidative metabolism during *Staphylococcus aureus* sepsis. *Am J Respir Crit Care Med.* 2007; 176(8):768–77. <https://doi.org/10.1164/rccm.200701-161OC> PMID: 17600279; PubMed Central PMCID: PMC2020830.
46. Hajizadeh S, DeGroot J, TeKoppele JM, Tarkowski A, Collins LV. Extracellular mitochondrial DNA and oxidatively damaged DNA in synovial fluid of patients with rheumatoid arthritis. *Arthritis Res Ther.* 2003; 5(5):R234–40. <https://doi.org/10.1186/ar787> PMID: 12932286; PubMed Central PMCID: PMC193725.
47. Sarma JV, Ward PA. Oxidants and redox signaling in acute lung injury. *Compr Physiol.* 2011; 1(3):1365–81. <https://doi.org/10.1002/cphy.c100068> PMID: 23733646.
48. Abraham E. Neutrophils and acute lung injury. *Crit Care Med.* 2003; 31(4 Suppl):S195–9. <https://doi.org/10.1097/01.CCM.0000057843.47705.E8> PMID: 12682440.
49. Crouser ED, Shao G, Julian MW, Macre JE, Shadel GS, Tridandapani S, et al. Monocyte activation by necrotic cells is promoted by mitochondrial proteins and formyl peptide receptors. *Crit Care Med.* 2009; 37(6):2000–9. <https://doi.org/10.1097/CCM.0b013e3181a001ae> PMID: 19384205; PubMed Central PMCID: PMC2743203.
50. Narimanbekov IO, Rozycki HJ. Effect of IL-1 blockade on inflammatory manifestations of acute ventilator-induced lung injury in a rabbit model. *Exp Lung Res.* 1995; 21(2):239–54. <https://doi.org/10.3109/01902149509068830> PMID: 7774527.
51. Gross O, Thomas CJ, Guarda G, Tschopp J. The inflammasome: an integrated view. *Immunol Rev.* 2011; 243(1):136–51. <https://doi.org/10.1111/j.1600-065X.2011.01046.x> PMID: 21884173.
52. Kuipers MT, Aslami H, Janczy JR, van der Sluijs KF, Vlaar AP, Wolthuis EK, et al. Ventilator-induced lung injury is mediated by the NLRP3 inflammasome. *Anesthesiology.* 2012; 116(5):1104–15. <https://doi.org/10.1097/ALN.0b013e3182518bc0> PMID: 22531249.
53. Nakahira K, Kyung SY, Rogers AJ, Gazourian L, Youn S, Massaro AF, et al. Circulating mitochondrial DNA in patients in the ICU as a marker of mortality: derivation and validation. *PLoS Med.* 2013; 10(12):e1001577; discussion e. <https://doi.org/10.1371/journal.pmed.1001577> PMID: 24391478; PubMed Central PMCID: PMC3876981.
54. Matzinger P. Tolerance, danger, and the extended family. *Annu Rev Immunol.* 1994; 12:991–1045. <https://doi.org/10.1146/annurev.iy.12.040194.005015> PMID: 8011301.
55. Matzinger P. Friendly and dangerous signals: is the tissue in control? *Nat Immunol.* 2007; 8(1):11–3. <https://doi.org/10.1038/ni0107-11> PMID: 17179963.
56. Bregeon F, Delpierre S, Chetaille B, Kajikawa O, Martin TR, Autillo-Touati A, et al. Mechanical ventilation affects lung function and cytokine production in an experimental model of endotoxemia. *Anesthesiology.* 2005; 102(2):331–9. <https://doi.org/10.1097/00000542-200502000-00015> PMID: 15681948.

➔ Synthèse de l'article 1 :

Ce premier travail a permis de mettre en évidence une libération d'alarmines mitochondrielles (en particulier l'ADN mitochondrial) par les cellules épithéliales pulmonaires soumises à l'étirement cyclique, mais aussi dans les alvéoles de lapins soumis à une VM agressive pendant 8 heures ou de patients ventilés en SDRA.

Le travail *in vitro* montre que sous l'effet du stretch, les cellules épithéliales pulmonaires libèrent à la fois de l'IL-8 et de l'ADNmt. La libération d'IL-8 était inhibée par l'antagonisme pharmacologique de TLR-9 (ODN TTAGGG), suggérant le rôle de l'ADNmt dans l'activation de la transcription du gène de l'IL-8 via la voie de signalisation TLR9. Parallèlement, le stretch de ces cellules entraîne la libération d'IL-1 β mature et d'ATP, avec un effet synergique de l'association stretch/LPS sur la sécrétion d'IL-1 β . Enfin, le surnageant des cellules stretchées induisait un chimiотactisme des PMN, essentiellement médié par le fMLP, puisque le blocage pharmacologique de son récepteur (anti-FPR1) limitait cet effet.

Dans le modèle *in vivo*, les lapins soumis à une VM agressive (Vt 20ml/kg, zero PEEP), en comparaison aux animaux en respiration spontanée, présentaient des concentrations alvéolaires élevées d'ADNmt (Cytochrome b, p=0,077 ; cytochrome c, p=0,052 ; NADH-I, p=0,08), d'ATP (p=0,067) et une augmentation du pouvoir chimiотактиque du surnageant du LBA, pouvant refléter la libération de fMLP mitochondrial en réponse au stress mécanique.

Enfin, les concentrations d'ADNmt étaient significativement plus élevées dans le surnageant des LBA de patients présentant un SDRA, en comparaison à des témoins sains, et ce d'autant plus que le liquide était inflammatoire en termes de concentrations de PMNs.

Ainsi, les alarmines mitochondrielles pourraient représenter le lien entre le stimulus mécanique subit par les cellules étirées, la libération locale de cytokines inflammatoires et le développement de lésions de VILI.

2.2 Article 2 (Dijon, Scientific Reports 2018)

Dans un contexte de pneumopathie bactérienne, VM et agent pathogène pourraient agir comme des signaux pro-inflammatoires synergiques, susceptibles de majorer les lésions tissulaires pulmonaires et d'altérer l'efficacité de la réponse antibactérienne de l'hôte (137). Les précédents travaux de l'équipe montrent que dans notre modèle animal, la combinaison des 2 agressions est particulièrement défavorable à l'hôte avec un excès de réponse inflammatoire tant au niveau local que systémique (127,132).

Au cours de ce travail, nous faisons l'hypothèse que la VM pourrait, au cours d'une pneumopathie bactérienne, avoir un effet synergique avec l'agression infectieuse sur la libération d'alarmes mitochondrielles, capable d'exacerber la réponse inflammatoire (Figure 14)

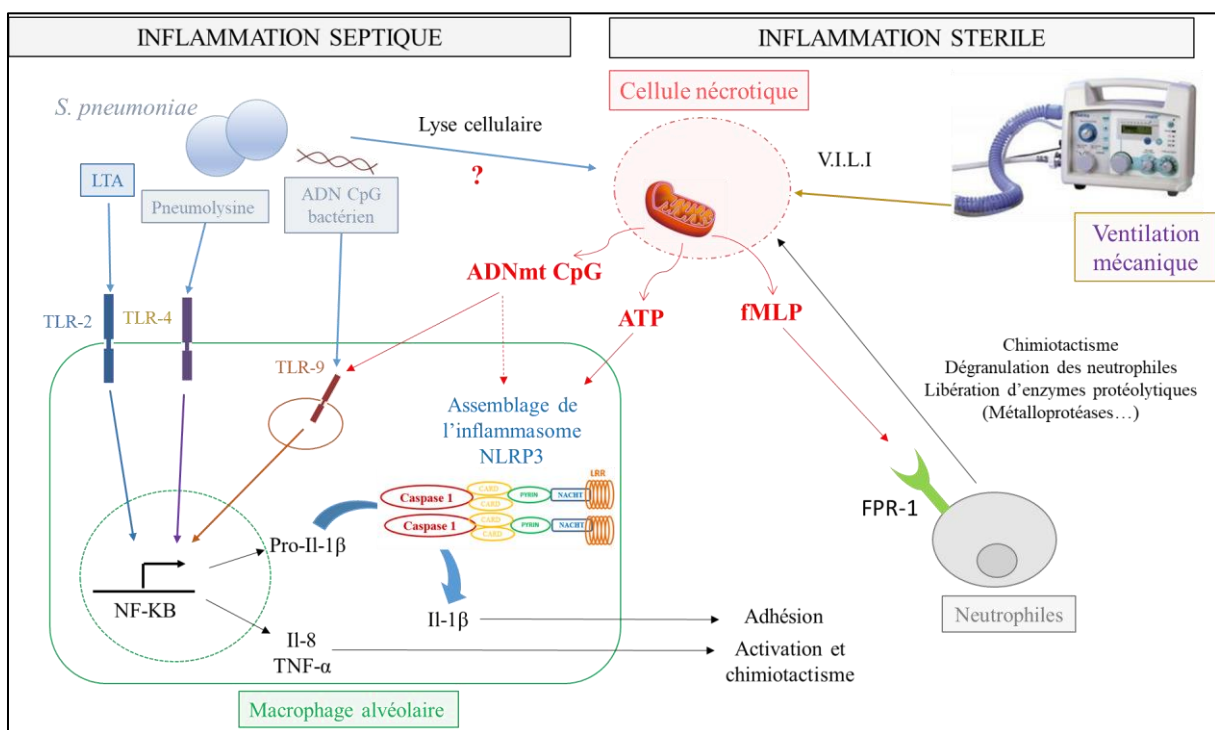


Figure 14. Hypothèses des déterminants et conséquences de la libération des alarmes mitochondrielles : modèle de pneumopathie à pneumocoque sous ventilation mécanique.

➔ Objectifs de l'étude :

- Evaluer dans quelle mesure la VM est capable d'induire la libération d'alarmes mitochondrielles dans les poumons de lapins infectés à pneumocoque.
- Evaluer dans quelle mesure la VM est capable d'induire la libération d'alarmes mitochondrielles dans les poumons de lapins sains et s'il existe une synergie pro-inflammatoire en cas d'infection bactérienne associée.

➔ **Participation personnelle :**

- Planification du design de l'étude
- Mise au point de plusieurs techniques utiles au projet
- Réalisation de toutes les expérimentations animales.
- Réalisation de tous les dosages avec l'aide de plusieurs étudiants qui ont pu valider leur stage à l'occasion de ce travail (Master 1 : Jennifer Donze, Stéphanie Malnuit ; Licence pro : Chloé Rebaud) et de Laure Anne Pauchard, doctorante.
- Analyse et interprétation des résultats.
- Ecriture et publication de l'article.

SCIENTIFIC REPORTS



OPEN

Mechanical ventilation and *Streptococcus pneumoniae* pneumonia alter mitochondrial homeostasis

Received: 19 March 2018

Accepted: 23 July 2018

Published online: 06 August 2018

Mathieu Blot^{1,2}, Laure-Anne Pauchard¹, Irène Dunn³, Jennifer Donze¹, Stéphanie Malnuit¹, Chloé Rebaud¹, Delphine Croisier¹, Lionel Piroth², Jérôme Pugin³ & Pierre-Emmanuel Charles^{1,5}

Required mechanical ventilation (MV) may contribute to bacterial dissemination in patients with *Streptococcus pneumoniae* pneumonia. Significant variations in plasma mitochondrial DNA (mtDNA) have been reported in sepsis according to the outcome. The impact of lung stretch during MV was addressed in a model of pneumonia. Healthy or *S. pneumoniae* infected rabbits were submitted to MV or kept spontaneously breathing (SB). Bacterial burden, cytokines release, mitochondrial DNA levels, integrity and transcription were assessed along with 48-hour mortality. Compared with infected SB rabbits, MV rabbits developed more severe pneumonia with greater concentrations of bacteria in the lungs, higher rates of systemic dissemination, higher levels of circulating inflammatory mediators and decreased survival. Pulmonary mtDNA levels were significantly lower in infected animals as compared to non-infected ones, whenever they were SB or MV. After a significant early drop, circulating mtDNA levels returned to baseline values in the infected SB rabbits, but remained low until death in the MV ones. Whole blood ex-vivo stimulation with *Streptococcus pneumoniae* resulted in a reduction of polymorphonuclear leukocytes mitochondrial density and plasma mtDNA concentrations. Thus, persistent mitochondrial depletion and dysfunction in the infected animals submitted to MV could account for their less efficient immune response against *S. pneumoniae*.

Community acquired pneumonia remains the main cause of death from infection, and *Streptococcus pneumoniae* is the main bacterial agent¹. In addition, in severely ill individuals, mechanical ventilation (MV) may contribute to bacterial dissemination^{2,3}. It is likely that the combination of the damaging effects of MV on the lungs (i.e., Ventilator-Induced Lung Injury [VILI], release of pro-inflammatory cytokines, recruitment and activation of polymorphonuclear leukocytes [PMNs]) and the onset of infection influences the severity of the disease^{4–7}. This pro-inflammatory state could alter host defenses against bacterial invasion^{8–10}. However, the relationship between excessive inflammation and resulting sepsis has been challenged by the concept of immune paralysis¹¹.

The inflammatory response to bacteria is initiated by the detection of pathogen-associated molecular patterns (PAMPs) by specialized cognate receptors, including toll-like receptors (TLRs)¹². Various kinds of molecules released from damaged or dying cells are also likely to activate immunity, and share signaling pathways and patterns of response with PAMPs¹³. Among the so-called damage-associated molecular patterns (DAMPs), some originate from mitochondria^{14,15}. Thus, mitochondrial DNA (mtDNA) activates and amplifies inflammation through the TLR9 ligation, as well as through the NLRP3 and the STING pathways^{13,16,17}. In addition, the formyl-Met-Leu-Phe (fMLP) peptide directs PMNs towards injured tissues, and might contribute to VILI^{18,19}. The extra-cellular release of the so called mitochondrial alarmins is the result of poorly understood mechanisms including extrusion²⁰. In addition, it is now well established that the metabolic disturbances subsequent to the activation of immune cells depend heavily on mitochondrial homeostasis, driving their ability to clear microbial invaders²¹. Thus, stressed mitochondria release ROS which likely contribute to the killing of bacteria by activated

¹Lipides Nutrition Cancer Lab, U.M.R. 1231, I.N.S.E.R.M., Faculty of Health Sciences, University of Burgundy, Dijon, France. ²Infectious Diseases Department, Dijon University Hospital, Dijon, France. ³Intensive Care Laboratory, University Hospitals of Geneva & Faculty of Medicine, University Hospital of Geneva, Geneva, Switzerland. ⁴Vivexia S.A.R.L., Gémeaux, France. ⁵Intensive Care Unit, Dijon University Hospital, Dijon, France. Correspondence and requests for materials should be addressed to P.-E.C. (email: pierre-emmanuel.charles@chu-dijon.fr)

immune cells. Moreover, mitophagy is enhanced in order to protect the cell against the “toxicity” of such damaged organelles, leading in turn to transient mitochondria depletion, reduction in energy expenditure and inflammation control. However, mitochondria involvement is not well understood in the context of bacterial infection or VILI. Some experimental reports suggest that fMLP might contribute to VILI^{18,19}. In contrast, there are conflicting results regarding the link between circulating mtDNA and outcomes of septic patients^{22–25}. Finally, mtDNA deletions have been reported in various chronic diseases and could be associated with substantial mitochondrial disturbances²⁶. Our investigation was therefore focused on whether MV and *S. pneumoniae* pneumonia could induce quantitative and qualitative mtDNA abnormalities in a rabbit model of infection²⁰.

Results

Mechanical ventilation worsens both clinical and microbiological outcomes of pneumococcal pneumonia in rabbits. Since uninfected animals subjected to 48 hours of MV were alive with arterial blood gases and lactate levels within the normal range, our MV protocol was considered safe (Supplementary Table S1). However, it is worth noting that MV alone led to mild lung injury (Supplementary Fig. S1).

Forty-eight-hour mortality in infected MV animals was dramatically higher than that in infected SB rabbits (100 vs. 0%, respectively; $p = 0.005$). Bacterial clearance in the lung was lower (6.0 [5.1–6.5] vs. 3.8 [1.0–4.8] log₁₀CFU/g of lung, $p = 0.04$), and the rate of systemic dissemination was higher (60 vs. 0%) (Fig. 1). In addition, pneumonia was multifocal in MV animals, whereas it was usually limited to one lobe in their SB counterparts.

Remarkably, MV did not lead to metabolic acidosis in rabbit despite adverse settings (Table S2), whereas such disturbances have been described in smaller animals²⁷.

Mechanical ventilation increases systemic but not pulmonary inflammation in rabbits with pneumonia. Pneumonia resulted in increased pulmonary concentrations and gene expression of both IL-8 and IL-1 β , but not TNF- α (Fig. 2). However, there was no significant difference between MV and SB infected animals. In contrast, systemic inflammation was enhanced in MV animals according to plasma concentrations of IL-8 and TNF- α , but not IL-1 β (Fig. 3). Obviously, the anti-inflammatory cytokine IL-10 was significantly more elevated in the lung as well as in the spleen of the infected rabbits submitted to MV as compared to SB ones.

In addition, according to our *ex vivo* assay which aimed at assessing the chemoattractive properties of BALF towards human PMNs, MV mildly decreased pulmonary migration of these cells in infected animals, but was shy of statistical significance (46 [22–59] vs 73 [52–76] % of attracted PMNs, $p = 0.09$) (Fig. 4).

Pulmonary mitochondrial DNA levels and integrity dramatically decrease during pneumococcal pneumonia. Adverse MV alone did not increase the amount of mtDNA released within the airway (i.e., extracellular mtDNA) as reflected by BALF concentrations (Fig. 5). In contrast, mtDNA tissue content (i.e., intracellular mtDNA) as well as the corresponding genes expression in the lung, reflecting mtDNA amount and integrity as well, were significantly decreased 48 hours after the onset of adverse MV (Fig. 6). In addition, the proportion of deleted mtDNA (i.e., damaged mtDNA) was increased by adverse MV.

In SB animals, mtDNA levels were found to be significantly lower in the BALF of infected rabbits than in the uninfected ones (Cytochrome b: 3792 [3700–7777] vs. 34528 [14479–71283] a.u., respectively; $p = 0.02$) (Fig. 5). The same results were obtained for both Cytochrome c and NADH I genes ($p = 0.02$), as well as in MV rabbits. We found also significantly smaller amounts of intracellular mtDNA within the lung in infected rabbits as compared to uninfected ones. Moreover, the expression of both NADH I and Cytochrome b genes was significantly decreased within the infected lung (Fig. 6). The same results were obtained in both SB and MV animals.

In addition, the proportion of deleted mtDNA was far greater in the infected animals than in the uninfected ones, regardless of ventilation.

Since *S. pneumoniae* usually release one endonuclease (i.e., EndA) likely to hydrolyze circulating bacterial DNA, we hypothesized that EndA could have damaged mtDNA within the tissues of infected animals. However, there was no substantial loss of mtDNA detection *in vitro* after co-incubation with increasing concentrations of *S. pneumoniae*, emphasizing thereby the validity of our findings (Fig. S2).

Circulating mitochondrial DNA levels decrease during *Streptococcus pneumoniae* pneumonia and return to baseline values only in the spontaneously breathing animals. Mitochondrial density and byproducts were also evaluated within the systemic compartment of infected animals. Thus, mtDNA concentrations were found to be significantly lower in the spleen of infected animals (i.e., intracellular mtDNA), whenever they were mechanically ventilated or not, whereas MV alone had no impact (Fig. 5).

Accordingly, plasma mtDNA level (i.e., extracellular mtDNA) decreased 8 hours after the onset of pneumonia in both infected groups. However, it rebounded and returned to baseline values 48 hours later in SB animals, whilst mtDNA concentrations remained low in MV animals, until death occurred.

In line with those findings, ATP plasma levels were found to be significantly lower in the animals subjected to MV than in their SB counterparts, as early as the 8th hour after bacterial challenge (Fig. 6).

We conducted *ex vivo* stimulation assays in an attempt to decipher what a decrease in mtDNA plasma concentrations resulting from bacterial insult meant in terms of mitochondrial density within the circulating immune cells (Fig. 7). Interestingly, when rabbit whole blood was submitted to heat-killed *S. pneumoniae*, greater was the bacteria number, lower was the PMNs mitochondrial density ($r = -0.34$; $p = 0.03$) in parallel with a drop of the plasma mtDNA concentration ($r = -0.42$; $p = 0.02$). In addition, the release of mtROS by PMNs was then blunted, but we failed to show any statistically significant correlation.

Mitochondrial depletion resulting from *Streptococcus pneumoniae* pneumonia may be related to defective biogenesis. Since mitochondrial density is thought to depend on mitochondrial biogenesis, we investigated the impact of MV and *S. pneumoniae* pneumonia on these pathways within the lung. Hence, we

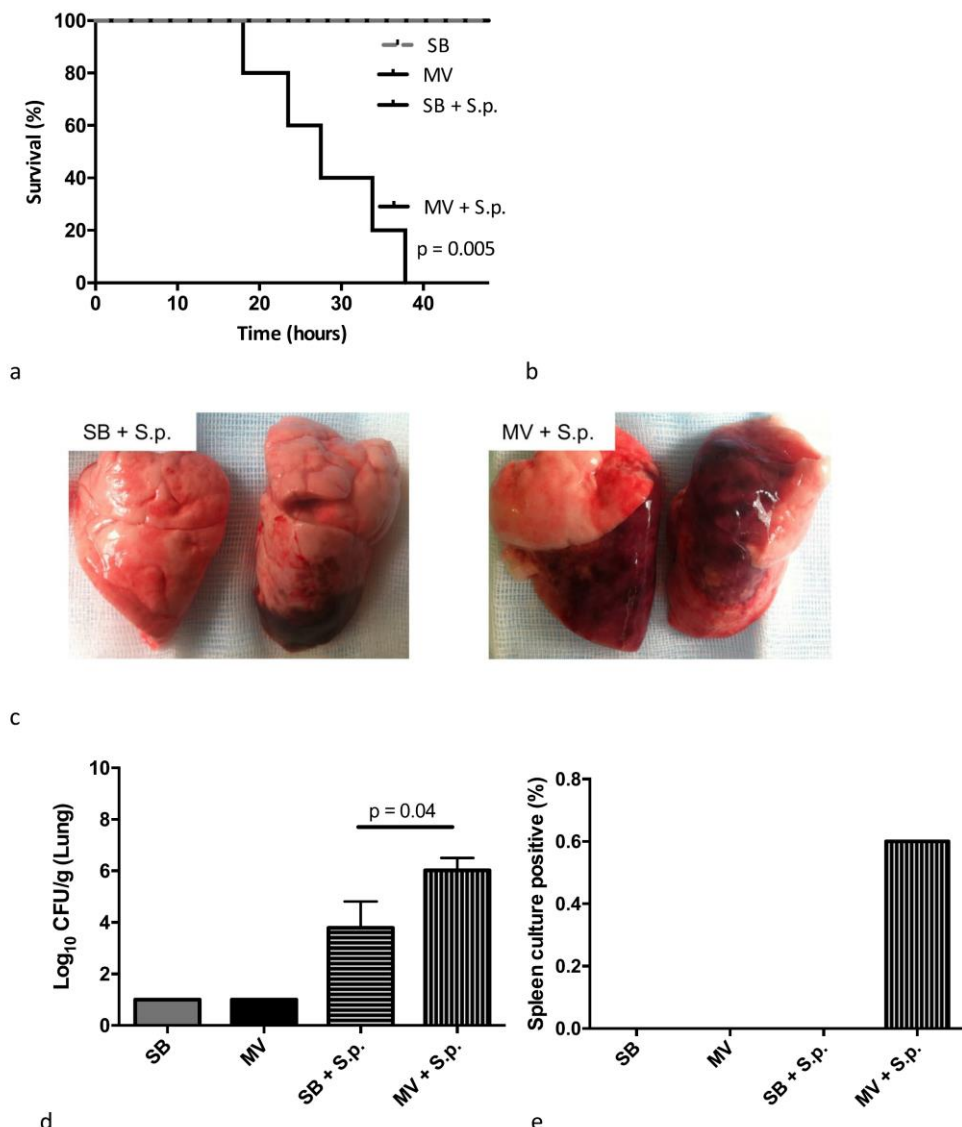


Figure 1. Main features of *Streptococcus pneumoniae* pneumonia in either spontaneously breathing or mechanically ventilated rabbits. (a) Time-dependent probability of survival (log rank test, $p = 0.005$); (b) Lung injury assessment according to macroscopic score calculation; (c) Lung pictures after pneumonia in either SB (left) or MV (right) animals; (d) pulmonary bacterial concentrations (Log_{10} CFU per gram of lung); (e) Pulmonary-to-systemic bacterial translocation expressed as the spleen positive culture rate 48 hours after bacteria instillation (or at the time of death if earlier). CFU: colony forming unit; MV: mechanical ventilation, SB: spontaneously breathing, S.p.: *Streptococcus pneumoniae*, IQR: interquartile range.

observed within the infected lung a down-regulation of the main regulator of mitochondrial biogenesis PGC1- α , as well as of the key regulator of mitochondrial genome copy number TFAM, especially in the MV animals (Fig. 8).

Discussion

As supported by our data, MV dramatically worsens the outcome of rabbits with *S. pneumoniae* pneumonia. Accordingly, the mortality rate reached 100% in the MV group whereas all the infected SB animals survived 48 hours after bacterial challenge. The substantially higher incidence of systemic dissemination in the ventilated rabbits, leading to overwhelming and unsolved systemic inflammation, could account for these differences, thus reflecting clinical observations²⁸. The lack of efficacy of the lung immune response might explain this increased pulmonary-to-systemic translocation rate since MV significantly decreased bacterial clearance in the lungs. Accordingly, we showed that PMN chemotaxis was decreased within the lung of infected animals subjected

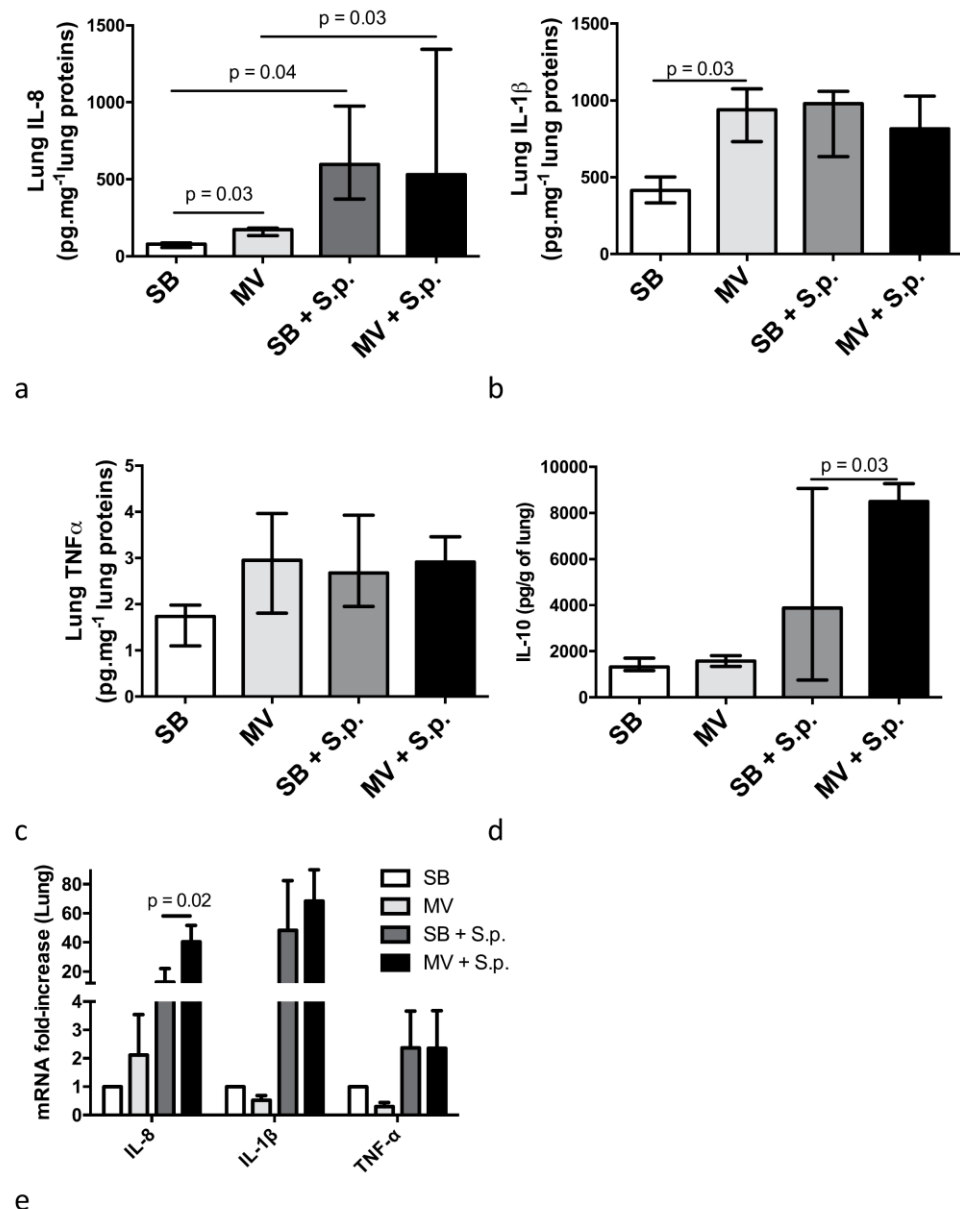


Figure 2. Inflammatory cytokine concentrations and gene expression in the lung tissue of spontaneously breathing or mechanically ventilated rabbits with or without *Streptococcus pneumoniae* pneumonia. Median (IQR) inflammatory cytokine concentrations (IL-8 [a], IL-1 β [b] and TNF- α [c]) in lung homogenates obtained 48 hours (or at the time of death if earlier) after tracheal instillation of saline (controls) or 5.108 CFU of *Streptococcus pneumoniae* in either spontaneously breathing or mechanically ventilated rabbits. Relative mRNA copies number of IL-8, IL-1 β and TNF- α genes within the lung were measured by the reverse transcriptase-polymerase chain reaction. All values are shown as the fold increase compared with uninfected spontaneous breathing rabbits - value set to 1. The Kruskall Wallis test and the Mann-Whitney U test were used successively for all intergroup comparisons and followed by post hoc corrections for multiple comparisons using the Bonferroni method. CFU: colony forming unit; SB: spontaneously breathing, MV: mechanical ventilation, S.p.: *Streptococcus pneumoniae*, IL: interleukin, TNF: tumor necrosis factor, mRNA: messenger ribonucleic acid, BALF: broncho-alveolar lavage fluid; IQR: interquartile range.

to MV independently from IL-8 production, together with the release of larger amounts of IL-10, a powerful anti-inflammatory cytokine. Given the mitochondrial involvement in the regulation of the immune response, we hypothesized that significant derangements of their homeostasis could contribute to the highly harmful effect

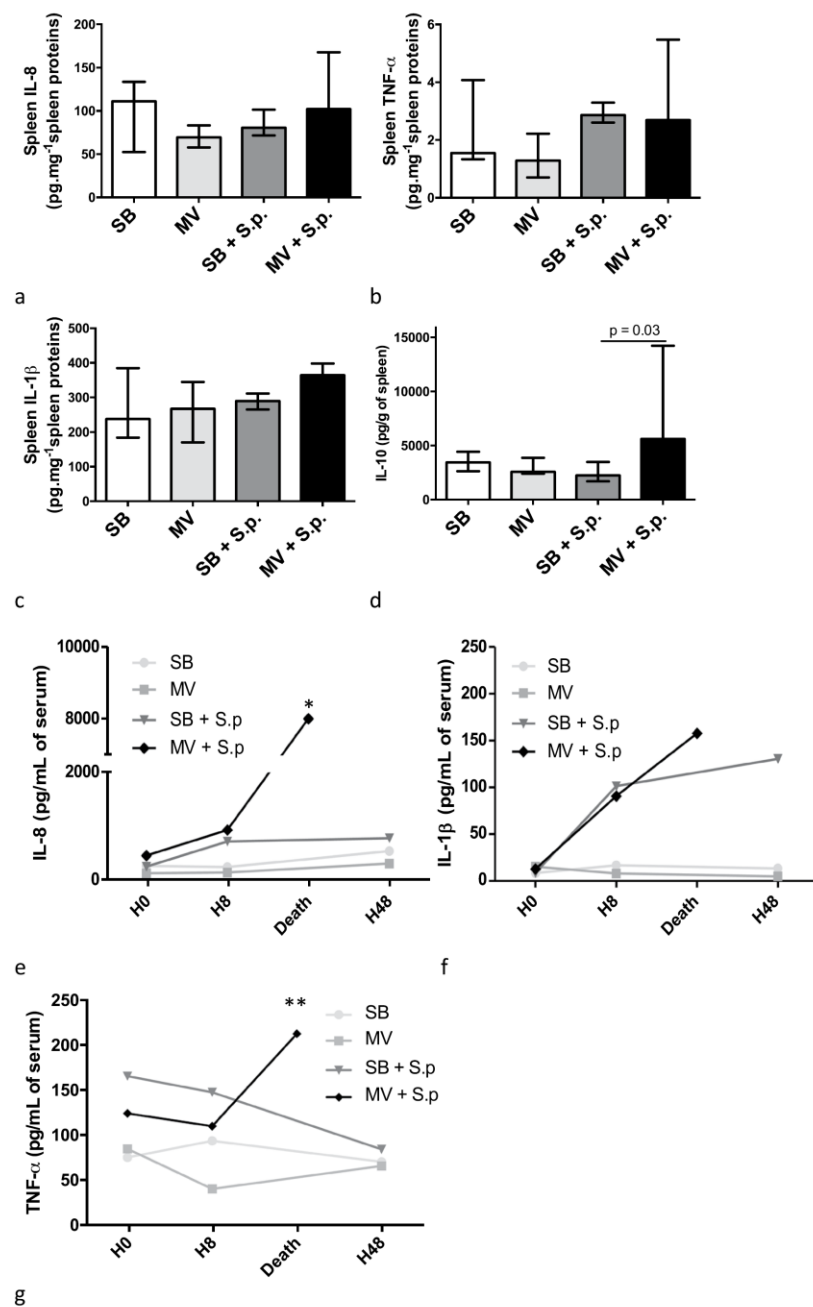


Figure 3. Inflammatory cytokine concentrations and gene expression in the systemic compartment of spontaneously breathing or mechanically ventilated rabbits with or without *Streptococcus pneumoniae* pneumonia. Median (IQR) inflammatory cytokine concentrations (IL-8 [A], IL-1 β [B] and TNF- α [C]) in spleen homogenates, 48 hours (or at the time of death if earlier) after tracheal instillation of saline (controls) or 5.108 CFU of *Streptococcus pneumoniae* in spontaneously breathing or mechanically ventilated rabbits. Relative mRNA copies numbers of IL-8, IL-1 β and TNF- α genes within the spleen were measured by the reverse transcriptase-polymerase chain reaction. All values are shown as the fold increase compared with uninfected spontaneous breathing rabbits - value set to 1. Median plasma concentrations of inflammatory cytokines (IL-8 [e], IL-1 β [f] and TNF- α [g]) were measured by ELISA at baseline, 8 or 48 hours (or at the time of death if earlier) after challenge. The Kruskall Wallis test and the Mann-Whitney U test were used successively for all intergroup comparisons and followed by post hoc corrections for multiple comparisons using the Bonferroni method.* and ** denote $p < 0.05$ between infected SB and MV rabbits at H48 or time of death, respectively. CFU: colony forming unit, SB: spontaneously breathing, MV: mechanical ventilation, S.p.: *Streptococcus pneumoniae*, IL: interleukin, TNF: tumor necrosis factor, mRNA: messenger ribonucleic acid, BALF: broncho-alveolar lavage fluid; IQR: Interquartile Range.

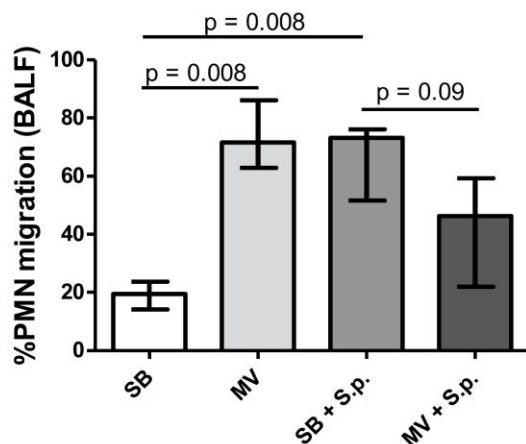


Figure 4. Polymorphonuclear leukocytes chemotaxis induced by broncho-alveolar lavage fluid in spontaneously breathing or mechanically ventilated rabbits with or without *Streptococcus pneumoniae* pneumonia. PMN chemotaxis was measured using a Boyden chamber, 48 hours (or at the time of death if earlier) after tracheal instillation of saline (controls) or 5.108 CFU of *Streptococcus pneumoniae* in either spontaneously breathing or mechanically ventilated rabbits. Results are expressed as the mean (SD) % of PMNs from healthy volunteers attracted by rabbit BALF. The Kruskall Wallis test and the Mann-Whitney U test were used successively for all intergroup comparisons and followed by post hoc corrections for multiple comparisons using the Bonferroni method. SB: spontaneous breathing, MV: mechanical ventilation, BALF: broncho-alveolar lavage fluid, IL: interleukin, PMN: polymorphonuclear leukocytes, S.p.: *Streptococcus pneumoniae*, SD: standard deviation.

of MV in the pneumonia setting. Indeed, our findings indicate that MV alone was associated with a significant decrease in mitochondrial density within the lung. Moreover, *S. pneumoniae* infection itself led to an obvious drop of the mitochondrial content in both pulmonary and systemic compartments, especially in the animals under MV. Thus, the PMNs recruitment deficiency measured in the ventilated lung could be subsequent to mitochondrial depletion, given the chemoattractant properties of fMLP. In addition, it is worth noting that circulating mtDNA levels fell continuously until death in the infected MV rabbits whereas they returned to baseline values in their SB counterparts. Assuming that mtDNA concentrations reflected mitochondrial density within immune cells, as suggested by our *ex vivo* findings as well as by the concomitant decrease of plasma ATP, one could consider that antimicrobial defenses were also impaired within the bloodstream. Thus, mitochondrial depletion could account for the host failure to clear circulating bacteria, leading in turn to higher levels of systemic inflammation^{24,29}. Mitochondrial depletion could result from a decreased biogenesis as reflected by the down regulation of both PGC1 α and TFAM genes. However, it remains difficult to delineate the respective effects of MV and infection on the reported mitochondrial disorders. Obviously, the effect of MV on pulmonary mitochondria density was hidden by the effect of infection when the animals were concomitantly submitted to both. Nevertheless, it is worth noting that: (i) down regulation of PGC1 gene expression within the lung was more pronounced in the ventilated and infected animals; (ii) constantly decreasing circulating mtDNA concentrations were only seen in the MV animals with pneumonia. Altogether, our findings suggest that MV does contribute to the poor outcome of rabbits with pneumonia by enhancing mitochondrial disturbances.

Mitochondrial involvement during the host response to bacterial insult is paramount³⁰. The clinical relevance of those findings has risen since some authors showed that on one hand, deep metabolic disturbances occurred in human cells, whereas on the other hand, more recently, others found that plasma concentrations of mtDNA were increased in both trauma and septic patients^{14,22,23,31,32}. This latter finding is however controversial in sepsis since mtDNA depletion in blood and mononuclear cells was reported elsewhere in patients with sepsis and correlated with disease severity^{24,29}. Similarly, a negative correlation between circulating cell-free mtDNA levels and all-cause mortality was found in a large cohort of patients, and in mechanically ventilated critically ill patients as well^{25,33}. However, the case mix of patients, the variability of the studied mitochondrial genes, as well as the various measurement methods used for mtDNA detection, may account for these differences.

To the best of our knowledge, experimental data published so far regarding the involvement of mitochondria in VILI and bacterial pneumonia are even sparser and conflicting¹⁸. Thus, mtDNA infusion is likely to cause lung injury in a rodent model mimicking the human polytrauma setting, while lung stretch-related mtDNA alterations promote VILI in mice submitted to adverse MV^{14,34}. In contrast, as we observed in our long-term adverse MV rabbit model, levels of mtDNA in BALF were not increased in mice ventilated for a short time with either low (8 mL/kg) or high (32 mL/kg) tidal volumes³⁵. The existing discrepancy between the findings obtained in animals submitted to lung stretch as compared to other trauma models could be related to the extent of tissue damage caused by mechanical stress exposure. In the setting of bacterial pneumonia, it has been shown that rising mtDNA levels were detected within isolated perfused rat lungs infected with *Pseudomonas aeruginosa*, thus accounting for the formation of tissue edema³⁶. Likewise, it has been recently reported *in vitro* that *S. pneumoniae* was likely to drive mitochondria disturbances leading to the release of mtDNA by infected alveolar cells through pneumolysin

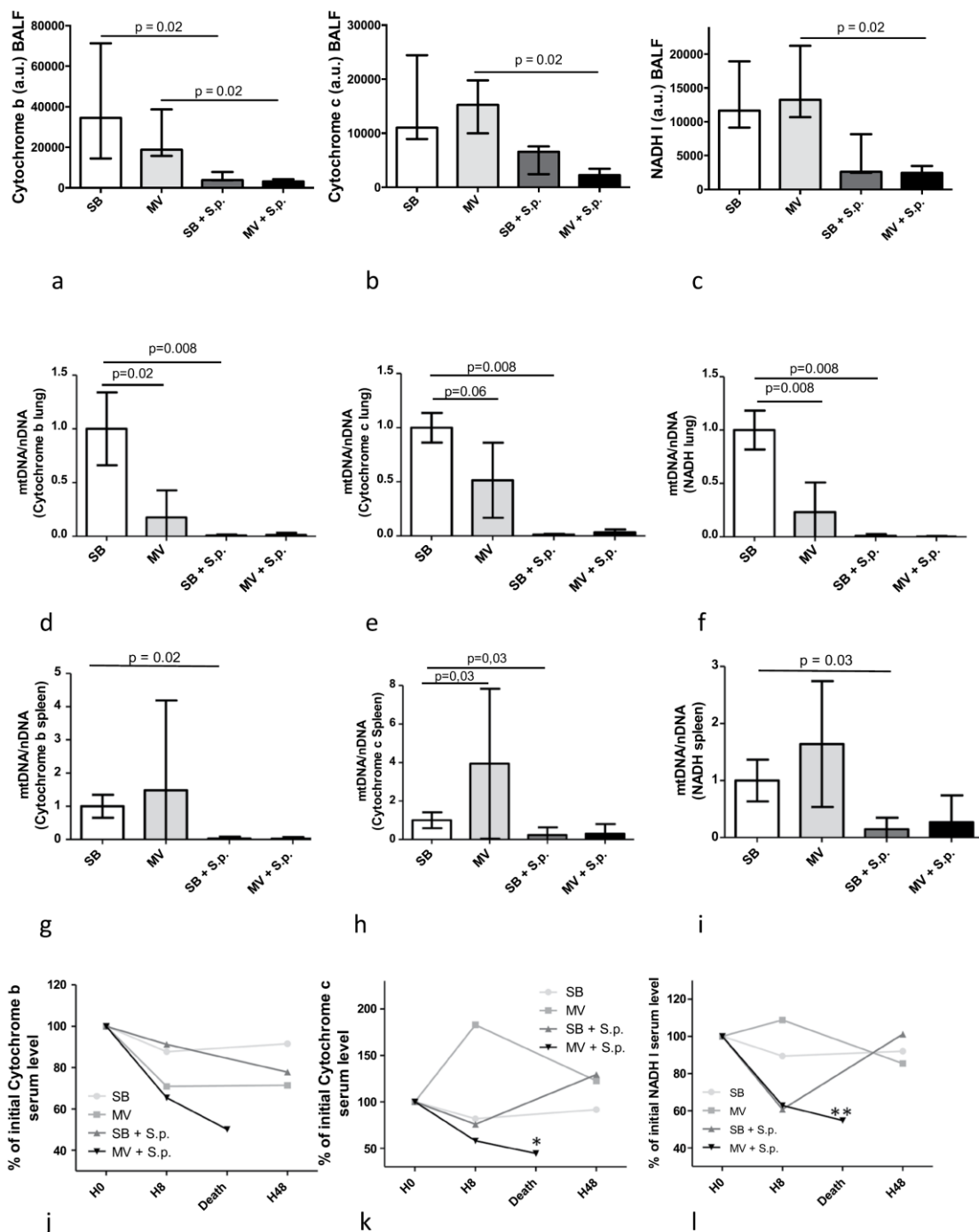


Figure 5. Mitochondrial DNA levels in broncho-alveolar lavage fluid, lung tissue, spleen and plasma in spontaneously breathing or mechanically ventilated rabbits with or without *Streptococcus pneumoniae* pneumonia. Median (IQR) mitochondrial DNA levels (Cytochrome b [a], Cytochrome c [b] and NADH I [c]) were measured in BALF, 48 hours (or at the time of death if earlier) after tracheal instillation of saline (controls) or 5.108 CFU of *Streptococcus pneumoniae* in spontaneously breathing rabbits or mechanically ventilated rabbits. Mitochondrial DNA levels were also measured in the lung (Cytochrome b [d], Cytochrome c [e] and NADH I [f]) and in the spleen (Cytochrome b [g], Cytochrome c [h] and NADH I [i]). Plasma concentrations (Cytochrome b [j], Cytochrome c [k] and NADH I [l]) were measured at baseline, 8 or 48 hours (or at the time of death if earlier) after saline or bacterial challenge. Results are expressed as percentage of baseline level. The Kruskall Wallis test and the Mann-Whitney U test were used successively for all intergroup comparisons and followed by post hoc corrections for multiple comparisons using the Bonferroni method. * denotes $p = 0.05$ and ** denotes $p = 0.08$ between infected SB and MV rabbits at H48 or time of death, respectively. SB: spontaneous breathing, MV: mechanical ventilation, BALF: broncho-alveolar lavage fluid, NADH: Nicotinamide adenine dinucleotide, PMN: polymorphonuclear leukocytes, S.p.: *Streptococcus pneumoniae*, IQR: interquartile range.

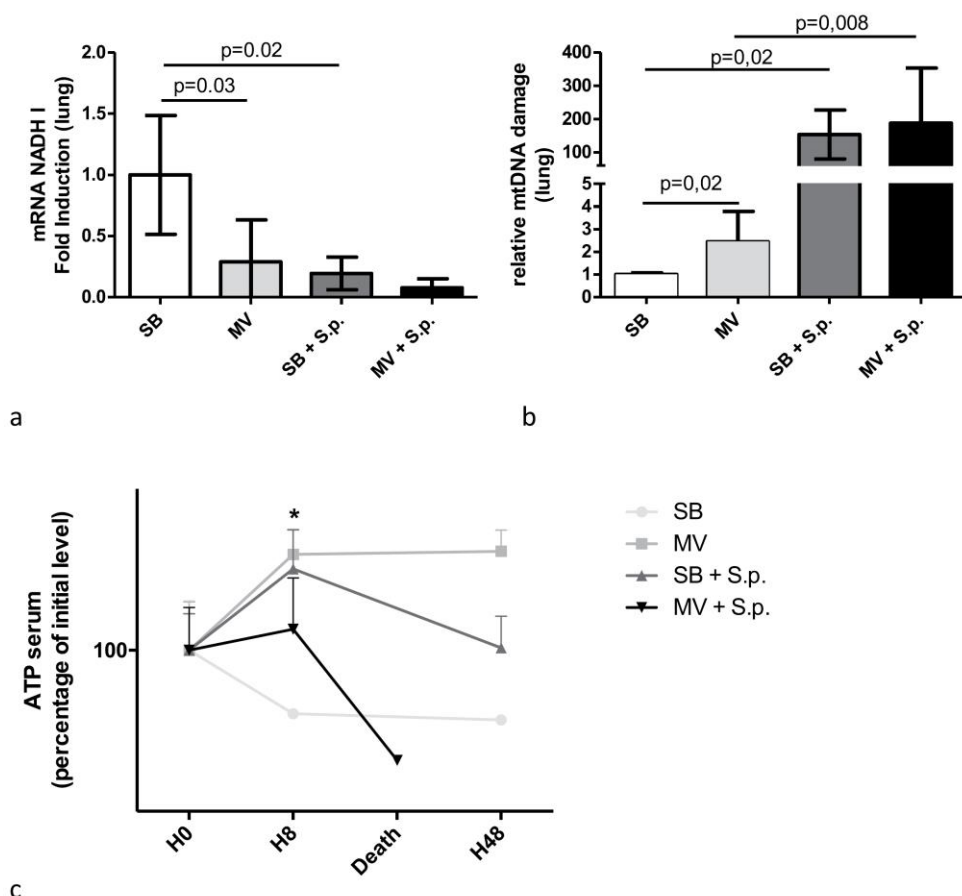


Figure 6. Pulmonary mitochondrial gene transcription, ATP plasma level and deleted mitochondrial DNA proportion in spontaneously breathing or mechanically ventilated rabbits with or without *Streptococcus pneumoniae* pneumonia. Pulmonary mitochondrial NADH-I mRNA was measured by reverse transcriptase-PCR (RT-qPCR), and normalized to GAPDH mRNA, 48 hours (or at the time of death if earlier) after tracheal instillation of saline (controls) or 5.108 CFU of *Streptococcus pneumoniae* in spontaneously breathing or mechanically ventilated rabbits [a]. Pulmonary mtDNA damage was assessed by quantifying the 4977bp deletion in mtDNA by PCR, and normalized to the mitochondrial NADH I gene [b]. The level of plasma ATP was measured at baseline, 8 or 48 hours (or at the time of death if earlier) after challenge [c]. The Kruskall Wallis test and the Mann-Whitney U test were used successively for all intergroup comparisons and followed by post hoc corrections for multiple comparisons using the Bonferroni method. ATP: adenosine triphosphate; SB: spontaneous breathing, MV: mechanical ventilation, RNA: ribonucleic acid, GAPDH: glyceraldehyde-3-phosphate dehydrogenase, NADH: Nicotinamide adenine dinucleotide, PCR: polymerase chain reaction, S.p.: *Streptococcus pneumoniae*.

secretion, one of its most important toxins³⁷. However, the animal model used in the present study has several advantages including the ability to assess long-term adverse MV and survival in animals with pneumonia.

In the context of sepsis, the link between mitochondrial homeostasis regarding the host immune response remains unsettled. Some authors reported that, in mice with *S. aureus* peritonitis, a significant decrease in liver concentrations of mtDNA occurred during the first two days, followed by complete restoration of mitochondrial density in survivors only, resulting from mitochondrial biogenesis enhancement³⁸. Similar data were obtained in the muscles of mice submitted to CLP³⁹. Our findings suggest an impairment of mitochondrial biogenesis within the lung of infected animals, accounting for depletion of protracted organelles. This finding paves the way for further therapeutic prospects, since increased mitochondrial biogenesis has been associated with survival in sepsis⁴⁰.

The pathophysiological link between such mitochondrial dysfunctions and the reduced efficacy of the host immune response is still an unsolved issue. Accordingly, mtDNA is required for NLRP3 inflammasome activation. Macrophages lacking mitochondria are thereby less likely to produce IL-1 β , since NLRP3 is required for the cleavage of pro-IL-1 β into bioactive IL-1 β , thus hampering their ability to clear pathogens¹⁶. Indeed, the beneficial effects of treatment with CpG ODN, a powerful TLR9-agonist, on bacterial clearance and mortality were demonstrated in animal models of *S. pneumoniae* and *S. aureus* pneumonia. These effects were achieved by

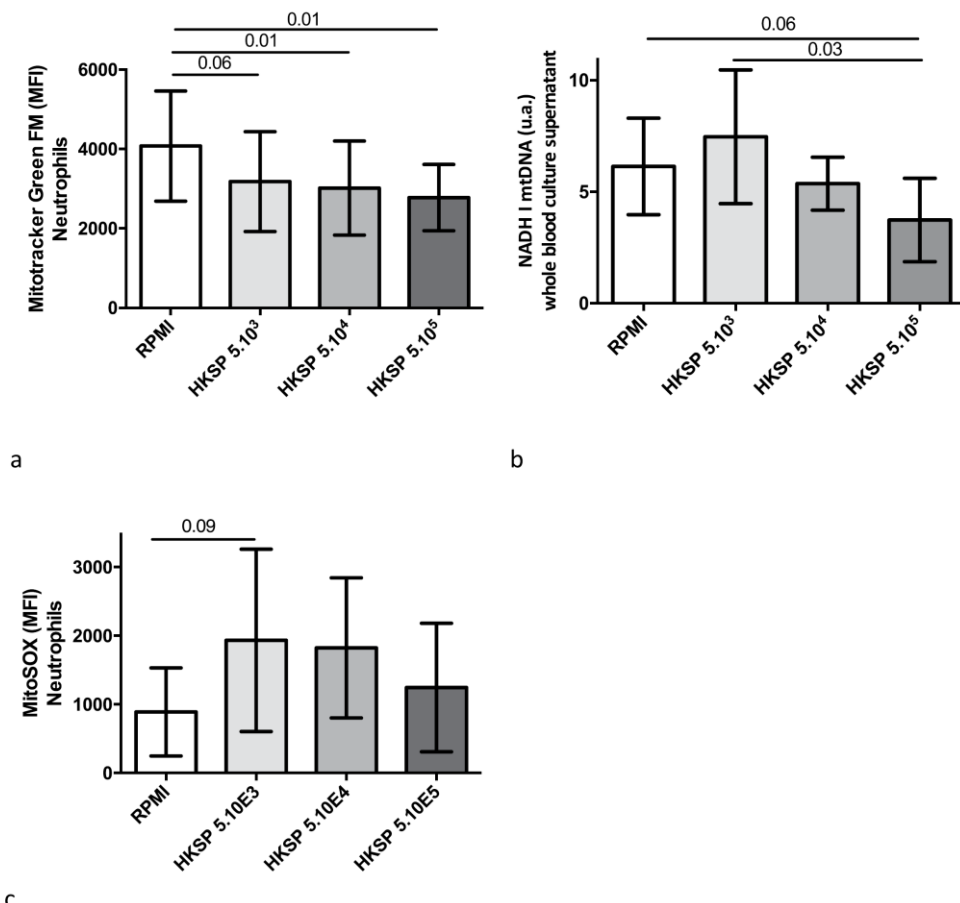


Figure 7. Mitochondrial homeostasis disturbance in whole blood stimulated ex vivo by Heat Killed Streptococcus pneumoniae (HKSP). **(a)** Neutrophil mitochondrial density assessed by flow cytometry with Mitotracker Green FM, and expressed as a median fluorescence intensity (MFI), in whole blood stimulated 16 hours with different concentrations of HKSP (5×10^3 , 5×10^4 , 5×10^5 bacteria/mL) or unstimulated (RPMI). Experiments were performed eight times. Data represent mean \pm SD, n=8 per condition. Normality distribution was verified with D'Agostino-Pearson normality test and t-test was used for all intergroup comparisons. A statistically significant correlation was demonstrated by the Spearmann test ($r = -0.34$; $p = 0.03$). **(b)** Mitochondrial DNA NADH I level in cell culture supernatant after whole blood stimulation by HKSP. t-test was used for all intergroup comparisons. A statistically significant correlation was demonstrated by the Spearmann test ($r = -0.34$; $p = 0.03$). **(c)** Mitochondrial ROS assessed by flow cytometry with MitoSOX expressed as a median fluorescence intensity (MFI) in the experimental conditions described above. Data represent mean \pm SD, n=8 per condition. t-test was used for all intergroup comparisons. DNA: deoxyribonucleic acid, HKSP: Heat Killed Streptococcus pneumoniae, MFI: Median fluorescence intensity, NADH: nicotinamide adenine dinucleotide dehydrogenase, RPMI: Roswell Park Memorial Institute medium, SD: standard deviation.

restoring immune functions^{41,42}. However, such findings are controversial since others have shown that a single mtDNA injection caused profound, TLR9-dependent immunosuppression in mice³².

Several limitations should be mentioned. First, the MV without PEEP we used could be considered not clinically relevant. However, it has recently been reported that such settings are still used, especially in the operating room⁴³. In addition, it is known that lung injury is heterogeneous in ARDS patients. As a result, poorly aerated areas of the lung usually coexist with overstretched ones, even if “low-V_T” is applied, as shown in human studies⁴⁴. Moreover, our model is likely to illustrate the respective effects of adverse MV (i.e. VILI features) and pneumococcal infection. We should also acknowledge that by using SB animals as controls, lung stretch was not the only factor evaluated. Actually, one cannot exclude the possibility that other mechanisms, such as impaired airway drainage subsequent to tracheal intubation, a prolonged supine position and general anesthesia could account, at least in part, for the lower bacterial clearance rate we report here. However, we have previously published data showing that when mild-stretch MV was compared with low-stretch MV in a Gram-negative bacteria VAP model, the latter strategy was likely to favor the host regarding this point⁸. We cannot exclude that mitochondrial

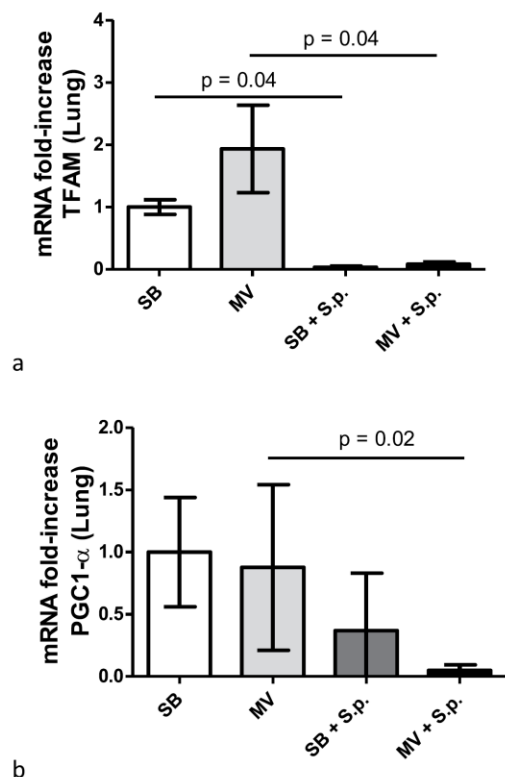


Figure 8. Lung mitochondrial biogenesis evaluation in spontaneously breathing or mechanically ventilated rabbits with or without *Streptococcus pneumoniae* pneumonia. Relative mRNA copy numbers of mitochondrial biogenesis genes (PGC1- α and TFAM) within the lung were measured by the reverse transcriptase-polymerase chain reaction. All values are shown as the fold increase compared with uninfected spontaneous breathing rabbits - value set to 1. The Kruskall Wallis test and the Mann-Whitney U test were used successively for all intergroup comparisons and followed by post hoc corrections for multiple comparisons using the Bonferroni method.

density was underestimated by mtDNA concentrations measurement since oxidized DNA as found in stressed organelles was not necessarily amplified. However, such a hypothesis is unlikely since 3 different mitochondrial genes were amplified with the same results. Finally, the fact that animals were not given antibiotics made any translation to clinical practice questionable. Further experimental studies are therefore needed.

In conclusion, MV impaired lung bacterial clearance and promoted pulmonary-to-systemic translocation in our model. As a result, higher levels of blood inflammation and increased mortality rates were observed. Simultaneously, these rabbits showed obvious signs of mitochondrial depletion in both the lungs and the overall system, together with evidence for deficient biogenesis. Altogether, although speculative, these data suggest that mitochondrial homeostasis is impaired in the setting of *S. pneumoniae* pneumonia, especially if the mechanical stretch resulting from MV is combined with the onset of infection, thereby opening new therapeutic avenues.

Methods

Animals. Male New Zealand White rabbits (3.0 to 3.3 kg) were bred in the University of Burgundy animal facility (Dijon, France). Animal use was approved by the local veterinary committee (i.e., Comité d'éthique de l'expérimentation animale Grand campus Dijon [C2EA Grand campus Dijon] n°105) and experiments were performed according to European laws for animal experimentation (European regulation on Animal Welfare).

Experimental Design. We conducted a prospective randomized animal study. Two sets of experiments were conducted, including uninfected and infected animals, respectively. Within each set, animals were randomized by drawing lots into spontaneously breathing or mechanical ventilation groups. The following groups were obtained: uninfected controls (SB [n = 5], or MV [n = 5]), infected (SB [n = 5] + S.p., or MV + S.p. [n = 5]) groups.

Mechanical Ventilation Model. The animals were intubated as previously described⁴⁵. Briefly, under general anesthesia provided by ketamine 20 mg/Kg (Panpharma, France) and xylazine 1.5 mg/Kg (Rompun®, Bayer, Germany), a cuff tube of 2.5 mm (Mallinckrodt™, Covidien®, U.S.A.) was orally introduced into the trachea under view control. The animal was put in the supine position and connected to a volume-controlled respirator (Servo ventilator 900 C, Siemens®, Germany) (12 mL/kg of tidal volume with zero end-expiratory pressure

[ZEEP], a respiratory rate of 30 bpm and an 0.5 inspired fraction of O₂), since it has been shown that VILI features are obtained with such settings^{46,47}. Only ventilated rabbits were kept anesthetized and paralyzed throughout the experiment with midazolam (0.2 mg/Kg/h) (Hypnovel®, Roche, Switzerland) and cisatracurium besilate (0.8 mg/Kg/h) (Nimbex®, GlaxoSmithKline, U.K). The animals were placed on a heating blanket, and isotonic serum was infused. Non-invasive monitoring was used to monitor heart rate (Hewlett Packard 78353B Monitor). Arterial blood lactate and gases were measured just after intubation to ascertain the safety of our “adverse” MV and at 48 hours (or immediately before death, when bradycardia prior to asystole occurred).

Experimental Pneumonia Induction. The pneumococcal clinical strain 16089 (9V serotype) was used (kindly provided the Centre National de Référence des Pneumocoques, France). Bacteria were grown in 5% CO₂ in brain heart infusion (BHI) broth (BioMérieux, Marcy l’Etoile, France). Before each experiment, bacteria from one frozen aliquot was cultured on agar plates and incubated for 24 h at 37°C. Twenty-five to 30 colonies were inoculated into 9 ml of BHI broth (BioMérieux, Marcy l’Etoile, France) for 6 h at 37°C, and then cultured on agar plates for 18 h at 37°C in an anaerobic atmosphere. This culture was diluted in physiologic saline to obtain a final inoculum of 8.5 log₁₀ colony-forming units (CFU)/ml in 0.5 ml of saline, according to optical density measurements in reference to a standard curve and confirmed by culture. Pneumonia was induced as previously described⁴⁸, by endobronchial challenge with 0.5 ml of this freshly calibrated bacterial inoculum in either SB or MV animals.

Pneumonia Evaluation. Forty-eight hours after pneumonia induction, the animals were euthanized by pentothal overdose following ketamine-xylazine injection as described above, and exsanguinated. However, if death occurred earlier (by asystole), animals were autopsied within the 2 minutes following exsanguination⁴⁵. Spontaneously breathing animals were euthanized if necessary (clinical signs of upcoming death), whereas the MV rabbits were already under general anesthesia. The lungs were removed via thoracotomy and lung injury evaluation was based on a macroscopic score and microscopic examination. For each lower lobe, a sample measuring 1 cm³ focused on a macroscopic lesion was excised, fixed in 10% buffered formalin, and embedded in paraffin. Hematoxylin-eosin staining was applied. Each specimen was graded using a score ranging from 0 to 3, based on the degree of neutrophil infiltration, hemorrhage, and edema⁴⁹.

Quantitative Bacteriology in Infected Lung and Spleen. Lungs and spleen from each animal were removed and homogenized. Bacteria were counted in a sample of this crude homogenate by plating 10-fold dilutions on sheep blood agar and incubating the plates for 24 h at 37°C. For each rabbit, the mean concentration was calculated (e.g., mean concentration = Σ [organ concentration × organ weight]/ Σ organ weights), and adjusted for the dilution.

Assessment of Inflammation. Blood samples were obtained just before experiment onset (H0), 8 hours later (H8) and at H48 (or just before death). Blood, lung and spleen concentrations of IL-8, IL-1 β , IL-10 and TNF- α were assessed by enzyme-linked immunosorbent assay (ELISA) (Euromedex). Lung and spleen pieces were taken and RNA was extracted using the RNA GenElute kit (Sigma). Complementary DNA (cDNA) was obtained by reverse transcription using random primers, RNAsin treatment, and ImProm II reverse transcriptase (Promega, Madison, WI). Quantitative PCR was then performed using the IQ5 thermocycler (Biorad, Hercules, CA) and the IQ™ Syber Green Supermix (Biorad) and rabbit-specific primers, designed using Primer3 software (version 0.4.0), and the rabbit (*Oryctolagus cuniculus*) sequence database. Melting curves were performed to ensure the presence of a single amplicon. The primers sequences for Gapdh, IL-8, IL-1 β , were reported in Table S1. The results are expressed as the fold induction using the Δ Ct method since the spontaneously breathing (SB) animals were always considered the baseline condition.

Mitochondrial DNA, mRNA and Mitochondrial Biogenesis Assessment. Mitochondrial DNA was measured in plasma and BALF (circulating cell-free mtDNA), as well as in lung and spleen tissue (reflecting mitochondrial density). Quantitative PCR was used to measure levels of mtDNA using specific PCR primers for rabbit cytochrome B, cytochrome C oxidase III, and NADH I¹⁴ (Table S1). Primers were designed using the *Oryctolagus cuniculus* mitochondrion complete genome NCB1 reference sequence (NC-001913.1), synthesized by Microsynth (Balgach, Switzerland), and had no significant homology with sequences from rabbit genomic DNA (Blast® site, <http://blast.ncbi.nlm.nih.gov>).

DNA was isolated from blood and BALF using the QIAamp DNA Mini Kit (Qiagen, Valencia, CA, USA), with a final volume of 200 μ l of DNA resuspended in elution buffer. Quantitative PCR was performed with one-tenth or one-hundredth dilutions of the final product, compared with a standard curve of rabbit mtDNA to quantify the amount of amplified mtDNA, and expressed as arbitrary units. Melting curves were performed to ascertain the amplification of a single amplicon. Rabbit mtDNA was isolated from peripheral blood mononuclear cells of healthy rabbits using the mitochondrial isolation kit for cultured cells from ThermoScientific (Rockford, IL, USA). To further ensure that cytochrome b, c and NADH-I primers were specific to mtDNA and did not amplify bacterial DNA sequences, we performed real-time PCR using DNA isolated from our *S. pneumoniae* strain. In order to assess the mitochondrial density within the lung and spleen parenchyma, mtDNA levels were then measured in tissue homogenates. Total cellular DNA was extracted from frozen lung and spleen with the DNeasy blood and Tissue kit (Qiagen, Valencia, CA, USA). The mtDNA copy number was obtained by real-time PCR as previously described and normalized to a nuclear house-keeping gene (i.e., GAPDH) expression, in order to ensure that these concentrations were not related to the number of live cells within the tissue sample⁵⁰. In addition, mitochondrial genes expression was also evaluated through the corresponding mRNA quantification by qPCR, as a reflect of mitochondrial proliferation and function. Mitochondrial DNA damage was assessed by quantifying a large base pair deletion along the major arch of the mitochondrial genome by quantitative PCR. A

common 4977 bp deletion in mtDNA was quantified by quantitative PCR using primers flanking the deletion and normalized to the mitochondrial NADH I gene.

Mitochondrial biogenesis was assessed through the measurement of PGC1- α and TFAM gene expression, in the lung tissue, by qPCR. The corresponding primers sequences for are reported in Table S1.

Neutrophils chemotaxis evaluation. Chemotaxis of human neutrophils induced by rabbits' BALF was measured using a modified Boyden chamber⁵¹. For each experiment, serial dilutions of prototypical chemotactic factors, such as human IL-8 (Merck-Serono, Geneva, Switzerland) and bacterial/mitochondrial fMLP (Sigma, St. Louis, MO, USA) served as a control for the maximal rate of neutrophil chemotaxis. Human neutrophils from healthy volunteers were isolated using a Ficoll-PaqueTM (GE Healthcare Bio-Sciences AB, Uppsala, Sweden) gradient and seeded into the upper well. Different samples of BALF were tested. Results were expressed as % of neutrophils from the upper well migrating across the filter to the lower well after 90 min. Neutrophils in the lower well were detected with the DraQ5TM dye (Biostatus), which stains neutrophil DNA, and counted using the Applied Biosystems 8200 Cellular Detection System (Life Technologies, Switzerland) in comparison with a known concentration of neutrophils as standard.

Circulating ATP concentrations measurement. Plasma ATP was quantified using the ATP bioluminescence assay kit CLS II with a detection range of 10^{-11} – 10^{-6} M (Roche Applied Science, Mannheim, Germany). A standard curve was performed with purified ATP.

Ex vivo whole blood stimulation assays. Fresh heparinized blood from healthy male rabbits was obtained by venipuncture and diluted 1:5 with RPMI 1640 medium (GibcoTM Life Technologies, Saint Aubin, France), supplemented with glutamine 2 mM (Gibco), and Fetal Bovine Serum 5% (Sigma). Blood was stimulated with 5×10^3 , 5×10^4 or 5×10^5 bacteria/mL heat-killed *S. pneumoniae* (HKSP) or left unstimulated. Viable bacteria were not used due their proliferation during the experiment and the need to control the inoculum size. HKSP were prepared by exposing a calibrated inoculum of *S. pneumoniae* (strain 16089), to 95 °C for 15 min. After 16 hours of incubation at 37 °C, diluted blood was centrifuged for 10 min at 500 g. Cell culture supernatant was removed and cell pellet used for mitochondrial staining after removing red blood cells with a 6 min red blood cells lysis. The supernatant was centrifuged for another 5 min at 5,000 g and kept frozen at –80 °C before use.

Mitochondrial labeling. For measuring the mitochondrial mass and mitochondrial ROS production, cells were labeled with respectively Mitotracker green FM and MitoSOX probes (Thermo), according to the manufacturer's instructions. In brief, cells were rinsed with PBS and resuspended in PBS-0.5% BSA before staining with Mitotracker green FM, or MitoSOX at a final concentration of respectively 150 nM and 5 nM, and incubated at 37 °C, 5% CO₂, during 20 min in dark. The concentration of mitochondrial dye used was selected by titrating with different concentrations and the same concentration was used throughout all experiments. Cells were then washed with 5 ml PBS and then centrifuged for 5 min at 500 g. Cell viability was determined by Zombie Violet staining (Biolegend). Cells were then washed with 5 ml PBS, centrifuged for 5 min at 500 g and scrapped in 300 µl PBS 0.5% BSA. Data were acquired on a BD LSRFortessaTM cytometer and analyzed using BD FACSDIVA (BD Biosciences, San Jose, CA) and FlowJo (TreeStar, Ashland, OR) software. Neutrophils were gated with SSC/FSC characteristics and doublets and dead cells were excluded. Results are expressed as a geometric median fluorescence intensity (MFI) of the mitochondrial labelling of the viable cells. Experiments were performed eight times.

Mitochondrial DNA concentrations were measured in the supernatant of whole blood stimulations assay according the method described above.

In vitro analysis to test mtDNA hydrolysis by *Streptococcus pneumoniae*. A defined quantity of mtDNA (3 ng) was incubated for 6 hours at 37 °C in an anaerobic atmosphere with seven different concentrations of *S. pneumoniae* inoculum diluted to 1/10th (7 to 1 log₁₀ CFU/mL), a negative (absence of *S. pneumoniae*) and a positive control (RQ1 Dnase (Promega, Madison, WI). DNA extraction and PCR were performed as described above for both cytochrome b and NADH genes. Experiments were performed four times.

Statistical analysis. Data are presented as medians (IQR). Group sizes were based on previous experiments in which statistically significant differences regarding, for instance, inflammatory mediator levels were achieved with similar numbers of animals^{46,47}. The Kruskall Wallis test was used for all intergroup comparisons of continuous variables. If the result was statistically significant, the Mann Whitney U test (or the Wilcoxon test if appropriate) was performed in order to compare the two groups, unless otherwise stated. Post hoc corrections for multiple comparisons were then applied using the Bonferroni method. Regarding *ex vivo* experimental data, correlations between *S. pneumoniae* inoculum concentrations and some mitochondrial parameters (i.e., mitochondrial DNA concentrations or others) were analyzed with the Spearman test. The cumulative probability of progression to death was compared between groups using the Kaplan-Meier method and the log-rank test. All tests were two-tailed. A *p* value lower than 0.05 was considered statistically significant. Data were analyzed with Prism software (GraphPad Prism[®], San Diego California, USA).

Availability of supporting data. All the data are available on demand.

References

1. Mandell, L. A. *et al.* Infectious Diseases Society of America/American Thoracic Society consensus guidelines on the management of community-acquired pneumonia in adults. *Clin Infect Dis* **44**(Suppl 2), S27–72, <https://doi.org/10.1086/511159> (2007).
2. Mongardon, N. *et al.* Epidemiology and outcome of severe pneumococcal pneumonia admitted to intensive care unit: a multicenter study. *Crit Care* **16**, R155, <https://doi.org/10.1186/cc11471> (2012).

common 4977 bp deletion in mtDNA was quantified by quantitative PCR using primers flanking the deletion and normalized to the mitochondrial NADH I gene.

Mitochondrial biogenesis was assessed through the measurement of PGC1- α and TFAM gene expression, in the lung tissue, by qPCR. The corresponding primers sequences for are reported in Table S1.

Neutrophils chemotaxis evaluation. Chemotaxis of human neutrophils induced by rabbits' BALF was measured using a modified Boyden chamber⁵¹. For each experiment, serial dilutions of prototypical chemotactic factors, such as human IL-8 (Merck-Serono, Geneva, Switzerland) and bacterial/mitochondrial fMLP (Sigma, St. Louis, MO, USA) served as a control for the maximal rate of neutrophil chemotaxis. Human neutrophils from healthy volunteers were isolated using a Ficoll-PaqueTM (GE Healthcare Bio-Sciences AB, Uppsala, Sweden) gradient and seeded into the upper well. Different samples of BALF were tested. Results were expressed as % of neutrophils from the upper well migrating across the filter to the lower well after 90 min. Neutrophils in the lower well were detected with the DraQ5TM dye (Biostatus), which stains neutrophil DNA, and counted using the Applied Biosystems 8200 Cellular Detection System (Life Technologies, Switzerland) in comparison with a known concentration of neutrophils as standard.

Circulating ATP concentrations measurement. Plasma ATP was quantified using the ATP bioluminescence assay kit CLS II with a detection range of 10^{-11} – 10^{-6} M (Roche Applied Science, Mannheim, Germany). A standard curve was performed with purified ATP.

Ex vivo whole blood stimulation assays. Fresh heparinized blood from healthy male rabbits was obtained by venipuncture and diluted 1:5 with RPMI 1640 medium (GibcoTM Life Technologies, Saint Aubin, France), supplemented with glutamine 2 mM (Gibco), and Fetal Bovine Serum 5% (Sigma). Blood was stimulated with 5×10^3 , 5×10^4 or 5×10^5 bacteria/mL heat-killed *S. pneumoniae* (HKSP) or left unstimulated. Viable bacteria were not used due their proliferation during the experiment and the need to control the inoculum size. HKSP were prepared by exposing a calibrated inoculum of *S. pneumoniae* (strain 16089), to 95 °C for 15 min. After 16 hours of incubation at 37 °C, diluted blood was centrifuged for 10 min at 500 g. Cell culture supernatant was removed and cell pellet used for mitochondrial staining after removing red blood cells with a 6 min red blood cells lysis. The supernatant was centrifuged for another 5 min at 5,000 g and kept frozen at –80 °C before use.

Mitochondrial labeling. For measuring the mitochondrial mass and mitochondrial ROS production, cells were labeled with respectively Mitotracker green FM and MitoSOX probes (Thermo), according to the manufacturer's instructions. In brief, cells were rinsed with PBS and resuspended in PBS-0.5% BSA before staining with Mitotracker green FM, or MitoSOX at a final concentration of respectively 150 nM and 5 nM, and incubated at 37 °C, 5% CO₂, during 20 min in dark. The concentration of mitochondrial dye used was selected by titrating with different concentrations and the same concentration was used throughout all experiments. Cells were then washed with 5 ml PBS and then centrifuged for 5 min at 500 g. Cell viability was determined by Zombie Violet staining (Biolegend). Cells were then washed with 5 ml PBS, centrifuged for 5 min at 500 g and scrapped in 300 μl PBS 0.5% BSA. Data were acquired on a BD LSRFortessaTM cytometer and analyzed using BD FACSDIVA (BD Biosciences, San Jose, CA) and FlowJo (TreeStar, Ashland, OR) software. Neutrophils were gated with SSC/FSC characteristics and doublets and dead cells were excluded. Results are expressed as a geometric median fluorescence intensity (MFI) of the mitochondrial labelling of the viable cells. Experiments were performed eight times.

Mitochondrial DNA concentrations were measured in the supernatant of whole blood stimulations assay according the method described above.

In vitro analysis to test mtDNA hydrolysis by *Streptococcus pneumoniae*. A defined quantity of mtDNA (3 ng) was incubated for 6 hours at 37 °C in an anaerobic atmosphere with seven different concentrations of *S. pneumoniae* inoculum diluted to 1/10th (7 to 1 log₁₀ CFU/mL), a negative (absence of *S. pneumoniae*) and a positive control (RQ1 Dnase (Promega, Madison, WI)). DNA extraction and PCR were performed as described above for both cytochrome b and NADH genes. Experiments were performed four times.

Statistical analysis. Data are presented as medians (IQR). Group sizes were based on previous experiments in which statistically significant differences regarding, for instance, inflammatory mediator levels were achieved with similar numbers of animals^{46,47}. The Kruskall Wallis test was used for all intergroup comparisons of continuous variables. If the result was statistically significant, the Mann Whitney U test (or the Wilcoxon test if appropriate) was performed in order to compare the two groups, unless otherwise stated. Post hoc corrections for multiple comparisons were then applied using the Bonferroni method. Regarding *ex vivo* experimental data, correlations between *S. pneumoniae* inoculum concentrations and some mitochondrial parameters (i.e., mitochondrial DNA concentrations or others) were analyzed with the Spearman test. The cumulative probability of progression to death was compared between groups using the Kaplan-Meier method and the log-rank test. All tests were two-tailed. A *p* value lower than 0.05 was considered statistically significant. Data were analyzed with Prism software (GraphPad Prism®, San Diego California, USA).

Availability of supporting data. All the data are available on demand.

References

1. Mandell, L. A. *et al.* Infectious Diseases Society of America/American Thoracic Society consensus guidelines on the management of community-acquired pneumonia in adults. *Clin Infect Dis* **44**(Suppl 2), S27–72, <https://doi.org/10.1086/511159> (2007).
2. Mongardon, N. *et al.* Epidemiology and outcome of severe pneumococcal pneumonia admitted to intensive care unit: a multicenter study. *Crit Care* **16**, R155, <https://doi.org/10.1186/cc11471> (2012).

3. Blot, M. *et al.* A leukocyte score to improve clinical outcome predictions in bacteremic pneumococcal pneumonia in adults. *Open Forum Infect Dis* **1**, ofu075, <https://doi.org/10.1093/ofid/ofu075> (2014).
4. Slutsky, A. S. & Ranieri, V. M. Ventilator-induced lung injury. *N Engl J Med* **369**, 2126–2136, <https://doi.org/10.1056/NEJMra1208707> (2013).
5. Pugin, J., Ricou, B., Steinberg, K. P., Suter, P. M. & Martin, T. R. Proinflammatory activity in bronchoalveolar lavage fluids from patients with ARDS, a prominent role for interleukin-1. *Am J Respir Crit Care Med* **153**, 1850–1856 (1996).
6. Pugin, J. Molecular mechanisms of lung cell activation induced by cyclic stretch. *Crit Care Med* **31**, S200–206 (2003).
7. Kawano, T. *et al.* Effect of granulocyte depletion in a ventilated surfactant-depleted lung. *J Appl Physiol* **62**, 27–33 (1987).
8. Ladoire, S. *et al.* Impact of the prone position in an animal model of unilateral bacterial pneumonia undergoing mechanical ventilation. *Anesthesiology* **118**, 1150–1159, <https://doi.org/10.1097/ALN.0b013e31828a7016> (2013).
9. Schortgen, F. *et al.* Infectious and inflammatory dissemination are affected by ventilation strategy in rats with unilateral pneumonia. *Intensive care medicine* **30**, 693–701, <https://doi.org/10.1007/s00134-003-2147-7> (2004).
10. Pauchard, L. A. *et al.* Linezolid and atorvastatin impact on pneumonia caused by *Staphylococcus aureus* in rabbits with or without mechanical ventilation. *PLoS One* **12**, e0187187, <https://doi.org/10.1371/journal.pone.0187187> (2017).
11. Hotchkiss, R. S., Monneret, G. & Payen, D. Sepsis-induced immunosuppression: from cellular dysfunctions to immunotherapy. *Nat Rev Immunol* **13**, 862–874, <https://doi.org/10.1038/nri3552> (2013).
12. van der Poll, T. & Opal, S. M. Host-pathogen interactions in sepsis. *Lancet Infect Dis* **8**, 32–43, [https://doi.org/10.1016/S1473-3099\(07\)70265-7](https://doi.org/10.1016/S1473-3099(07)70265-7) (2008).
13. Pugin, J. How tissue injury alarms the immune system and causes a systemic inflammatory response syndrome. *Ann Intensive Care* **2**, 27, <https://doi.org/10.1186/2110-5820-2-27> (2012).
14. Zhang, Q. *et al.* Circulating mitochondrial DAMPs cause inflammatory responses to injury. *Nature* **464**, 104–107, <https://doi.org/10.1038/nature08780> (2010).
15. McDonald, B. *et al.* Intravascular danger signals guide neutrophils to sites of sterile inflammation. *Science* **330**, 362–366, <https://doi.org/10.1126/science.1195491> (2010).
16. Shimada, K. *et al.* Oxidized mitochondrial DNA activates the NLRP3 inflammasome during apoptosis. *Immunity* **36**, 401–414, <https://doi.org/10.1016/j.immuni.2012.01.009> (2012).
17. West, A. P. *et al.* Mitochondrial DNA stress primes the antiviral innate immune response. *Nature* **520**, 553–557, <https://doi.org/10.1038/nature14156> (2015).
18. Kuipers, M. T., van der Poll, T., Schultz, M. J. & Wieland, C. W. Bench-to-bedside review: Damage-associated molecular patterns in the onset of ventilator-induced lung injury. *Critical care* **15**, 235, <https://doi.org/10.1186/cc10437> (2011).
19. Matsuyama, H. *et al.* Acute lung inflammation and ventilator-induced lung injury caused by ATP via the P2Y receptors: an experimental study. *Respir Res* **9**, 79, <https://doi.org/10.1186/1465-9921-9-79> (2008).
20. Unuma, K., Aki, T., Funakoshi, T., Hashimoto, K. & Uemura, K. Extrusion of mitochondrial contents from lipopolysaccharide-stimulated cells: Involvement of autophagy. *Autophagy* **11**, 1520–1536, <https://doi.org/10.1080/15548627.2015.1063765> (2015).
21. West, A. P. *et al.* TLR signalling augments macrophage bactericidal activity through mitochondrial ROS. *Nature* **472**, 476–480, <https://doi.org/10.1038/nature09973> (2011).
22. Bhagirath, V. C., Dwivedi, D. J. & Liaw, P. C. Comparison of the Proinflammatory and Procoagulant Properties of Nuclear, Mitochondrial, and Bacterial DNA. *Shock* **44**, 265–271, <https://doi.org/10.1097/SHK.0000000000000397> (2015).
23. Nakahira, K. *et al.* Circulating mitochondrial DNA in patients in the ICU as a marker of mortality: derivation and validation. *PLoS Med* **10**, e1001577, <https://doi.org/10.1371/journal.pmed.1001577> (2013).
24. Pyle, A. *et al.* Fall in circulating mononuclear cell mitochondrial DNA content in human sepsis. *Intensive Care Med* **36**, 956–962, <https://doi.org/10.1007/s00134-010-1823-7> (2010).
25. Cote, H. C., Day, A. G. & Heyland, D. K. Longitudinal increases in mitochondrial DNA levels in blood cells are associated with survival in critically ill patients. *Crit Care* **11**, R88, <https://doi.org/10.1186/cc6096> (2007).
26. Chen, T. *et al.* The mitochondrial DNA 4,977-bp deletion and its implication in copy number alteration in colorectal cancer. *BMC Med Genet* **12**, 8, <https://doi.org/10.1186/1471-2350-12-8> (2011).
27. Wolthuis, E. K. *et al.* Mechanical ventilation using non-injurious ventilation settings causes lung injury in the absence of pre-existing lung injury in healthy mice. *Crit Care* **13**, R1, <https://doi.org/10.1186/c7688> (2009).
28. Kellum, J. A. *et al.* Understanding the inflammatory cytokine response in pneumonia and sepsis: results of the Genetic and Inflammatory Markers of Sepsis (GenIMMS) Study. *Arch Intern Med* **167**, 1655–1663 (2007).
29. Puskarich, M. A., Shapiro, N. I., Trzeciak, S., Kline, J. A. & Jones, A. E. Plasma levels of mitochondrial DNA in patients presenting to the emergency department with sepsis. *Shock* **38**, 337–340, <https://doi.org/10.1097/SHK.0b013e31826ea169> (2012).
30. Ho, J. *et al.* Autophagy in sepsis: Degradation into exhaustion? *Autophagy* **12**, 1073–1082, <https://doi.org/10.1080/15548627.2016.1179410> (2016).
31. Singer, M. The role of mitochondrial dysfunction in sepsis-induced multi-organ failure. *Virulence* **5**, 66–72, <https://doi.org/10.4161/viru.26907> (2014).
32. Schafer, S. T. *et al.* Mitochondrial DNA: An Endogenous Trigger for Immune Paralysis. *Anesthesiology* **124**, 923–933, <https://doi.org/10.1097/ALN.0000000000001008> (2016).
33. Ashar, F. N. *et al.* Association of mitochondrial DNA levels with frailty and all-cause mortality. *J Mol Med (Berl)* **93**, 177–186, <https://doi.org/10.1007/s00109-014-1233-3> (2015).
34. Hashizume, M. *et al.* Mitochondrial-targeted DNA repair enzyme 8-oxoguanine DNA glycosylase 1 protects against ventilator-induced lung injury in intact mice. *Am J Physiol Lung Cell Mol Physiol* **304**, L287–297, <https://doi.org/10.1152/ajplung.00071.2012> (2013).
35. Timmermans, K., Kox, M., Vaneker, M., Pickkers, P. & Scheffer, G. J. Mitochondrial DNA and TLR9 Signaling Is Not Involved in Mechanical Ventilation-Induced Inflammation. *Anesth Analg* **124**, 531–534, <https://doi.org/10.1213/ANE.0000000000001554> (2017).
36. Kuck, J. L. *et al.* Mitochondrial DNA damage-associated molecular patterns mediate a feed-forward cycle of bacteria-induced vascular injury in perfused rat lungs. *Am J Physiol Lung Cell Mol Physiol* **308**, L1078–1085, <https://doi.org/10.1152/ajplung.00015.2015> (2015).
37. Nerlich, A. *et al.* Pneumolysin induced mitochondrial dysfunction leads to release of mitochondrial DNA. *Sci Rep* **8**, 182, <https://doi.org/10.1038/s41598-017-18468-7> (2018).
38. Haden, D. W. *et al.* Mitochondrial biogenesis restores oxidative metabolism during *Staphylococcus aureus* sepsis. *American journal of respiratory and critical care medicine* **176**, 768–777, <https://doi.org/10.1164/rccm.200701-161OC> (2007).
39. Rocheteau, P. *et al.* Sepsis induces long-term metabolic and mitochondrial muscle stem cell dysfunction amenable by mesenchymal stem cell therapy. *Nat Commun* **6**, 10145, <https://doi.org/10.1038/ncomms10145> (2015).
40. Athale, J. *et al.* Nrf2 promotes alveolar mitochondrial biogenesis and resolution of lung injury in *Staphylococcus aureus* pneumonia in mice. *Free Radic Biol Med* **53**, 1584–1594, <https://doi.org/10.1016/j.freeradbiomed.2012.08.009> (2012).
41. Wanke-Jellinek, L. *et al.* Beneficial Effects of CpG-Oligodeoxynucleotide Treatment on Trauma and Secondary Lung Infection. *J Immunol* **196**, 767–777, <https://doi.org/10.4049/jimmunol.1500597> (2016).
42. Roquilly, A. *et al.* CpG-ODN and MPLA prevent mortality in a murine model of post-hemorrhage-*Staphylococcus aureus* pneumonia. *PLoS One* **5**, e13228, <https://doi.org/10.1371/journal.pone.0013228> (2010).

43. Futier, E. *et al.* A trial of intraoperative low-tidal-volume ventilation in abdominal surgery. *N Engl J Med* **369**, 428–437, <https://doi.org/10.1056/NEJMoa1301082> (2013).
44. Terragni, P. P. *et al.* Tidal hyperinflation during low tidal volume ventilation in acute respiratory distress syndrome. *American journal of respiratory and critical care medicine* **175**, 160–166, <https://doi.org/10.1164/rccm.200607-915OC> (2007).
45. Charles, P. E. *et al.* New model of ventilator-associated pneumonia in immunocompetent rabbits. *Critical care medicine* **30**, 2278–2283, <https://doi.org/10.1097/01.CCM.0000025914.47112.77> (2002).
46. Charles, P. E. *et al.* Mild-stretch mechanical ventilation up-regulates toll-like receptor 2 and sensitizes the lung to bacterial lipopeptide. *Critical care* **15**, R181, <https://doi.org/10.1186/cc10330> (2011).
47. Barbar, S. D. *et al.* Mechanical Ventilation Alters the Development of *Staphylococcus aureus* Pneumonia in Rabbit. *PLoS One* **11**, e0158799, <https://doi.org/10.1371/journal.pone.0158799> (2016).
48. Piroth, L. *et al.* Development of a new experimental model of penicillin-resistant *Streptococcus pneumoniae* pneumonia and amoxicillin treatment by reproducing human pharmacokinetics. *Antimicrob Agents Chemother* **43**, 2484–2492 (1999).
49. Broccard, A. *et al.* Prone positioning attenuates and redistributes ventilator-induced lung injury in dogs. *Crit Care Med* **28**, 295–303 (2000).
50. Piantadosi, C. A. & Suliman, H. B. Mitochondrial transcription factor A induction by redox activation of nuclear respiratory factor 1. *J Biol Chem* **281**, 324–333, <https://doi.org/10.1074/jbc.M508805200> (2006).
51. Drife, G., Dunn-Siegrist, I., Tissieres, P. & Pugin, J. Innate immune functions of immature neutrophils in patients with sepsis and severe systemic inflammatory response syndrome. *Critical care medicine* **41**, 820–832, <https://doi.org/10.1097/CCM.0b013e318274647d> (2013).

Acknowledgements

We are indebted to P. Bastable and S. Rankin for editing assistance, and to the Cytometry and CellimaP core facilities of the University of Burgundy which are supported by the following institutions: Conseil Régional de Bourgogne Franche-Comté, FEDER, etc.

Author Contributions

M.B., L.A.P., J.P. and P.E.C. designed the experiments and analyzed the data. M.B., L.A.P., I.D., J.D., S.M. and C.R. conducted the experiments. M.B. and P.E.C. drafted the manuscript. D.C., L.P. and J.P. revised the manuscript.

Additional Information

Supplementary information accompanies this paper at <https://doi.org/10.1038/s41598-018-30226-x>.

Competing Interests: The authors declare no competing interests.

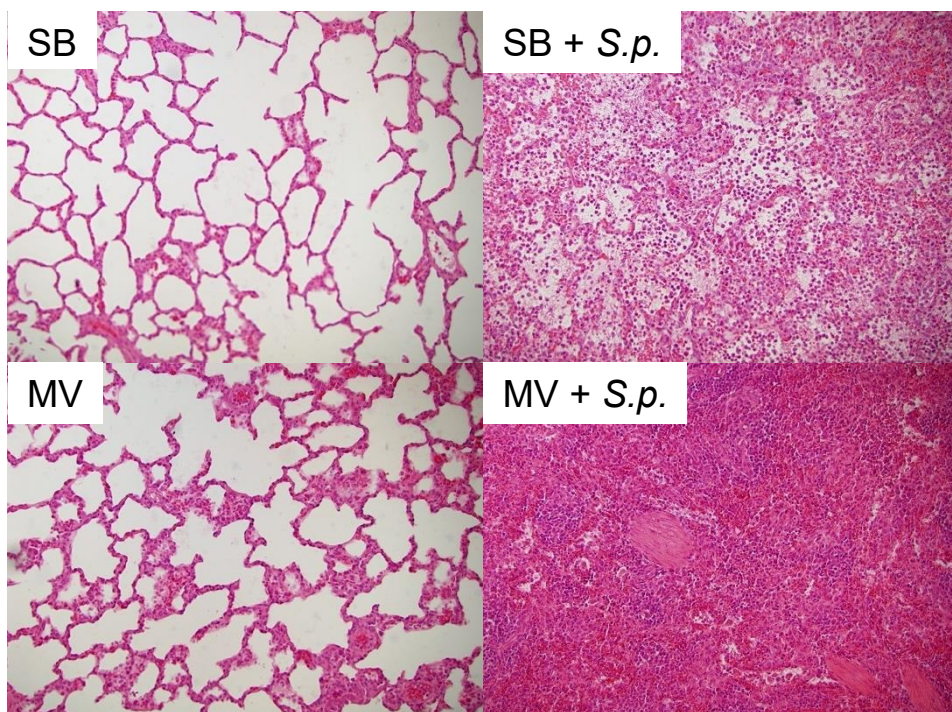
Publisher's note: Springer Nature remains neutral with regard to jurisdictional claims in published maps and institutional affiliations.



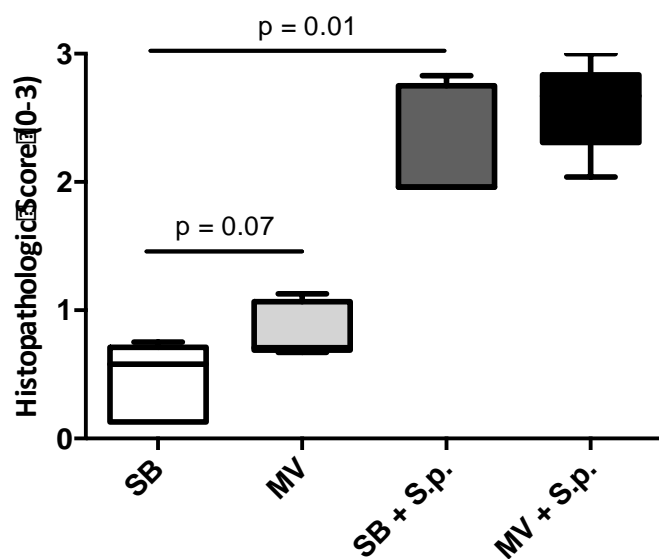
Open Access This article is licensed under a Creative Commons Attribution 4.0 International License, which permits use, sharing, adaptation, distribution and reproduction in any medium or format, as long as you give appropriate credit to the original author(s) and the source, provide a link to the Creative Commons license, and indicate if changes were made. The images or other third party material in this article are included in the article's Creative Commons license, unless indicated otherwise in a credit line to the material. If material is not included in the article's Creative Commons license and your intended use is not permitted by statutory regulation or exceeds the permitted use, you will need to obtain permission directly from the copyright holder. To view a copy of this license, visit <http://creativecommons.org/licenses/by/4.0/>.

© The Author(s) 2018

Supplementary data :



a



b

Figure S1: Main features of lung injury in spontaneously breathing or mechanically ventilated rabbits with or without *Streptococcus pneumoniae* pneumonia.

(A) Representative microphotographs of rabbit lungs fixed at the same transpulmonary pressure (hematoxylin and eosin x400) in various conditions: following tracheal instillation of saline (controls) or 8.5 log₁₀ CFU of *Streptococcus pneumoniae* in spontaneously breathing or mechanically ventilated

animals. (B) Histopathology score of Ventilator Induced Lung Injury ranging from 0 to 3, based on the degree of polymorphonuclear infiltration, hemorrhage, and edema in the interstitial and alveolar spaces, in spontaneous breathing or mechanically ventilated rabbits (B).

The two-tailed Mann-Whitney U test was used for all intergroup comparisons followed by appropriate corrections for multiple comparisons.

CFU: colony forming unit; MV: mechanical ventilation, SB: spontaneously breathing, *S.p.*: *Streptococcus pneumoniae*.

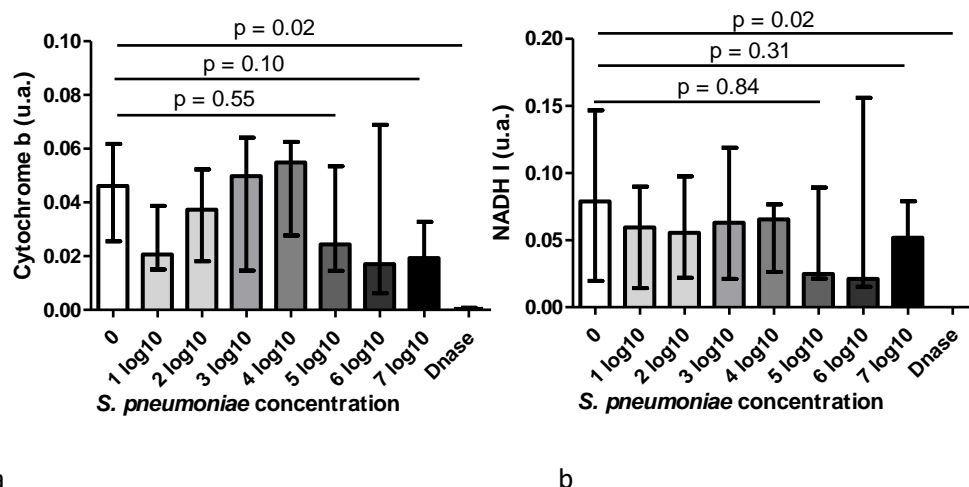


Figure S2. *in vitro* hydrolysis of mitochondrial DNA by *Streptococcus pneumoniae*.

Median concentrations (IQR) of mitochondrial DNA (Cytochrome b [A], NADH I [B]) were measured 6 hours after co-incubation with increasing concentrations of *Streptococcus pneumoniae*.

The two-tailed Mann-Whitney U test was used for all intergroup comparisons.

Deoxyribonucleic acid, Dnase: Desoxyribonuclease, NADH: nicotamide adenine dinucleotide hydrogen, PCR: polymerase chain reaction, IQR: interquartile range.

The two-tailed Mann-Whitney U test was used for all intergroup comparisons followed by appropriate corrections for multiple comparisons.

	FORWARD	REVERSE
GAPDH	5'-ATG TTT GTG ATG GGC GTG AAC C- 3'	5'-CCC AGC ATC GAA GGT AGA GGA- 3'
IL-8	5'-AAC CTT CCT GCT GCT TCT GA- 3'	5'-TCT GCA CCC ACT TTT TCC TTG- 3'
IL-1B	5'-CCT GTC CTG CGT GAT GAA AG- 3'	5'-GAC GGG CAT GTA CTC TGT CT- 3'
CYT-B	5'-CCA TCC TTG TTC TAG CCT TCA- 3'	5'-AAT GGT GAT GAA CGG GTG TT- 3'
CYT-C	5'-GAA GGC AAT CGC AAA AAC AT- 3'	5'-ACG TGA AGA CCG TGA AAT CC- 3'
NADH-I	5' -GCC CCA ACC CTA GCT CTA AC- 3'	5'-GCT CGG AGA GCA CCA AAT AG- 3'
PGC1-A	5' -TAG AGT CTT GGA GCT CCT- 3'	5' -TCC TCT GAC CCC AGA CTC AC- 3'
TFAM	5' -TAT AAG CTG AAC GAG GTC- 3'	5' -ACA ACT ACC CAT ATT TAA AGC- 3'
MTDNA_{4977PB}	5'-CCTTACACTATTCCCTCATCACC-3'	5'-TGTGGTCTTGGAGTAGAAACC-3'

Table S1: Polymerase chain reaction rabbit-specific primers sequences.

Abbreviations: GAPDH: glyceraldehyde-3-phosphate dehydrogenase, IL: interleukin, Cyt: cytochrome, NADH: nicotamide adenine dinucleotide, ATG: autophagy-related, PGC1: peroxisome proliferator-activated receptor gamma coactivator 1, TFAM: mitochondrial transcription factor A.

	PaO ₂ /FIO ₂ ratio		Arterial lactate concentration (mmol/L)		Arterial pH	
	H0	H48	H0	H48	H0	H48
MV	453 (412-459)	420 (409-437)	1.4 (1-1.5)	1.0 (0.8-1.3)	7.49 (7.43-7.51)	7.48 (7.47-7.49)
MV + S.p.	413 (397-431)	142 (78-215)*	1.6 (1.4-1.9)	7.3)*	7.53 (7.50-7.56)	7.16 (7.14-7.26)

Table S2: Arterial blood oxygenation, pH and lactate concentration in rabbits subjected to mechanical ventilation with or without *Streptococcus pneumoniae* pneumonia.

Blood samples were obtained at baseline (H0), and after 48 hours of mechanical ventilation or earlier if death occurred**.

Data are expressed as median (IQR). *indicates p<0.05

The two-tailed Mann-Whitney U test was used for all intergroup comparisons.

**blood was drawn just before death, at the onset of bradycardia. SB: spontaneous breathing,

MV: mechanical ventilation, S.p.: *Streptococcus pneumoniae*, PaO₂/FIO₂ ratio: ratio of arterial partial oxygen pressure /fraction of inspired oxygen.

➔ Synthèse de l'article 2

Dans notre modèle de pneumopathie à *S.p.* chez le lapin, les animaux ventilés avec un schéma jugé modérément agressif (Vt 12 ml/kg, zero PEEP), développent des pneumopathies plus sévères (défaut de clairance bactérienne pulmonaire et systémique, surmortalité), comparés aux animaux en ventilation spontanée (VS). Les concentrations intracellulaires pulmonaires d'ADN mitochondrial (ADNmt), reflet du pool mitochondrial, sont significativement diminuées chez les lapins ventilés, en comparaison aux lapins en VS, et chez les lapins infectés en comparaison aux lapins non infectés. Parallèlement les concentrations plasmatiques d'ADNmt diminuent précocement (H8) chez tous les lapins infectés, mais n'est restauré que chez les lapins en VS, c'est-à-dire ceux qui survivent à la pneumonie. Il existe également une altération qualitative de l'ADNmt dans le compartiment pulmonaire, en particulier chez les animaux infectés et ventilés. Ces délétions de l'ADNmt, survenant en contexte de stress oxydatif, sont source de dysfonction mitochondriale et pourraient expliquer en partie l'altération de l'expression génique des protéines mitochondrielles observée dans notre modèle.

Des tests *ex vivo* complémentaires ont permis de montrer que :

- L'ADNmt circulant n'était pas digéré par une Dnase de notre souche de *Streptococcus pneumoniae*.
- Des tests de stimulation *ex vivo* de sang total de lapin avec notre souche de *Streptococcus pneumoniae* entraînaient une réduction inoculum-dépendante de la densité mitochondriale des PMNs avec parallèlement une diminution des concentrations d'ADNmt dans le surnageant. Ces données suggèrent que l'ADNmt circulant pourrait être le reflet de la densité mitochondriale des PMNs.

Parallèlement, il existe dans notre modèle un défaut d'activation de la biogénèse mitochondriale dans le compartiment pulmonaire chez les lapins infectés, et particulièrement au cours de la double agression infection/ventilation.

Ces résultats suggèrent une diminution drastique du pool mitochondrial dans les compartiments pulmonaire et systémique dans notre modèle de pneumonie bactérienne, avec un rôle potentiellement aggravant de la VM dans ce contexte. Le défaut d'activation de la biogénèse mitochondriale pourrait expliquer l'absence de restauration du pool mitochondrial, et la surmortalité des animaux ventilés qui en découle.

Plusieurs limites et questions étaient soulevées au terme de ces deux travaux :

- Concernant le modèle expérimental :
 - Les anomalies observées au cours de la VM agressive ne permettent pas de les attribuer au seul effet du stretch des cellules pulmonaires dans la mesure où les animaux ventilés, à la différence de ceux en respiration spontanée, bénéficient d'une anesthésie générale, d'une curarisation, d'une hydratation intraveineuse continue, de variations thermiques induite par la procédure, malgré la mise en place d'un tapis chauffant. L'étude d'un groupe soumis à une VM protectrice permettrait de répondre à cette limite.
- Nous n'avons pas observé d'augmentation des niveaux d'ADNmt dans le surnageant des LBA au cours de la VM et de l'infection respectivement, en comparaison à la situation contrôle. Plusieurs hypothèses pourraient permettre de l'expliquer :
 - Ce modèle expérimental permet l'évaluation d'une VM prolongée, à la différence des modèles de VM chez le petit rongeur (maximum 8 heures). Néanmoins, il est possible que la libération d'ADNmt soit très précoce. Deux temps d'évaluation, l'un précoce, l'autre plus tardif seraient alors nécessaires pour mieux évaluer cette mesure. Par ailleurs, la mitophagie semble être un processus activé très précocement au cours des situations de stress infectieux (dans les premières heures), et qui pourrait expliquer la baisse du pool mitochondrial observées dans le tissu pulmonaire et splénique.
 - Les données de la littérature concernant les variations d'ADNmt plasmatique au cours de situations infectieuses (sepsis, choc septique), sont comme nous l'avons vu dans l'introduction, très discordantes. Nos résultats obtenus chez le lapin retrouvent plutôt une baisse, parallèlement à la baisse de la densité mitochondriale des cellules immunitaires (rates des animaux infectés, PMNs lors des tests ex vivo avec sang total stimulé par du pneumocoque inactivé à la chaleur). Une des explications pourrait être les méthodes de centrifugation. En effet, il est impératif de bien centrifuger les fluides pour exclure les cellules et débris cellulaires, au risque que la mesure soit le reflet de l'ADNmt intracellulaire, plus qu'extracellulaire. Les protocoles retrouvés dans la littérature sont très différents d'un travail à l'autre, allant de centrifugations classiques à l'enchainement de plusieurs centrifugations. Il est très probable que les protocoles de centrifugation appliqués dans notre travail (1600 rpm pendant 10 min) soient insuffisants et méritent d'être optimisés.
- La densité mitochondriale mesurée par PCR dans les tissus pulmonaire et splénique n'est qu'une évaluation grossière de la masse mitochondriale. Or, les situations analysées dans

notre étude (VS, VM, infection, double agression) imposent de considérer l'infiltat cellulaire immunitaire des tissus, qui pourraient expliquer en partie les variations de pool mitochondrial global du tissu. Une mesure des altérations mitochondriales à l'échelle d'un type cellule précis serait nécessaire pour statuer plus finement sur des variations de pool mitochondrial.

- La pertinence de ce modèle pourrait également être améliorée par l'étude des altérations mitochondriales au cours de la pneumopathie à pneumocoque traitée par un antibiotique afin de se rapprocher de la situation clinique.
- Enfin, l'impact de la correction des altérations mitochondriales au cours du sepsis ou du VILI, ne sont pas connues. Il est très probable que cette adaptation mitochondriale, en réponse au stress, mécanique ou infectieux, soit bénéfique : phénomène d'hibernation, ou protection des cellules face au stress oxydatif, au prix d'une perte de fonctionnalité cellulaire, dont la durée pourrait être déterminée par l'efficacité de la clairance bactérienne, l'activation des voies de régulation (balance mitophagie/biogénèse mitochondriale). Le bénéfice éventuel résultant de la correction de ces altérations mériterait ainsi d'être évaluée.

2.3 Article 3 : Dysfonction mitochondriale et réponse immune de l'hôte au cours de la pneumopathie à *Streptococcus pneumoniae* : impact de la ventilation mécanique ? (Travail en cours de publication)

Au terme de ces 2 premiers travaux, nous avons souhaité mieux préciser l'impact de la VM comme agression surajoutée au cours de la pneumopathie à pneumocoque sur la réponse immune et la dysfonction mitochondriale. Des méthodes d'analyse complémentaires ont été développées pour répondre à certaines interrogations et limites des précédents travaux. Le modèle expérimental a été optimisé.

→ Objectifs de l'étude

Décrire certains aspects de la réponse immune et les phénomènes de dysfonction mitochondriale au cours du temps dans les compartiments pulmonaires et extra-pulmonaires :

- Au cours de la VM selon deux modalités (protectrice et agressive)
- Au cours de la pneumopathie à *S.p.*, chez l'animal ventilé ou non, en corrélant ces anomalies à la mortalité, à la clairance bactérienne, à la diffusion systémique de l'infection.

Evaluer l'impact de l'injection de cellules souches/stromales mésenchymateuses humaines, seules, en comparaison ou à une antibiothérapie, ou en association avec celle-ci, sur le devenir, la restauration de l'homéostasie mitochondriale et de l'immunité innée.

→ Participation personnelle :

- Planification du design de l'étude avec le Pr P.E. Charles
- Réalisation de toutes les expérimentations animales sur 3 ans avec l'aide de Marine Jacquier (Master 2), Laure-Anne Pauchard (Ingénieur recherche), Chloé Rebaud (Licence pro), Camille Hamelle (Master 1).
- Plusieurs mises au point nécessaires au projet (validation de la sécurité clinique des 2 schémas de VM, méthode de mesure des altérations mitochondrielles par cytométrie en flux...).
- Réalisation de tous les dosages avec l'aide de Marine Jacquier (Master 2), Camille Hamelle (Master 1), Charline Marlin (BTS).
- Analyse et interprétation des résultats, écriture de l'article avec le Pr P.E. Charles.

Mesenchymal stem cells as an adjunctive therapy during severe ventilated pneumococcal pneumonia.

Mathieu Blot^{1,2}, Marine Jacquier¹, Laure-Anne Pauchard¹, Chloé Rebaud¹, Charline Marlin¹, Camille Hamelle¹, Amandine Bataille³, Delphine Croisier⁴, Charles Thomas¹, Danielle Bensoussan⁵, Loic Reppel⁵, Pierre-Emmanuel Charles^{1,6}.

¹ INSERM, LabEx LipSTIC, Univ. Bourgogne Franche-Comté, LNC UMR1231, Dijon, France

² Infectious Diseases Department, University Hospital, Dijon, France

³ Cell imaging platerform, CellImaP/DimaCell, INSERM LNC UMR1231, 21000, Dijon, France.

⁴ Vivexia S.A.R.L., Gémeaux, France

⁵ University hospital, Cell therapy and tissue bank Unit, CNRS, UMR 7365, 54500 Vandoeuvre-lès-Nancy, France

⁶ Intensive Care Unit, University Hospital, Dijon, France.

Corresponding author:

Pierre-Emmanuel Charles

pierre-emmanuel.charles@chu-dijon.fr

+33 3 80 29 31 27

Medical Intensive Care Unit.

University Hospital

14, rue Gaffarel

21000 Dijon

FRANCE

Author's contributions :

Study design and concept: M.B., M.J., L.A.P., P.E.C., L.R.

Acquisition of data: M.B., M.J., L.A.P., C.M., C.R., C.H., A.B.

Analysis and interpretation of data: M.B., P.E.C., L.R., D.B., C.T.

Drafting the manuscript: M.B., P.E.C., L.R., D.B.

Statistical analysis: M.B., M.J., L.A.P., P.E.C., P.C.

Administrative, technical, or material support: M.B., P.E.C., A.B., D.C., L.P., P.C.

Study supervision: P.E.C., D.B., P.C.

Sources of support: This work was supported by a grant (MSD Avenir 2018 – sponsorship agreement), INSERM (Institut national de la santé et de la recherche médicale) U.M.R. 1231 (Labex Lipstic), and the UBFC (Université Bourgogne Franche Comté).

Running title: Mesenchymal stem cells for ventilated pneumonia.

Subject Category:

1.19 Immunology/Inflammation: Animal Models

4.8 Mechanical Ventilation: Physiology & Pathophysiology

10.10 Pathogenic Mechanisms of Infections

Impact:

Mechanical ventilation dramatically worsens pneumococcal pneumonia in rabbits, by causing immune and mitochondrial dysfunctions. Mesenchymal stem cells administration is likely to substantially alleviate those deleterious effects and in turn to improve the outcome. In addition, MSCs mitigates the pro-inflammatory effect resulting from the early administration of antimicrobial agents when both treatments are given simultaneously, thus enhancing the beneficial effect of antibiotics. Mesenchymal stem cells represent therefore a promising adjunctive therapy for severe pneumococcal pneumonia.

Abstract

Rationale: Ventilator-induced lung injury (VILI) worsens severe pneumonia. Mitochondrial dysfunction might be critical.

Objectives: We addressed the impact on survival, lung injury, immune response and mitochondrial homeostasis of prolonged mechanical ventilation (MV) in rabbits with pneumococcal pneumonia, and whether mesenchymal stem cells (MSCs) could be protective.

Methods: Healthy or infected rabbits (n=105) were submitted to either protective or adverse MV, or kept spontaneously breathing. Survival, bacterial burden, immune and mitochondrial derangements were assessed. In a second set of experiments, rabbits submitted to adverse MV were infused with MSCs and/or ceftaroline upon pneumonia onset.

Measurements and main results: Adverse MV alone caused VILI as well as mitochondrial alterations (mitochondrial DNA [mtDNA] release, increased mitochondrial membrane potential [$\Delta\Psi_m$]) in alveolar polymorphonuclear neutrophils [PMNs], decreased pulmonary mitochondria density). Pneumonia survival dramatically fell from 86% to 0% ($p<0.001$) if adverse instead of protective MV was applied, along with lower pulmonary bacterial clearance and greater levels of inflammation. Similarly, mitochondrial disturbances were then obvious since larger amounts of mtDNA were released and alterations of $\Delta\Psi_m$ were detected in both alveolar and circulating immune cells. Survival was enhanced by MSCs or ceftaroline (57% for each, $p<0.01$), and even more by the combination of both (86%, $p<0.001$). MSCs by themselves reduced VILI, and promoted inflammation and mitochondrial alterations resolution in both pulmonary and systemic compartments.

Conclusions: In this proof-of-concept study, MSCs improve the outcome of rabbits submitted to pneumonia and MV by correcting immune and mitochondrial dysfunctions, thus representing a promising adjunctive therapy to antibiotics.

Word count: 248

Introduction

Community-acquired pneumonia (CAP) remains the leading cause of mortality from infection, and *Streptococcus pneumoniae* the main bacterial agent (1). Severe pneumonia often requires mechanical ventilation (MV) and as such is very frequently encountered in the ICUs with high fatality rates despite effective and early antibiotics, thus emphasizing the urgent need for adjunctive therapies (2,3). Growing evidence supports mitochondrial depletion and dysfunction as important events in the pathogenesis of sepsis-induced multiple organ failure and immune deficiency (4–6). We recently demonstrated that cyclic stretch of human alveolar epithelial cells, as well as of healthy rabbit lung, was likely to promote polymorphonuclear neutrophils (PMNs) chemotaxis and activation subsequently to the release of the so called mitochondrial alarmins (i.e., fMLP, mtDNA and ATP) (7). In addition, we showed that MV worsens the prognosis of pneumococcal pneumonia in rabbits, and was associated with substantial mitochondrial disturbances (e.g. decrease in mitochondrial density within the lung) that could result from a decreased biogenesis (6).

The host immune response diversity in the setting of severe pneumonia leads to various outcomes regardless of antibiotics and supportive care appropriateness. That's why developing personalized medicine targeting relevant and critical pathogenesis steps is paramount (8,9). Accordingly, mesenchymal stem cells (MSCs) has been advocated as a promising adjunctive therapy for pneumonia and acute respiratory distress syndrome (ARDS), since they could provide environment-dependent immunomodulatory and cellular protective effects (10). Interestingly, MSCs were shown to restore alveolar epithelial and macrophages bioenergetics through mitochondrial transfer during acute lung injury (11,12).

Here, we evaluated the impact of MV on immune and mitochondrial derangements in healthy rabbits, and in those with pneumococcal pneumonia. Then, we determine the effect of cord-derived MSCs alone or as an adjunctive therapy of antibiotics in the setting of ventilated pneumococcal pneumonia.

Detailed Methods

Animals

Pathogen free male New Zealand White rabbits (3.0 to 3.3 kg) were bred in the University of Burgundy animal facility under standard care (Dijon, France). All experiments were performed in line with the National Institute of Health guidelines on the Use of Laboratory Animals and were approved by the University Animal Care Committee (i.e., Comité d'éthique de l'expérimentation animale Grand campus Dijon [C2EA Grand campus Dijon] n°105), authorization numbers: APAFIS#9858-2017051014111311v1 and APAFIS#17870-2018112915119912v1.

Experimental design

We conducted a prospective randomized animal study. Two sets of experiments were conducted, including uninfected and infected animals, respectively. Within each set, animals were randomized by drawing lots into spontaneously breathing or mechanical ventilation groups (either protective, or adverse). Rabbits were euthanized 8 or 24 hours thereafter. During the condition associating pneumonia and adverse MV, rabbits were randomly allocated to receive: NaCl (control group), cord-derived Mesenchymal Stem Cells (MSCs), ceftaroline-fosamil (ceftaroline) or ceftaroline+MSCs. Fifteen groups (n=7/group) were evaluated (Table S2).

Mechanical Ventilation Model

The animals were intubated as previously described (13). Briefly, under general anesthesia provided by ketamine 27 mg/Kg (Panpharma, France) and xylazine 2 mg/Kg (Rompun®, Bayer, Germany), a cuff tube of 2.5 mm (Mallinckrodt™, Covidien®, U.S.A.) was orally introduced into the trachea under view control. The animal was put in the supine position and connected to a volume-controlled respirator (Servo ventilator 900 C, Siemens®, Germany). Animals were subjected to either “adverse” (20 mL/kg of tidal volume (Vt) with zero end-expiratory pressure (ZEEP), a respiratory rate of 15 bpm and an 0.5 inspired fraction of O₂), since it has previously been shown that VILI features are obtained with such settings (7), or “protective” (8 mL/kg of Vt with 5 cmH₂O positive end-expiratory pressure (PEEP), a respiratory rate of 35 bpm and an 0.5 inspired fraction of O₂) (14). Only ventilated rabbits were kept anesthetized and paralyzed throughout the experiment with ketamine (1mg/Kg/h), midazolam (0.2 mg/Kg/h) (Hypnovel®,

Roche, Switzerland) and cisatracurium besilate (0.8 mg/Kg/h) (Nimbex®, GlaxoSmithKline, U.K). The animals were placed on a heating blanket, and isotonic saline was infused. Non-invasive monitoring was used to monitor heart rate (Hewlett Packard 78353B Monitor). Venous blood lactate and gases were measured just after intubation to ascertain the safety of our MV and at 8 hours, 16 hours, 24 hours (or immediately before death, when bradycardia prior to asystole occurred).

Experimental Pneumonia Induction

The pneumococcal clinical strain 16089 (9V serotype, penicillin-intermediate and ceftaroline-susceptible) was used (kindly provided the Centre National de Référence des Pneumocoques, France). Bacteria were grown in 5% CO₂ in brain heart infusion (BHI) broth (BioMérieux, Marcy l'Etoile, France). Before each experiment, bacteria from one frozen aliquot was cultured on agar plates and incubated for 24 hours at 37 °C. Twenty-five to 30 colonies were inoculated into 9 ml of BHI broth (BioMérieux, Marcy l'Etoile, France) for 6 hours at 37 °C, and then cultured on agar plates for 18 hours at 37 °C in an anaerobic atmosphere. This culture was diluted in isotonic saline to obtain a final inoculum of 8.8 log₁₀ colony-forming units (CFU)/ml in 0.5 ml of isotonic saline, according to optical density measurements in reference to a standard curve and confirmed by culture. Pneumonia was induced as previously described (6,15), by endobronchial challenge with 0.5 ml of this freshly calibrated bacterial inoculum in either SB or MV animals.

Therapeutics delivery

Previous work of our group showed that a significant bacteremic pneumonia was already observed 4 hours after inoculation (15). As a result, therapeutics (NaCl, MSCs (3.10⁶/Kg), ceftaroline (20mg/Kg) or ceftaroline+MSCs) were administrated once, 4 hours after pneumonia induction. Ceftaroline (Pfizer, New York, USA) was reconstituted in isotonic saline at a final concentration of 30mg/ml and administrated intramuscularly in the right thigh at the dose of 20mg/kg. It was previously showed an eradication of infection and a pharmacodynamic simulating human dose regimen with such settings in non-ventilated infected rabbits with this same pneumococcal strain (16). The concentrations of ceftaroline in plasma were determined from iterative blood samples (just before administration and 1, 2 and 4 hours thereafter) to analyze pharmacokinetic as previously reported (16).

MSC preparation, administration and characterization

Umbilical cord-derived MSCs were prepared as described previously (17). Umbilical cord was collected at Nancy Maternity Hospital from a single mother who had signed an informed consent form in compliance with the French national legislation regarding human sample collection, manipulation, and personal data protection. The collection protocol was approved by the local ethics committee and the French ministry for research (No. DC-2014-2114). All MSCs were produced at clinical-grade in α -MEM culture medium (Macopharma, Mouvaux, France) enriched with 5% platelet lysate (Macopharma, Mouvaux, France) and applying good manufacturing practices. Briefly, umbilical cord was immersed in an antibiotic-antifungal solution composed of gentamicin, amoxicillin, vancomycin, and amphotericin B for 1 hr. at room temperature. The cord was then cut into thin pieces which were placed in complete medium. The culture was carried out at 37 °C and in hypoxic conditions (5% of O₂ and 5% of CO₂). MSCs were cultured until passage three and then frozen and stored in vapor phase nitrogen. MSCs were characterized as previously described (17). After thawing, MSCs were washed once in α -MEM to remove the cryoprotectant and used within 1 hour. Rabbits were intravenously infused with 3×10^6 viable MSCs/kg at 4 hours after pneumonia induction. MSCs were administrated in 10 mL of isotonic saline.

Material harvesting and sample collection

Blood samples were obtained from the venous catheter just before experiment onset (H0) and 8, 16 and 24 hours later (or just before death when bradycardia occurred). Lactate concentration was measured within 30 min. from venous plasma transported at 4°C. Ethylenediaminetetraacetic acid anticoagulated blood was centrifuged immediately at 2,000 g during 10 min. and the plasma collected and stored at -80°C until further analyses.

Twenty-four hours after pneumonia induction, the animals were euthanized by ketamine xylazine injection, following by euthasol overdose and exsanguinated. However, if death occurred earlier (by asystole), animals were autopsied within the 2 min. following exsanguination (6). Spontaneously breathing animals were euthanized if necessary (clinical signs of upcoming death), whereas the MV rabbits were already under general anesthesia. The lungs were removed via thoracotomy. Each lower pulmonary lobe was instilled twice with 2.5 mL of sterile PBS1x. The broncho-alveolar lavage fluid (BALF) was centrifugated at 500 g during 10 min. to collect the cell pellet. The supernatant was centrifugated again at 3,200 g during 5 min. to remove potential remaining cells and debris.

Pneumonia Evaluation.

Lung injury evaluation was based on a macroscopic score and microscopic examination of lungs, as previously reported (13). A sample measuring 1 cm³ of the right lower lobe was excised, fixed in 10% buffered formalin, and embedded in paraffin. Hematoxylin-eosin staining was applied. Each specimen was scored by the same pathologist blinded for experimental groups, using the following parameters and a scale of 0 (absent), 1 (mild), 2 (moderate), 3 (severe), and 4 (very severe): interstitial damage, vasculitis, peribronchitis, edema, thrombus formation, and pleuritis as previously reported (18).

Quantitative Bacteriology in Infected Lung and Spleen.

Lungs and spleen from each animal were homogenized. Bacteria were counted in a sample of this crude homogenate by plating 10-fold dilutions on sheep blood agar and incubating the plates for 24 h at 37 °C. For each rabbit, the mean concentration was calculated (e.g., mean concentration = Σ [organ concentration × organ weight]/ Σ organ weights), and adjusted for the dilution.

Assessment of Inflammation.

A piece of fresh lung was immediately placed into a tissue protein extraction reagent (T-PER, Thermo) with protease inhibitors (Thermo) and stored at -80°C for cytokine measurement. Total protein concentration was measured with the BCA protein assay kit (Sigma). Plasma and lung concentrations of IL-8, IL-1 β , IL-10 and TNF- α were assessed by enzyme-linked immunosorbent assay (ELISA) (Uscn Life Science Inc., Wuhan, China).

Mitochondrial DNA Assessment. Mitochondrial DNA was measured in plasma and BALF (circulating cell-free mtDNA), as well as in lung and spleen tissue (reflecting mitochondrial density). Quantitative PCR was used to measure levels of mtDNA using specific PCR primers for NADH I (Table S2) (6). Primers were designed using the *Oryctolagus cuniculus* mitochondrion complete genome NCB1 reference sequence (NC-001913.1), synthesized by Microsynth (Balgach, Switzerland), and had no significant homology with sequences from rabbit genomic DNA (Blast® site, <http://blast.ncbi.nlm.nih.gov>). DNA was isolated from plasma and BALF, using the QIAamp DNA Mini Kit (Qiagen, Valencia, CA, USA), with a final volume of 200 μ l of DNA resuspended in elution buffer. Quantitative PCR was performed with one-tenth or one-hundredth dilutions of the final product, compared with a standard curve of rabbit mtDNA to quantify the amount of amplified mtDNA, and expressed as arbitrary units. Melting curves were performed to ascertain the amplification of a single amplicon. Rabbit mtDNA was

isolated from peripheral blood mononuclear cells of healthy rabbits using the mitochondrial isolation kit for cultured cells from ThermoScientific (Rockford, IL, USA). In order to assess the mitochondrial density within the lung and spleen parenchyma, mtDNA levels were then measured in tissue homogenates. Total cellular DNA was extracted from frozen lung and spleen with the DNeasy blood and Tissue kit (Qiagen, Valencia, CA, USA). The mtDNA copy number was obtained by real-time PCR as previously described, and normalized to a nuclear house-keeping gene (i.e., GAPDH) expression, in order to ensure that these concentrations were not related to the number of live cells within the tissue sample. Non infected and non-ventilated animals (H8 and H24) were considered the baseline condition for the other groups evaluated at H8 and H24 respectively. The group submitted to pneumonia and adverse MV (H24) and treated with Isotonic Saline was considered the baseline of other therapeutic groups.

Circulating ATP concentrations measurement. Plasma and BALF ATP concentrations were quantified using the ATP bioluminescence assay kit HS II with a detection range of 10^{-12} – 10^{-5} M (Roche Applied Science, Mannheim, Germany). A standard curve was performed with purified ATP.

Mitochondrial mRNA and Mitochondrial Biogenesis Assessment

Mitochondrial genes expression was also evaluated through the corresponding mRNA quantification by qPCR, as a reflect of mitochondrial proliferation and function. Mitochondrial biogenesis was then assessed through the measurement of PGC1- α and TFAM gene expression, in the lung tissue, by qPCR. In brief, lung pieces were taken, and total RNAs were extracted using the RNA GenElute kit (Sigma). Then, RQ1Dnase (Promega) treatment was performed and RNA was reverse transcribed with random primers and ImProm II reverse transcriptase (Promega, Madison, WI). Real time quantitative PCR was performed on a StepOnePlusTM Real-Time PCR (Applied Biosystem), with SYBR green reagent (PowerUp®, Thermo) and rabbit-specific primers, designed using Primer3 software (version 0.4.0), and the rabbit (*Oryctolagus cuniculus*) sequence database. Melting curves were performed to ensure the presence of a single amplicon. Results show averages of experiments normalized to Gapdh and expressed as a fold change relative to control values as described in each figure (ΔCt method). The primers sequences were reported in Table S1.

Mitochondrial measurement with flow cytometry

Blood cells were collected after red blood cell lysis (5 min). Spleen cells were collected after mechanical dissociation in RPMI and a red blood cell lysis (30 sec). Spleen and BAL cells were filtered through a cell strainer of 70 µm (Falcon®). All were resuspended in PBS-0.5% BSA before staining.

Four mitochondrial probes (Thermo) were used at the indicated concentrations to measure mitochondrial mass (Mitotracker green FM, 200 nM), mitochondrial membrane potential ($\Delta\Psi_m$)/active mitochondria (Mitotracker Red CMXRos, 150 nM and Tetramethylrhodamine, Methyl Ester, Perchlorate (TMRM), 100 nM), and mitochondrial ROS production (MitoSOX, 5µM). Cells were incubated separately, with these 4 probes, at 37 °C, 5% CO₂, during 20 min in the dark, according to the manufacturer's instructions. The concentration of mitochondrial dye used was selected by titrating with different concentrations and the same concentration was used throughout all experiments. Cells were then washed with 5 ml PBS and then centrifuged for 5 min at 500 g. Then, cells were incubated with a mouse anti rabbit CD45 (Clone L12/201) APC-Cy7 (Lynx rapid conjugaison kit) (Biorad) and a mouse anti-rabbit Neutrophils (RPN3/57, Biorad) Dylight® 680 (Fast conjugaison kit, Abcam), at 4°C, during 20 min in PBS-2%BSA in the dark. Cell viability was determined by Zombie Violet staining (Biolegend). Cells were then washed with 5 ml PBS, centrifuged for 5 min at 500 g and scrapped in 300 µl PBS 0.5% BSA. Data were acquired on a BD LSRIIcytometer and analyzed using BD FACSDIVA (BD Biosciences, San Jose, CA) and FlowJo (TreeStar, Ashland, OR) software. Blood and alveolar neutrophils were gated with SSC/FSC characteristics and identified as CD45+PNN+ cells. Alveolar macrophages were gated with SSC/FSC characteristics and identified as CD45+PNN- cells. Doublets and dead cells were excluded. Geometric median fluorescence intensity (MFI) of each mitochondrial labelling of the viable cells were measured and autofluorescence of unstained cells used as control for each sample (MFI ratio of stained cells/unstained cells).

Statistical analysis. Data are expressed as box-and-whisker plots, or as mean with SEM as indicated. Comparisons between multiple groups were first performed using Kruskall Wallis analysis of variance test. To account for multiple comparisons, the *p* value was adjusted for a false discovery rate (FDR) using the Benjamini and Hochberg method. Eight- and 24-hours. groups were analyzed separately. Correlations were analyzed with the Spearman test. The cumulative probability of progression to death was compared between groups using the Kaplan-Meier method and the log-rank test. All tests were two-tailed. A *p* value lower than

0.05 was considered statistically significant. Data were analyzed with Prism software (GraphPad Prism®, San Diego California, USA).

Availability of supporting data. All the data are available on demand.

Results

Adverse mechanical ventilation causes mild lung damage, inflammation, and mitochondrial derangements in the pulmonary compartment.

We first investigated the effect of short and long-term protective MV (pMV) and adverse MV (aMV) in non-infected rabbits. The MV settings we applied were considered as safe since all ventilated animals were kept alive, without macroscopic lung damage (Figure E1A), or metabolic disturbances (Figures E1E, E1F). Only aMV was associated with an early but transient decrease of central body temperature (Figure E1B). As expected, blood oxygenation was increased by aMV, along with hypocapnia (Figures E1C, E1D), despite the lower respiratory rate we applied, as compared to the settings in the pMV group.

Then, we investigated the effect of MV on inflammation and mitochondrial homeostasis in the pulmonary compartment. In our rabbit model, only the aMV regimen induced IL-8 release within the airways, PMN cells recruitment, and lung injury (Figure 1A, 1B, 1C, E2A), whereas IL-1 β , TNF- α and IL-10 pulmonary concentrations remained low (Figures E2B, E2C, E2D). In addition, larger amounts of mtDNA were recovered from their BAL fluids, as compared to those obtained in the pMV_{H24} group (0.77 [0.50-1.15] vs. 0.46 [0.43-0.52] ng/ μ L, *p=0.051) (Figure 1D). Mitochondrial DNA lung tissue content (i.e. intracellular mtDNA), was significantly reduced in aMV_{H24} as compared to pMV_{H24} (0.61 [0.47-0.78] vs. 0.85 [0.72-1.51] NADH-I/GAPDH fold induction, *p<0.05) (Figure 1F). Alveolar neutrophils displayed an increase in $\Delta\Psi_m$ in aMV_{H24} animals, as compared to their SB counterparts (496 [340-689] vs. 42 [42-171] median of fluorescence (MFI) ratio, **p<0.001) (Figures 1G, 1H). Conversely, alveolar macrophages displayed a decrease in $\Delta\Psi_m$ in pMV_{H24} animals, as compared to their SB counterparts (*p<0.05) (Figure 1I and 1J).

In the systemic compartment, meaningful rising levels of circulating ATP were measured in aMV animals, as compared to SB animals, whereas no inflammation was detected if leukocytes, IL-8 and IL-1 β concentrations were considered (Figures E3A, E3B, E3C, E3E). Similarly, plasma mtDNA concentrations, mitochondria liver content, $\Delta\Psi_m$ and ROS production in blood neutrophils remain unchanged whenever animals were ventilated or not (Figures E3D, E3F, E3G, E3H, E3I).

Adverse mechanical ventilation worsens the prognosis of pneumococcal pneumonia and is associated with profound immune and mitochondrial derangements in both pulmonary and systemic compartments.

Then, we investigated the effect of MV in the setting of pneumococcal pneumonia. During pneumonia, 24 hours survival was dramatically lower in animals submitted to aMV (0%), as compared to pMV (86%; ***p<0.001), or those kept in SB (100%; ***p<0.001) (Figure 2A). In this setting, only the aMV regimen led to a drop of central body temperature, gas exchanges deep alterations as well as lactic acidosis as compared to pMV or SB animals (Figures 2B, 2C, 2D, 2E, 2F). Animals submitted to aMV, as compared to others, presented more severe lung damages (extensive pneumonia, and lung injury) (Figures 2G, 3C and E4A), and a lower pulmonary bacterial clearance (7.1 [5.0-7.2] vs. 4.0 [3.5-5.7] log₁₀CFU/g of tissue, *p<0.05) together with a higher rate of pulmonary-to-systemic translocation (29% vs 0%) (Figures 2H and 2I). Alveolar inflammation was enhanced by aMV since a significantly greater alveolar PMM recruitment (2.8E⁷ [1.2E⁷ vs. 5.11E⁷] vs. 8.2E⁶ [4.2E⁶-1.5E⁷] cells/mL; *p<0.05) together with a higher IL-8 (804 [753-868] vs. 337 [193-357] pg/g of proteins, °p<0.1) and lower IL-10 pulmonary concentrations in this group (Figures 3A, 3B, 3C and E4D). However, no significant difference in the pulmonary concentrations of IL-1β and TNF-α was measured (Figures E4B, E4C).

As compared to animals submitted to pMV, infected animals in which adverse MV was applied, exhibited larger amounts of cell-free mtDNA (0.98 [0.76-1.21] vs. 0.39 [0.30-0.44] ng/mL; **p<0.01) and ATP (2.6E⁻¹⁰ [2.3E⁻¹⁰-5.4E⁻¹⁰] vs. 1.2E⁻¹⁰ [9.E⁻¹¹-2E⁻¹⁰] M; *p<0.05), within the alveolar space (Figures 3D and 3E). Interestingly, the release of ATP was even earlier (i.e., as soon as H8), in all infected and ventilated animals but remained high solely in those submitted to aMV (Figure 3E). Pulmonary mtDNA levels were significantly lower in infected animals, as compared to non-infected ones (*p<0.05), whenever they were SB or MV (Figure 3F). Alveolar neutrophils displayed an early and persistent increase in ΔΨm in all infected animals, earlier in the aMV as compared to the pMV group (Mitotracker Red/Green, *p<0.05; TMRM, °p<0.1) (Figures 3F, 3G). In contrast, alveolar macrophages exhibited significantly decreased ΔΨm in all infected groups, as compared to the controls (*p<0.05), regardless of MV (Figures 3H and 3I).

In the systemic compartment, leukocytes count dropped early in all infected groups, but remains low in the only animals submitted to aMV, as compared to the SB (****p=0.0001) or pMV animals (*p<0.05) (Figure E5A). Interleukin-8 concentrations were significantly higher in animals submitted to aMV, as compared to SB and those submitted to pMV (Figures 3K and E5B). Mitochondrial alarmins concentrations (i.e., mtDNA and ATP) increased continuously in SB animals, while they dropped in the aMV group (Figures 3L and 3M). Mitochondrial DNA liver content was significantly lower in infected animals that underwent MV (either protective or adverse), as compared to uninfected SB animals (Figure E5F). Blood neutrophils displayed a significant decrease in $\Delta\Psi_m$ in infected animals under adverse MV, as compared to uninfected SB animals (*p<0.05), and a non-significant increase of the production of mitochondrial ROS, as compared to infected SB animals (^p<0.1) (Figures 3N, 3K, E5I).

Mesenchymal stem cells contributed to *Streptococcus pneumoniae* ventilated pneumonia outcome improvement through both pulmonary and systemic inflammatory response and mitochondrial derangements modulation.

In the setting of pneumococcal pneumonia and adverse MV, rabbits were randomized in four therapeutic strategies arms, all administrated 4 hours after the bacterial challenge: NaCl (control group), 3.10^6 human cord-derived MSCs/kg, ceftaroline 20mg/kg, or both treatments (ceftaroline+MSCs). First, 24-hours survival was dramatically improved by MSCs or ceftaroline treatment as compared to the control group (both 57% vs 0% for the control group, **p<0.01), but was the higher when both treatments were combined (86% vs 0%, ***p<0.001) (Figure E4A). The combined therapy significantly reduced lung damage, improved gas exchange, and alleviated lactacidemia (Figures 4B, 4C, 4D, 4E, 4F and 4G), along with a dramatic improvement of lung bacterial clearance (Figure 4H). In the meantime, pulmonary-to-systemic translocation was abrogated (Figure 4I). As compared to the control group, ceftaroline+MSCs treatment reduced alveolar PMNs recruitment (^p<0.1), and IL-8 pulmonary concentrations (Figures 4J and 4K), but IL-1 β , TNF- α and IL-10 concentrations remained unchanged (Figures E7A, E7B, E7C). In addition, the release of mtDNA within the alveolar compartment was decreased (*p<0.05), but ATP levels remained unchanged (Figures 4L and E7D). As compared to the control group, the combined therapy led to a further increase of the $\Delta\Psi_m$ of alveolar PMNs (Mitotracker Red/Green, **p<0.01; TMRM, *p<0.05) (Figures 4M, 4N). Similarly, $\Delta\Psi_m$ was restored in alveolar macrophages (Mitotracker Red/Green, **p<0.01, TMRM, p=NS) (Figures

4O and 4P). In the systemic compartment, ceftaroline+MSCs was associated with reduced IL-8 plasma concentrations, rising mtDNA and ATP plasma concentrations (Figures 4Q, E7H, E7I), and enhanced $\Delta\Psi_m$ of circulating PMNs (Mitotracker Red/Green, * $p<0.05$ and TMRM, ** $p<0.01$), with a non-significant reduction of neutrophil-dependent ROS production (Figures 4R, 4S, E7K).

The respective effects of each treatment (i.e., ceftaroline and MSCs) was also sought. Thus, ceftaroline alone, although reducing significantly the pulmonary bacterial burden, increased TNF- α (** $p<0.001$) and IL-10 (** $p<0.001$) release within the alveolar compartment (Figures 4H, E7B, E7C). In addition, $\Delta\Psi_m$ of both alveolar and circulating PMNs remained unchanged in the ceftaroline group when compared to controls (Figures 4M, 4N, 4O, 4P).

In contrast, MSCs administration by itself attenuated lung damages, improved markedly gas exchange and mitigated lactacidemia (Figures 4B, 4C, 4D, 4E, 4F and 4G). Although not statistically significant, MSCs reduced pulmonary bacterial concentrations by 1.4 log (5.7 [4.2-5.7] vs. 7.1 [5.0-7.2] \log_{10} CFU/g of tissue, $p=0.30$, along with pulmonary-to-systemic translocation abrogation (Figures 4H and 4I). Interestingly, MSCs alone didn't significantly reduced IL-8 and TNF- α pulmonary concentrations, but compensated the overproduction of these mediators subsequent to antibiotic exposure (Figure 4K, E7B). Over time, MSCs was associated with an increase in plasma mtDNA concentrations (NaCl vs. MSCs, $p=NS$; ceftaroline vs. ceftaroline+MSCs , $p<0.05$) (Figure E7H). In addition, alveolar neutrophils $\Delta\Psi_m$ was significantly increased as a result of MSCs administration alone (Mitotracker red/green, ** $p<0.01$; TMRM, * $p<0.05$), or in combination with ceftaroline (* $p<0.05$) (Figures 4M and 4N). Similar findings were obtained in alveolar macrophages (** $p<0.01$), as well as in circulating PMNs from animals treated with MSCs alone (Mitotracker red/green, * $p<0.05$; TMRM, ° $p<0.1$) (Figures 4O and 4P).

Discussion

Herein, we showed in our rabbit model of prolonged MV, that lung stretch worsened pneumococcal pneumonia, leading to sepsis and ARDS features, as a result of VILI. Accordingly, adverse ventilatory settings promoted profound immune and mitochondrial derangements likely to dramatically increase the risk of death. In this context, we showed that MSCs improved markedly pneumonia outcome, through some significant modulations in host response and mitochondrial homeostasis, thus acting synergistically with antibiotics.

Severe pneumonia often requires MV and as such is very frequently encountered in the ICUs with high fatality rates despite effective and early antibiotics, thus emphasizing the urgent need for adjunctive therapies (2,3). In addition, MV is known to be harmful by itself, especially through airspace overdistension when applied to pre-injured lungs (e.g., bacterial pneumonia). Both additional lung damages and exacerbated pulmonary and systemic inflammatory response leading to remote organs failure have been associated with a poor outcome in this context (19–22). There is growing evidence that supports the involvement of mitochondrial depletion/dysfunction in the development of one dysregulated host immune response leading to multiple organ failure in septic patients (4–6). In the current study, we used a prolonged MV experimental model to unravel the clinically relevant pathophysiological interplay between VILI and pneumococcal pneumonia, especially in terms of mitochondrial homeostasis, as well as the therapeutic potency of MSCs, alone or in combination with antibiotics.

Our data are in line with previous findings demonstrating that PMNs involvement is of paramount importance in both pneumonia-associated ARDS and VILI pathogenesis (2,19). Thus, a tight correlation between PMNs alveolar recruitment magnitude and clinical outcome has been shown for long, suggesting that such an inappropriate accumulation and activation of those cells within the lung, could seriously compromise inflammation resolution and tissue repair as well (23,24). Accordingly, we show that lung stretch resulting from adverse MV markedly increased PMNs alveolar recruitment, especially if concurrent bacterial infection occurred, leading paradoxically to a striking deficiency of bacterial clearance, in addition to superimposed lung damages. Improving our knowledge of the underlying mechanisms is therefore mandatory.

We recently demonstrated that cyclic stretch of human alveolar epithelial cells, and of healthy rabbit lung as well, was likely to promote PMNs chemotaxis and activation subsequently to the release of the so called mitochondrial alarmins (i.e., fMLP, mtDNA and ATP), in part through the concomitant triggering of the TLR-9 and the NLRP-3 inflammasome pathways (7). Interestingly, mtDNA levels were found to be much elevated in the BAL fluid from ARDS patients, especially if highly neutrophilic (7). The present study provides further insights since we show that one superimposed infectious insult, results in the release of even greater amount of mtDNA, as well as ATP, in the alveolar compartment. Thus, in addition to PAMPs harbored by infecting *S. pneumoniae*, one could assume that mtDNA stimulates IL-8 secretion through the TLR-9 activation, leading in turn to neutrophils chemotaxis and lung recruitment, contributing thereby to lung injury (7,25). Thus, some authors showed that blocking TLR-9 could protect against VILI in a short-term MV rodent models (26). Although others reported conflicting findings regarding this issue, our data support also the involvement of mtDNA within the alveolar space in the context of VILI (27). Nonetheless, such data raise some questions about alveolar mtDNA origins since the following mechanisms should be addressed: (i) cell death by necrosis or necroptosis; (ii) PMNs netosis; (iii) mitochondrial permeability transition (MPT) pore opening upon cell stimulation by microbial products, thus creating a channel whereby mtDNA can translocate from mitochondria to cytosol, and then possibly outside the cell through extrusion (28,29). In addition, the latter mechanism implies that the cell is unable to prevent mtDNA release from damaged mitochondria or to clear it within the cytosolic compartment, through mitophagy enhancement or cytosolic DNases engagement, respectively (30). Our findings provide some clues likely to decipher with alveolar mtDNA origin as well as with potential mitochondrial disturbances underlying mechanisms. Firstly, *S. pneumoniae* toxin pneumolysin, is one of the potential culprit, since it can trigger the loss of $\Delta\psi_m$, resulting in opening of the MPT pore and mtDNA release, as shown in human alveolar epithelial cells (31). Secondly, we found that $\Delta\psi_m$ was decreased in alveolar macrophages, that might reflect their metabolic switch toward glycolysis rather than OXPHOS, resulting in a M1 pro-inflammatory profile, as far as the host response is concerned, with possible subsequent mtDNA loss. Lower IL-10 pulmonary concentrations might account for such macrophages reprogramming. This finding is however conflicting with recently published experimental data showing that cyclic stretch was likely to promote alveolar macrophages polarization toward a M2 phenotype through the release of IL-4 (32). In contrast, $\Delta\psi_m$ striking

elevation in PMNs suggest OXPHOS activation, accounting at least in part for the high levels of ATP measured within the alveolar space, since cyclic stretch *per se* could have evoked ATP released by epithelial cells (7). Of note, ATP could have thus acted as a pro-inflammatory signal for PMNs through either autocrine or paracrine pathways, involving their purinergic receptors, driving chemotaxis and cell activation (33). However, it is worth noting that surprisingly, IL-1 β pulmonary concentrations were not heightened by the release of larger amounts of either ATP or mtDNA, whereas these two alarmins are known to activate the NLRP3 inflammasome (34). This strong $\Delta\Psi_m$ elevation should also be considered as a marker of increased PMNs life-span resulting from delayed apoptosis. Accordingly, PMN apoptosis was shown to be inversely proportional to the severity of sepsis and associated lung injury (35). Altogether, the combination of lung stretch subsequent to adverse MV and pneumococcal infection drives a hyperinflammatory state relying on the alveolar recruitment and activation of PMNs together with a macrophage reprogramming, and reduced bacterial clearance. As a result, lung injury is markedly worsened leading in turn to major disturbances in gas exchanges including hypoxemia and dead space enlargement. Such findings emphasize the clinical relevance of our model since increasing dead space has been consistently associated with poor prognosis in the patients with ARDS, and even early during the course of the disease (36).

Beside the above described pulmonary effects of the deadly combination of MV and infection, differences arose regarding inflammation within the blood compartment. First, rising IL-8 levels were measured in the only animals submitted to aMV. The link between systemic release of IL-8 and poor outcome in the setting of ventilated pneumonia has already been reported in numbers of experimental and clinical studies (37,14,38,39). Pulmonary-to-systemic translocation of inflammatory mediators, as frequently suggested, cannot fully explain such an hyperinflammatory state. Another relevant hypothesis is that the higher rate of bacteremia was likely to mount a greater inflammatory response from circulating leucocytes. It is worth noting that in the meantime, blood leucocytes count fell dramatically regardless of ventilation before returning to baseline values in all but the rabbits submitted to aMV. Interestingly, this finding parallels with clinical features, since we identified leucopenia as a strong predictor of early death during pneumococcal pneumonia (3). Since the drop of $\Delta\Psi_m$ we measured in circulating PMNs could then indicate apoptosis enhancement, resulting from overstimulation of these cells, cell death could account for leucopenia in our model, and

in the clinical setting as well. As a result, systemic clearance of *S. pneumoniae* would be hampered leading in turn to protracted inflammation and poorer outcome. In line with those findings, plasma mtDNA and ATP concentrations tended to decrease until death in the infected rabbits submitted to adverse MV, while in contrast they augmented in those in which protective MV was applied, and most of all in the SB group. As suggested by previous *ex vivo* findings of our group, plasma mtDNA concentrations could reflect mitochondrial density within circulating immune cells, in particular PMNs cells (6). In addition, we found in the present work a significant correlation between cell-free mtDNA serum concentrations and the circulating leukocytes count, as we did in the alveolar compartment (Figure E8). Those data suggest that mtDNA could act as, or be a surrogate of (e.g., fMLP), one powerful chemotactic agent for PMNs that enabled those inflammatory cells sequestration within the alveolar space, whereas they were allowed to recirculate in the infected animals not submitted to adverse MV, accounting for leucopenia recovery. Nonetheless, the origin of circulating mtDNA is probably more complex during sepsis, since many processes are acting together, as mentioned above. However, it has been shown recently that NETs, a relevant source of extra-cellular mtDNA, were commonly found in both the serum and the BAL fluid from patients with ARDS (40). Although speculative, one could then hypothesize that circulating PMNs in the aMV group failed to enter netosis, and rather die from apoptosis, contributing thereby to defective bacterial clearance within the blood compartment.

Finally, the present study illustrates the deleterious systemic impact of the double lung insult as far as energetic metabolism is concerned. Lactacidemia could be at least in part subsequent to septic shock, hepatic failure, as well as mitochondrial dysfunction. Actually, the significant decrease of the liver mtDNA content may reflect the mitochondrial mass reduction in remote organs. Similar findings were obtained in a peritonitis mice model (41). Interestingly, the authors showed that mitochondria depletion reversal through biogenesis activation was tightly linked with sepsis recovery. Our previously published results as well as the present ones support this hypothesis.

Overall, our data illustrate the close relationship between lung stretch, hyperinflammatory state and increased risk of death in the setting of pneumonia/ARDS as recently underscored by cohort studies dealing with both clinical and biological data including transcriptome analysis. Accordingly, some authors found that 2 distinct phenotypes could be described

among ARDS patients (42,43). Those with the highest levels of systemic inflammation together with lactacidemia and the greatest plateau pressures values, reflecting excessive lung stretch, had clearly the poorest outcome.

In addition, the immune response compartmentalization issue is raised by the present data. Actually, it remains poorly understood, while evidences supporting organ-specific immunology have arisen. It has even been pointed out as a current gap in the host immune response understanding (44). Interestingly, our findings illustrate to which extent immune cells can behave differently with regard to the considered compartment. For instance, as suggested herein in the worst clinical scenario (i.e., adverse MV plus pneumonia), PMNs harbored mitochondria with contrasted activation levels in terms of $\Delta\Psi_m$, if considering the blood and the alveolar compartments, maybe as a result of differences in inflammatory and metabolic environment. This finding contrast with those obtained in patients with or without ARDS in study that addressed the PMNs cells traffic issue (45). These authors showed that PMNs were unprimed within the pulmonary vasculature in healthy lungs, whereas they remained primed if circulating through injured lungs. Overall, these results might witness the difficulty to reliably assess the host response on the only immune circulating cells and in turn to design tailored therapies on this basis (44).

Finally, we addressed in our clinically relevant model of ventilated pneumococcal pneumonia, the effect of clinical-grade human cord-derived MSCs, a promising adjunctive therapy for sepsis and ARDS. As noted by Perlee *et al.*, earlier studies that documented beneficial effects of MSCs mainly relied on the *Escherichia coli* pneumonia model (18). Conversely, little is known about the impact of MSCs administration on the outcome of pneumococcal pneumonia, the main cause of severe pneumonia (46). Furthermore, to the best of our knowledge, no preclinical study has investigated its effect in the peculiar setting of ventilated pneumonia. The clinical relevance of the present model is also enhanced by the implementation of antibiotics, alone or in combination with MSCs. We used human clinical grade MSCs, immediately used after thawing, just as done in the clinical setting. Finally, among potential sources of MSCs, unlike bone marrow and adipose tissue, fetal cord source could display a much greater availability, a critical point given the high incidence of bacterial pneumonia (47,48).

Either antibiotics administration or MSCs injection resulted in a dramatic mortality decline along with reduced lung damages and improved gas exchanges. The best outcome was achieved when both treatments were given simultaneously. Although worthy, lower lung bacterial concentrations resulting from antibiotics exposure alone could not account for such beneficial effects. According to the results of several preclinical models of sepsis and lung-injury, the beneficial effects of MSCs relied mainly on apparently paradoxical antimicrobial and anti-inflammatory properties (5,18,17,10). Accordingly, in the present study, while antibiotics led to enhanced pulmonary bacterial clearance, MSCs themselves were likely to dampen pulmonary inflammation, since they reduced IL8 alveolar release and subsequent PMN cells alveolar recruitment when both therapies were given to the infected rabbits. Moreover, the rising TNF-alpha concentrations subsequent to bacterial lysis in antibiotics-treated animals were counteracted by MSCs. Then, we observed greater concentrations of pulmonary IL-10 concentrations in the group treated by MSCs, that could reflect repolarization of monocytes and/or macrophages from a type 1 (proinflammatory) to a type 2 (anti-inflammatory) phenotype (10,49). Finally, antibiotics and MSCs acted synergistically as far as bacterial lung clearance was concerned.

Some previous experimental studies provide clues regarding the underlying mechanisms. Thus, mitochondria transfers from MSCs to injured epithelial cells or alveolar macrophages has been described as a subtle way likely to constitute alveolar cells bioenergetics and phagocytic activity, in the context of lung injury (11,12). Accordingly, we showed herein that MSCs significantly reduced mitochondrial damage (lower mtDNA release in BALF) and improved mitochondrial function of immune cells (increasing $\Delta\Psi_m$ in alveolar and circulating neutrophils, as well as in alveolar macrophages). Therefore, we assume, that the delayed mitochondrial apoptosis we observed in alveolar and circulating myeloid cells could improve bacterial clearance, just as reported in mice with pneumococcal pneumonia after Fas/FasL mediated apoptosis disruption (50). Conflicting results remain however, since other authors observed that induction of apoptosis contributes to macrophages phagocytosis (51,52).

Since pulmonary-to-systemic *S. pneumoniae* translocation was less likely in the animals treated with either antibiotics or CSMs, one could hypothesize that activated circulating PMN cells microbicidal properties were then enhanced. The higher $\Delta\Psi_m$ we measured in those PMN cells could thus reflect an increase of OXPHOS. However, we cannot exclude a

redistribution of alveolar neutrophils toward the blood flow, driven by a paracrine effect of MSCs, since we observed concomitantly lower alveolar infiltration and higher blood leukocytes count. Basically, pulmonary-to-systemic PMNs trafficking has been described in the setting of ARDS (45).

The strengths of our model rely mainly on the prolonged MV it allows, in contrast to those that used rodents. It was thus possible to assess “long-term” outcomes such as survival in animals with pneumonia. Moreover, it is worth noting that some differences between groups (e.g., lung bacterial burden) did not appear as soon as the 8th hour following the onset of the disease, becoming obvious thereafter. In addition, we have evaluated the effects of MSCs in animals under antibiotics, to be more clinically relevant. Actually, only very few studies tested MSCs in combination with antibiotics (53).

Several limitations should however be mentioned. First, the adverse MV settings (high VT plus ZEEP) we used could be considered not clinically relevant. However, the present study is a proof-of-concept one. In addition, it is known that lung injury is heterogeneous in ARDS patients. As a result, poorly aerated areas of the lung usually coexist with overstretched ones, even if “low-V_T” is applied, as shown in human studies (21). Second, our findings regarding mitochondria metabolic function disturbances should be taken cautiously since we did not explore the respiratory chain at the cell level. Too many cells were mandatory for performing such analysis in addition to FACS.

Acknowledgements

The authors acknowledge Cytometry and CellimaP core facilities of the University of Burgundy which are supported by the following institutions: Conseil Régional de Bourgogne Franche-Comté, FEDER, etc. We thank V. Saint-Giorgio and her staff (Animal Facility), V. Aubert (Electronic Microscopy Facility – INRA), for technical expertise, and S. Rankin for editing assistance. We thank the Centre National de Référence des Pneumocoques (France) for providing us the pneumococcal strain and Vivexia® staff for his assistance for the experiments.

Funding

This work was supported by grants: MSD-Avenir, the Institut National de la Santé et de la Recherche Médicale (INSERM), and by a French government grant managed by the French National Research Agency under the programme ‘Investissements d’Avenir’ with reference ANR-11-LABX-0021 (Lipstic Labex).

REFERENCES:

1. Torres A, Blasi F, Peetermans WE, Viegi G, Welte T. The aetiology and antibiotic management of community-acquired pneumonia in adults in Europe: a literature review. *Eur J Clin Microbiol Infect Dis.* juill 2014;33(7):1065-79.
2. Slutsky AS, Ranieri VM. Ventilator-induced lung injury. *N Engl J Med.* 28 nov 2013;369(22):2126-36.
3. Blot M, Croisier D, Péchinot A, Vagner A, Putot A, Fillion A, et al. A leukocyte score to improve clinical outcome predictions in bacteremic pneumococcal pneumonia in adults. *Open Forum Infect Dis.* sept 2014;1(2):ofu075.
4. Brealey D, Brand M, Hargreaves I, Heales S, Land J, Smolenski R, et al. Association between mitochondrial dysfunction and severity and outcome of septic shock. *Lancet.* 20 juill 2002;360(9328):219-23.
5. Rocheteau P, Chatre L, Briand D, Mebarki M, Jouvion G, Bardon J, et al. Sepsis induces long-term metabolic and mitochondrial muscle stem cell dysfunction amenable by mesenchymal stem cell therapy. *Nat Commun.* 2015;6:10145.
6. Blot M, Pauchard L-A, Dunn I, Donze J, Malnuit S, Rebaud C, et al. Mechanical ventilation and *Streptococcus pneumoniae* pneumonia alter mitochondrial homeostasis. *Sci Rep.* 6 août 2018;8(1):11718.
7. Grazioli S, Dunn-Siegrist I, Pauchard L-A, Blot M, Charles P-E, Pugin J. Mitochondrial alarmins are tissue mediators of ventilator-induced lung injury and ARDS. *PLoS ONE.* 2019;14(11):e0225468.
8. Davenport EE, Burnham KL, Radhakrishnan J, Humburg P, Hutton P, Mills TC, et al. Genomic landscape of the individual host response and outcomes in sepsis: a prospective cohort study. *Lancet Respir Med.* 2016;4(4):259-71.
9. van der Poll T, van de Veerdonk FL, Scicluna BP, Netea MG. The immunopathology of sepsis and potential therapeutic targets. *Nat Rev Immunol.* juill 2017;17(7):407-20.
10. Laroye C, Gibot S, Reppel L, Bensoussan D. Concise Review: Mesenchymal Stromal/Stem Cells: A New Treatment for Sepsis and Septic Shock? *Stem Cells.* déc 2017;35(12):2331-9.
11. Islam MN, Das SR, Emin MT, Wei M, Sun L, Westphalen K, et al. Mitochondrial transfer from bone-marrow-derived stromal cells to pulmonary alveoli protects against acute lung injury. *Nat Med.* 15 avr 2012;18(5):759-65.
12. Jackson MV, Morrison TJ, Doherty DF, McAuley DF, Matthay MA, Kisselpfennig A, et al. Mitochondrial Transfer via Tunneling Nanotubes is an Important Mechanism by Which Mesenchymal Stem Cells Enhance Macrophage Phagocytosis in the In Vitro and In Vivo Models of ARDS. *Stem Cells.* 2016;34(8):2210-23.

13. Charles P-E, Piroth L, Desbiolles N, Lequeu C, Martin L, Portier H, et al. New model of ventilator-associated pneumonia in immunocompetent rabbits. *Crit Care Med.* oct 2002;30(10):2278-83.
14. Ladoire S, Pauchard L-A, Barbar S-D, Tissieres P, Croisier-Bertin D, Charles P-E. Impact of the prone position in an animal model of unilateral bacterial pneumonia undergoing mechanical ventilation. *Anesthesiology.* mai 2013;118(5):1150-9.
15. Piroth L, Martin L, Coulon A, Lequeu C, Duong M, Buisson M, et al. Development of a new experimental model of penicillin-resistant *Streptococcus pneumoniae* pneumonia and amoxicillin treatment by reproducing human pharmacokinetics. *Antimicrob Agents Chemother.* oct 1999;43(10):2484-92.
16. Croisier-Bertin D, Piroth L, Charles P-E, Larribeau A, Biek D, Ge Y, et al. Ceftaroline versus ceftriaxone in a highly penicillin-resistant pneumococcal pneumonia rabbit model using simulated human dosing. *Antimicrob Agents Chemother.* juill 2011;55(7):3557-63.
17. Laroye C, Lemarié J, Boufenzer A, Labroca P, Cunat L, Alauzet C, et al. Clinical-grade mesenchymal stem cells derived from umbilical cord improve septic shock in pigs. *Intensive Care Med Exp.* 8 août 2018;6(1):24.
18. Perlee D, de Vos AF, Scicluna BP, Mancheño P, de la Rosa O, Dalemans W, et al. Human Adipose-Derived Mesenchymal Stem Cells Modify Lung Immunity and Improve Antibacterial Defense in Pneumosepsis Caused by *Klebsiella pneumoniae*. *Stem Cells Transl Med.* août 2019;8(8):785-96.
19. Acute Respiratory Distress Syndrome Network, Brower RG, Matthay MA, Morris A, Schoenfeld D, Thompson BT, et al. Ventilation with lower tidal volumes as compared with traditional tidal volumes for acute lung injury and the acute respiratory distress syndrome. *N Engl J Med.* 04 2000;342(18):1301-8.
20. Amato MBP, Meade MO, Slutsky AS, Brochard L, Costa ELV, Schoenfeld DA, et al. Driving pressure and survival in the acute respiratory distress syndrome. *N Engl J Med.* 19 févr 2015;372(8):747-55.
21. Terragni PP, Rosboch G, Tealdi A, Corno E, Menaldo E, Davini O, et al. Tidal hyperinflation during low tidal volume ventilation in acute respiratory distress syndrome. *Am J Respir Crit Care Med.* 15 janv 2007;175(2):160-6.
22. Stüber F, Wrigge H, Schroeder S, Wetegrove S, Zinserling J, Hoeft A, et al. Kinetic and reversibility of mechanical ventilation-associated pulmonary and systemic inflammatory response in patients with acute lung injury. *Intensive Care Med.* juill 2002;28(7):834-41.
23. Steinberg KP, Milberg JA, Martin TR, Maudner RJ, Cockrill BA, Hudson LD. Evolution of bronchoalveolar cell populations in the adult respiratory distress syndrome. *Am J Respir Crit Care Med.* juill 1994;150(1):113-22.
24. Cowburn AS, Condliffe AM, Farahi N, Summers C, Chilvers ER. Advances in neutrophil biology: clinical implications. *Chest.* sept 2008;134(3):606-12.

25. Zhang Q, Raoof M, Chen Y, Sumi Y, Sursal T, Junger W, et al. Circulating mitochondrial DAMPs cause inflammatory responses to injury. *Nature*. 4 mars 2010;464(7285):104-7.
26. Lin J-Y, Jing R, Lin F, Ge W-Y, Dai H-J, Pan L. High Tidal Volume Induces Mitochondria Damage and Releases Mitochondrial DNA to Aggravate the Ventilator-Induced Lung Injury. *Front Immunol*. 2018;9:1477.
27. Timmermans K, Kox M, Vaneker M, Pickkers P, Scheffer GJ. Mitochondrial DNA and TLR9 Signaling Is Not Involved in Mechanical Ventilation-Induced Inflammation. *Anesth Analg*. févr 2017;124(2):531-4.
28. Nakahira K, Haspel JA, Rathinam VAK, Lee S-J, Dolinay T, Lam HC, et al. Autophagy proteins regulate innate immune responses by inhibiting the release of mitochondrial DNA mediated by the NALP3 inflammasome. *Nat Immunol*. mars 2011;12(3):222-30.
29. Unuma K, Aki T, Funakoshi T, Hashimoto K, Uemura K. Extrusion of mitochondrial contents from lipopolysaccharide-stimulated cells: Involvement of autophagy. *Autophagy*. 2015;11(9):1520-36.
30. Piantadosi CA. Mitochondrial DNA, oxidants, and innate immunity. *Free Radic Biol Med*. 17 janv 2020;
31. Nerlich A, Mieth M, Letsiou E, Fatykhova D, Zscheppang K, Imai-Matsushima A, et al. Pneumolysin induced mitochondrial dysfunction leads to release of mitochondrial DNA. *Sci Rep*. 09 2018;8(1):182.
32. Bielen K, 's Jongers B, Boddaert J, Lammens C, Jorens PG, Malhotra-Kumar S, et al. Mechanical Ventilation Induces Interleukin 4 Secretion in Lungs and Reduces the Phagocytic Capacity of Lung Macrophages. *J Infect Dis*. 23 2018;217(10):1645-55.
33. Chen Y, Corriden R, Inoue Y, Yip L, Hashiguchi N, Zinkernagel A, et al. ATP release guides neutrophil chemotaxis via P2Y2 and A3 receptors. *Science*. 15 déc 2006;314(5806):1792-5.
34. Shimada K, Crother TR, Karlin J, Dagvadorj J, Chiba N, Chen S, et al. Oxidized mitochondrial DNA activates the NLRP3 inflammasome during apoptosis. *Immunity*. 23 mars 2012;36(3):401-14.
35. Fialkow L, Fochesatto Filho L, Bozzetti MC, Milani AR, Rodrigues Filho EM, Ladniuk RM, et al. Neutrophil apoptosis: a marker of disease severity in sepsis and sepsis-induced acute respiratory distress syndrome. *Crit Care*. 2006;10(6):R155.
36. Morales-Quinteros L, Schultz MJ, Bringué J, Calfee CS, Camprubí M, Cremer OL, et al. Estimated dead space fraction and the ventilatory ratio are associated with mortality in early ARDS. *Ann Intensive Care*. 21 nov 2019;9(1):128.
37. Bonten MJ, Froon AH, Gaillard CA, Greve JW, de Leeuw PW, Drent M, et al. The systemic inflammatory response in the development of ventilator-associated pneumonia. *Am J Respir Crit Care Med*. oct 1997;156(4 Pt 1):1105-13.

38. Barbar S-D, Pauchard L-A, Bruyère R, Bruillard C, Hayez D, Croisier D, et al. Mechanical Ventilation Alters the Development of *Staphylococcus aureus* Pneumonia in Rabbit. *PLoS ONE*. 2016;11(7):e0158799.
39. Pauchard L-A, Blot M, Bruyere R, Barbar S-D, Croisier D, Piroth L, et al. Linezolid and atorvastatin impact on pneumonia caused by *Staphylococcus aureus* in rabbits with or without mechanical ventilation. *PLoS ONE*. 2017;12(11):e0187187.
40. Bendib I, de Chaisemartin L, Granger V, Schlemmer F, Maitre B, Hüe S, et al. Neutrophil Extracellular Traps Are Elevated in Patients with Pneumonia-related Acute Respiratory Distress Syndrome. *Anesthesiology*. 2019;130(4):581-91.
41. Haden DW, Suliman HB, Carraway MS, Welty-Wolf KE, Ali AS, Shitara H, et al. Mitochondrial biogenesis restores oxidative metabolism during *Staphylococcus aureus* sepsis. *Am J Respir Crit Care Med*. 15 oct 2007;176(8):768-77.
42. Calfee CS, Delucchi KL, Sinha P, Matthay MA, Hackett J, Shankar-Hari M, et al. Acute respiratory distress syndrome subphenotypes and differential response to simvastatin: secondary analysis of a randomised controlled trial. *Lancet Respir Med*. 2018;6(9):691-8.
43. Bos LDJ, Scicluna BP, Ong DSY, Cremer O, van der Poll T, Schultz MJ. Understanding Heterogeneity in Biologic Phenotypes of Acute Respiratory Distress Syndrome by Leukocyte Expression Profiles. *Am J Respir Crit Care Med*. 1 juill 2019;200(1):42-50.
44. Rubio I, Osuchowski MF, Shankar-Hari M, Skirecki T, Winkler MS, Lachmann G, et al. Current gaps in sepsis immunology: new opportunities for translational research. *Lancet Infect Dis*. déc 2019;19(12):e422-36.
45. Summers C, Singh NR, White JF, Mackenzie IM, Johnston A, Solanki C, et al. Pulmonary retention of primed neutrophils: a novel protective host response, which is impaired in the acute respiratory distress syndrome. *Thorax*. juill 2014;69(7):623-9.
46. Asami T, Ishii M, Namkoong H, Yagi K, Tasaka S, Asakura T, et al. Anti-inflammatory roles of mesenchymal stromal cells during acute *Streptococcus pneumoniae* pulmonary infection in mice. *Cytotherapy*. mars 2018;20(3):302-13.
47. Laroye C, Boufenzer A, Jolly L, Cunat L, Alauzet C, Merlin J-L, et al. Bone marrow vs Wharton's jelly mesenchymal stem cells in experimental sepsis: a comparative study. *Stem Cell Res Ther*. 27 juin 2019;10(1):192.
48. Laroye C, Gauthier M, Antonot H, Decot V, Reppel L, Bensoussan D. Mesenchymal Stem/Stromal Cell Production Compliant with Good Manufacturing Practice: Comparison between Bone Marrow, the Gold Standard Adult Source, and Wharton's Jelly, an Extraembryonic Source. *J Clin Med*. 14 déc 2019;8(12).
49. Rabani R, Volchuk A, Jerkic M, Ormesher L, Garces-Ramirez L, Canton J, et al. Mesenchymal stem cells enhance NOX2 dependent ROS production and bacterial killing in macrophages during sepsis. *Eur Respir J*. 8 mars 2018;

50. Matute-Bello G, Liles WC, Frevert CW, Dhanireddy S, Ballman K, Wong V, et al. Blockade of the Fas/FasL system improves pneumococcal clearance from the lungs without preventing dissemination of bacteria to the spleen. *J Infect Dis.* 15 févr 2005;191(4):596-606.
51. Ali F, Lee ME, Iannelli F, Pozzi G, Mitchell TJ, Read RC, et al. Streptococcus pneumoniae-associated human macrophage apoptosis after bacterial internalization via complement and Fc γ receptors correlates with intracellular bacterial load. *J Infect Dis.* 15 oct 2003;188(8):1119-31.
52. Preston JA, Bewley MA, Marriott HM, McGarry Houghton A, Mohasin M, Jubrail J, et al. Alveolar Macrophage Apoptosis-associated Bacterial Killing Helps Prevent Murine Pneumonia. *Am J Respir Crit Care Med.* 1 juill 2019;200(1):84-97.
53. Alcayaga-Miranda F, Cuenca J, Martin A, Contreras L, Figueroa FE, Khouri M. Combination therapy of menstrual derived mesenchymal stem cells and antibiotics ameliorates survival in sepsis. *Stem Cell Res Ther.* 16 oct 2015;6:199.

FIGURES LEGENDS

Figure 1. Prolonged adverse mechanical ventilation causes mild lung damage, inflammation and mitochondrial derangements in the pulmonary compartment.

Rabbits were submitted to either protective or adverse MV, or kept SB during 8 or 24 hours. Inflammation and mitochondrial derangements were measured within the lung: (A) interleukin-8 BAL fluid concentrations by ELISA; (B) polymorphonuclear cells accumulation within the alveolar compartment; (C) extent of inflammation scored on hematoxylin-eosin stained lung tissue sections. Mitochondrial alarmins were measured in BAL fluids at H8 or H24 ((D) cell-free mitochondrial DNA levels (NADH I) by qPCR, and (E) ATP levels by bioluminescence assay). (F) Mitochondrial DNA levels were also measured in the lung tissue (as a reflect of mitochondrial density). Mitochondrial membrane potential ($\Delta\Psi_m$) of alveolar immune cells was measured by flow cytometry and using mitochondrial fluorescent probes (alveolar neutrophils $\Delta\Psi_m$ assessed by (G) Mitotracker Red/Green or (H) TMRM and alveolar macrophages $\Delta\Psi_m$ assessed by (I) Mitotracker Red/Green or (J) TMRM).

Data are expressed as box-and-whisker diagrams (n=7 at H8 and H24). The Kruskal-Wallis test with FDR post-hoc correction was used for multiple comparisons. *, p < .05; **, p < .01; ***, p < .001; ****, p < .0001.

Abbreviations: ATP: adenosine triphosphate; BAL: broncho-alveolar lavage; DNA: deoxyribonucleic acid; ELISA: enzyme-linked immunosorbent assay; MV: mechanical ventilation; NADH: nicotinamide adenine dinucleotide; qPCR: quantitative polymerase chain reaction; SB: spontaneous breathing; TMRM: tetramethylrhodamine; $\Delta\Psi_m$: mitochondrial membrane potential.

Figure 2. Adverse mechanical ventilation worsens the prognosis of pneumococcal pneumonia.

Main features of *Streptococcus pneumoniae* pneumonia in either spontaneously breathing or mechanically ventilated rabbits submitted to either protective or adverse MV. (A) Time-dependent probability of survival (Kaplan-Meier survival curves, log rank tests: adverse MV + S.p vs. protective MV + Sp. (**p=0.0004); adverse MV + S.p. vs. SB (###p=0.0002); adverse MV + S.p. vs. SB + S.p (\$\$\$p=0.0002)). (B) Central temperature was measured at baseline (H0), H8 and H24 (or just prior to death if appropriate). Blood samples were obtained at H0, H8 and

H24 (or just prior death if appropriate) to measure: venous (C) oxygen partial pressure (PvO₂), (D) partial pressure of carbon dioxide (PvCO₂), (E) pH, and (F) lactate concentrations. (G) Lung injury assessment according to macroscopic score calculation. Bacterial loads (\log_{10} colony-forming units per gram of lung) in (H) the lung and (I) the spleen (as the reflect of pulmonary-to-systemic bacterial translocation), at H8 or H24 (or just prior death if appropriate) after airways' bacterial challenge.

(B-F) Data are expressed as mean \pm SEM. *: Adverse MV + S.p vs. protective MV + Sp. ; # : adverse MV + S.p. vs. SB ; \$: adverse MV + S.p. vs. SB + S.p. (G-H) Data are expressed as box-and-whisker diagrams (n=7 at H8 and H24). The Kruskal-Wallis test and FDR post-hoc correction for multiple comparisons was used. *, p < .05; **, p < .01; ***, p < .001; ****, p < .0001.

Abbreviations: FDR: false discovery rate; MV: mechanical ventilation; SB: spontaneous breathing; SEM: standard error of the mean.

Figure 3. In the setting of pneumococcal pneumonia, adverse mechanical ventilation is associated with deep immune and mitochondrial derangements in both the pulmonary and the systemic compartments.

Rabbits'airways were challenged with *Streptococcus pneumoniae* or NaCl (control group) and submitted to protective or adverse MV or kept SB during 8 or 24 hours. Inflammation and mitochondrial derangements were measured within the lung: (A) polymorphonuclear cells accumulation within the alveolar compartment; (B) interleukin-8 BAL fluid concentrations; (C) the extent of inflammation scored on H&E stained tissue sections expressed as total HE score and confluent inflammation score. Mitochondrial alarmins were measured in BAL fluids at H8 or H24. ((D) cell-free mitochondrial DNA levels (NADH I) by qPCR, and (E) ATP levels by bioluminescence assay). (F) Mitochondrial DNA levels were measured in the lung tissue (as a reflect of mitochondrial density). Mitochondrial membrane potential ($\Delta\Psi_m$) of alveolar immune cells was measured by flow cytometry and using mitochondrial fluorescent probes (alveolar neutrophils $\Delta\Psi_m$ assessed by (G) Mitotracker Red/Green or (H) TMRM and alveolar macrophages $\Delta\Psi_m$ assessed by (I) Mitotracker Red/Green or (J) TMRM. Blood samples were obtained at baseline (H0), H8 and H24 (or just prior to death if appropriate) to measure: (K) interleukin-8, and mitochondrial alarmins plasma concentrations ((L) cell-free mitochondrial

DNA (NADH-I) and (M) cell-free ATP, expressed as percentage of baseline level). Mitochondrial membrane potential ($\Delta\Psi_m$) of blood PMN was measured by flow cytometry and using (N) Mitotracker Red/Green or (O) TMRM probes.

(A-J and N-O) Data are expressed as box-and-whisker diagrams (n=7 at H8 and H24). (K-M) Data are expressed as means \pm SEM. *: Adverse MV + S.p vs. protective MV + Sp. ; #: adverse MV + S.p. vs. SB ; \$: adverse MV + S.p. vs. SB + S.p.. The Kruskal-Wallis test with FDR post-hoc correction for multiple comparisons was used. *, p < .05; **, p < .01; ***, p < .001; ****, p < .0001.

Abbreviations: ATP: adenosine triphosphate; BAL: broncho-alveolar lavage; DNA: deoxyribonucleic acid; FDR: false discovery rate; HE: hematoxylin and eosin; MV: mechanical ventilation; NADH: nicotinamide adenine dinucleotide; PMN: polymorphonuclear leukocytes; qPCR: quantitative polymerase chain reaction; SB: spontaneous breathing; SEM: standard error of the mean; TMRM: tetramethylrhodamine; $\Delta\Psi_m$: mitochondrial membrane potential.

Figure 4. Mesenchymal stem cells contributed to pneumococcal ventilated pneumonia outcome improvement.

In the setting of pneumococcal pneumonia and adverse MV, rabbits were randomized to receive 4 hours after the insult: NaCl (control group), intravenous infusion of 3.10^6 human cord-derived MSCs/kg, intramuscular injection of ceftaroline 20mg/kg, or both treatments. (A) Time-dependent probability of survival (Kaplan-Meier survival curves, log rank tests: control vs. MSCs (**p=0.0012); control vs. ceftaroline (&&p=0.0091); control vs. ceftaroline+MSCs (###p=0.004); ceftaroline vs. ceftaroline+MSCs (p=0.11)). Blood samples were obtained at baseline (H0), H8 and H24 (or just prior to death if appropriate) to measure venous (B) oxygen partial pressure (PvO₂); (C) partial pressure of carbon dioxide (PvCO₂); (D) pH; and (E) lactate concentrations. (F) Lung injury assessment according to macroscopic score calculation. Bacterial loads (log₁₀ colony-forming units per gram of lung) in (G) the lung and (H) the spleen (as the reflect of pulmonary-to-systemic bacterial translocation), at H8 or H24 (or just prior death if appropriate) after bacterial challenge.

(B-E) Data are expressed as mean \pm SEM. *: control vs. MSCs, &: control vs. ceftaroline, #: control vs. ceftaroline+MSCs. (F-G) Data are expressed as box-and-whisker diagrams (n=7 at H8 and H24). The Kruskal-Wallis test and FDR post-hoc correction for multiple comparisons was used. *, p < .05; **, p < .01; ***, p < .001; ****, p < .0001.

Abbreviations: FDR: false discovery rate; MSCs: mesenchymal stem cells; MV: mechanical ventilation; SB: spontaneous breathing; SEM: standard error of the mean.

Figure 5. Mesenchymal stem cells contributed to the modulation of both pulmonary and systemic inflammatory response to pneumococcal pneumonia and resolution of mitochondrial derangements as well, in ventilated rabbits.

In the setting of pneumococcal pneumonia and adverse MV, rabbits were randomized to receive, 4 hours after the insult: NaCl (control group), intravenous infusion of 3.10^6 human cord-derived MSCs/kg, intramuscular injection of ceftaroline 20mg/kg, or both treatments. Inflammation and mitochondrial derangements were measured within the lung: (A) interleukin-8 BAL fluid concentrations; (B) polymorphonuclear cells accumulation within the alveolar compartment; (C) the extent of inflammation scored on H&E stained tissue sections expressed as total HE score and confluent inflammation score. Mitochondrial alarmins were measured in BAL fluids at H8 or H24 ((D) cell-free mitochondrial DNA levels (NADH I) by qPCR, and (E) ATP levels by bioluminescence assay). Mitochondrial membrane potential ($\Delta\Psi_m$) of alveolar immune cells was measured by flow cytometry and using mitochondrial fluorescent probes (alveolar neutrophils $\Delta\Psi_m$ assessed by (F) Mitotracker Red/Green or (G) TMRM and alveolar macrophages $\Delta\Psi_m$ assessed by (H) Mitotracker Red/Green or (I) TMRM. Blood samples were obtained at baseline (H0), H8 and H24 (or just prior to death if appropriate) to measure: (J) interleukin-8 and mitochondrial alarmins plasma concentrations ((K) cell-free mitochondrial DNA (NADH-I) and (L) cell-free ATP, and expressed as percentage of baseline level). $\Delta\Psi_m$ of blood PMN was measured by flow cytometry and using (M) Mitotracker Red/Green or (N) TMRM probes.

(A-I and M-N) Data are expressed as box-and-whisker diagrams (n=7 at H8 and H24). (J-L) Data are expressed as means \pm SEM. *: control vs. MSCs, &: control vs. ceftaroline, #: control vs. ceftaroline+MSCs. The Kruskal-Wallis test with FDR post-hoc correction for multiple comparisons was used. *, p < .05; **, p < .01; ***, p < .001; ****, p < .0001.

Abbreviations: ATP: adenosine triphosphate; BAL: broncho-alveolar lavage; DNA: deoxyribonucleic acid; ELISA: enzyme-linked immunosorbent assay; FDR: false discovery rate; HE: hematoxylin and eosin; MV: mechanical ventilation; NADH: nicotinamide adenine dinucleotide; PMN: polymorphonuclear leukocytes; qPCR: quantitative polymerase chain

reaction; SB: spontaneous breathing; SEM: standard error of the mean; TMRM: tetramethylrhodamine; $\Delta\Psi_m$: mitochondrial membrane potential.

Figure 1

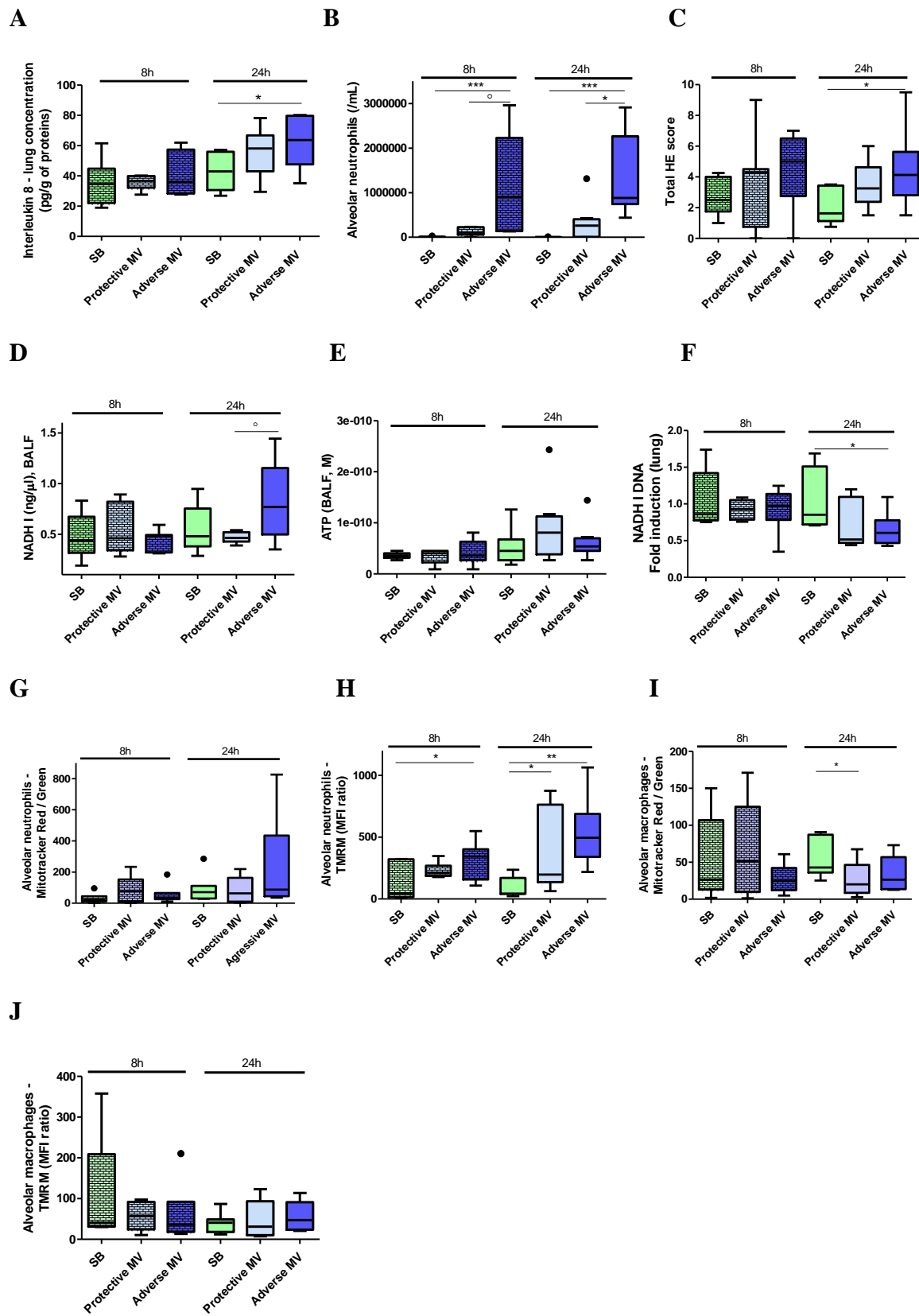
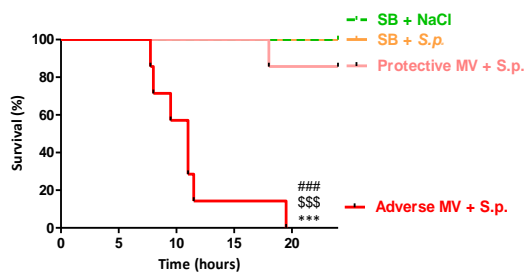
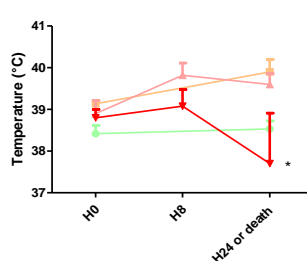


Figure 2

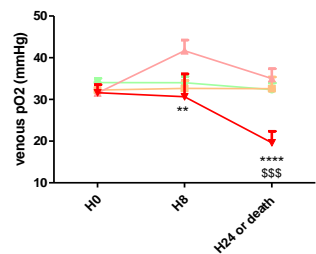
A



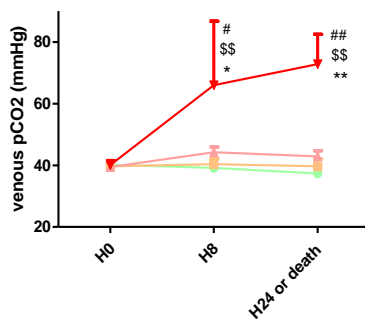
B



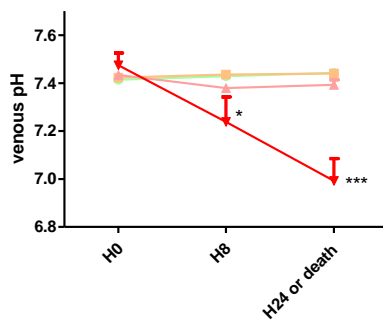
C



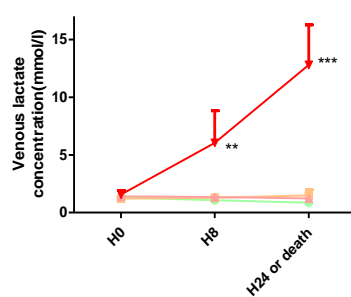
D



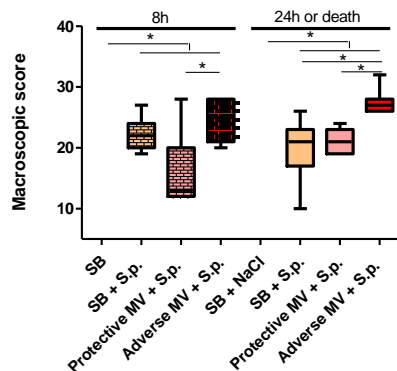
E



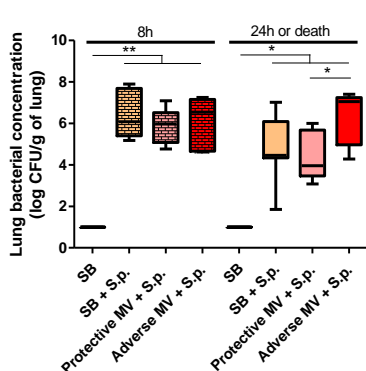
F



G



H



I

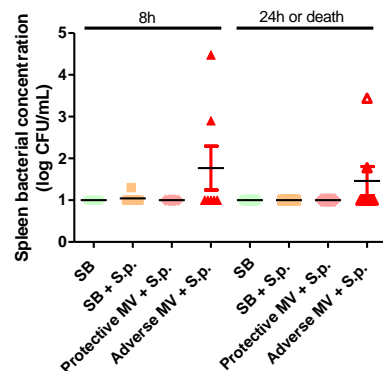
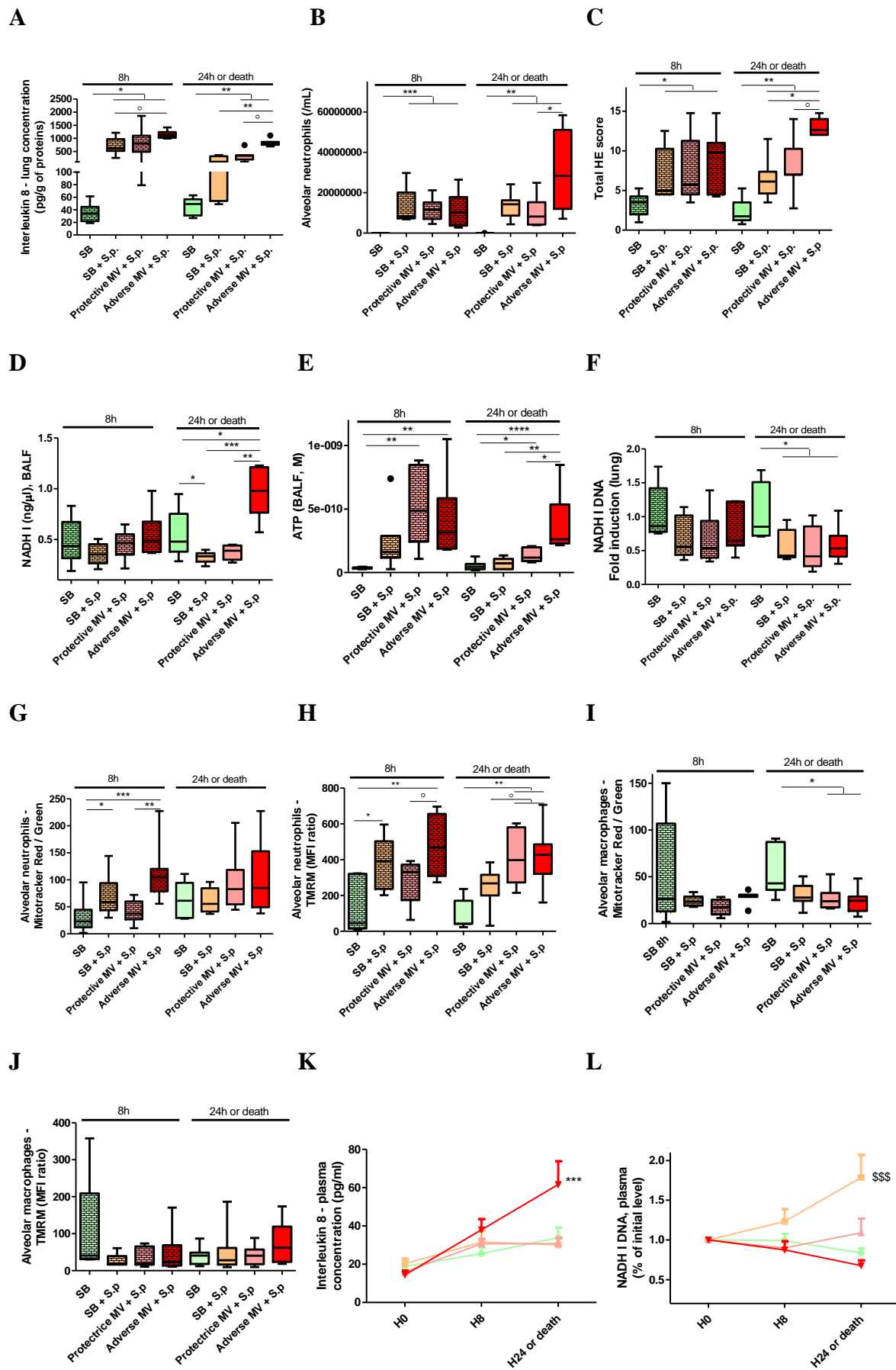


Figure 3



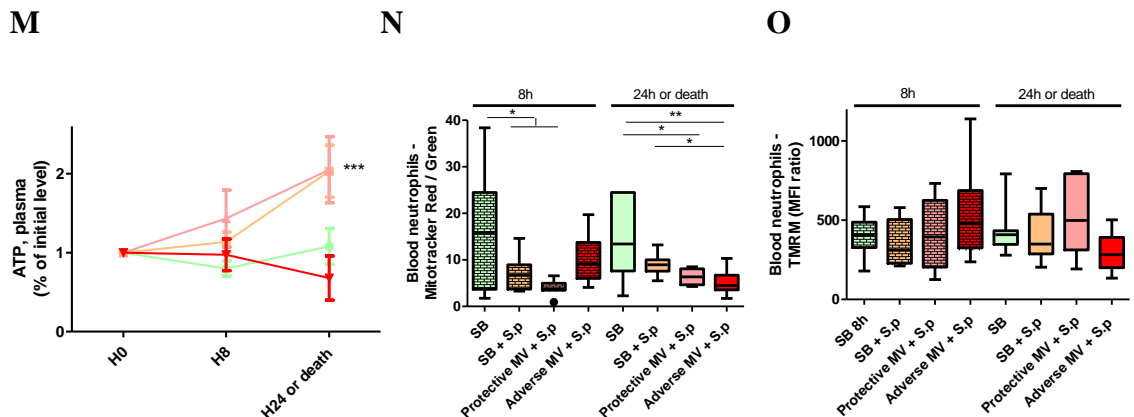


Figure 4

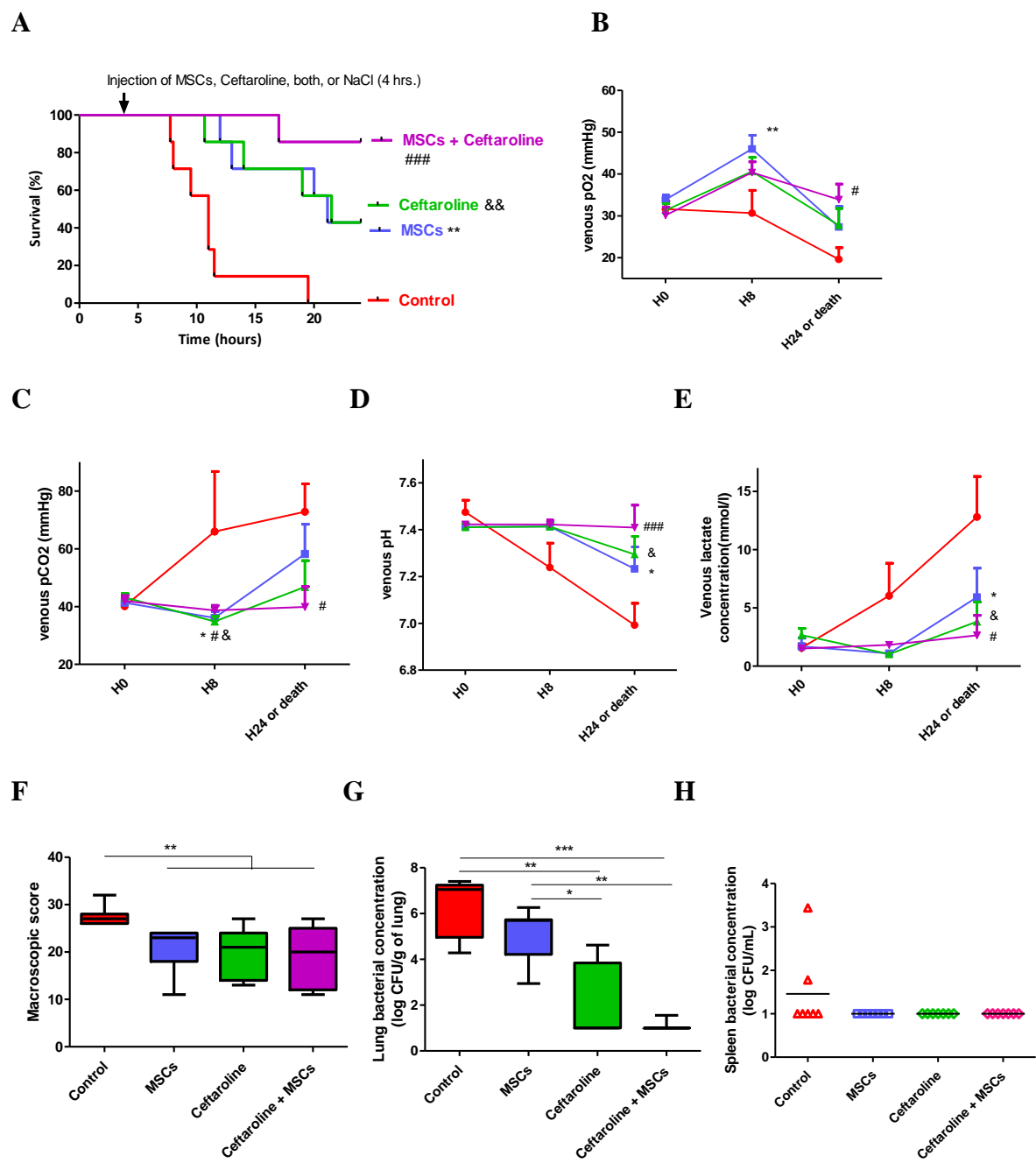
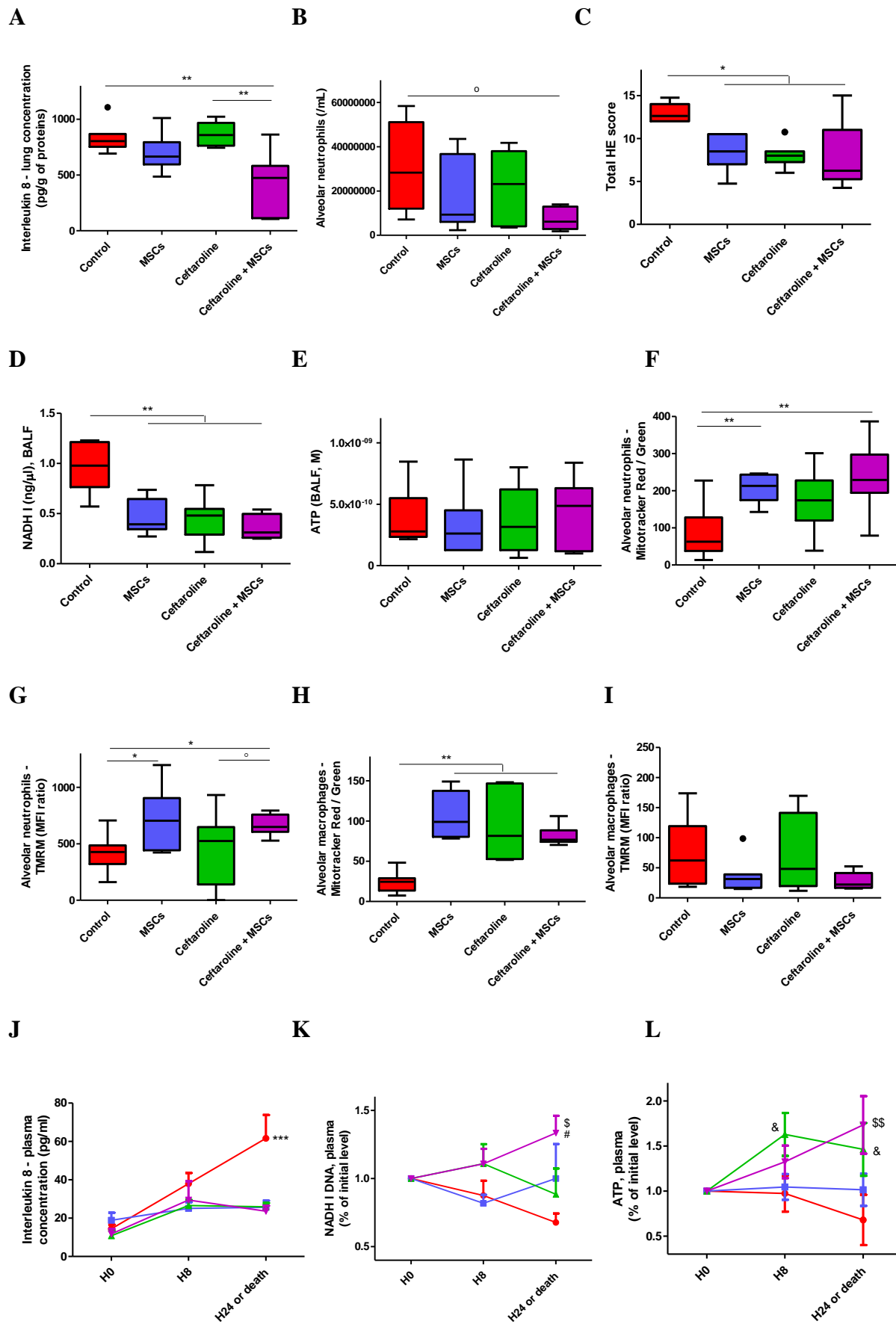
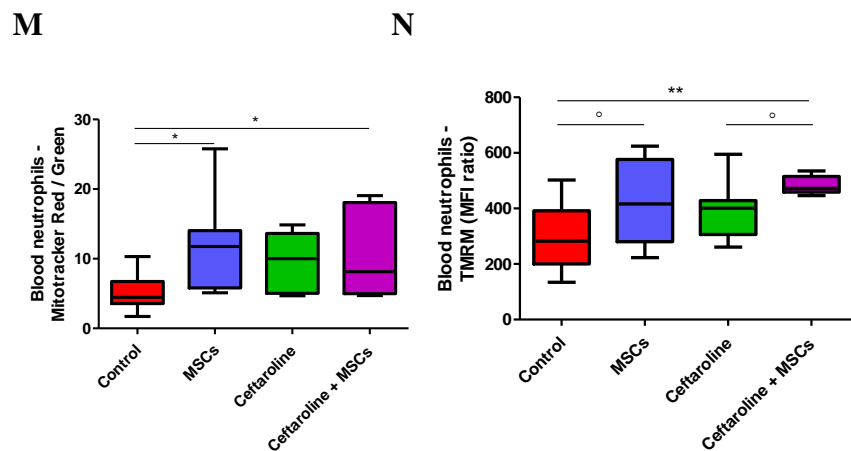


Figure 5





Supplementary data

Figure E1. Safety of either protective or adverse prolonged mechanical ventilation protocols in rabbits.

Rabbits were submitted to protective or adverse mechanical ventilation, or kept spontaneous breathing during 8 or 24 hours. (A) Lung representative photographs; (B) Central temperature was measured at baseline (H0), H8 and H24. Blood samples were obtained at H0, H8 and H24 to measure venous (C) oxygen partial pressure (PvO₂); (D) partial pressure of carbon dioxide (PvCO₂); (E) pH; and (F) lactate concentrations.

Data are expressed as mean ± standard error of the mean (n=7 per group). * : protective MV vs. Adverse MV; # : protective MV vs. SB ; \$: adverse MV vs. SB. The Kruskal-Wallis test and False Discovery Rate post-hoc correction multiple comparisons was used at each time point.

*, p < .05; **, p < .01; ***, p < .001; ****, p < .0001.

Figure E2. Lung damage, inflammation and mitochondrial homeostasis during either protective or adverse prolonged mechanical ventilation.

Rabbits were submitted to protective or adverse MV or kept SB during 8 or 24 hours. (A) representative photographs of H&E-stained lung tissue sections. BAL fluid concentrations of inflammatory cytokines were measured by ELISA : (B) Interleukin-1 β , (C) TNF- α , (D) Interleukin-10.

Data are expressed as box-and-whisker diagrams (n=7 rabbits per group at H8 and H24). The Kruskal-Wallis test with FDR post-hoc multiple comparisons correction was used . *, p < .05; **, p < .01; ***, p < .001; ****, p < .0001.

Abbreviations: ELISA: enzyme-linked immunosorbent assay; FDR: false discovery rate; HE: hematoxylin and eosin; MV: mechanical ventilation; SB: spontaneous breathing; SEM: standard error of the mean; TNF: tumor necrosis factor.

Figure E3. Inflammation and mitochondrial homeostasis in the systemic compartment during mechanical ventilation.

Rabbits were submitted to protective or adverse MV or kept SB, during 8 or 24 hours. Blood samples were obtained at baseline (H0), H8 and H24 to measure: (A) leukocytes count, (B) plasma concentrations of interleukin-8 and (C) interleukin-1 β by ELISA, mitochondrial alarmins ((D) cell-free mitochondrial DNA (NADH I) by qPCR, and (E) ATP by bioluminescence assay). (F) Mitochondrial DNA levels were measured in the spleen tissue (as a reflect of mitochondrial density). (H) Mitochondrial membrane potential ($\Delta\Psi_m$) of blood PMN was measured by flow cytometry and using (G) Mitotracker Red/Green or (H) TMRM. (I) Mitochondrial ROS production of blood PMN was measured by flow cytometry and using the MitoSOX probe.

(A-E) Data are expressed as means \pm SEM. * : protective MV vs. Adverse MV; # : protective MV vs. SB ; \$: adverse MV vs. SB. (F-I) Data are expressed as box-and-whisker diagrams (n=7 at H8 and H24). The Kruskal-Wallis test with FDR post-hoc correction for multiple comparisons was used. *, p < .05; **, p < .01; ***, p < .001; ****, p < .0001.

Abbreviations: ATP: adenosine triphosphate; DNA: deoxyribonucleic acid; ELISA: enzyme-linked immunosorbent assay; FDR: false discovery rate; MV: mechanical ventilation; NADH: nicotinamide adenine dinucleotide; PMN: polymorphonuclear leukocytes; qPCR: quantitative chain reaction; ROS: reactive oxygen species; SB: spontaneous breathing; SEM: standard error of the mean; TMRM: tetramethylrhodamine; $\Delta\Psi_m$: mitochondrial membrane potential.

Figure E4. In the setting of pneumococcal pneumonia, adverse mechanical ventilation increased lung damage, and led to immune and mitochondrial derangements in the lung compartment.

Rabbits' airways were challenged with *Streptococcus pneumoniae* or NaCl (control group) and submitted to protective or adverse MV or kept in SB during 8 or 24 hours. (A) representative photographs of H&E-stained lung tissue sections. BAL fluid concentrations of inflammatory cytokines measured by ELISA: (B) interleukin-1 β , (C) TNF- α , and (D) interleukin-10.

Data are expressed as box-and-whisker diagrams (n=7 rabbits at H8 and H24). The Kruskal-Wallis test with FDR post-hoc correction for multiple comparisons was used. *, p < .05; **, p < .01; ***, p < .001; ****, p < .0001.

Abbreviations: ELISA: enzyme-linked immunosorbent assay; FDR: false discovery rate; HE: hematoxylin and eosin; MV: mechanical ventilation; qPCR: quantitative polymerase chain reaction; SB: spontaneous breathing; SEM: standard error of the mean; TNF: tumor necrosis factor

Figure E5. In the setting of pneumococcal pneumonia, adverse MV led to immune and mitochondrial derangements in the systemic compartment.

Rabbits were inoculated with *Streptococcus pneumoniae* or NaCl (control group) and submitted protective or adverse MV or kept SB, during 8 or 24 hours. Blood samples were obtained at baseline (H0), H8 and H24 (or just prior to death if appropriate) to measure: (E) leukocyte count, and (F) interleukin-1 β plasma concentrations. (C) Mitochondrial DNA (NADH-

I) levels were measured in the spleen tissue (as a reflect of mitochondrial density) by qPCR. Mitochondrial membrane potential ($\Delta\Psi_m$) of blood PMN was measured by flow cytometry and using (D) Mitotracker Red/Green or (E) TMRM probes. (F) Mitochondrial ROS production of blood PMN was measured by flow cytometry and using the MitoSOX probe.

(A-B) Data are expressed as means \pm SEM. *: Adverse MV + S.p vs. protective MV + Sp. ; # : adverse MV + S.p. vs. SB ; \$: adverse MV + S.p. vs. SB + S.p. (C-F) Data are expressed as box-and-whisker diagrams (n=7 at H8 and H24). The Kruskal-Wallis test with FDR post-hoc correction for multiple comparisons was used. *, p < .05; **, p < .01; ***, p < .001; ****, p < .0001.

Abbreviations: DNA: deoxyribonucleic acid; ELISA: enzyme-linked immunosorbent assay; FDR: false discovery rate; MV: mechanical ventilation; NADH: nicotinamide adenine dinucleotide; PMN: polymorphonuclear leukocytes; qPCR: quantitative polymerase chain reaction; ROS: reactive oxygen species; SB: spontaneous breathing; SEM: standard error of the mean; TMRM: tetramethylrhodamine; $\Delta\Psi_m$: mitochondrial membrane potential.

Figure E6. Mesenchymal stem cells contributed to the reduction of lung damages and to the improvement of the physiological response to pneumococcal pneumonia in rabbits submitted to adverse MV.

In the setting of pneumococcal pneumonia and adverse MV, rabbits were randomized to receive, 4 hours after the insult: NaCl (control group), intravenous infusion of 3.10^6 human cord-derived MSCs/kg, intramuscular injection of ceftaroline 20mg/kg, or both treatments. (A) lung pictures; (B) representative photographs of H&E-stained lung tissue sections; (c) body temperature was measured at baseline (H0), at H8 or H24 (or just prior death if appropriate)

after bacterial challenge. Data are expressed as mean \pm SEM (n=7 rabbits per group). *: control vs. MSCs, &: control vs. ceftaroline, #: control vs. ceftaroline+MSCs. The Kruskal-Wallis test and FDR post-hoc correction for multiple comparisons was used at H8 and H24. *, p < .05; **, p < .01; ***, p < .001; ****, p < .0001. Abbreviations: FDR: false discovery rate; H&E: hematoxylin and eosin; MV: mechanical ventilation, MSCs: mesenchymal stem cells, SEM: standard error of mean

Figure E7 : Mesenchymal stem cells contributed to the modulation of both pulmonary and systemic inflammatory response to pneumococcal pneumonia, along with the resolution of mitochondrial derangements, in rabbits submitted to adverse MV.

In the setting of pneumococcal pneumonia and adverse MV, rabbits were randomized to receive, 4 hours after the insult: NaCl (control group), intravenous infusion of 3.10^6 human cord-derived MSCs/kg, intramuscular injection of ceftaroline 20mg/kg, or both treatments. Inflammation and mitochondrial derangements were measured within the lung and systemic compartments. Pulmonary concentrations of inflammatory cytokines measured by ELISA: (B) interleukin-1 β , (C) TNF- α , and (D) interleukin-10. (D) Mitochondrial DNA levels were measured in the lung tissue (as a reflect of mitochondrial density) by qPCR. Blood samples were obtained at baseline (H0), H8 and H24 (or just prior death if occurred) to measure: (E) leukocyte count, and (F) interleukin-1 β plasma concentrations. (G) Mitochondrial DNA levels were measured in the spleen tissue (as a reflect of mitochondrial density). (H) Mitochondrial ROS production of blood PMN was measured by flow cytometry and using the MitoSOX probe. (A-D) Data are expressed as box-and-whisker diagrams (n= 7 rabbits per group at H8 and H24). (E-F) Data are expressed as means \pm SEM. The Kruskal-Wallis test with FDR post-hoc correction for multiple comparisons was used. *, p < .05; **, p < .01; ***, p < .001; ****, p < .0001. Abbreviations:

BAL: broncho-alveolar lavage; DNA: deoxyribonucleic acid; ELISA: enzyme-linked immunosorbent assay; FDR: False Discovery Rate; MV: mechanical ventilation; MSCs: mesenchymal stem cells; NADH: Nicotinamide adenine dinucleotide; PMN: polymorphonuclear leukocytes; qPCR: quantitative polymerase chain reaction; ROS: reactive oxygen species; SB: spontaneous breathing; SEM: standard error of the mean; TNF: tumor necrosis factor

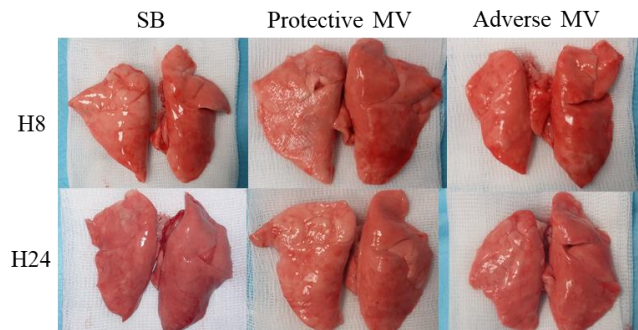
Figure E8. Cell-free extracellular mitochondrial DNA concentrations and blood leukocyte count are closely related in both BAL fluids and plasma.

All rabbits infected with *Streptococcus pneumoniae* and assessed at H24 (or before if death occurred earlier) were considered for the analysis, regardless of MV and treatment as well. First, we observed a significant correlation (A) between BAL fluids mitochondrial DNA concentrations measured by qPCR, and alveolar neutrophils count, and (B) between plasma mitochondrial DNA concentrations and blood leukocyte count. Then, we investigate the prognostic value of BAL fluids and plasma mitochondrial DNA concentrations and found (C) a significant association between mitochondrial DNA alveolar concentration and mortality ($p=0.004$) and (D) an inverse association between plasma mitochondrial DNA concentration and mortality ($p=0.042$). Abbreviations: BAL: broncho-alveolar lavage; DNA: deoxynucleic acid; PMN: polymorphonuclear leukocytes; qPCR: quantitative polymerase chain reaction.

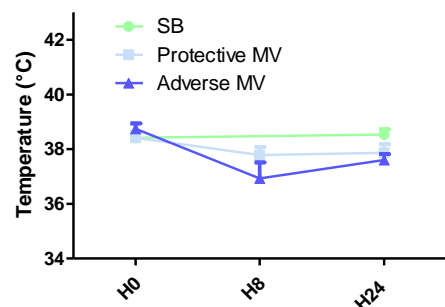
SUPPLEMENTARY FIGURES

Figure E1

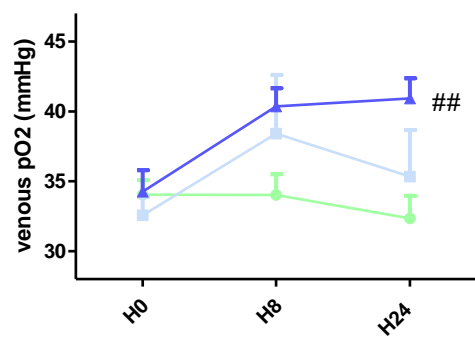
A



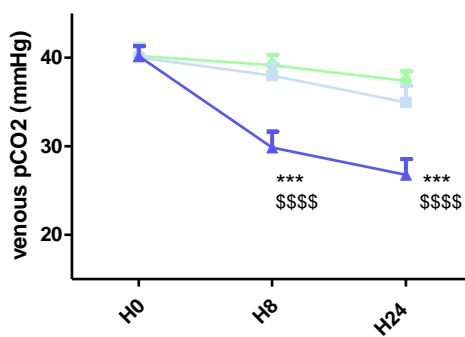
B



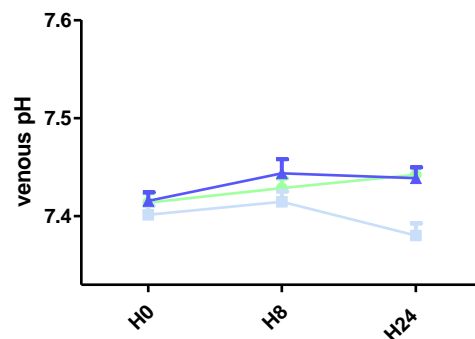
C



D



E



F

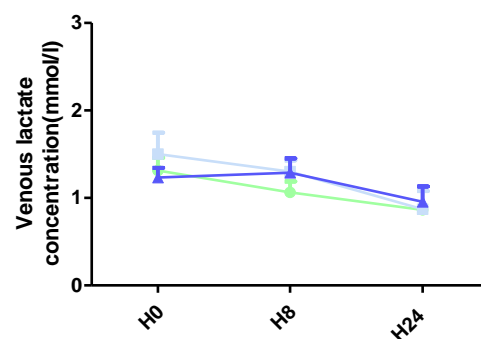
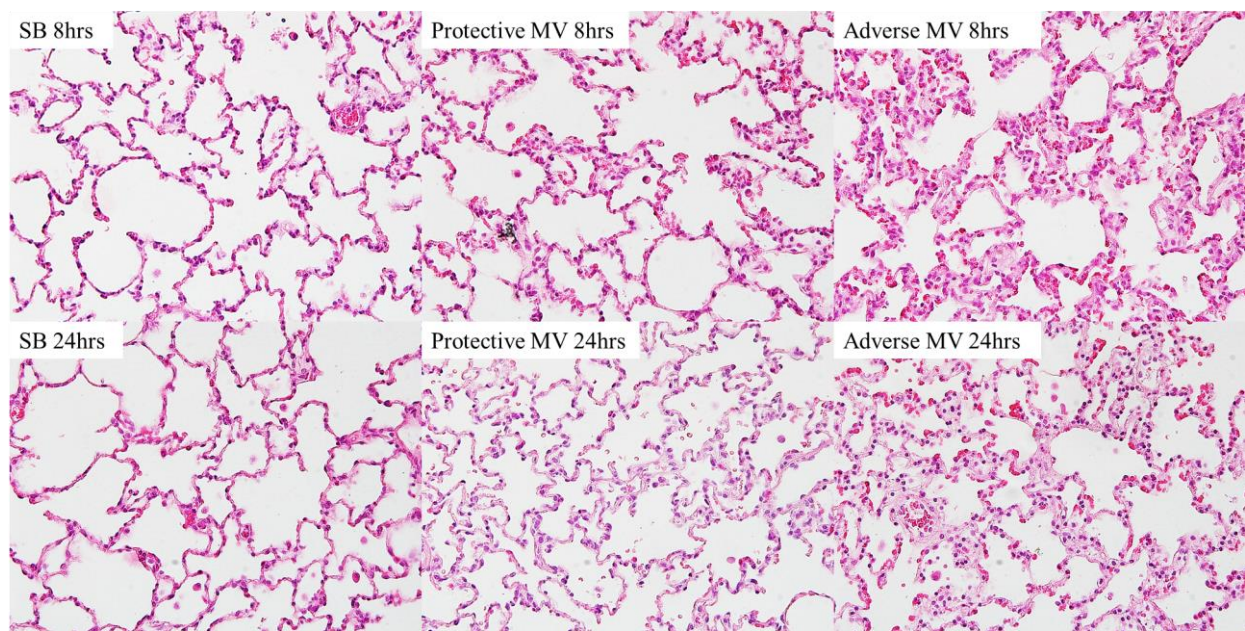
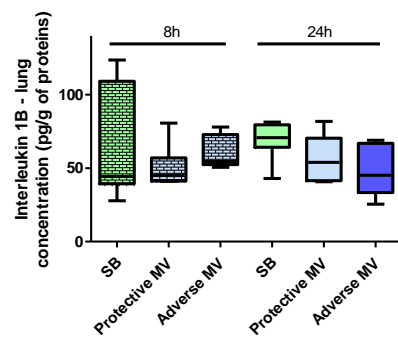


Figure E2

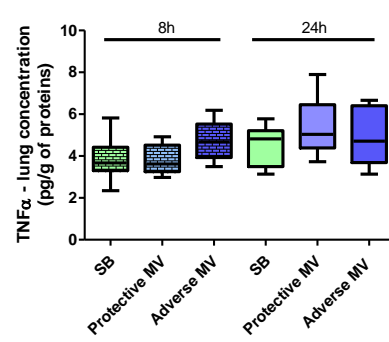
A



B



C



D

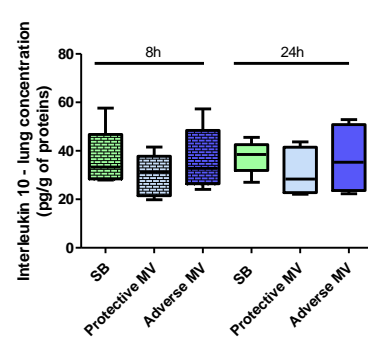


Figure E3

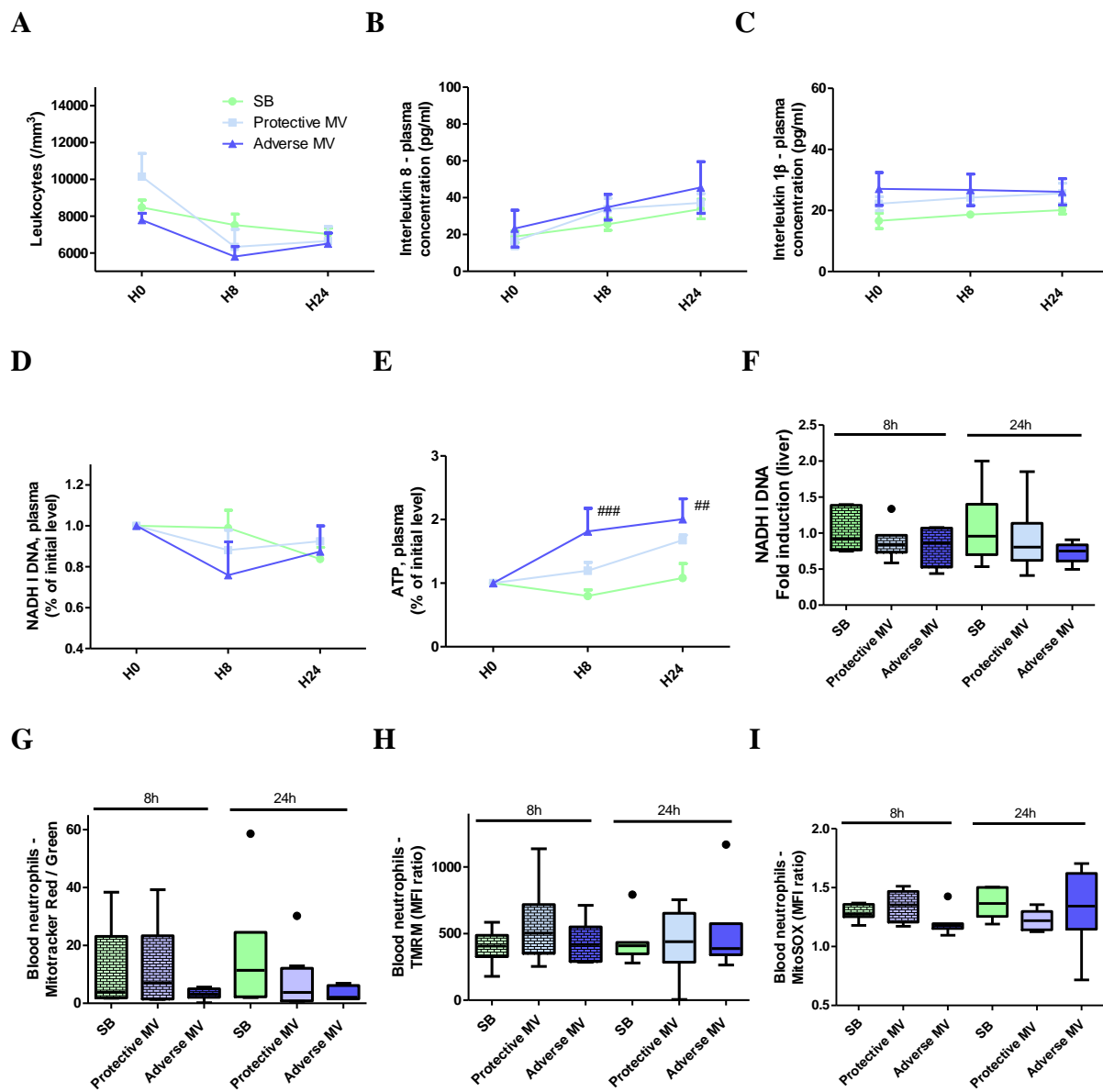
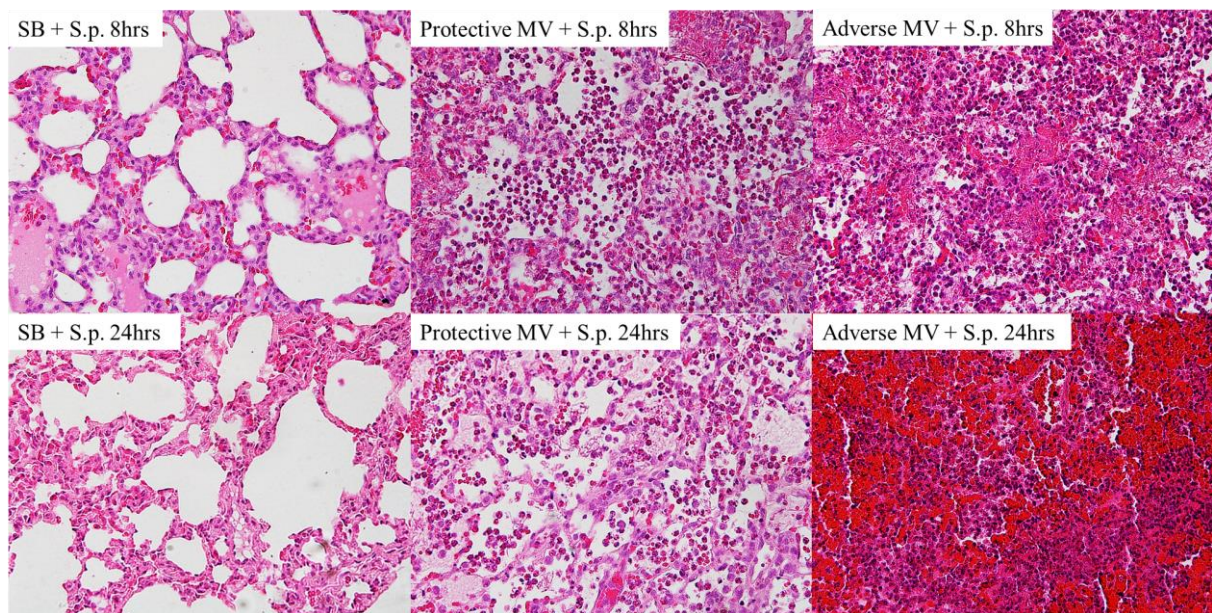
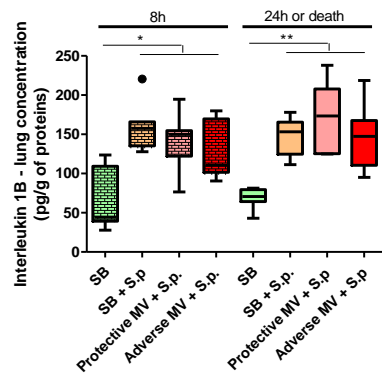


Figure E4

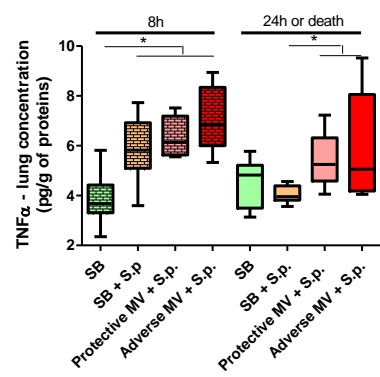
A



B



C



D

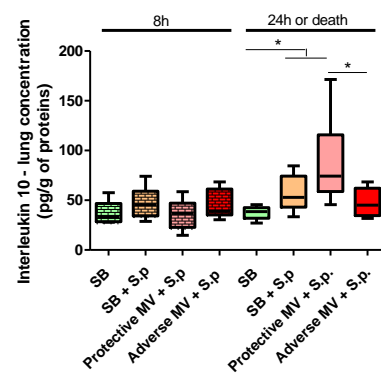


Figure E5

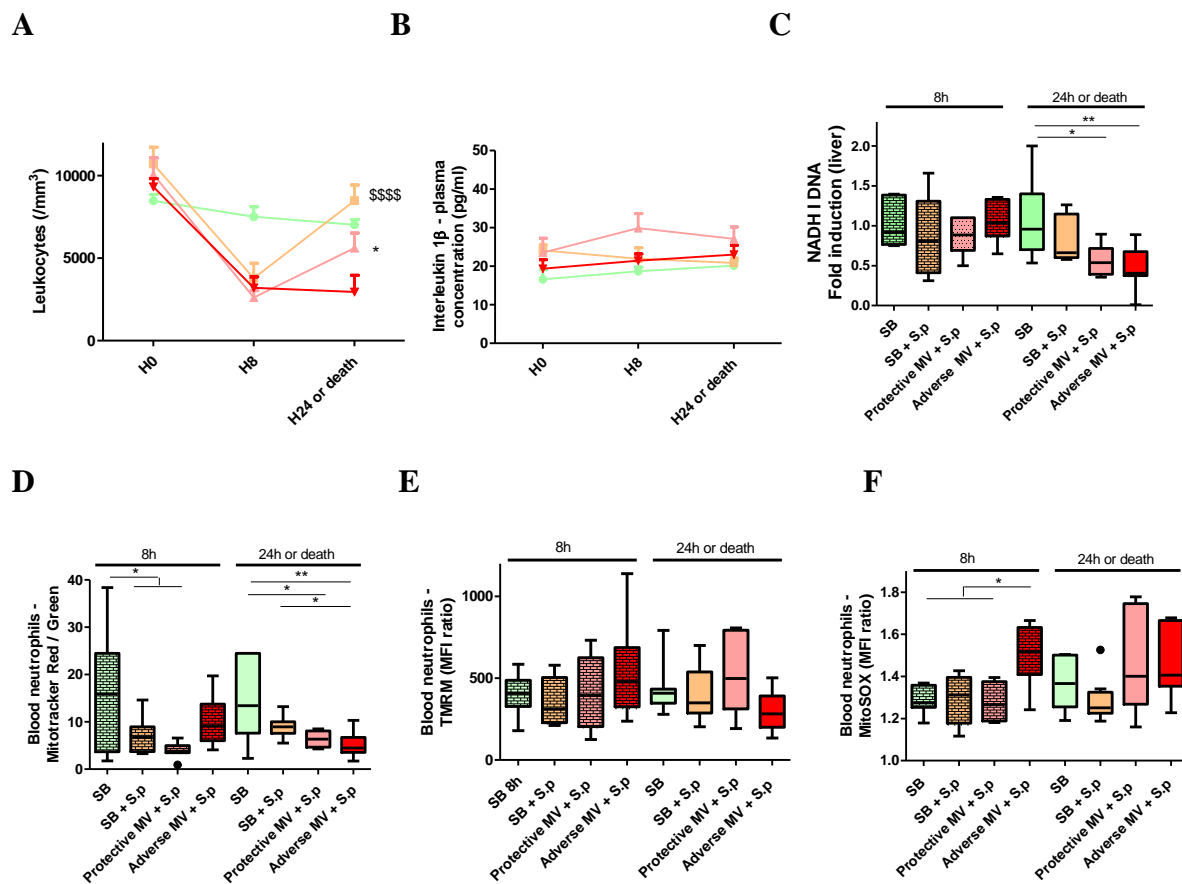
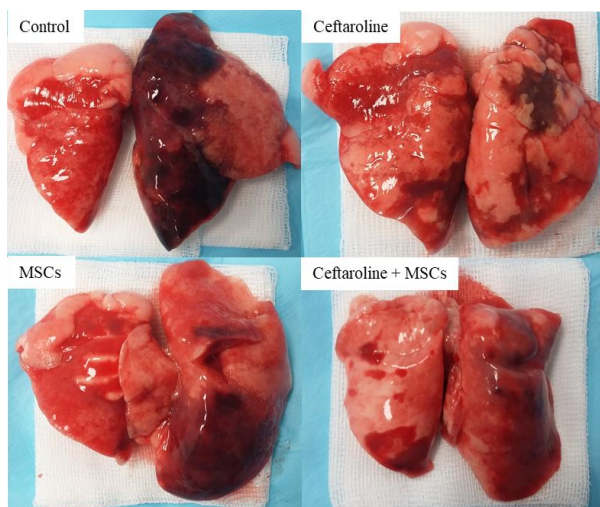
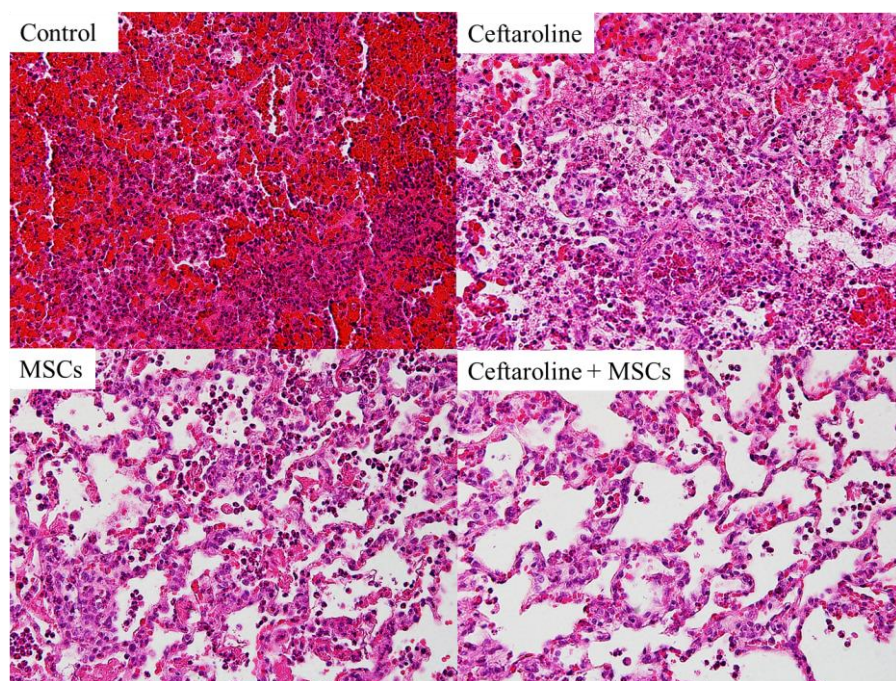


Figure E6

A



B



C

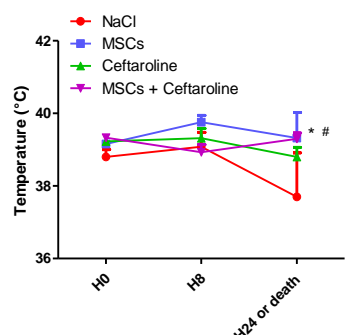


Figure E7

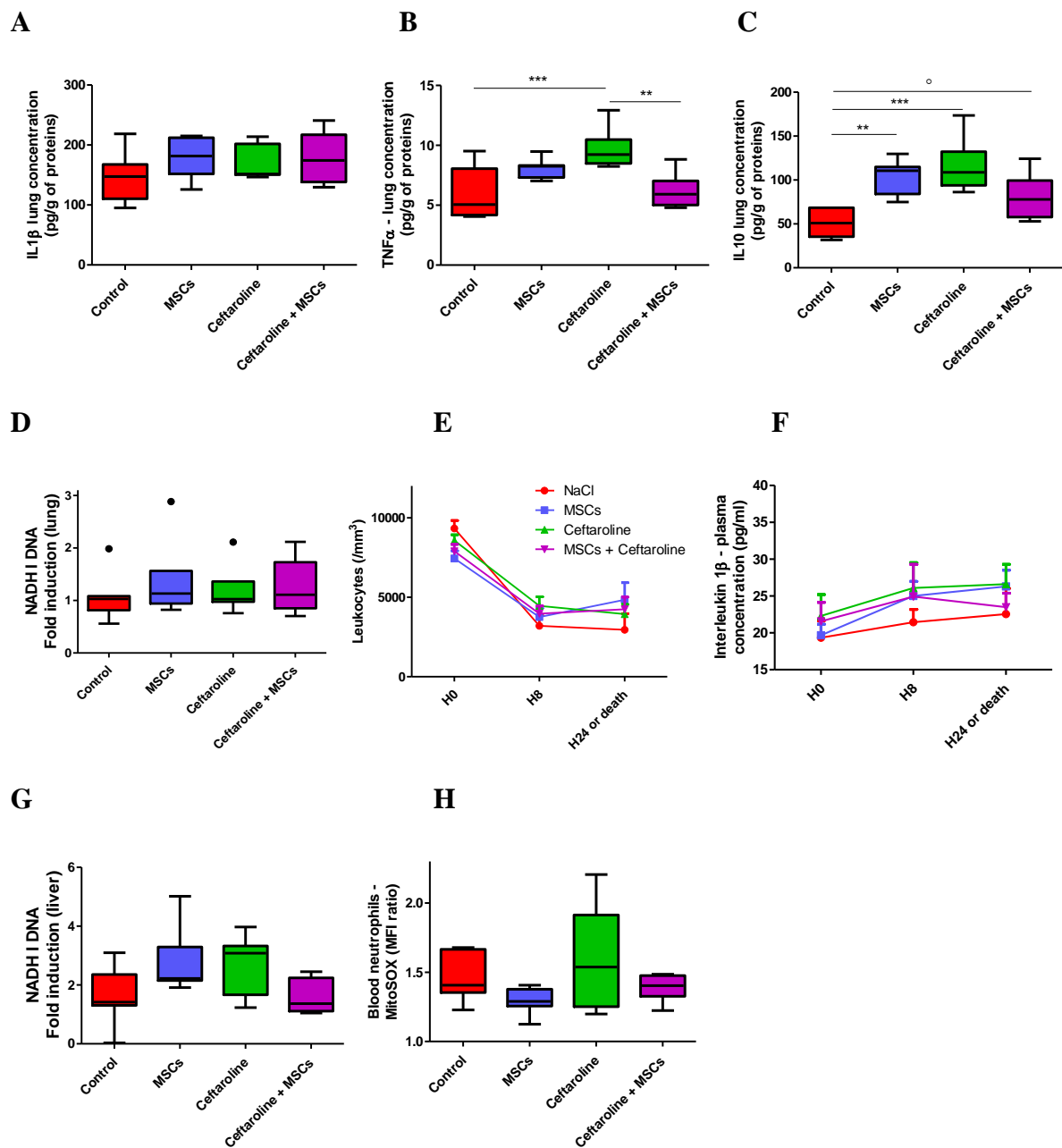
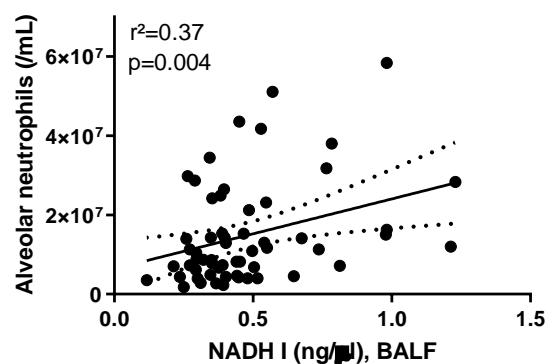
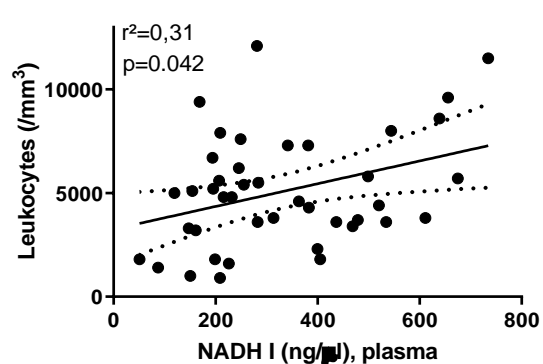


Figure E8

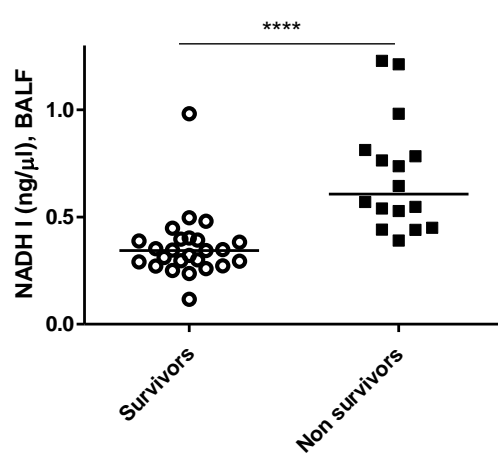
A



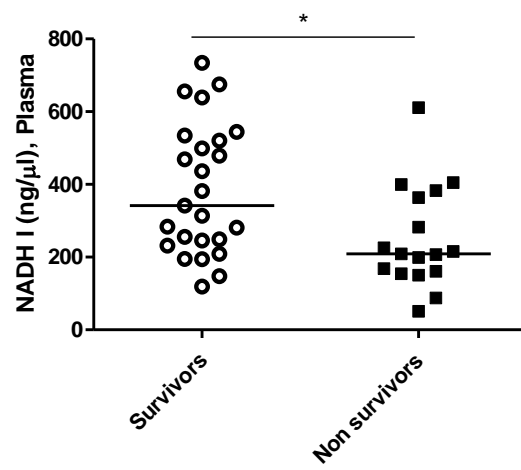
B



C



D



SUPPLEMENTARY TABLE

Table E1: Experimental groups (n=7 rabbits/group). CPT: ceftaroline fosamil, MSCs: mesenchymal stem cells, MV: mechanical ventilation, NaCl: isotonic saline, SB: spontaneous breathing, S.p.: *Streptococcus pneumoniae*.

		H8			H24		
Intra-tracheal inoculation	Treatment administrated at H4	Spontaneous breathing	Protective MV	Adverse MV	Spontaneous breathing	Protective MV	Adverse MV
NaCl	NaCl	SB _{H8}	pMV _{H8}	aMV _{H8}	SB _{H24}	pMV _{H24}	aMV _{H24}
S.p.	<i>S.pneumoniae</i>	SBP _{H8}	pMVP _{H8}	aMVP _{H8}	SBP _{H24}	pMVP _{H24}	aMVP _{H24} Control
S.p.	MSCs						MSCs
S.p.	Ceftaroline						CPT
S.p.	MSCs+Ceftaroline						MSCs + CPT

3 Travaux cliniques en cours

3.1 Etude PNEUMOCHONDRIE.

Dysfonction mitochondriale des cellules immunitaires alvéolaires et circulantes au cours du syndrome de détresse respiratoire aigüe : impact de l'agression infectieuse et de l'étirement alvéolaire lié à la ventilation mécanique.

Investigateur principal : Dr Mathieu BLOT

Responsable scientifique : Pr Pierre-Emmanuel CHARLES

Méthodologiste : Dr Serge Aho

Etudiante encadrée lors de ce travail et validant son Master 2 (2019) : Marine Jacquier

Promoteur : CHU Dijon Bourgogne

Approuvée le 29/05/2018 par le CPP SUD-EST III

Enregistrement Clinical Trial : NCT03955887

Financement obtenu en décembre 2018 : Bourse Appel d'Offre Jeune Chercheur (50 000 euros)

Résumé du protocole :

a. Rationnel

Le sepsis conduit à une réponse dérégulée de l'hôte susceptible d'entraîner des défaillances d'organes. Au cours du sepsis, des données expérimentales et cliniques suggèrent la survenue de dysfonctions mitochondrielles, particulièrement dans le muscle et les monocytes circulants, susceptibles de contribuer aux défaillances d'organes et au décès. Les pneumopathies aiguës communautaires (PAC), représentent la principale cause de décès d'origine infectieuse. La ventilation mécanique (VM) s'impose dans 20% des cas de pneumopathies bactériémiques à *Streptococcus pneumoniae* (S.p.), la mortalité atteignant alors 50%. Il existe alors fréquemment des critères de syndrome de détresse respiratoire aigüe (SDRA), associant une atteinte pulmonaire bilatérale et une hypoxémie marquée. L'étirement cyclique des cellules pulmonaires induit par la VM, génère une inflammation stérile et des dommages tissulaires (i.e. ventilator-induced lung injury [VILI]), responsables de dysfonctions

cellulaires de nature à modifier la réponse immunitaire, notamment au cours du SDRA. C'est pourquoi l'application d'une VM dite protectrice est alors requise. Cela n'empêche pas néanmoins qu'environ un tiers des patients présentent des signes de surdistension alvéolaire, ce dont témoigne une élévation de la pression motrice (PM) ($PM \geq 15$ cmH₂O), associée à une surmortalité. Les effets délétères de la VM pourraient s'expliquer par la survenue d'anomalies mitochondrielles. En effet, l'étirement cyclique de cellules pulmonaires entraîne des dysfonctions de la chaîne respiratoire et la production de radicaux libres de l'oxygène (ROS), altérant la perméabilité membranaire. Ces phénomènes pourraient favoriser le VILI, faciliter la translocation de bactéries du poumon vers le compartiment systémique et entraîner des altérations de la réponse immunitaire. Dans notre modèle de pneumopathie à *S.p.* chez le lapin, les animaux sous VM développent des pneumopathies plus sévères (défaut de clairance pulmonaire des bactéries, translocation bactérienne dans le sang, surmortalité), comparés aux animaux en ventilation spontanée (VS). Les concentrations intracellulaires pulmonaires d'ADN mitochondrial (ADNmt), reflet du pool mitochondrial, sont significativement diminuées chez les lapins ventilés, en comparaison aux lapins en VS, et chez les lapins infectés en comparaison aux lapins non infectés. Parallèlement le contenu mitochondrial des cellules circulantes diminue précocement (H8) chez tous les lapins infectés, mais n'est restauré que chez les lapins en VS, ceux qui survivent à la pneumonie (Blot *et al*, poster ECCMID 2015, article soumis). Ces données suggèrent une altération des mécanismes de restauration de l'homéostasie mitochondriale (biogénèse mitochondriale et mitophagie) au cours de la double agression infection/VM, susceptible d'expliquer la surmortalité observée. D'autres travaux de notre équipe illustrent l'importance de ces phénomènes en montrant dans un modèle murin d'infection polymicrobienne, que l'inhibition de la mitophagie chez les macrophages favorisait la survie (Patoli *et al*, en préparation). Les données humaines sur ce sujet sont inexistantes. Ces phénomènes de dysfonction mitochondriale méritent néanmoins d'être explorés chez l'homme, au cours de l'agression combinée VM/pneumopathie, afin de comprendre son impact éventuel sur l'efficacité de la réponse immune de l'hôte. Dans une démarche de médecine personnalisée, ces données ouvriraient des perspectives de thérapies ciblées, capables d'activer la biogénèse mitochondriale et/ou de moduler la mitophagie, afin de prévenir les dysfonctions d'organes et la mortalité au cours des PAC graves traitées par antibiothérapie.

b. Objectifs

Principal : Mesurer l'impact de la double agression VM/pneumopathie sur l'importance du pool de mitochondries actives dans les macrophages alvéolaires de patients, isolés à partir du liquide de lavage broncho-alvéolaire (LBA).

Secondaires :

- 1) Mesurer l'impact de la double agression VM/pneumopathie sur :
 - La dysfonction mitochondriale des cellules immunitaires alvéolaires et circulantes
 - La régulation de la biogénèse mitochondriale et de la mitophagie
 - Certains aspects de la réponse immunitaire innée alvéolaire et systémique
- 2) Mesurer l'effet propre de la VM (amplitude de la distension alvéolaire évaluée par le niveau de pression motrice (PM)) en comparant les patients en SDRA soumis à une VM la moins protectrice ($PM \geq 15 \text{ cmH}_2\text{O}$) à ceux soumis à une VM la plus protectrice ($PM < 15 \text{ cmH}_2\text{O}$) sur :
 - La dysfonction mitochondriale des cellules immunitaires alvéolaires et circulantes
 - La régulation de la biogénèse mitochondriale et de la mitophagie
 - Certains aspects de la réponse immunitaire innée alvéolaire et systémique
- 3) Etudier les corrélations entre les altérations mitochondrielles des cellules immunitaires alvéolaires et circulantes, l'activation immunitaire de ces cellules et la sévérité clinique.

c. Design

Etude prospective, monocentrique au CHU de Dijon, non interventionnelle incluant 51 patients:

- Groupe expérimental (groupe 1, 34 patients) : Patient présentant une pneumopathie aigue sévère compliquée d'un SDRA avec un rapport $\text{PaO}_2/\text{FiO}_2 < 150$ et nécessitant le recours à la VM.
- Groupe contrôle (groupe 2, 17 patients) : Patients bénéficiant d'un LBA en routine pour une pathologie non suspecte d'une infection aigue.

Pour chaque patient inclus, 3 tubes de sang supplémentaires et 10 ml de LBA seront dédiés à la recherche.

d. Critères de jugement

Principal : Contenu en mitochondries actives des macrophages alvéolaires (marqueur de dysfonction mitochondriale) : exprimé par la médiane de fluorescence (MFI) du marquage Mitotracker Red CMXROS®, dépendant du potentiel de membrane mitochondrial (cytométrie en flux).

Secondaires :

- Autres marqueurs de dysfonction mitochondriale des cellules immunitaires alvéolaires et circulantes :
 - o Pool mitochondrial global (marquage Mitotracker Green FM), pool de mitochondries actives (Mitotracker Red CMXRos), production de ROS mitochondriaux (MitoSOX, cytométrie en flux).
 - o Concentrations intra-cellulaires d'ADNmt (cyt B rapportée à celles du GAPDH)

- Libération extracellulaire alvéolaire et systémique d'ADNmt (dommage mitochondrial) et altération qualitative de l'ADNmt (oxydation, PCR)
 - Expression des gènes mitochondriaux (RTqPCR)
 - Anomalies de l'ultrastructure mitochondriale (microscopie électronique).
- Evaluation de la balance mitophagie/biogénèse mitochondriale dans les cellules immunitaires alvéolaires :
 - Expression des gènes de la mitophagie (p62, Parkin, Pink1) et de la biogénèse mitochondriale (TFAM, PGC1 α) (RTqPCR).
 - Evaluation du flux autophagique/mitophagique et de la biogénèse mitochondriale au sein des macrophages alvéolaires et des polynucléaires neutrophiles par microscopie confocale.
- Réponse immunitaire innée alvéolaire et circulante :
 - Concentration des cytokines inflammatoires (IL-1, IL-6, IL-8, TNF- α , INF- γ) et anti-inflammatoires (IL-4, IL-10) dans le surnageant des LBA et le plasma.
 - Activation immunitaire des cellules immunitaires (expression membranaire de HLA-DR, CD206 et CD64 mesurée par cytométrie en flux).
 - Capacités phagocytaires mesurées par test PhagotestTM (cytométrie en flux).
- Sévérité clinique évaluée par :
 - Mortalité à J30,
 - Score Sequential Organ Failure Assessment (SOFA) à l'inclusion
 - Sévérité du SDRA selon les critères de Berlin (rapport PaO₂/FiO₂) à l'inclusion

e. Critères d'inclusion et de non-inclusion

Critères d'inclusion :

- Personne majeure ayant donné son consentement écrit ou oral ou sa non-opposition (ou consentement obtenu auprès de la personne de confiance)
- Groupe 1 : patient présentant :
 - Une pneumopathie aigue définie par :
 - Signes et symptômes aigus de pneumopathie (nouveaux ou s'aggravant, dans les 7 derniers jours), au moins 2 parmi :
 - Toux
 - Crachat purulent
 - Dyspnée

- Douleur thoracique
 - Température < 35°C ou ≥ 38°C
 - Et un nouvel infiltrat radiologique pulmonaire (radiographie ou scanner à l'admission)
 - Non acquise sous ventilation mécanique
 - Compliquée de SDRA selon la nouvelle définition de Berlin,
 - Radiographie thoracique retrouvant des opacités parenchymateuses bilatérales non entièrement expliquée par des épanchements pleuraux, des nodules ou des atélectasies.
 - Insuffisance respiratoire non expliquée par une dysfonction cardiaque ou un remplissage excessif. Une échocardiographie sera réalisée en cas de doute diagnostique.
 - Rapport PaO₂/FiO₂ < 300 et PEEP ≥ 5 cmH₂O
 - Nécessitant le recours à la VM.
 - Avec réalisation d'un LBA à visée diagnostique dans les 72 heures qui suivent le début de la VM
- Groupe 2 : patients :
- Absence de fièvre durant les 15 derniers jours (rapportée ou mesurée ≥ 37,8°C).
 - Ne bénéficiant pas de VM,
 - Et bénéficiant d'un LBA pour une pathologie non suspecte d'infection aigüe (ex : syndrome interstitiel chronique, nodule ou masse pulmonaire).

Critères de non-inclusion :

- Patient non affilié à un régime de sécurité sociale
- Personne sous protection de justice (curatelle, tutelle, sauvegarde de justice)
- Femme enceinte, parturiante ou allaitante
- Déficit immunitaire primitif ou secondaire connu (radiothérapie, chimiothérapie, traitement immunosuppresseur ou corticothérapie systémique (> 10mg/j d'équivalent prednisone pendant plus de 7 jours) dans les 6 mois qui précèdent l'inclusion, infection par le VIH, déficit immunitaire primitif cellulaire).

- Patients bénéficiant d'un traitement connu pour moduler la fonction mitochondriale, la biogénèse et/ou la mitophagie (chloroquine, hydroxychloroquine, rapamycine, carbamazépine, resveratrol, metformine, sildénafil).
- Patients présentant une fibrose pulmonaire ou une mucoviscidose, connues pour être associées à des altérations mitochondrielles

Critères d'exclusion :

- Quantité du prélèvement de LBA insuffisante, ne permettant pas la réalisation des investigations biologiques
- Qualité du LBA insuffisante : au moins 1 des 3 items :
 - Cellularité < 50 000 / ml (LBA non représentatif)
 - Plus de 15% de cellules bronchiques
 - LBA non interprétable (coagulum, très hémorragique)
- Groupe 2 : diagnostic d'une pathologie infectieuse pulmonaire au décours du LBA et du reste du bilan réalisé

f. Méthode statistique

Comparaison des médianes (\pm IQR) par des tests non paramétriques, et des variables qualitatives par le test exact de Fisher. Les corrélations entre les variables quantitatives évaluant les altérations mitochondrielles et celles évaluant l'activation immunitaire d'une part, et la sévérité clinique d'autre part seront étudiées par le test de Spearman.

g. Avancée des travaux

Au 10 mars 2020, 14 patients ont été inclus (7 cas, 7 témoins).

Suite à l'épidémie de pneumopathies liées au Coronavirus Covid-19, l'étude princeps a été interrompue mais une étude ancillaire a été créée.

3.2 Etude Ancillaire PNEUMOCHONDRIE COVID-19

Réponse cytokinique et alarmines mitochondrielles dans les compartiments alvéolaire et systémique au cours du syndrome de détresse respiratoire aigüe lié au COVID19 : comparaison avec les autres agents pathogènes respiratoires.

a. Rationnel

L'infection par le Covid19 est responsable du syndrome respiratoire aigu sévère (SRAS) chez certains patients à risque, une forme particulièrement sévère de SDRA. Une alvéolite extrêmement intense semble en effet se développer chez les patients les plus gravement atteints. Une inflammation systémique intense est également présente, d'où le risque élevé de défaillance d'organe à distance du poumon, notamment rénale. Certaines études ayant mesuré la réponse inflammatoire systémique ont montré un lien possible entre son intensité, ses caractéristiques et le devenir des patients. En l'absence de traitement étiologique actuellement disponible, la prise en charge se limite à la ventilation mécanique, seul moyen de rétablir l'oxygénation de ces patients, mais susceptible d'exacerber cette inflammation notamment par le risque de volotraumatisme auquel elle expose. L'atteinte pulmonaire de certains patients augmente en effet considérablement le risque de surdistension alvéolaire. Analyser de façon qualitative et quantitative la réponse inflammatoire intra-alvéolaire est donc cruciale car son atténuation pourrait constituer une cible thérapeutique. Celle-ci pourrait être globale (e.g., corticothérapie) ou bien sélective vis-à-vis de certains médiateurs (e.g., thérapies ciblées anti-IL6 ou anti-IL1 β). Enfin, le rôle des alarmines mitochondrielles et notamment de l'ADNmt pourrait être critique dans l'initiation et l'amplification de cette inflammation, comme cela est suggéré de manière générale au cours du SDRA. La chloroquine, une molécule proposée dans le traitement de la pneumopathie à Covid19, pourrait agir en bloquant la reconnaissance de l'ADNmt par TLR9, atténuant l'inflammation alvéolaire.

b. Objectifs

Principal : comparer les caractéristiques de la réponse cytokinique au cours du SDRA COVID19 dans le compartiment alvéolaire (surnageant LBA) à celle observée chez les patients souffrant de SDRA d'autre étiologie

Secondaires :

- Comparer les caractéristiques de la réponse cytokinique au cours du SDRA COVID19 dans le compartiment systémique (plasma) à celle observée chez les patients souffrant de SDRA d'autre étiologie
- Evaluer la relation entre les concentrations d'ADNmt et l'amplitude de la réponse inflammatoire dans le compartiment alvéolaire.

- Evaluer la relation entre les concentrations d'ADNmt et l'amplitude de la réponse inflammatoire dans le compartiment systémique.
- Mesurer l'impact de la distension alvéolaire évaluée en termes de pression motrice sur les caractéristiques de la réponse cytokiniques alvéolaire.
- Comparaison des concentrations cytokiniques (LBA + plasma) et en ADNmt et ATP entre le groupe SDRA Covid19 et le groupe de patients témoins

c. Critères de jugement

Principal : Concentrations de cytokines inflammatoires dans le surnageant de patients en SDRA

Secondaires :

- Concentrations de cytokines inflammatoires dans le plasma de patients en SDRA
- Concentrations d'ADNmt et d'ATP dans le LBA de patients en SDRA
- Concentrations d'ADNmt et d'ATP dans plasma de patients en SDRA

d. Critères d'inclusion

- Groupe SDRA Covid19 :

- o Critères d'inclusion de l'étude principale +
 - Prélèvement(s) respiratoire(s) positif(s) pour Covid19

- Groupe SDRA non Covid19 (pour les patients nouvellement inclus au cours de l'épidémie Covid-19) :

- o Critères d'inclusion de l'étude principale +
 - Prélèvement(s) respiratoire(s) négatif(s) pour Covid19
 - Scanner thoracique non en faveur d'une infection à Covid19

Au 18 mai 2020, 14 patients en SDRA lié à une infection à SARS-CoV2 ont pu être inclus avec des LBA collectés pour les différentes analyses. Les dosages immunologiques, des alarmines mitochondrielles et les données cliniques sont en cours d'analyse.

3.3 Etude LYMPHONIE

Evaluation d'un test fonctionnel lymphocytaire (QuantiFERON Monitor®) comme marqueur pronostique au cours de la pneumonie aigue communautaire (Etude LYMPHONIE – Etude préliminaire).

Investigateur principal : Dr Mathieu BLOT

Responsable scientifique : Pr Lionel PIROTH

Méthodologiste : Pr Christine BINQUET

Promoteur : CHU Dijon Bourgogne

Approuvée le 09/01/2018 par le CPP Sud Méditerranée V

Enregistrement Clinical Trial : NCT03505281

Suite à l'épidémie de pneumopathies liées au Coronavirus Covid-19, l'étude princeps a été adaptée avec de nouveaux objectifs.

3.4 Etude ancillaire LYMPHONIE Covid-19

Objectif secondaire ayant fait l'objet d'un amendement : Etudier les différences entre les altérations fonctionnelles lymphocytaires des PAC sévères liée au SARS-Cov2 de celles qui ne le sont pas.

Au 1^{er} avril 2020, 14 nouveaux patients présentant une PAC sévère liée au Covid-19, dans les 48 heures suivant l'admission à l'hôpital, ont été inclus.

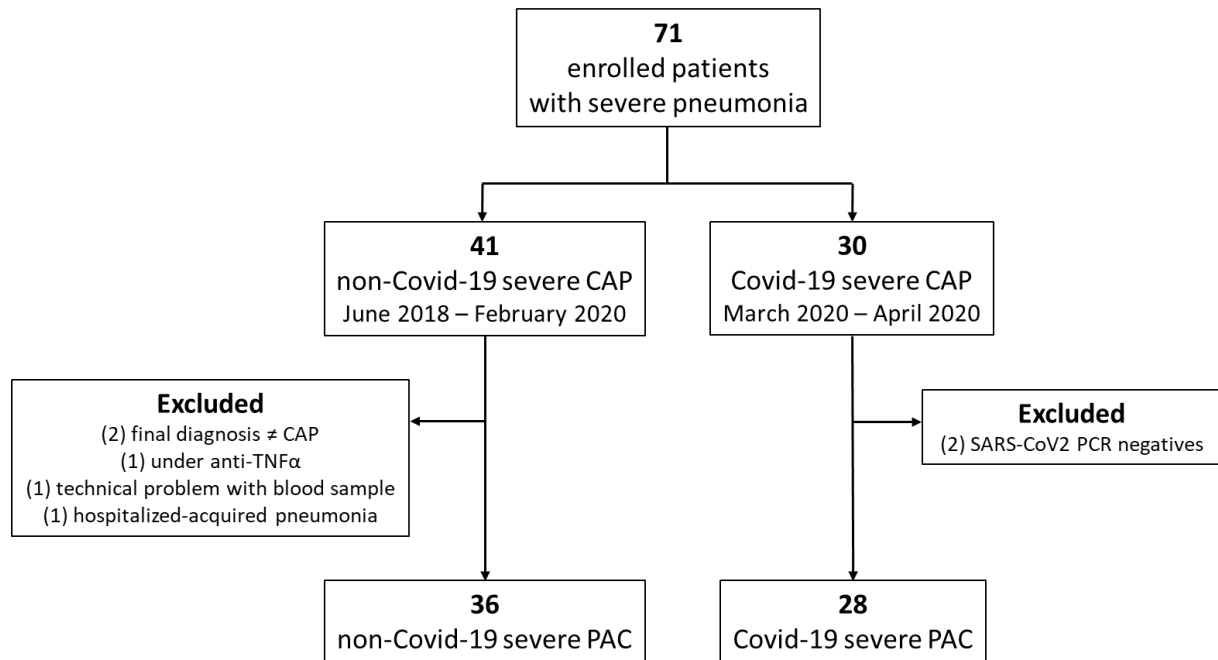
L'objectif est d'inclure 38 patients, qui seront comparés aux 37 premiers patients ayant une PAC non liée au Covid-19 afin de comparer :

- La réponse cytokinique dans le plasma afin d'identifier s'il existe un pattern inflammatoire lié au COVID-19 et qui pourrait faire l'objet d'une cible thérapeutique
- La réponse lymphocytaire : quantitative (sous population lymphocytaires) et qualitative (fonctionnalité lymphocytaire évaluée par le test standardisé Quantiféron Monitor, Qiagen).

Des études ancillaires seront aussi réalisées afin d'étudier :

- Les alarmines mitochondrielles plasmatiques
- Les anomalies lipidiques plasmatiques et les marqueurs d'inflammation liés aux lipoprotéines

Au 18 mai 2020, 71 patients ont été inclus, parmi lesquels 64 n'ont pas été exclus (36 dans le groupe non Covid-19 et 28 dans le groupe Covid-19)



4 Perspectives

Plusieurs perspectives sont envisagées :

A court terme, nous souhaitons finaliser ce travail de thèse avec plusieurs analyses complémentaires :

- Analyse de la biogénèse mitochondriale (PGC1- α , TFAM, NRF2) et de la voie Sirtuin par RTqPCR dans le tissu pulmonaire.
- Analyse transcriptomique du tissu pulmonaire afin de comparer 5 conditions (n=7/groupe) et d'étudier l'effet des CSMs sur la régulation des gènes impliqués dans la réponse immunitaire et l'homéostasie mitochondriale (Analyse en cours par la plateforme de transcriptomique de Paris Saclay):
 - o Lapins témoins
 - o Lapins infectés + VM agressive
 - o Idem + MSCs
 - o Idem + Ceftaroline
 - o Idem + MSCs + Ceftaroline
- Analyse de la microscopie électronique des tissus pulmonaires et hépatiques dans les différentes conditions d'étude (Figure 15).

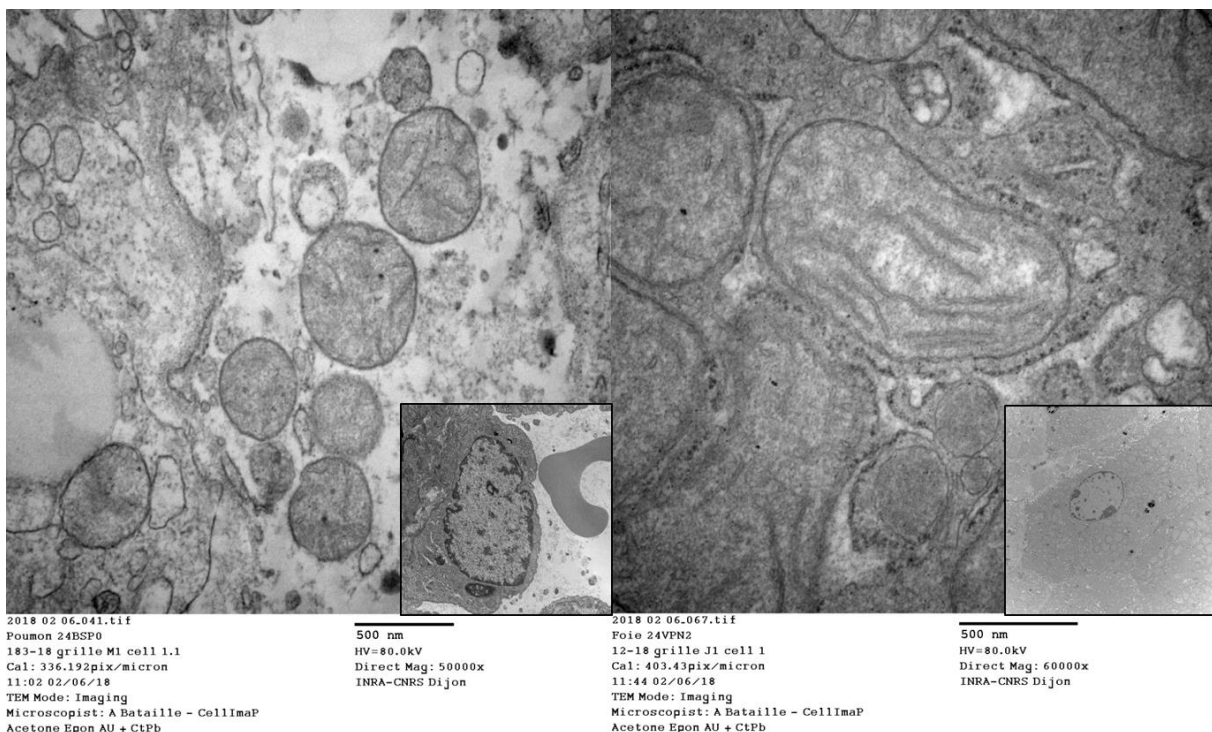


Figure 15. Analyse morphologique des mitochondries d'un lapin sain par microscopie électronique d'un pneumocyte de type II (grossissement 50 000 x) et (B) d'un hépatocyte (grossissement 60 000 x).

A moyen terme, je réaliseraï une mobilité dans le laboratoire du Pr Tom van der Poll à Amsterdam de septembre 2020 à aout 2021 sur un projet intitulé « **Impact of Sirt-1 on mitochondrial recovery, innate immune response and outcome during pneumonia** ». Un modèle de souris avec délétion conditionnelle de Sirt1 dans les cellules myéloïdes sera utilisé. Ce projet a été financé par deux bourses RICAI (35 000 euros) et ESCMID (20 000 euros).

A plus long terme, à mon retour de mobilité, je souhaite co-encadrer le travail de thèse de Science de Marine Jacquier, actuellement interne en réanimation, sur la thématique de la réponse immunitaire au cours de la pneumopathie grave ventilée et l'impact des CSMs avec un travail expérimental, un travail *ex vivo* sur du sang total stimulé et traité ou non par CSMs et la finalisation de l'étude PNEUMOCHONDRIE.

5 Conclusion générale

Ces travaux *in vitro*, expérimentaux chez le lapin, et les données obtenues chez des patients en SDRA et ventilés, montrent que des alarmines mitochondrielles, en particulier l'ADNmt, sont libérées dans le compartiment alvéolaire suite au stretch des cellules alvéolaires, et pourraient représenter le lien entre agression mécanique, et réponse inflammatoire stérile à l'origine du VILI (Figure 16).

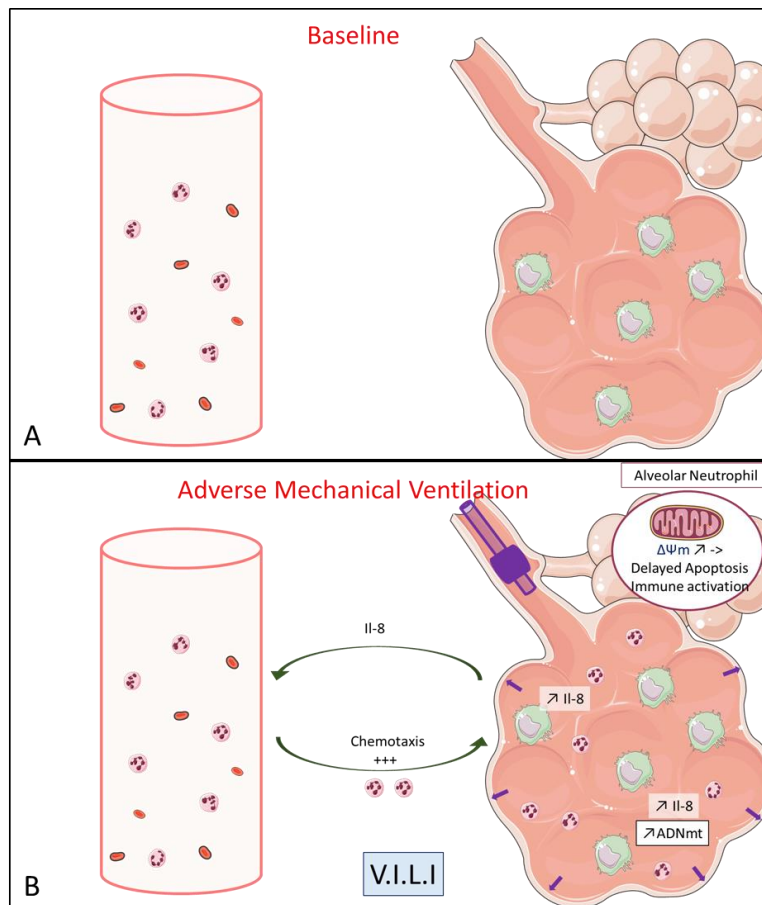


Figure 16. Réponse immunitaire et déterminants mitochondriaux dans les compartiments alvéolaires et systémiques : (A) situation basale et (B) au cours de l'agression mécanique que représente la ventilation mécanique agressive. L'étirement cyclique des alvéoles est à l'origine 1) d'une activation des macrophages alvéolaires libérant de l'IL-8 à l'origine du chimiotactisme des PMNs, mais aussi 2) d'une libération d'ADNmt dans le compartiment alvéolaire, potentialisant la libération d'IL-8 et accentuant ainsi le chimiotactisme des PMNs sur le site alvéolaire. Une libération de fMLP mitochondrial pourrait aussi aggraver ce phénomène. Parallèlement, l'augmentation du potentiel de membrane mitochondrial des PMNs alvéolaires faciliterait leur activation et un défaut de clairance en retardant leur apoptose. Le biotrauma ainsi généré (accumulation des PMNs et réponse immunitaire cytokinique), signature du VILI, pourraient ainsi avoir une origine mitochondriale.

Ces travaux montrent aussi que la VM joue un rôle délétère dans le pronostic de la pneumopathie à pneumocoque, et s'associant à des altérations mitochondrielles (Figure 17)

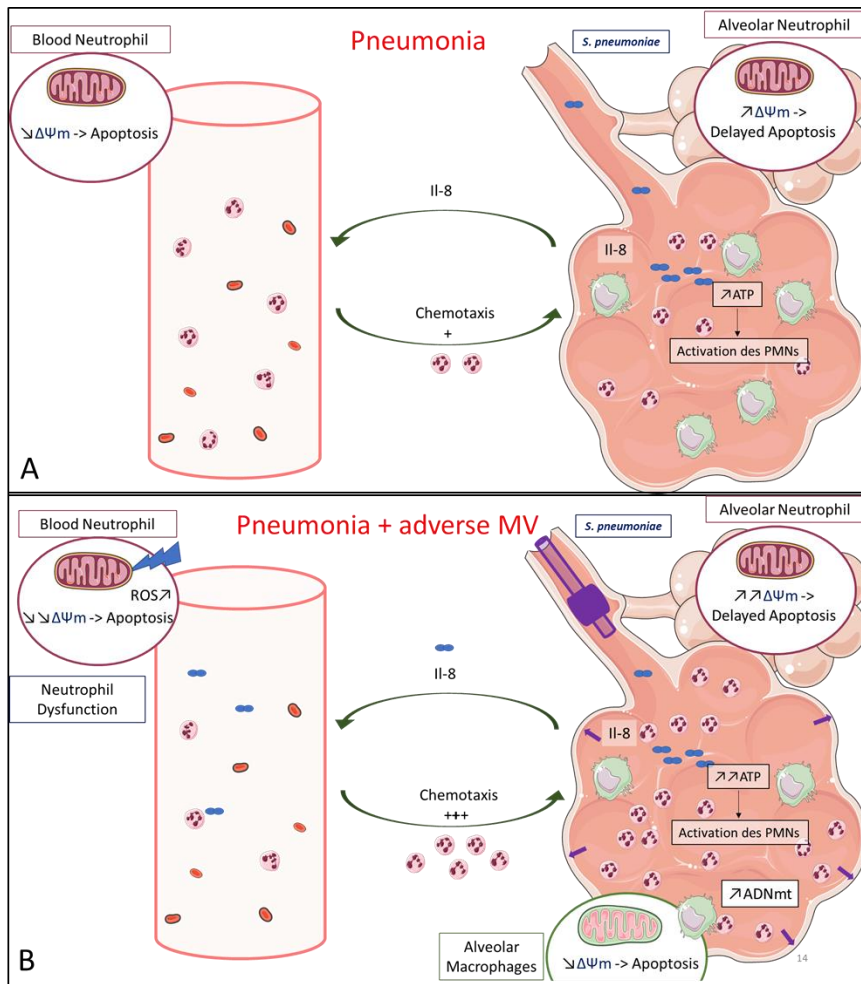


Figure 17. Réponse immunitaire et déterminants mitochondriaux dans les compartiments alvéolaires et systémiques : (A) au cours de la pneumopathie à pneumocoque, et (B) effet de l'agression surajoutée de la ventilation mécanique. Au cours de la pneumopathie à pneumocoque, la reconnaissance des PAMPs bactériens, en particulier la Pneumolysine reconnue par TLR-4 active la sécrétion de cytokines inflammatoires par les macrophages et les cellules épithéliales (en particulier l'IL-8) responsable du chimiotactisme des PMNs. La libération d'ATP dans le compartiment alvéolaire, dont l'origine pourrait être mixte (bactérienne et mitochondriale), est à l'origine de l'activation des PMNs. Lors de l'agression mécanique liée à la VM, l'étirement cyclique des cellules alvéolaires libère de l'ADNmt potentialisant la sécrétion d'IL-8 et l'afflux de PMN, qui s'activent sous l'effet de l'environnement inflammatoire, et des concentrations élevées d'ATP. L'agression infectieuse entraîne une augmentation du potentiel de membrane mitochondrial ($\Delta\Psi_m$) des PMNs alvéolaires et une diminution du $\Delta\Psi_m$ des macrophages alvéolaires et des PMNs circulants, avec un rôle aggravant de la VM. Les conséquences seraient une séquestration alvéolaire/pulmonaire des PMNs par apoptose

mitochondriale retardée. A l'inverse une apoptose mitochondriale accélérée expliquerait la raréfaction des macrophages alvéolaires et des PMNs circulants. La surproduction de ROS par les PMNs circulants agraverait les phénomènes de dysfonction mitochondriale au cours de la double agression et facilitant la chute du $\Delta\text{Ψ}_m$ et leur apoptose.

Ces données in-vivo témoignent de la complexité de la physiopathologie de la réponse immunitaire au cours de la pneumopathie à pneumocoque, qui ne peuvent être résumées par des modèles in-vitro. La compartmentalisation de la réponse immunitaire entre le site infecté et le compartiment systémique et les profils d'activation mitochondrial parfaitement inverses entre PMNs alvéolaires et circulants, et entre PMNs et macrophages alvéolaires en sont l'exemple même.

Ces données compromettent aussi l'idée qu'une approche thérapeutique immunomodulatrice ciblée, qu'elle soit anti ou pro inflammatoire, pourrait permettre d'améliorer le pronostic au cours de la pneumopathie grave ventilée.

Les CSMs pourraient être considérées comme une approche intelligente, dont l'effet est déterminé par l'environnement inflammatoire, oxydatif, et capable de moduler la réponse immunitaire en fonction du stade physiopathologique, de l'état immunitaire...

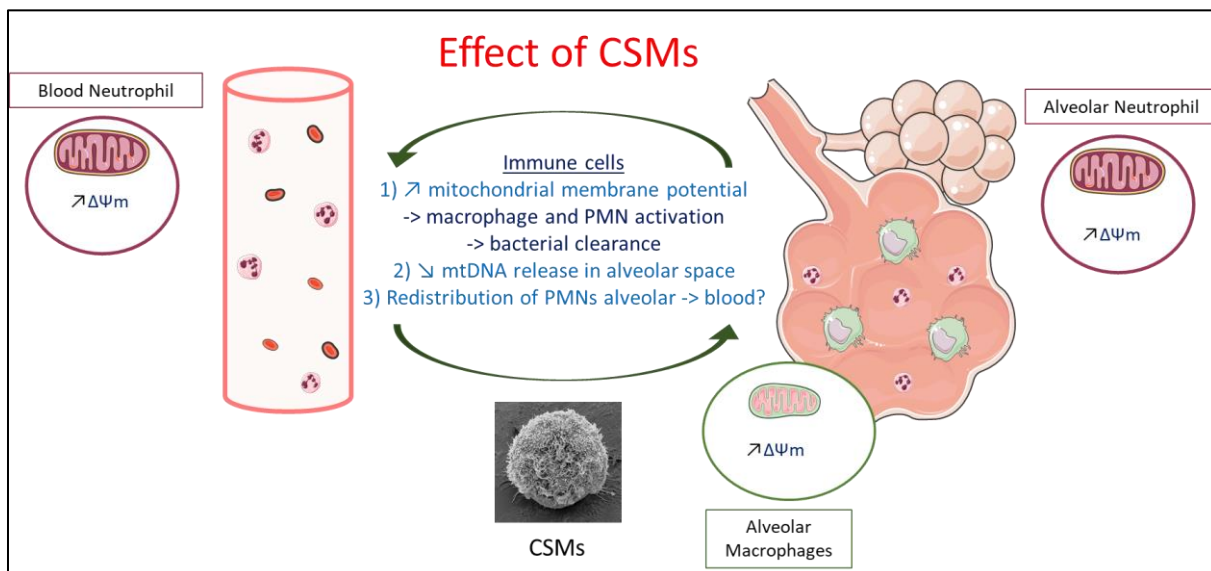


Figure 18. Effet des CSMs au cours de la pneumopathie à pneumocoque grave ventilée. L'augmentation du $\Delta\text{Ψ}_m$ observée dans les cellules immunitaires alvéolaires et circulantes pourrait faciliter la clairance bactérienne et limiter la translocation systémique. Si celle-ci n'expliquant pas la diminution de la séquestration des PMNs sur le site alvéolaire, l'on pourrait faire l'hypothèse qu'il existe une redistribution des PMNs alvéolaires activés dans le compartiment sanguin. La limitation de la libération d'ADNmt dans le compartiment alvéolaire et l'augmentation parallèle des niveaux d'ADNmt circulants, observées au cours du traitement par CSMs pourrait permettre cette

redistribution en corrigeant le gradient d'ADNmt alvéolaire/circulant. Cette modulation immunitaire et mitochondriale s'associe à une meilleure clairance bactérienne, à une limitation du VILI et une amélioration de la survie. Enfin, les CSMs semblent limiter les effets pro-inflammatoires (libération d'IL-8 et de TNF- α) produits par l'antibiothérapie.

Ces données méritent néanmoins d'être confirmées par une mesure plus précise de la fonction mitochondriale des cellules immunitaires (mesure de la respiration mitochondriale par Seahorse®), et une mesure plus précise de l'activation immunitaire. De telles mesures dans un modèle *in vivo* restent complexes et délicates à interpréter dans la mesure où les cellules doivent être préalablement triées et que toute manipulation reste une agression susceptible de perturber son homéostasie mitochondriale, et tout retard à la mesure est aussi un biais de mesure surajouté.

En conclusion, les CSMs améliorent le pronostic de la pneumopathie à pneumocoque ventilée, *via* la correction de dysfonctions immunitaires et mitochondrielles, représentant ainsi une stratégie adjuvante à l'antibiothérapie prometteuse.

6 Bibliographie

1. Mackenzie G. The definition and classification of pneumonia. *Pneumonia (Nathan)*. 2016;8:14.
2. Flateau C, Le Bel J, Tubiana S, Blanc F-X, Choquet C, Rammaert B, et al. High heterogeneity in community-acquired pneumonia inclusion criteria: does this impact on the validity of the results of randomized controlled trials? *BMC Infect Dis [Internet]*. 3 déc 2018 [cité 28 nov 2019];18. Disponible sur: <https://www.ncbi.nlm.nih.gov/pmc/articles/PMC6276130/>
3. Levy ML, Le Jeune I, Woodhead MA, Macfarlane JT, Lim WS, British Thoracic Society Community Acquired Pneumonia in Adults Guideline Group. Primary care summary of the British Thoracic Society Guidelines for the management of community acquired pneumonia in adults: 2009 update. Endorsed by the Royal College of General Practitioners and the Primary Care Respiratory Society UK. *Prim Care Respir J*. mars 2010;19(1):21-7.
4. Mandell LA, Wunderink RG, Anzueto A, Bartlett JG, Campbell GD, Dean NC, et al. Infectious Diseases Society of America/American Thoracic Society consensus guidelines on the management of community-acquired pneumonia in adults. *Clin Infect Dis*. 1 mars 2007;44 Suppl 2:S27-72.
5. Woodhead M, Blasi F, Ewig S, Garau J, Huchon G, Ieven M, et al. Guidelines for the management of adult lower respiratory tract infections--summary. *Clin Microbiol Infect*. nov 2011;17 Suppl 6:1-24.
6. European Respiratory Society. European lung whitebook 2013. <https://www.erswhitebook.org/chapters/acute-lower-respiratory-infections/>.
7. Welte T, Torres A, Nathwani D. Clinical and economic burden of community-acquired pneumonia among adults in Europe. *Thorax*. janv 2012;67(1):71-9.
8. Top 10 causes of death. Global Health Observatory, Who. http://www.who.int/gho/mortality_burden_disease/causes_death/top_10/en/. Disponible le 20 octobre 2018.
9. GBD 2017 Causes of Death Collaborators. Global, regional, and national age-sex-specific mortality for 282 causes of death in 195 countries and territories, 1980-2017: a systematic analysis for the Global Burden of Disease Study 2017. *Lancet*. 10 2018;392(10159):1736-88.
10. Garcia-Vidal C, Fernández-Sabé N, Carratalà J, Díaz V, Verdaguer R, Dorca J, et al. Early mortality in patients with community-acquired pneumonia: causes and risk factors. *Eur Respir J*. sept 2008;32(3):733-9.
11. Peyrani P, Arnold FW, Bordon J, Furmanek S, Luna CM, Cavallazzi R, et al. Incidence and Mortality of Adults Hospitalized With Community-Acquired Pneumonia According to Clinical Course. *Chest*. 11 oct 2019;
12. Daniel P, Woodhead M, Welham S, McKeever TM, Lim WS, British Thoracic Society. Mortality reduction in adult community-acquired pneumonia in the UK (2009-2014): results from the British Thoracic Society audit programme. *Thorax*. 2016;71(11):1061-3.
13. Kolditz M, Ewig S, Klapdor B, Schütte H, Winning J, Rupp J, et al. Community-acquired pneumonia as medical emergency: predictors of early deterioration. *Thorax*. juin 2015;70(6):551-8.

14. Simonetti AF, Garcia-Vidal C, Viasus D, García-Somoza D, Dorca J, Gudiol F, et al. Declining mortality among hospitalized patients with community-acquired pneumonia. *Clin Microbiol Infect.* juin 2016;22(6):567.e1-7.
15. Cilloniz C, Ferrer M, Liapikou A, Garcia-Vidal C, Gabarrus A, Ceccato A, et al. Acute respiratory distress syndrome in mechanically ventilated patients with community-acquired pneumonia. *Eur Respir J.* 2018;51(3).
16. Blot M, Croisier D, Péchinot A, Vagner A, Putot A, Fillion A, et al. A leukocyte score to improve clinical outcome predictions in bacteremic pneumococcal pneumonia in adults. *Open Forum Infect Dis.* sept 2014;1(2):ofu075.
17. ARDS Definition Task Force, Ranieri VM, Rubenfeld GD, Thompson BT, Ferguson ND, Caldwell E, et al. Acute respiratory distress syndrome: the Berlin Definition. *JAMA.* 20 juin 2012;307(23):2526-33.
18. Mortensen EM, Coley CM, Singer DE, Marrie TJ, Obrosky DS, Kapoor WN, et al. Causes of death for patients with community-acquired pneumonia: results from the Pneumonia Patient Outcomes Research Team cohort study. *Arch Intern Med.* 13 mai 2002;162(9):1059-64.
19. Eurich DT, Marrie TJ, Minhas-Sandhu JK, Majumdar SR. Ten-Year Mortality after Community-acquired Pneumonia. A Prospective Cohort. *Am J Respir Crit Care Med.* 1 sept 2015;192(5):597-604.
20. Eurich DT, Marrie TJ, Minhas-Sandhu JK, Majumdar SR. Risk of heart failure after community acquired pneumonia: prospective controlled study with 10 years of follow-up. *BMJ.* 13 févr 2017;356:j413.
21. Corrales-Medina VF, Suh KN, Rose G, Chirinos JA, Doucette S, Cameron DW, et al. Cardiac complications in patients with community-acquired pneumonia: a systematic review and meta-analysis of observational studies. *PLoS Med.* juin 2011;8(6):e1001048.
22. Divino V, Schranz J, Early M, Shah H, Jiang M, DeKoven M. The annual economic burden among patients hospitalized for community-acquired pneumonia (CAP): a retrospective US cohort study. *Curr Med Res Opin.* 17 oct 2019;1-10.
23. Saba G, Andrade LF, Gaillat J, Bonnin P, Chidiac C, Illes H-G, et al. Costs associated with community acquired pneumonia in France. *Eur J Health Econ.* mai 2018;19(4):533-44.
24. van der Poll T, Opal SM. Pathogenesis, treatment, and prevention of pneumococcal pneumonia. *Lancet.* 31 oct 2009;374(9700):1543-56.
25. Torres A, Blasi F, Peetermans WE, Viegi G, Welte T. The aetiology and antibiotic management of community-acquired pneumonia in adults in Europe: a literature review. *Eur J Clin Microbiol Infect Dis.* juill 2014;33(7):1065-79.
26. Said MA, Johnson HL, Nonyane BAS, Deloria-Knoll M, O'Brien KL, AGEDD Adult Pneumococcal Burden Study Team, et al. Estimating the burden of pneumococcal pneumonia among adults: a systematic review and meta-analysis of diagnostic techniques. *PLoS ONE.* 2013;8(4):e60273.
27. Jain S, Self WH, Wunderink RG, Fakhru S, Balk R, Bramley AM, et al. Community-Acquired Pneumonia Requiring Hospitalization among U.S. Adults. *N Engl J Med.* 30 juill 2015;373(5):415-27.

28. Gadsby NJ, Russell CD, McHugh MP, Mark H, Conway Morris A, Laurenson IF, et al. Comprehensive Molecular Testing for Respiratory Pathogens in Community-Acquired Pneumonia. *Clin Infect Dis.* 1 avr 2016;62(7):817-23.
29. McCullers JA. The co-pathogenesis of influenza viruses with bacteria in the lung. *Nat Rev Microbiol.* avr 2014;12(4):252-62.
30. Blot M, Chavanel P, Piroth L. Procalcitonin to Distinguish Viral From Bacterial Origin of Pneumonia: No Premature Conclusion! *Clin Infect Dis.* 17 déc 2019;
31. Prina E, Ranzani OT, Torres A. Community-acquired pneumonia. *Lancet.* 12 sept 2015;386(9998):1097-108.
32. Waterer GW, Rello J, Wunderink RG. Management of community-acquired pneumonia in adults. *Am J Respir Crit Care Med.* 15 janv 2011;183(2):157-64.
33. van der Poll T, van de Veerdonk FL, Scicluna BP, Netea MG. The immunopathology of sepsis and potential therapeutic targets. *Nat Rev Immunol.* juill 2017;17(7):407-20.
34. Mogensen TH. Pathogen recognition and inflammatory signaling in innate immune defenses. *Clin Microbiol Rev.* avr 2009;22(2):240-73, Table of Contents.
35. Vernatter J, Pirofski L. Current concepts in host-microbe interaction leading to pneumococcal pneumonia. *Curr Opin Infect Dis.* juin 2013;26(3):277-83.
36. Pham CTN. Neutrophil serine proteases: specific regulators of inflammation. *Nat Rev Immunol.* juill 2006;6(7):541-50.
37. Papayannopoulos V. Neutrophil extracellular traps in immunity and disease. *Nat Rev Immunol.* 2018;18(2):134-47.
38. Yipp BG, Petri B, Salina D, Jenne CN, Scott BNV, Zbytnuik LD, et al. Infection-induced NETosis is a dynamic process involving neutrophil multitasking in vivo. *Nat Med.* sept 2012;18(9):1386-93.
39. Manfredi AA, Ramirez GA, Rovere-Querini P, Maugeri N. The Neutrophil's Choice: Phagocytose vs Make Neutrophil Extracellular Traps. *Front Immunol.* 2018;9:288.
40. Knapp S, Leemans JC, Florquin S, Branger J, Maris NA, Pater J, et al. Alveolar macrophages have a protective antiinflammatory role during murine pneumococcal pneumonia. *Am J Respir Crit Care Med.* 15 janv 2003;167(2):171-9.
41. Thompson BT, Chambers RC, Liu KD. Acute Respiratory Distress Syndrome. *N Engl J Med.* 10 août 2017;377(6):562-72.
42. Fialkow L, Fochesatto Filho L, Bozzetti MC, Milani AR, Rodrigues Filho EM, Ladniuk RM, et al. Neutrophil apoptosis: a marker of disease severity in sepsis and sepsis-induced acute respiratory distress syndrome. *Crit Care.* 2006;10(6):R155.
43. Dehoux MS, Boutten A, Ostinelli J, Seta N, Dombret MC, Crestani B, et al. Compartmentalized cytokine production within the human lung in unilateral pneumonia. *Am J Respir Crit Care Med.* sept 1994;150(3):710-6.

44. Boutten A, Dehoux MS, Seta N, Ostinelli J, Venembre P, Crestani B, et al. Compartmentalized IL-8 and elastase release within the human lung in unilateral pneumonia. *Am J Respir Crit Care Med.* janv 1996;153(1):336-42.
45. Fernandez-Botran R, Uriarte SM, Arnold FW, Rodriguez-Hernandez L, Rane MJ, Peyrani P, et al. Contrasting inflammatory responses in severe and non-severe community-acquired pneumonia. *Inflammation.* août 2014;37(4):1158-66.
46. Hotchkiss RS, Moldawer LL, Opal SM, Reinhart K, Turnbull IR, Vincent J-L. Sepsis and septic shock. *Nat Rev Dis Primers.* 30 juin 2016;2:16045.
47. Siemieniuk RAC, Meade MO, Alonso-Coello P, Briel M, Evaniew N, Prasad M, et al. Corticosteroid Therapy for Patients Hospitalized With Community-Acquired Pneumonia: A Systematic Review and Meta-analysis. *Ann Intern Med.* 6 oct 2015;163(7):519-28.
48. Sibila O, Rodrigo-Troyano A, Torres A. Nonantibiotic Adjunctive Therapies for Community-Acquired Pneumonia (Corticosteroids and Beyond): Where Are We with Them? *Semin Respir Crit Care Med.* 2016;37(6):913-22.
49. Postma DF, van Werkhoven CH, van Elden LJR, Thijsen SFT, Hoepelman AIM, Kluytmans JAJW, et al. Antibiotic treatment strategies for community-acquired pneumonia in adults. *N Engl J Med.* 2 avr 2015;372(14):1312-23.
50. Hotchkiss RS, Monneret G, Payen D. Sepsis-induced immunosuppression: from cellular dysfunctions to immunotherapy. *Nat Rev Immunol.* déc 2013;13(12):862-74.
51. Venet F, Monneret G. Advances in the understanding and treatment of sepsis-induced immunosuppression. *Nat Rev Nephrol.* 2018;14(2):121-37.
52. Arraes SMA, Freitas MS, da Silva SV, de Paula Neto HA, Alves-Filho JC, Auxiliadora Martins M, et al. Impaired neutrophil chemotaxis in sepsis associates with GRK expression and inhibition of actin assembly and tyrosine phosphorylation. *Blood.* 1 nov 2006;108(9):2906-13.
53. Tavares-Murta BM, Zaporoli M, Ferreira RB, Silva-Vergara ML, Oliveira CHB, Murta EFC, et al. Failure of neutrophil chemotactic function in septic patients. *Crit Care Med.* mai 2002;30(5):1056-61.
54. Maianski NA, Maianski AN, Kuijpers TW, Roos D. Apoptosis of neutrophils. *Acta Haematol.* 2004;111(1-2):56-66.
55. Blot M, Chavanet P, Piroth L. [Influenza infection: An update for clinicians]. *Rev Med Interne.* mars 2019;40(3):158-65.
56. Grousd JA, Rich HE, Alcorn JF. Host-Pathogen Interactions in Gram-Positive Bacterial Pneumonia. *Clin Microbiol Rev.* 19 2019;32(3).
57. Hotchkiss RS, Colston E, Yende S, Crouser ED, Martin GS, Albertson T, et al. Immune checkpoint inhibition in sepsis: a Phase 1b randomized study to evaluate the safety, tolerability, pharmacokinetics, and pharmacodynamics of nivolumab. *Intensive Care Med.* 2019;45(10):1360-71.

58. Davenport EE, Burnham KL, Radhakrishnan J, Humburg P, Hutton P, Mills TC, et al. Genomic landscape of the individual host response and outcomes in sepsis: a prospective cohort study. *Lancet Respir Med.* 2016;4(4):259-71.
59. Scicluna BP, van Vugt LA, Zwinderman AH, Wiewel MA, Davenport EE, Burnham KL, et al. Classification of patients with sepsis according to blood genomic endotype: a prospective cohort study. *Lancet Respir Med.* 2017;5(10):816-26.
60. Antcliffe DB, Burnham KL, Al-Beidh F, Santhakumaran S, Brett SJ, Hinds CJ, et al. Transcriptomic Signatures in Sepsis and a Differential Response to Steroids. From the VANISH Randomized Trial. *Am J Respir Crit Care Med.* 15 2019;199(8):980-6.
61. Antcliffe DB, Gordon AC. Why Understanding Sepsis Endotypes Is Important for Steroid Trials in Septic Shock. *Crit Care Med.* déc 2019;47(12):1782-4.
62. Cheng S-C, Scicluna BP, Arts RJW, Gresnigt MS, Lachmandas E, Giamarellos-Bourboulis EJ, et al. Broad defects in the energy metabolism of leukocytes underlie immunoparalysis in sepsis. *Nat Immunol.* avr 2016;17(4):406-13.
63. Archibald JM. Endosymbiosis and Eukaryotic Cell Evolution. *Curr Biol.* 5 oct 2015;25(19):R911-921.
64. Hemmi H, Takeuchi O, Kawai T, Kaisho T, Sato S, Sanjo H, et al. A Toll-like receptor recognizes bacterial DNA. *Nature.* 7 déc 2000;408(6813):740-5.
65. Zhang Q, Raoof M, Chen Y, Sumi Y, Sursal T, Junger W, et al. Circulating mitochondrial DAMPs cause inflammatory responses to injury. *Nature.* 4 mars 2010;464(7285):104-7.
66. Meyer A, Laverny G, Bernardi L, Charles AL, Alsaleh G, Pottecher J, et al. Mitochondria: An Organelle of Bacterial Origin Controlling Inflammation. *Front Immunol.* 2018;9:536.
67. Jakobs S. High resolution imaging of live mitochondria. *Biochim Biophys Acta.* juin 2006;1763(5-6):561-75.
68. Matzinger P. Tolerance, danger, and the extended family. *Annu Rev Immunol.* 1994;12:991-1045.
69. Seong S-Y, Matzinger P. Hydrophobicity: an ancient damage-associated molecular pattern that initiates innate immune responses. *Nat Rev Immunol.* juin 2004;4(6):469-78.
70. Bianchi ME. DAMPs, PAMPs and alarmins: all we need to know about danger. *J Leukoc Biol.* janv 2007;81(1):1-5.
71. Fang C, Wei X, Wei Y. Mitochondrial DNA in the regulation of innate immune responses. *Protein Cell.* janv 2016;7(1):11-6.
72. Piantadosi CA. Mitochondrial DNA, oxidants, and innate immunity. *Free Radic Biol Med.* 17 janv 2020;
73. Rodríguez-Nuevo A, Zorzano A. The sensing of mitochondrial DAMPs by non-immune cells. *Cell Stress.* 23 mai 2019;3(6):195-207.
74. Grazioli S, Pugin J. Mitochondrial Damage-Associated Molecular Patterns: From Inflammatory Signaling to Human Diseases. *Front Immunol.* 2018;9:832.

75. West AP, Shadel GS. Mitochondrial DNA in innate immune responses and inflammatory pathology. *Nat Rev Immunol.* juin 2017;17(6):363-75.
76. Patrushev M, Kasymov V, Patrusheva V, Ushakova T, Gogvadze V, Gaziev A. Mitochondrial permeability transition triggers the release of mtDNA fragments. *Cell Mol Life Sci.* déc 2004;61(24):3100-3.
77. Lood C, Blanco LP, Purmalek MM, Carmona-Rivera C, De Ravin SS, Smith CK, et al. Neutrophil extracellular traps enriched in oxidized mitochondrial DNA are interferogenic and contribute to lupus-like disease. *Nat Med.* févr 2016;22(2):146-53.
78. Nakahira K, Haspel JA, Rathinam VAK, Lee S-J, Dolinay T, Lam HC, et al. Autophagy proteins regulate innate immune responses by inhibiting the release of mitochondrial DNA mediated by the NALP3 inflammasome. *Nat Immunol.* mars 2011;12(3):222-30.
79. Pugin J. How tissue injury alarms the immune system and causes a systemic inflammatory response syndrome. *Ann Intensive Care.* 2012;2(1):27.
80. Van Houten B, Hunter SE, Meyer JN. Mitochondrial DNA damage induced autophagy, cell death, and disease. *Front Biosci (Landmark Ed).* 1 janv 2016;21:42-54.
81. Nissanka N, Minczuk M, Moraes CT. Mechanisms of Mitochondrial DNA Deletion Formation. *Trends Genet.* 2019;35(3):235-44.
82. Shimada K, Crother TR, Karlin J, Dagvadorj J, Chiba N, Chen S, et al. Oxidized mitochondrial DNA activates the NLRP3 inflammasome during apoptosis. *Immunity.* 23 mars 2012;36(3):401-14.
83. Harrington JS, Choi AMK, Nakahira K. Mitochondrial DNA in Sepsis. *Curr Opin Crit Care.* août 2017;23(4):284-90.
84. Krychtiuk KA, Ruhittel S, Hohensinner PJ, Koller L, Kaun C, Lenz M, et al. Mitochondrial DNA and Toll-Like Receptor-9 Are Associated With Mortality in Critically Ill Patients. *Crit Care Med.* déc 2015;43(12):2633-41.
85. Timmermans K, Kox M, Scheffer GJ, Pickkers P. Plasma Nuclear and Mitochondrial DNA Levels, and Markers of Inflammation, Shock, and Organ Damage in Patients with Septic Shock. *Shock.* 2016;45(6):607-12.
86. Puskarich MA, Shapiro NI, Trzeciak S, Kline JA, Jones AE. Plasma levels of mitochondrial DNA in patients presenting to the emergency department with sepsis. *Shock.* oct 2012;38(4):337-40.
87. Chen Y, Corriden R, Inoue Y, Yip L, Hashiguchi N, Zinkernagel A, et al. ATP release guides neutrophil chemotaxis via P2Y2 and A3 receptors. *Science.* 15 déc 2006;314(5806):1792-5.
88. McDonald B, Pittman K, Menezes GB, Hirota SA, Slaba I, Waterhouse CCM, et al. Intravascular danger signals guide neutrophils to sites of sterile inflammation. *Science.* 15 oct 2010;330(6002):362-6.
89. Eltzschig HK, Sitkovsky MV, Robson SC. Purinergic signaling during inflammation. *N Engl J Med.* 13 déc 2012;367(24):2322-33.
90. Zhou R, Yazdi AS, Menu P, Tschopp J. A role for mitochondria in NLRP3 inflammasome activation. *Nature.* 13 janv 2011;469(7329):221-5.

91. Sumi Y, Woehrle T, Chen Y, Bao Y, Li X, Yao Y, et al. Plasma ATP is required for neutrophil activation in a mouse sepsis model. *Shock*. août 2014;42(2):142-7.
92. Bao Y, Ledderose C, Seier T, Graf AF, Brix B, Chong E, et al. Mitochondria regulate neutrophil activation by generating ATP for autocrine purinergic signaling. *J Biol Chem*. 26 sept 2014;289(39):26794-803.
93. Scarpulla RC. Transcriptional paradigms in mammalian mitochondrial biogenesis and function. *Physiol Rev*. avr 2008;88(2):611-38.
94. Lemarie A, Grimm S. Mitochondrial respiratory chain complexes: apoptosis sensors mutated in cancer? *Oncogene*. 22 sept 2011;30(38):3985-4003.
95. Boveris A, Costa LE, Poderoso JJ, Carreras MC, Cadena E. Regulation of mitochondrial respiration by oxygen and nitric oxide. *Ann N Y Acad Sci*. 2000;899:121-35.
96. West AP, Shadel GS, Ghosh S. Mitochondria in innate immune responses. *Nat Rev Immunol*. juin 2011;11(6):389-402.
97. Clere-Jehl R, Helms J, Kassem M, Le Borgne P, Delabranche X, Charles A-L, et al. Septic Shock Alters Mitochondrial Respiration of Lymphoid Cell-Lines and Human Peripheral Blood Mononuclear Cells: The Role of Plasma. *Shock*. 14 févr 2018;
98. Weiss SL, Zhang D, Bush J, Graham K, Starr J, Murray J, et al. MITOCHONDRIAL DYSFUNCTION IS ASSOCIATED WITH AN IMMUNE PARALYSIS PHENOTYPE IN PEDIATRIC SEPSIS. *Shock*. 20 nov 2019;
99. Japiassú AM, Santiago APSA, d'Avila J da CP, Garcia-Souza LF, Galina A, Castro Faria-Neto HC, et al. Bioenergetic failure of human peripheral blood monocytes in patients with septic shock is mediated by reduced F1Fo adenosine-5'-triphosphate synthase activity. *Crit Care Med*. mai 2011;39(5):1056-63.
100. Gong Y, Zou L, Feng Y, Li D, Cai J, Chen D, et al. Importance of Toll-like receptor 2 in mitochondrial dysfunction during polymicrobial sepsis. *Anesthesiology*. déc 2014;121(6):1236-47.
101. Park DW, Jiang S, Tadie J-M, Stigler WS, Gao Y, Deshane J, et al. Activation of AMPK enhances neutrophil chemotaxis and bacterial killing. *Mol Med*. 8 nov 2013;19:387-98.
102. Park DW, Zmijewski JW. Mitochondrial Dysfunction and Immune Cell Metabolism in Sepsis. *Infect Chemother*. mars 2017;49(1):10-21.
103. Zmijewski JW, Lorne E, Banerjee S, Abraham E. Participation of mitochondrial respiratory complex III in neutrophil activation and lung injury. *Am J Physiol Lung Cell Mol Physiol*. avr 2009;296(4):L624-634.
104. Stienstra R, Netea-Maier RT, Riksen NP, Joosten LAB, Netea MG. Specific and Complex Reprogramming of Cellular Metabolism in Myeloid Cells during Innate Immune Responses. *Cell Metab*. 5 juill 2017;26(1):142-56.
105. Netea MG, Joosten LAB, Latz E, Mills KHG, Natoli G, Stunnenberg HG, et al. Trained immunity: A program of innate immune memory in health and disease. *Science*. 22 avr 2016;352(6284):aaf1098.

106. Kroemer G, Galluzzi L, Brenner C. Mitochondrial membrane permeabilization in cell death. *Physiol Rev.* janv 2007;87(1):99-163.
107. Tait SWG, Green DR. Mitochondria and cell death: outer membrane permeabilization and beyond. *Nat Rev Mol Cell Biol.* sept 2010;11(9):621-32.
108. Chang KC, Unsinger J, Davis CG, Schwulst SJ, Muenzer JT, Strasser A, et al. Multiple triggers of cell death in sepsis: death receptor and mitochondrial-mediated apoptosis. *FASEB J.* mars 2007;21(3):708-19.
109. Gustave C-A, Gossez M, Demaret J, Rimmelé T, Lepape A, Malcus C, et al. Septic Shock Shapes B Cell Response toward an Exhausted-like/Immunoregulatory Profile in Patients. *J Immunol.* 01 2018;200(7):2418-25.
110. Whitaker RM, Corum D, Beeson CC, Schnellmann RG. Mitochondrial Biogenesis as a Pharmacological Target: A New Approach to Acute and Chronic Diseases. *Annu Rev Pharmacol Toxicol.* 2016;56:229-49.
111. Gkikas I, Palikaras K, Tavernarakis N. The Role of Mitophagy in Innate Immunity. *Front Immunol.* 2018;9:1283.
112. Youle RJ, Narendra DP. Mechanisms of mitophagy. *Nat Rev Mol Cell Biol.* janv 2011;12(1):9-14.
113. Archer SL. Mitochondrial dynamics--mitochondrial fission and fusion in human diseases. *N Engl J Med.* 5 déc 2013;369(23):2236-51.
114. Singer M. The role of mitochondrial dysfunction in sepsis-induced multi-organ failure. *Virulence.* 1 janv 2014;5(1):66-72.
115. Kraft BD, Chen L, Suliman HB, Piantadosi CA, Welty-Wolf KE. Peripheral Blood Mononuclear Cells Demonstrate Mitochondrial Damage Clearance During Sepsis. *Crit Care Med.* mai 2019;47(5):651-8.
116. Angus DC, van der Poll T. Severe sepsis and septic shock. *N Engl J Med.* 29 août 2013;369(9):840-51.
117. Singer M. Critical illness and flat batteries. *Crit Care.* 28 2017;21(Suppl 3):309.
118. Kreymann G, Grosser S, Buggisch P, Gottschall C, Matthaei S, Greten H. Oxygen consumption and resting metabolic rate in sepsis, sepsis syndrome, and septic shock. *Crit Care Med.* juill 1993;21(7):1012-9.
119. Haden DW, Suliman HB, Carraway MS, Welty-Wolf KE, Ali AS, Shitara H, et al. Mitochondrial biogenesis restores oxidative metabolism during *Staphylococcus aureus* sepsis. *Am J Respir Crit Care Med.* 15 oct 2007;176(8):768-77.
120. Protti A, Singer M. Bench-to-bedside review: potential strategies to protect or reverse mitochondrial dysfunction in sepsis-induced organ failure. *Crit Care.* 2006;10(5):228.
121. Calvano SE, Xiao W, Richards DR, Felciano RM, Baker HV, Cho RJ, et al. A network-based analysis of systemic inflammation in humans. *Nature.* 13 oct 2005;437(7061):1032-7.

122. Carré JE, Orban J-C, Re L, Felsmann K, Iffert W, Bauer M, et al. Survival in critical illness is associated with early activation of mitochondrial biogenesis. *Am J Respir Crit Care Med.* 15 sept 2010;182(6):745-51.
123. Brealey D, Brand M, Hargreaves I, Heales S, Land J, Smolenski R, et al. Association between mitochondrial dysfunction and severity and outcome of septic shock. *Lancet.* 20 juill 2002;360(9328):219-23.
124. Hotchkiss RS, Swanson PE, Freeman BD, Tinsley KW, Cobb JP, Matuschak GM, et al. Apoptotic cell death in patients with sepsis, shock, and multiple organ dysfunction. *Crit Care Med.* juill 1999;27(7):1230-51.
125. Takasu O, Gaut JP, Watanabe E, To K, Fagley RE, Sato B, et al. Mechanisms of cardiac and renal dysfunction in patients dying of sepsis. *Am J Respir Crit Care Med.* 1 mars 2013;187(5):509-17.
126. Slutsky AS, Ranieri VM. Ventilator-induced lung injury. *N Engl J Med.* 28 nov 2013;369(22):2126-36.
127. Charles P-E, Tissières P, Barbar SD, Croisier D, Dufour J, Dunn-Siegrist I, et al. Mild-stretch mechanical ventilation upregulates toll-like receptor 2 and sensitizes the lung to bacterial lipopeptide. *Crit Care.* 2011;15(4):R181.
128. Kuipers MT, van der Poll T, Schultz MJ, Wieland CW. Bench-to-bedside review: Damage-associated molecular patterns in the onset of ventilator-induced lung injury. *Crit Care.* 2011;15(6):235.
129. Kawano T, Mori S, Cybulsky M, Burger R, Ballin A, Cutz E, et al. Effect of granulocyte depletion in a ventilated surfactant-depleted lung. *J Appl Physiol.* janv 1987;62(1):27-33.
130. Grommes J, Soehnlein O. Contribution of neutrophils to acute lung injury. *Mol Med.* avr 2011;17(3-4):293-307.
131. Yildiz C, Palaniyar N, Otulakowski G, Khan MA, Post M, Kuebler WM, et al. Mechanical ventilation induces neutrophil extracellular trap formation. *Anesthesiology.* avr 2015;122(4):864-75.
132. Charles PE, Etienne M, Croisier D, Piroth L, Lequeu C, Pugin J, et al. The impact of mechanical ventilation on the moxifloxacin treatment of experimental pneumonia caused by *Streptococcus pneumoniae*. *Crit Care Med.* mai 2005;33(5):1029-35.
133. Barbar S-D, Pauchard L-A, Bruyère R, Bruillard C, Hayez D, Croisier D, et al. Mechanical Ventilation Alters the Development of *Staphylococcus aureus* Pneumonia in Rabbit. *PLoS ONE.* 2016;11(7):e0158799.
134. Pauchard L-A, Blot M, Bruyere R, Barbar S-D, Croisier D, Piroth L, et al. Linezolid and atorvastatin impact on pneumonia caused by *Staphylococcus aureus* in rabbits with or without mechanical ventilation. *PLoS ONE.* 2017;12(11):e0187187.
135. Charles PE, Martin L, Etienne M, Croisier D, Piroth L, Lequeu C, et al. Influence of positive end-expiratory pressure (PEEP) on histopathological and bacteriological aspects of pneumonia during low tidal volume mechanical ventilation. *Intensive Care Med.* déc 2004;30(12):2263-70.

136. Ladoire S, Pauchard L-A, Barbar S-D, Tissieres P, Croisier-Bertin D, Charles P-E. Impact of the prone position in an animal model of unilateral bacterial pneumonia undergoing mechanical ventilation. *Anesthesiology*. mai 2013;118(5):1150-9.
137. Charles P-E, Piroth L, Desbiolles N, Lequeu C, Martin L, Portier H, et al. New model of ventilator-associated pneumonia in immunocompetent rabbits. *Crit Care Med*. oct 2002;30(10):2278-83.
138. Ventilation with lower tidal volumes as compared with traditional tidal volumes for acute lung injury and the acute respiratory distress syndrome. The Acute Respiratory Distress Syndrome Network. *N Engl J Med*. 4 mai 2000;342(18):1301-8.
139. Thompson BT, Chambers RC, Liu KD. Acute Respiratory Distress Syndrome. *N Engl J Med*. 09 2017;377(19):1904-5.
140. Stüber F, Wrigge H, Schroeder S, Wetegrove S, Zinserling J, Hoeft A, et al. Kinetic and reversibility of mechanical ventilation-associated pulmonary and systemic inflammatory response in patients with acute lung injury. *Intensive Care Med*. juill 2002;28(7):834-41.
141. Guérin C, Reignier J, Richard J-C, Beuret P, Gacouin A, Boulain T, et al. Prone positioning in severe acute respiratory distress syndrome. *N Engl J Med*. 6 juin 2013;368(23):2159-68.
142. Terragni PP, Rosboch G, Tealdi A, Corno E, Menaldo E, Davini O, et al. Tidal hyperinflation during low tidal volume ventilation in acute respiratory distress syndrome. *Am J Respir Crit Care Med*. 15 janv 2007;175(2):160-6.
143. Amato MBP, Meade MO, Slutsky AS, Brochard L, Costa ELV, Schoenfeld DA, et al. Driving pressure and survival in the acute respiratory distress syndrome. *N Engl J Med*. 19 févr 2015;372(8):747-55.
144. Aoyama H, Pettenuzzo T, Aoyama K, Pinto R, Englesakis M, Fan E. Association of Driving Pressure With Mortality Among Ventilated Patients With Acute Respiratory Distress Syndrome: A Systematic Review and Meta-Analysis. *Crit Care Med*. 10 nov 2017;
145. Chapman KE, Sinclair SE, Zhuang D, Hassid A, Desai LP, Waters CM. Cyclic mechanical strain increases reactive oxygen species production in pulmonary epithelial cells. *Am J Physiol Lung Cell Mol Physiol*. nov 2005;289(5):L834-841.
146. Davidovich N, DiPaolo BC, Lawrence GG, Chhour P, Yehya N, Margulies SS. Cyclic stretch-induced oxidative stress increases pulmonary alveolar epithelial permeability. *Am J Respir Cell Mol Biol*. juill 2013;49(1):156-64.
147. Ratner V, Sosunov SA, Niatsetskaya ZV, Utkina-Sosunova IV, Ten VS. Mechanical ventilation causes pulmonary mitochondrial dysfunction and delayed alveolarization in neonatal mice. *Am J Respir Cell Mol Biol*. déc 2013;49(6):943-50.
148. Lin J-Y, Jing R, Lin F, Ge W-Y, Dai H-J, Pan L. High Tidal Volume Induces Mitochondria Damage and Releases Mitochondrial DNA to Aggravate the Ventilator-Induced Lung Injury. *Front Immunol*. 2018;9:1477.
149. Timmermans K, Kox M, Vaneker M, Pickkers P, Scheffer GJ. Mitochondrial DNA and TLR9 Signaling Is Not Involved in Mechanical Ventilation-Induced Inflammation. *Anesth Analg*. févr 2017;124(2):531-4.

150. Papaiahgari S, Yerrapureddy A, Reddy SR, Reddy NM, Dodd-O JM, Crow MT, et al. Genetic and pharmacologic evidence links oxidative stress to ventilator-induced lung injury in mice. *Am J Respir Crit Care Med.* 15 déc 2007;176(12):1222-35.
151. Tang H, Shrager JB. The Signaling Network Resulting in Ventilator-induced Diaphragm Dysfunction. *Am J Respir Cell Mol Biol.* 2018;59(4):417-27.
152. Horwitz EM, Le Blanc K, Dominici M, Mueller I, Slaper-Cortenbach I, Marini FC, et al. Clarification of the nomenclature for MSC: The International Society for Cellular Therapy position statement. *Cytotherapy.* 2005;7(5):393-5.
153. Laroye C, Gibot S, Reppel L, Bensoussan D. Concise Review: Mesenchymal Stromal/Stem Cells: A New Treatment for Sepsis and Septic Shock? *Stem Cells.* déc 2017;35(12):2331-9.
154. Walter J, Ware LB, Matthay MA. Mesenchymal stem cells: mechanisms of potential therapeutic benefit in ARDS and sepsis. *Lancet Respir Med.* déc 2014;2(12):1016-26.
155. Huppert LA, Liu KD, Matthay MA. Therapeutic potential of mesenchymal stromal cells in the treatment of ARDS. *Transfusion.* 2019;59(S1):869-75.
156. Prockop DJ, Gregory CA, Spees JL. One strategy for cell and gene therapy: harnessing the power of adult stem cells to repair tissues. *Proc Natl Acad Sci USA.* 30 sept 2003;100 Suppl 1:11917-23.
157. Horák J, Nalos L, Martínková V, Beneš J, Štengl M, Matějovič M. Mesenchymal Stem Cells in Sepsis and Associated Organ Dysfunction: A Promising Future or Blind Alley? *Stem Cells Int.* 2017;2017:7304121.
158. Perlee D, van Vugt LA, Scicluna BP, Maag A, Lutter R, Kemper EM, et al. Intravenous Infusion of Human Adipose Mesenchymal Stem Cells Modifies the Host Response to Lipopolysaccharide in Humans: A Randomized, Single-Blind, Parallel Group, Placebo Controlled Trial. *Stem Cells.* 2018;36(11):1778-88.
159. Mei SHJ, Haitsma JJ, Dos Santos CC, Deng Y, Lai PFH, Slutsky AS, et al. Mesenchymal stem cells reduce inflammation while enhancing bacterial clearance and improving survival in sepsis. *Am J Respir Crit Care Med.* 2010;182(8):1047-57.
160. Jackson MV, Morrison TJ, Doherty DF, McAuley DF, Matthay MA, Kisselkell A, et al. Mitochondrial Transfer via Tunneling Nanotubes is an Important Mechanism by Which Mesenchymal Stem Cells Enhance Macrophage Phagocytosis in the In Vitro and In Vivo Models of ARDS. *Stem Cells.* 2016;34(8):2210-23.
161. Hall SRR, Tsioyi K, Ith B, Padera RF, Lederer JA, Wang Z, et al. Mesenchymal Stromal Cells Improve Survival During Sepsis in the Absence of Heme Oxygenase-1: The Importance of Neutrophils. *STEM CELLS.* 2013;31(2):397-407.
162. Devaney J, Horie S, Masterson C, Elliman S, Barry F, O'Brien T, et al. Human mesenchymal stromal cells decrease the severity of acute lung injury induced by *E. coli* in the rat. *Thorax.* 2015;70(7):625-35.
163. Alcayaga-Miranda F, Cuenca J, Martin A, Contreras L, Figueroa FE, Khouri M. Combination therapy of menstrual derived mesenchymal stem cells and antibiotics ameliorates survival in sepsis. *Stem Cell Res Ther.* 2015;6:199.

164. Rocheteau P, Chatre L, Briand D, Mebarki M, Jouvon G, Bardon J, et al. Sepsis induces long-term metabolic and mitochondrial muscle stem cell dysfunction amenable by mesenchymal stem cell therapy. *Nat Commun.* 2015;6:10145.
165. Németh K, Leelahavanichkul A, Yuen PST, Mayer B, Parmelee A, Doi K, et al. Bone marrow stromal cells attenuate sepsis via prostaglandin E(2)-dependent reprogramming of host macrophages to increase their interleukin-10 production. *Nat Med.* 2009;15(1):42-9.
166. Weil BR, Herrmann JL, Abarbanell AM, Manukyan MC, Poynter JA, Meldrum DR. Intravenous infusion of mesenchymal stem cells is associated with improved myocardial function during endotoxemia. *Shock.* 2011;36(3):235-41.
167. Laroye C, Lemarié J, Boufenzer A, Labroca P, Cunat L, Alauzet C, et al. Clinical-grade mesenchymal stem cells derived from umbilical cord improve septic shock in pigs. *Intensive Care Med Exp.* 8 2018;6(1):24.
168. Gupta N, Krasnodembskaya A, Kapetanaki M, Mouded M, Tan X, Serikov V, et al. Mesenchymal stem cells enhance survival and bacterial clearance in murine Escherichia coli pneumonia. *Thorax.* 2012;67(6):533-9.
169. Laffey JG, Matthay MA. Fifty Years of Research in ARDS. Cell-based Therapy for Acute Respiratory Distress Syndrome. Biology and Potential Therapeutic Value. *Am J Respir Crit Care Med.* 2017;196(3):266-73.
170. Zheng G, Huang L, Tong H, Shu Q, Hu Y, Ge M, et al. Treatment of acute respiratory distress syndrome with allogeneic adipose-derived mesenchymal stem cells: a randomized, placebo-controlled pilot study. *Respir Res.* 2014;15:39.
171. Wilson JG, Liu KD, Zhuo H, Caballero L, McMillan M, Fang X, et al. Mesenchymal stem (stromal) cells for treatment of ARDS: a phase 1 clinical trial. *Lancet Respir Med.* 2015;3(1):24-32.
172. Matthay MA, Calfee CS, Zhuo H, Thompson BT, Wilson JG, Levitt JE, et al. Treatment with allogeneic mesenchymal stromal cells for moderate to severe acute respiratory distress syndrome (START study): a randomised phase 2a safety trial. *Lancet Respir Med.* 2019;7(2):154-62.
173. Hayes M, Masterson C, Devaney J, Barry F, Elliman S, O'Brien T, et al. Therapeutic efficacy of human mesenchymal stromal cells in the repair of established ventilator-induced lung injury in the rat. *Anesthesiology.* 2015;122(2):363-73.
174. Curley GF, Hayes M, Ansari B, Shaw G, Ryan A, Barry F, et al. Mesenchymal stem cells enhance recovery and repair following ventilator-induced lung injury in the rat. *Thorax.* 2012;67(6):496-501.
175. Masterson C, Devaney J, Horie S, O'Flynn L, Deedigan L, Elliman S, et al. Syndecan-2-positive, Bone Marrow-derived Human Mesenchymal Stromal Cells Attenuate Bacterial-induced Acute Lung Injury and Enhance Resolution of Ventilator-induced Lung Injury in Rats. *Anesthesiology.* 2018;129(3):502-16.
176. Islam MN, Das SR, Emin MT, Wei M, Sun L, Westphalen K, et al. Mitochondrial transfer from bone-marrow-derived stromal cells to pulmonary alveoli protects against acute lung injury. *Nat Med.* 2012;18(5):759-65.

177. Ahmad T, Mukherjee S, Pattnaik B, Kumar M, Singh S, Kumar M, et al. Miro1 regulates intercellular mitochondrial transport & enhances mesenchymal stem cell rescue efficacy. EMBO J. 2 mai 2014;33(9):994-1010.
178. Liu K, Ji K, Guo L, Wu W, Lu H, Shan P, et al. Mesenchymal stem cells rescue injured endothelial cells in an in vitro ischemia-reperfusion model via tunneling nanotube like structure-mediated mitochondrial transfer. Microvasc Res. 2014;92:10-8.

RESUME

Les dommages pulmonaires induits par la ventilation mécanique (VM) appelés Ventilator-induced lung injury (VILI) pourraient aggraver le pronostic des pneumopathies. La survenue d'anomalies mitochondrielles pourrait contribuer aux effets délétères de la VM. Nos travaux, menés *in vitro* et *in vivo* chez le lapin, ainsi que des données obtenues chez les patient ventilés en syndrome de détresse respiratoire aiguë, montrent que des alarmes mitochondrielles, en particulier l'ADN mitochondrial, sont libérées dans les alvéoles suite à l'étiènement des pneumocytes, ce qui pourrait constituer un lien entre l'agression mécanique et la réponse l'inflammation stérile à l'origine du VILI. Chez le lapin, nous montrons qu'une VM agressive et prolongée aggrave le pronostic de la pneumopathie à pneumocoque et s'associe à des altérations immunitaires et mitochondrielles. Ces données obtenues *in vivo* illustrent aussi la complexité et la compartmentalisation de la réponse immunitaire et de l'homéostasie mitochondriale. Enfin, nous observons que l'administration de cellules souches mésenchymateuses stromales améliore le pronostic des lapins soumis à la double agression VM-pneumopathie, en corrigeant certaines dysfonctions immunitaires et mitochondrielles, représentant ainsi une thérapie adjutante à l'antibiothérapie prometteuse.

Mots clés : pneumopathie, ventilation mécanique, dysfonction mitochondriale, cellules souches mésenchymateuses stromales

ABSTRACT

Lung damage induced by mechanical ventilation (MV) worsens the prognosis of pneumonia. Mitochondrial dysfunctions could account for such deleterious effects. Accordingly, data obtained from both *in vitro* and *in vivo* experimental studies, as well as in ventilated patients with acute respiratory distress syndrome, show that mitochondrial alarmins, especially mitochondrial DNA, are released in the alveolar compartment as a result of the cyclic stretch, and could thus represent one link between the mechanical insult and the sterile inflammation leading to VILI (ventilator-induced lung injury). In rabbits, we show herein that adverse and prolonged MV worsens the prognosis of pneumococcal pneumonia, and is associated with different immune and mitochondrial patterns of response according to the considered body compartment (i.e., lung or blood flow). Finally, mesenchymal stem cells administration improves the outcome of rabbits submitted to the combination of pneumonia and MV by correcting some immune and mitochondrial dysfunctions, thus representing a promising adjunctive therapy to antibiotics.

Keywords : pneumonia, mechanical ventilation, mitochondrial dysfunction, mesenchymal stem cells